

Flow Electrification in Aged Transformer Oils

by

Darrell Eugene Schlicker

B.S., Michigan Technological University, 1994

Submitted to the
Department of Electrical Engineering and Computer Science
in partial fulfillment of the requirements
for the degree of

Master of Science in Electrical Engineering

at the

Massachusetts Institute of Technology

September 1996

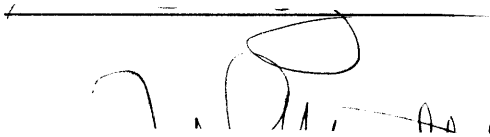
© Massachusetts Institute of Technology, 1996
All Rights Reserved

Signature of Author



Department of Electrical Engineering and Computer Science
September 6, 1996

Certified by



Markus Zahn
Thesis Supervisor

Accepted by



Frederic R. Morgenthaler
Chairman, Departmental Committee on Graduate Students

MASSACHUSETTS INSTITUTE
OF TECHNOLOGY

OCT 15 1996

ENG

LIBRARIES

Flow Electrification in Aged Transformer Oils

by

Darrell Eugene Schlicker

Submitted to the Department of Electrical Engineering and Computer Science on September 6, 1996 in partial fulfillment of the requirements for the degree of Master of Science in Electrical Engineering.

Abstract

Flow electrification is a problem occurring in many industries in which the transport of highly insulating fluid is required. Flow electrification results from the entrainment of electrical double layer charge into the fluid. This double layer charge is initially located at an interface between the insulating liquid and a second solid material and exists because of the difference in Fermi energy (or band potential) of the materials. Once the charge enters the liquid it is transported along with the fluid flow and can accumulate in the volume or on insulating surfaces. In addition the counter charge left on the interface can also rise to high levels which may cause tracking and electric discharges. As the potentials increase with charge accumulation it becomes possible for the electric field strength to exceed the breakdown strength of the materials in which the fields exist at both upstream and downstream locations.

This phenomena of fluid electrification occurs in large power transformers, where oil is used as the liquid dielectric to insulate the spaces between windings. The solid surfaces are covered with solid dielectric of cellulose pressboard which also acts as a source of double layer charge. The flow of fluid is used as cooling mechanism to remove heat dissipated through conduction losses in the transformer. Unfortunately, this flow also brings with it some degree of charge transport and additional electrical fields are superimposed on the already present electric fields from the transformer windings. Under certain circumstances this can lead to a break down and catastrophic transformer failure. The study of the electrification can help to better describe the circumstances under which flow electrification phenomena is at its peak.

Flow electrification has two major areas of study: the first being the microscopic origin of the charge which is the electrical double layer itself, and the second being the more macroscopic results of this charge transport including the transformer charge distributions and resulting potentials. The first area will be concentrated on, as it is the source of charge and also it is much less dependent on exact geometry which only tends to suppress or enhance the entrainment of double layer charge and alter the resulting potential distribution.

The study of the electrical double layer charge is done in an apparatus consisting of two coaxial steel cylinders, with the region between the cylinders filled with oil. The inner cylinder is rotated creating a well-mixed core region in the fluid. The extent of the electrification is characterized by the measurement of the charge density of the fluid, open circuit voltage potential between the cylinders, and current flow between the cylinders under short circuit conditions. Parameters such as temperature and rotational rate are imposed, while conductivity, dielectric constant, and moisture levels are measured. AC and DC Voltages are also applied between the cylinders to alter the fluid charging.

The focus of the measurements made are on electrification in new oils and oils taken from transformers which were in service. The measurements also focus on the effects, in new and used oils, of an additive of 1,2,3 benzotriazole (BTA), which has been shown to reduce the relative amount of charge entrained in the flow.

Thesis Supervisor: Markus Zahn
Title: Professor of Electrical Engineering

Acknowledgments

The research presented in this thesis was performed in the Laboratory for Electromagnetic and Electronic Systems and was sponsored by the Electrical Power Research Institute (WO 334-1) under the management of Stan Lindgren. Oil samples were provided by Dan Crofts of Texas Utilities. Additional instrumentation was provided by Tettex Instruments. This thesis was supervised by Professor Markus Zahn at the Massachusetts Institute of Technology.

In the completion of any thesis there are always many people to thank who have contributed in many different ways, but first of all I would like to thank Prof. Zahn, who has both guided my research and who has helped to keep my enthusiasm high even in difficult times. I am fortunate to have had the opportunity to learn from his wide range of knowledge in both the classroom and in our meetings. Most of all I would like to praise the joy and excitement that he demonstrates in the search for understanding.

I would also like to thank Professor Bernard Lesieutre who joined our research group on a separate project, but also contributed to this research.

Along with any research project comes the need for people who assist in both administrative and technical areas. Here I would like to thank LEES staff members Kathy McCue and Paul Warren for the administrative component of this work. I would also like to acknowledge machinists Rocco Albano and Michael Grossman for their excellent construction of various components of the apparatus. Additionally I would like to thank LEES staff member Wayne Ryan who tended to fall into at least these two categories and who is also good friend.

In the day to day life of a student, it is the interaction with the other students in your lab which proves very valuable. These are the people with whom you spend much time with and become most familiar and who are simultaneously friends and also assistants with whom you can discuss both your successes and setbacks. In particular I would like to acknowledge Yanqing Du, Robert Lyons, Alexander Mamishev, and Mitchell Meinhold. I would also like to thank former Ph.D. students Andrew Washabaugh, who

has made great contributions in this research area, and Philip von Guggenberg, who has offered his suggestions in several meetings.

I also want to thank several of my friends, Tina, J-Jay, Pam and Amy, with whom I have kept in contact with over the years. Even though most of our communication is through phone calls and e-mail, their support and friendship has been invaluable in reaching many of my goals such as this.

Finally I would like to thank my parents Barbara Schlicker and Eugene Schlicker, who have given me their support and praise all of my life. They have helped to give me the opportunities, which have made me what I am today and for that I am very grateful.

Contents

| | |
|---|-----------|
| 1 Introduction..... | 19 |
| 1.1 Electrification Phenomena | 19 |
| 1.2 Electrification in the Power Industry..... | 22 |
| 1.3 Characterization of Electrification..... | 24 |
| 1.4 Scope of Thesis..... | 24 |
| 2 Apparatus | 27 |
| 2.1 Couette Facility | 27 |
| 2.1.1 Couette Charger..... | 27 |
| 2.1.2 Reservoir | 30 |
| 2.1.3 System Control and Data Acquisition | 30 |
| 3 Preliminary Measurements | 33 |
| 3.1 Introduction | 33 |
| 3.2 Varied Rotation and Temperature..... | 33 |
| 3.3 Applied Voltage | 42 |
| 4 Transient Behavior..... | 47 |
| 4.1 Introduction | 47 |
| 4.2 Initial System Conditioning..... | 47 |
| 4.3 Rotation Induced Transients | 51 |
| 4.4 Voltage Induced Transients | 56 |
| 5 Fresh Oil Measurements | 63 |

Contents

| | |
|---|------------|
| 5.1 Introduction | 63 |
| 5.2 Baseline Measurements | 63 |
| 5.3 Addition of BTA | 67 |
| 6 Aged Oil Measurements | 77 |
| 6.1 Introduction | 77 |
| 6.2 Oil Drying | 77 |
| 6.3 Baseline Measurements | 81 |
| 6.3.1 Rotation and Temperature Dependence | 81 |
| 6.3.2 Applied DC Voltage Dependence | 87 |
| 6.3.3 Applied AC Voltage Dependence | 91 |
| 6.4 Addition of BTA | 95 |
| 6.5 Effects of BTA | 101 |
| 6.5.1 Concentration Dependence | 101 |
| 6.5.2 Rotation and Temperature Dependence | 105 |
| 6.5.3 Applied DC Voltage | 112 |
| 6.5.4 Applied AC Voltage | 116 |
| 7 Conclusions | 121 |
| 7.1 Transients | 121 |
| 7.2 Fresh and Aged Oils | 122 |
| 7.3 BTA Effects | 123 |

Appendix

| | |
|--|------------|
| A BTA Addition | 125 |
| A.1 BTA Concentrate Preparation | 125 |
| A.1.1 BTA Concentration Calculations | 125 |
| A.1.2 BTA Solution/Suspension Preparation | 127 |
| A.2 Addition of BTA to the Couette Charger | 127 |
| B Acquisition and System Control Software and Plotting Routines | 129 |
| B.1 Acquisition and Control Software | 129 |

| | |
|--|------------|
| B.1.1 Schedule Description | 129 |
| B.1.2 Scheduler Commands | 132 |
| B.1.3 Instrument Commands | 137 |
| B.1.4 Software Module Descriptions | 150 |
| B.1.5 Experiment Schedules | 152 |
| B.2 Data Plotting and Manipulation | 158 |
| B.2.1 Exported MAT File Contents | 158 |
| B.2.2 Matlab Data Manipulation and Utility Scripts | 164 |
| B.2.3 Plotting and Analysis Scripts for Experiment Schedules | 187 |
| C Recovery Voltage Simulation | 237 |
| C.1 Recovery Voltage Measurement | 237 |
| C.2 Recovery Voltage for a Second Order RC Network | 238 |
| C.2.1 Measurements | 238 |
| C.2.2 Comparison with Theory | 241 |
| C.2.3 Simulation of Recovery Voltage | 243 |
| C.3 Recovery Voltage for a Pressboard/Oil System | 249 |
| C.3.1 Pressboard Dielectric Spectrum | 250 |
| C.3.2 Simulation of Recovery Voltage | 252 |
| C.4 Scripts Used for Recovery Voltage Simulations | 257 |
| C.4.1 RC Network Simulation | 257 |
| C.4.2 Function to Generate Pressboard Spectrum | 264 |
| C.4.3 Recovery Voltage Simulation for Couette Charger | 269 |
| D Impedance Measurement of Interdigitated Electrode Sensor | 280 |
| D.1 Interdigital Sensor | 280 |
| D.2 Admittance Divider Technique | 282 |
| D.3 Current Integration Technique | 285 |
| D.3.1 Representative Data | 289 |
| D.3.2 Analysis Script | 294 |
| D.3.3 Circuit Board Layout | 310 |
| D.4 Proposed Zero-Order Inversion Technique for Homogeneous Material | 312 |

Contents

List of Figures

Figure 2-1: Couette Facility consisting of Couette Charger (left chamber) and Reservoir (right chamber). Oil is dried and degassed in the reservoir and then moved to the CC where controlled rotation of the inner cylinder generates a turbulent fluid flow. The temperature of the CC and reservoir are controlled through external heating tape and cooling coils, while the oil temperature, moisture, conductivity, and charge density are measured. Inner and outer cylinders are also utilized as terminals for current and voltage measurements, application of AC and DC voltages, and dielectric measurements. 28

Figure 3-1: Measurement of terminal current and charge density at stepped rotation rates. The temperature of the oil was 45°C, while the conductivity and moisture of the oil were approximately 2.5 pS/m and 32 ppm respectively..... 36

Figure 3-2: Summary of measurement data from Figure 3-1 demonstrating charge density and terminal current dependence on rotation. Increase in charge densities with rotation rate results from the decrease in the sublayer thickness at the interfaces, which allows more double layer charge to become mixed in the turbulent core region between cylinders..... 37

Figure 3-3: Measurement of terminal voltage and charge density at stepped rotation rates. The temperature of the oil was 15°C, while the conductivity and moisture of the oil were approximately 0.3 pS/m and 5 ppm, respectively..... 38

Figure 3-4: Summary of measurement data from Figure 3-3 demonstrating charge density and terminal voltage dependence on rotation..... 39

Figure 3-5: Summary of open circuit terminal voltage and charge density as functions of rotational rate and temperature. Competing effects between conductivity and interfacial parameters results in the non-monotonic variation of charge density as a function of temperature. Contributions to the terminal voltages are made by both inner and outer cylinder double layers and the bulk charge which are also dependent on competing effects..... 40

Figure 3-6: Summary of terminal short circuit current as a function of temperature and rotation rate. Charge densities are again non-monotonic as in Figure 3-5. Charge densities increase with rotation due to decreasing sublayer thickness at the interfaces

List of Figures

| | |
|--|----|
| allowing more charge to become entrained. The dominant effect on the terminal current as a function of temperature is the increase in conductivity which tends to reduce the equivalent series resistance of the CC and increase the currents. | 41 |
| Figure 3-7: Effects of applied AC and DC voltages on measured charged density with CC rotational rate held constant at 400 RPM. | 44 |
| Figure 3-8: Effects of applied AC voltages as a function of frequency on measured charged density with CC rotational rate held constant at 400 RPM. | 45 |
| Figure 4-1: Initial conditioning transient observed during first measurements after cleaning and reassembly of the CC. The rotation rate was held at a constant 400 RPM, yet the terminal voltage and charge density continued to change for many hours. The measurements are continued in Figure 4-2. | 49 |
| Figure 4-2: Continuation of measurements started in Figure 4-1. Rotation was stopped for several minutes between measurements while data acquisition was reset, but when the rotation was restarted for this measurement, the terminal voltage and charge density basically continued near the ending levels of Figure 4-1. The conditioning transient continues for approximately 45 minutes before the measured parameters reach a stable value. | 50 |
| Figure 4-3: Transient induced by a step in the rotational rate. Since the terminal voltage time constant involved is not comparable to known time constants of the system, it is hypothesized that the momentary impulse in the shear stress on the inner cylinder may have altered the interface. A second hypothesis is that the rapid increase in rotation may have momentarily reduced the sublayer thickness allowing additional charge to be. | 52 |
| removed from the double layer, reaction rates of charge across the surface may then result in a long time constant. | 53 |
| Figure 4-4: Transients observed in the terminal voltage due to steps in the rotational rate. Time constants of the transients are again longer than system time constants. | 53 |
| Figure 4-5: Transients observed in the terminal current due to steps in rotation. Time constants of the transients are on the order of the relaxation time of the oil as expected. | 54 |
| Figure 4-6: Transients in terminal voltage and charge density induced by steps in rotational rate. Notice that each step results in a small transient with relatively long time constant, however the step from 700 to 800 RPM resulted in a rather large negative transient in the terminal voltage and an associated transient in the charge density. ... | 55 |
| Figure 4-7: Baseline data of terminal voltage and charge density at constant rotation and temperature with no pre-stressing. | 58 |
| Figure 4-8: Terminal voltage and charge density after pre-stressing with a DC voltage. Before these measurements were started, 500 V was applied between terminals for one hour. The applied voltage was then disconnected and the charger was allowed to relax for ten minutes, which is nearly 600 times longer than the oil relaxation time. However when rotation is started a transient with a relatively long time constant is observed. | 59 |
| Figure 4-9: Measurements showing the relaxation of an applied terminal voltage of 180V for ten minutes. The application and relaxation was repeated four times in the measurement. The first was with no rotation, the second was with 400 RPM | |

rotation, the third was with 800 RPM rotation, and in the fourth measurement the rotation was simultaneously stopped as the applied voltage was removed..... 60

Figure 4-10: Charge densities during the application and relaxation of the terminal voltages in Figure 4-9. 61

Figure 4-11: Comparison of terminal voltages under the four conditions of the measurement shown in Figure 4-9. The terminal voltages have been normalized by removing their final value and dividing by their peak magnitude. The terminal voltage with no rotation and with the rotation stopped match the decay based on only relaxation, while the decays with rotation contain a second longer time constant. ... 62

Figure 5-1: Dependence of terminal voltage and charge density on rotation and temperature for fresh Shell Diala A oil. Measurements were made using stepped rotation, values of terminal voltage and charge density were then averaged over each step..... 65

Figure 5-2: Dependence of terminal current and charge density on rotation and temperature for new Shell Diala A oil..... 66

Figure 5-3: Addition of BTA at 1 hour into the measurement to raise the oil concentration from 0 ppm to 5 ppm. 70

Figure 5-4: Addition of BTA at 1 hour into the measurement to raise the oil concentration from 5 ppm to 10 ppm. 71

Figure 5-5: Addition of BTA at 1.75 hours into the measurement to raise the oil concentration from 10 ppm to 15 ppm. 72

Figure 5-6: Effects of BTA addition on conductivity cell offset voltage and streaming current from the tip of the absolute charge sensor for each BTA addition. 73

Figure 5-7: Effects of BTA on terminal current and charge density as a function of concentration and rotational rate. 74

Figure 5-8: Effects of BTA on oil conductivity as a function of concentration. 75

Figure 6-1: Drying process of aged transformer oil. 79

Figure 6-2: Summary of effects of oil drying on oil dielectric properties as functions of moisture and frequency. 80

Figure 6-3: Measurements of terminal current and voltage with varied rotation. 83

Figure 6-4: Measurement of charge density with varied rotation. 84

Figure 6-5: Summary of rotation and temperature dependence of terminal voltage and charge density for aged transformer oil..... 85

Figure 6-6: Summary of rotation and temperature dependence of terminal current and charge density for aged transformer oil..... 86

Figure 6-7: Effects of applied DC voltage on charge density. 89

Figure 6-8: Summary of applied DC voltage on charge density for 400 and 800 RPM rotation at varied temperature. 90

Figure 6-9: Effects of applied AC voltage frequency on charge density. The erratic behavior for low frequencies occurs as the frequency becomes comparable to the time required for a charge measurement. 93

Figure 6-10: Summary of applied AC voltage effects on charge density for 400 and 800 RPM rotation at varied temperature. 94

Figure 6-11: Addition of BTA in used transformer oil to bring concentration from 0 to 5 ppm. 97

List of Figures

Figure 6-12: Addition of BTA in used transformer oil at approximately 100 minutes to bring concentration from 0 to 5 ppm. 98

Figure 6-13: Addition of BTA in used transformer oil at approximately 100 minutes to bring concentration from 5 to 10 ppm. 99

Figure 6-14: Addition of BTA in used transformer oil at approximately 100 minutes to bring concentration from 10 to 15 ppm. 100

Figure 6-15: Addition of BTA in used transformer oil at approximately 100 minutes to bring concentration from 10 to 15 ppm. 101

Figure 6-16: Summary of BTA effects as a function of concentration. 103

Figure 6-17: Summary of BTA effects as a function of concentration. 104

Figure 6-18: Temperature and rotation dependence of terminal voltage and charge density with 15 ppm BTA. 107

Figure 6-19: Temperature and rotation dependence of terminal current and charge density with 15 ppm BTA. 108

Figure 6-20: Comparison of terminal voltages with and without BTA at varied temperature. 109

Figure 6-21: Comparison of terminal current with and without BTA at varied temperature. 110

Figure 6-22: Comparison of charge density with and without BTA at varied temperature. 111

Figure 6-23: Temperature and applied DC voltage dependence on charge density with 15 ppm BTA. 114

Figure 6-24: Comparison of charge density with and without BTA at varied applied DC voltage and temperature with the rotation rate at a constant 400 RPM. 115

Figure 6-25: Comparison of charge density with and without BTA at varied applied DC voltage at 60°C with the rotation rate at a constant 400 RPM. 116

Figure 6-26: Temperature and applied AC voltage dependence on charge density with 15 ppm BTA. 118

Figure 6-27: Comparison of charge density with and without BTA at varied applied AC voltage and temperature. 119

Figure 6-28: Comparison of charge density with and without BTA at varied applied AC voltage and temperature. 120

Figure C-1: Second order RC network used for initial recovery voltage measurements. 238

Figure C-2: Comparison of measured recovery voltage and theoretical recovery voltage for network with $R_1=1.05\text{ M}\Omega$, $R_2=10.3\text{ M}\Omega$, $C_1=330\text{ nF}$, and $C_2=335\text{ nF}$. The charging voltage was 200 V, while the charging time was .5 seconds and the discharging time was .25 seconds. 239

Figure C-5: Simulation of recovery voltage. Top) FFT of current after imposing zero current for recovery stage. Middle) Magnitude of network impedance. Bottom) FFT of network voltage after imposing open circuit condition for recovery period. 247

Figure C-6: Simulation of recovery voltage. Top) Applied and recovery voltage after IFFT. Middle) Applied and recovery voltage. Bottom) Simulated recovery voltage. 248

Figure C-7: Dielectric spectrum of pressboard at two levels of moisture. 251

Figure C-8: Simulation of recovery voltage. Top) Applied voltage, recovery voltage is unknown and is therefore set to zero. Middle) FFT of applied voltage. Bottom) Magnitude of admittance as a function of frequency for modeled oil/pressboard system. 253

Figure C-9: Simulation of recovery voltage. Top) FFT of current flowing pressboard/oil system due to applied voltage. Middle) IFFT of current. Bottom) Current after imposing open circuit conditions at recovery period. 254

Figure C-10: Simulation of recovery voltage. Top) FFT of current after imposing zero current for recovery stage. Middle) Magnitude of network impedance. Bottom) FFT of network voltage after imposing open circuit condition for recovery period. 255

Figure D-1: Top view of interdigital electrode sensor containing three different spatial periodicity's. 281

Figure D-2: Lumped-element equivalent circuit of one set of interdigitated electrodes.. 282

Figure D-3: Lumped-element equivalent circuit of dielectric sensor as an admittance divider. 284

Figure D-4: Bode plot of admittance divider response..... 284

Figure D-5: Simple Current Measurement..... 286

Figure D-6: Active current integration circuit..... 286

Figure D-7: Bode plot for system response of current integration technique. 288

Figure D-8: Magnitude and phase measurement using current integration technique. 290

Figure D-9: Sensor capacitance and conductance measurement in air using current integration technique. Since both sensor and air are pure dielectrics, no conductance is observed..... 291

Figure D-10: Sensor magnitude and phase response in pressboard. The behavior of the gain and phase is due to the highly dispersive nature of the pressboard. 292

Figure D-11: Sensor capacitance and conductance when in contact with pressboard. The behavior of the capacitance and conductance signifies the known non-ohmic characteristics of the pressboard's dielectric spectrum. 293

Figure D-12: Solder side of interdigital sensor interface using current intergration techniques (viewed from component side). 310

Figure D-13: Component side of interdigital sensor interface using current intergration techniques (viewed from component side). 311

Figure D-14: Parts placement for interdigital sensor interface using current integration techniques (viewed from component side). 312

List of Tables

Table C-1: Comparison of measured and theoretical values for peak value of recovery voltage for network with $R_1=1.05\text{ M}\Omega$, $R_2=10.3\text{ M}\Omega$, $C_1=330\text{ nF}$, and $C_2=335\text{ nF}$ using a 200 V charging voltage. 239

Table C-2: Comparison of measured and theoretical values of recovery voltage peak time for network with $R_1=1.05\text{ M}\Omega$, $R_2=10.3\text{ M}\Omega$, $C_1=330\text{ nF}$, and $C_2=335\text{ nF}$ using a 200 V charging voltage..... 240

Table C-3: Comparison of measured and theoretical values for peak value of recovery voltage for network with $R_1=9.96\text{ M}\Omega$, $R_2=10.2\text{ M}\Omega$, $C_1=317\text{ nF}$, and $C_2=103\text{ nF}$ using a 200 V charging voltage. 240

Table C-4: Comparison of measured and theoretical values of recovery voltage peak time for network with $R_1=9.96\text{ M}\Omega$, $R_2=10.2\text{ M}\Omega$, $C_1=317\text{ nF}$, and $C_2=103\text{ nF}$ using a 200 V charging voltage..... 241

1 Introduction

1.1 Electrification Phenomena

Flow electrification involves the entrainment of electrical double layer charge, located at interfaces between solids and liquids, into the flow of a fluid. The flow of the fluid then tends to redistribute the charge through convection and simultaneous relaxation of the charge to new regions of the flow and adjoining solid materials. This redistribution of charge further results in electric fields which may create additional charge transport through conduction. However, in order for a significant amount of electrification to occur several criteria must be met.

Firstly, an electrical double layer must be present at the interfaces, since this is the charge source for the fluid. An electrical double layer is simply the separation of charge that may occur at the interface of two materials due to their molecular dissimilarity, atomic makeup or structure. The term “double layer” arises from one method of modeling the charge as two sheets of opposite polarity located at specified distances from the interface. However, a more physical model for the actual distribution of the charge is an exponential decay away from the interface with the counter charge on the surface. This distribution is justified by assuming the dominant phenomena determining the distributions

Chapter 1: Introduction

are electrical conduction and diffusion of the charge or charged ions. The decay length of the exponential distribution under these assumptions can be determined for equilibrium conditions and is known as the Debye length which can be written as

$$\lambda_d = \sqrt{\frac{\epsilon D}{\sigma}} \quad (1.1)$$

where λ_d is the Debye length, ϵ is the dielectric constant of the material, σ is the conductivity of the material, and D is the diffusivity of the charge or charged ions in the material. From Eq. 1.1 it can be observed that the Debye length is inversely proportional to the square root of the material's conductivity and proportional to the square root of the product of dielectric constant and diffusivity. However, this only relates the thickness of the Debye layer to the material and not the actual magnitude of the charge to the material. Predicting the actual charge is a very difficult, if not impossible task especially for materials such as transformer oil which is composed of many hydrocarbons and trace impurities. Yet with the assumption of an exponential distribution, it becomes possible to assign a boundary charge density at the interface which then can be calculated from measurement. So in general it is possible to determine the approximate size of the double layer from simple material properties, but not the absolute magnitude of the charge density of the distribution.

The second requirement necessary for electrification to occur is that the charge in the double layer becomes entrained in the fluid flow. This entrainment of the double layer charge is a result of an enhancement of the molecular diffusivity in a region of the fluid extending from the bulk of the fluid to a region near the interface. The thickness of the layer between the interface and this region of enhanced diffusivity is known as the diffusion sublayer and is defined as the distance from the interface at which the molecular diffusivity balances the diffusivity due to the fluid flow. The sublayer thickness is dependent on several parameters of the fluid including its viscosity and density. It is also dependent on the roughness of the surface and overall flow geometry and velocity. The important characteristic of the sublayer thickness in regard to electrification is that it is on the order of the Debye length which allows the fluid flow to remove the charge from the

double layer. It should be somewhat obvious that a smaller sublayer thickness will result in the removal of more charge from the double layer and in general increase the charge entrained in the fluid, while a decrease in the sublayer thickness will act to reduce the charging of the fluid.

The previous conditions mentioned for electrification are sufficient to allow the fluid to become charged, at least near the interface. However, problems resulting from fluid electrification generally require some additional conditions and an even more specific knowledge of the system in which electrification is occurring.

The first of these additional requirements is that the charge now entrained in the fluid, near the double layer charge source, is transported away due to the bulk convection caused by the flow. Since the fluid is assumed to be flowing, there is definitely a means for bulk convection of the charge. However, simultaneous to the movement of charge, is the relaxation of charge due to the conductivity of the fluid. If the velocity of the fluid is such that the charge is transported a characteristic distance of the system in a shorter period of time than the charge tends to decay, then charge can successfully be redistributed. This relation between charge movement and relaxation is expressed in the electric Reynolds Number as

$$R_e = \frac{U \varepsilon}{\ell \sigma} \tag{1.2}$$

where U is the flow velocity, ℓ is a characteristic length of the system, ε is the dielectric constant of fluid, and σ is the fluid conductivity. If the electric Reynolds number is sufficiently large, significant charge transport will occur.

With the electrical double layer charge now being transported away from the double layer source, charge redistribution and accumulation can occur in the system. Determining the transient, or even steady-state charge distributions within a system will be of varying difficulty depending on the flow characteristics, materials, and overall complexity of the geometry of the system. The importance of the redistribution and accumulation of charge lies in the new electric fields which are generated by the charge.

Chapter 1: Introduction

These electric fields are key to most problems associated with the flow electrification phenomena.

The development of these electric fields creates current flow which tends to relax the redistributed charge and also creates electrical stress on the materials in the system. Under steady state conditions the redistribution of the charge through electrification and convective transport balance the relaxation of charge. However, in reaching this steady state condition the electric fields due to the redistributed charge will grow and increase the electrical stress on the materials in the system. If this stress is near the electrical breakdown strength of the material a breakdown may occur in the system, which is in general the greatest problem of electrification. But even if the system can reach a steady state charge distribution without breakdown, the electric fields present can still pose a problem. These fields may make unsafe working conditions or can result in an unexpected discharge if the system is then perturbed.

1.2 Electrification in the Power Industry

One important industrial situation where the conditions for electrification phenomena are generally good is in large power transformers using oil/pressboard dielectrics. There are several primary reasons why electrification is possible in these transformers. The materials used between the windings of the transformer must be highly insulating in order to protect from breakdown due to the energization voltages and to reduce conduction losses. This highly insulating environment results in the slow relaxation of charge accumulated in the system. The structure of the transformer is also rather complex containing many pressboard surfaces to isolate and support the windings. The oil dielectric then fills the remaining regions between pressboard surfaces creating many interfaces between pressboard and oil at which a double layer necessary for electrification can exist. Finally the flow required to remove and transport the double layer charge, results from the cooling techniques employed. The heat dissipated in the windings is removed by the circulation of the oil dielectric through the transformer and external heat exchangers. All these factors help contribute to the flow electrification which occurs in these transformers.

The real problem with flow electrification in these transformers is the possibility of electrical breakdown in the dielectric materials. The chance for breakdowns is worsened by the presence of already large AC electric fields from energized windings which are superimposed on fields developed by electrification. Breakdowns can have the effect of degrading the dielectric materials, making them more susceptible to additional breakdown. Furthermore if these breakdowns are severe enough or the insulation isolating the high voltages between windings becomes damaged, the transformer may fail catastrophically.

In order to reduce the chance of electrification problems several precautionary steps have been taken in the design and operation of many of these transformers. One major design improvement is the reduction of the fluid velocity of the oil being circulated. By allowing larger ducts in the flow path, flow rates can be maintained, but the lower velocities tend to increase the sublayer thickness and reduce the amount of double layer charge entrained in the flow. Another design improvement has been made in the control of the circulation of oil. Since the purpose of the oil circulation is to remove thermal energy to prevent overheating and insulation damage, the pumping of the oil is only necessary when internal temperatures reach a certain level. By only pumping the oil when these temperatures are reached, the total operating time for which electrification can occur is reduced. Furthermore the dielectric materials are more conductive at these higher temperatures which results in faster charge relaxation times which help to reduce charge accumulation. This idea of increased conductivity to reduce charge accumulation is widely used in the petroleum industry where additives which increase the conductivity of insulating liquids are utilized. However severely increasing the conductivity of the dielectric materials in the transformers is undesirable because of the loss in efficiency and potential loss of breakdown strength.

Another additive, 1,2,3 benzotriazole (BTA), has been shown to reduce the electrification phenomena without increasing the conductivity of the oil. This additive which is widely accepted and used in the Japanese power industry has met much hesitation in the U.S. industry. Part of this reluctance is due to the incomplete understanding of all of the mechanisms and effects of this additive on the total transformer system. Continuing

Chapter 1: Introduction

research and long term studies should reveal any adverse effects of the additive in the transformer system.

1.3 Characterization of Electrification

Characterizing the degree of electrification for a complete system is in general a difficult task because it involves material properties, flow patterns, and electric field distributions in a potentially complex geometry. Fortunately some generic observations can be made about electrification, such as: reducing flow rates and increasing the conductivity of the fluid tends to reduce the charge entrained in the flow. Controlling flow velocities in a fluid system is a generally well understood area of mechanics, while measurements of dielectric properties and their dependencies on parameters such as temperature and moisture are common. However electrification in a system is also very dependent on the interaction of solids and liquids at interfaces where double layer charge forms. It is the exact properties of the double layer that are much more difficult to predict, yet have such great effects on the total charging of fluid.

Several models for parameters which characterize this interface have been developed in [6]. These parameters demonstrate one method of ideally describing the interface under steady state conditions. A second method for describing the interfaces is by looking at only the effects of the double layer, namely the charging of the fluid in a geometrically simple system where double layer effects are exemplified. This method has the main disadvantage in not allowing absolute numbers for fundamental parameters to be compared. However in practice repeatability issues can cause difficulty in comparing even fundamental parameters which helps to warrant this type of comparison.

1.4 Scope of Thesis

In this thesis many electrification measurements in a Couette facility are presented for new and aged oils under various imposed conditions. Chapter two describes the apparatus and instrumentation utilized in the measurement of the electrification phenomena. Chapter three presents some preliminary data and general trends of the electrification measurements on imposed parameters. Chapter four concentrates on many transient behaviors which were observed in response to fluid velocity changes, applied voltages, and

system conditioning. Chapter five demonstrates dependencies for fresh oil including the addition of BTA. Chapter six is dedicated to a number of comparisons for aged oil with and without BTA for many imposed conditions.

In addition the appendix includes additional information on electrification and other topics peripherally related to electrification. Appendix A includes techniques and calculations used in the addition of BTA in electrification measurements. Appendix B covers the usage of the software application “Spin” and supporting utilities specifically developed to allow fine and flexible control of experiments and measurements. Appendix C contains preliminary work in developing comparisons between measured dielectric spectral data in the frequency domain and recovery voltage measurements in the time domain. Finally, Appendix D introduces and compares a current measurement technique for use in interdigital electrode sensors, currently being developed for the measurement of dielectric material properties.

Chapter 1: Introduction

2 Apparatus

2.1 Couette Facility

Flow electrification measurements were carried out in an apparatus designed to create a turbulent flow of oil in which imposed parameters such as flow rate, temperature, and moisture could be controlled. In addition other properties of the oil were measured, including conductivity, dielectric constant, and charge density. The complete facility consists of two major units the first being the actual charger in which the flow of oil results in the entrainment of electrical double layer charge, and the reservoir which is used for processing of the oil. The complete facility, referred to as the Couette Facility is shown in Figure 2-1.

2.1.1 Couette Charger

The Couette Charger (CC) consists of two coaxial stainless steel cylinders with the region between cylinders filled with transformer oil. The top and bottom of the chamber are sealed with polycarbonate pieces which contain the fluid and provide electrical isolation between cylinders. A shaft extends from the inner cylinder and out of a sealed port in the top of the charger, allowing it to be rotated at variable speeds by an electric motor. This rotation results in a turbulent flow of the oil between cylinders for rotational rates greater than 60 RPM [3]. The turbulent flow is advantageous in that it creates a core region of uniform charge density between cylinders. Having a uniform charge density allows a charge density measurement at a single location to characterize the charging of the fluid.

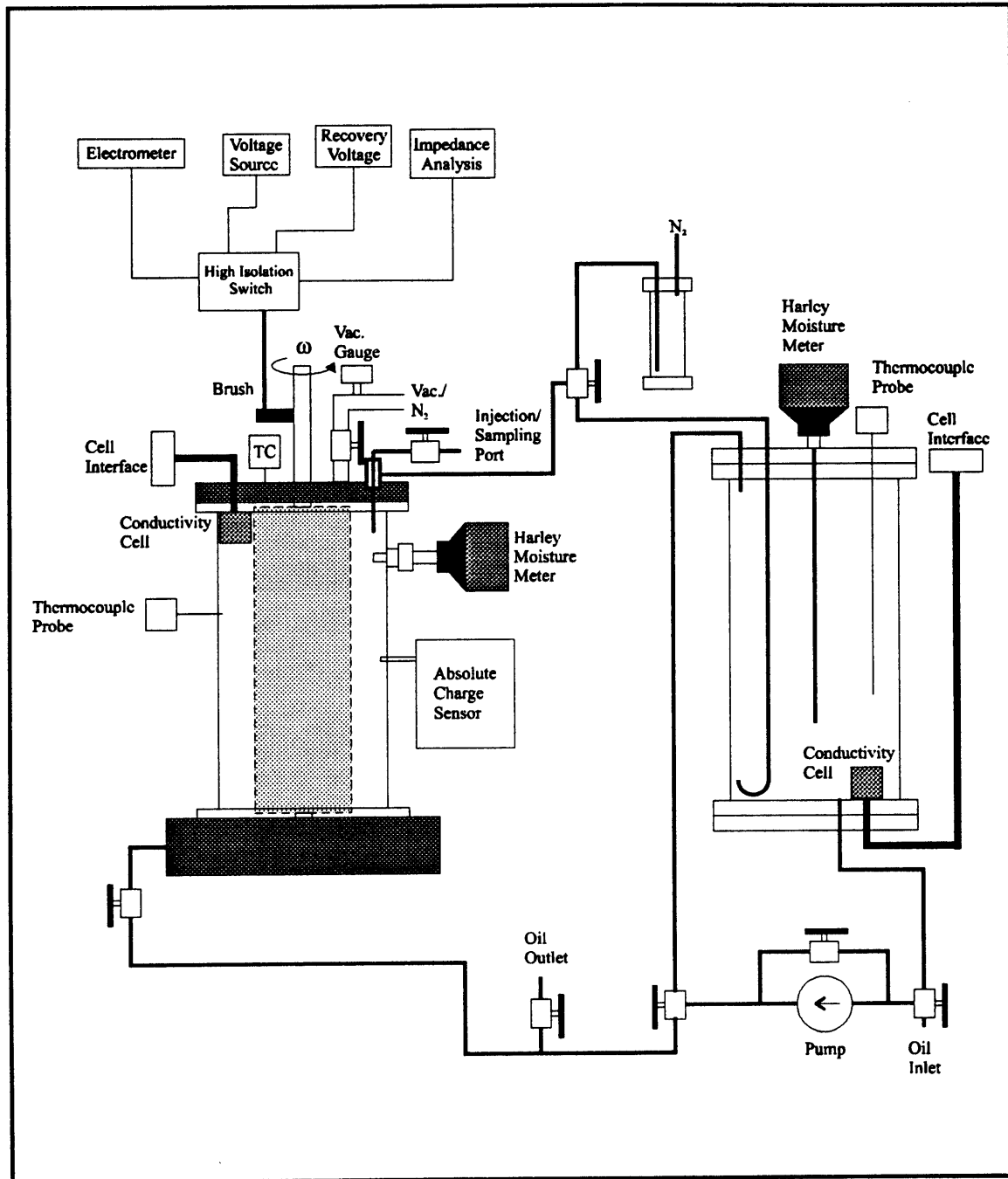


Figure 2-1: Couette Facility consisting of Couette Charger (left chamber) and Reservoir (right chamber). Oil is dried and degassed in the reservoir and then moved to the CC where controlled rotation of the inner cylinder generates a turbulent fluid flow. The temperature of the CC and reservoir are controlled through external heating tape and cooling coils, while the oil temperature, moisture, conductivity, and charge density are measured. Inner and outer cylinders are also utilized as terminals for current and voltage measurements, application of AC and DC voltages, and dielectric measurements.

Terminal Constraints

Since the inner and outer cylinder are electrically isolated, they can be utilized as electrical terminals from which various constraints may be imposed and measurements can be made. The connection of the terminals is selected through an automated high voltage, high cross-impedance switch that allows either of an electrometer, high-voltage amplifier, recovery voltage meter, or impedance meter to be connected. The electrometer is used when the terminals are to be short circuited or open circuited which also allows the short circuit terminal current or open circuit voltage to be measured. Application of both AC and DC voltages is achieved with a high voltage amplifier and allows the charge densities to be perturbed from their open circuit or short circuit values. Both recovery voltage measurements and impedance measurements are useful for monitoring the dielectric properties of the material filling the space between cylinders. These measurements have importance when the cylinders are covered with a solid dielectric such as pressboard, in which case the total terminal impedance becomes a function of moisture distributed in the system.

Oil Properties

Several properties of the oil are monitored during electrification measurements including oil conductivity, dielectric constant, moisture, charge density and temperature. Dielectric properties of the oil are monitored using a ganged capacitor consisting of many parallel plates which are submerged in the oil. Measurements of the capacitors impedance can then be used to calculate the oil's conductivity and dielectric constant. Thermocouples are placed in the top and the side of the CC for measuring the bulk oil temperature and the outer cylinder temperature, respectively. Moisture measurements are carried out using a moisture sensor developed by J.W. Harley, Inc. for measuring moisture in transformer oil. These sensors measure the relative saturation of moisture in the oil, but ppm concentrations can be calculated from saturation curves since the oil temperature is known. Oil charge density measurements are made with an absolute charge sensor which utilizes an expanding metal bellows as a faraday cage [4].

Chapter 2: Apparatus

BTA Addition

In experiments using the additive BTA, it was introduced as a concentrate in oil, through the injection/sampling port consisting of a valve and a teflon tube extending through a top port in the CC and into the gap between cylinders. Additions of BTA were generally made at elevated temperatures, where the solubility of the BTA in oil was enhanced allowing higher concentrations and smaller injection volumes.

During the injections, the large reservoir was sealed from the CC, which was connected to a mini-reservoir. This allowed the volume of oil into which the BTA concentrate was being injected to be minimized, creating a more reliable final BTA concentration in the CC. The specifics of the BTA preparation and concentration calculations can be found in Appendix A.

2.1.2 Reservoir

The reservoir is utilized in processing of the oil before measurements. General processing of the oil involves degassing and drying using a vacuum pump. Measurements of the oil properties including temperature, moisture, dielectric constant, and conductivity are also made as in the CC during the drying process.

The reservoir can also be utilized for increasing or decreasing the moisture of the oil in the CC during measurements. This is accomplished by using a recirculatory flow between the CC and the reservoir. The bottom of the reservoir contains a connection to a source of both wet and dry nitrogen, and as either wet or dry nitrogen bubbles through the oil in the reservoir, oil moisture is increased or decreased. This is especially useful for observing moisture transients when pressboard has been placed on either inner or outer cylinders.

2.1.3 System Control and Data Acquisition

The Couette Facility consists of many instruments, several for control and several for measurements. The instruments which are involved in the control of the system are the CC motor, recirculatory motor, terminal selector, wetting/drying system, and high voltage

supply. The instruments involved in measurements are the electrometers, thermocouples, moisture meters, absolute charge sensor, impedance measurements (dielectric properties), and recovery voltage measurements.

In order to control and monitor all of these instruments software was developed which allowed flexibility in the creation of specific experiments with a minimal specification of instrument behaviors for each new experiment. This flexibility was accomplished by creating an interpreter of a language consisting of commands specific to the instruments present in the Couette Facility. The software also assists in the configuration and calibration of instruments as well as handling the multitasking in the execution of commands for each instrument.

New experiments are created by placing commands in a schedule file, which is then run to carry out the experiment. Data generated by the control and measurement instruments is then simultaneously collected and placed in a file which can be imported as numerical matrices into the Matlab mathematical software package (product of The MathWorks, Inc.), where it can be plotted and further analyzed. The software developed for the Couette Facility, further described in Appendix B, allows future researchers the ability to carry out new experimentation with ease.

The software was run on a Pentium PC using the Windows 95 operating system. Data acquisition and instrument control was accomplished using serial communications, GPIB protocol, digital IO interfaces, A/D interfaces, and D/A interfaces.

Chapter 2: Apparatus

3 Preliminary Measurements

3.1 Introduction

In preparation for measurements on new and aged oils several preliminary measurements were made using fresh oil. These measurements demonstrate general trends for electrification in the Couette geometry under varying rotational rates, temperatures, and applied AC and DC voltages.

3.2 Varied Rotation and Temperature

The following measurements were carried out in the Couette Facility with the inner and outer stainless steel cylinders left bare and the gap filled with new Shell Diala A transformer oil.

Figure 3-1 shows the temporal data for a measurement of charge density and terminal current with rotation increased in steps of 100 RPM. Figure 3-2 summarizes the dependence of the fluid charge density in the turbulent core region as measured with the absolute charge sensor, and the terminal current measured between cylinders, both as a function of the rotational rate. The charge density increases monotonically with the increase in rotation rate. This is due to the monotonic decrease in the sublayer thickness at oil/cylinder interfaces with increasing fluid velocities. The decrease in the sublayer thickness allows more of the double layer charge to become entrained in the turbulent core.

Chapter 3: Preliminary Measurements

The terminal current in these measurements becomes increasingly negative with rotational rate. The short circuit currents are created by the dissimilarity of the interfaces due to the different cylinder radii and possible differences in the interfacial parameters between inner and outer cylinders. The currents also depend on the oil's conductivity and the charge transport rates through the interfaces. This results in the measured current containing much information about the system, but in a rather complex manner.

The measurement in Figure 3-3 shows the temporal data for the open circuit terminal voltage and charge density with stepped rotation. Figure 3-4 summarizes the voltage and charge density as a function of rotation rate. The charge densities again have a similar dependence as described previously. The terminal voltage, which in this case tends to increase with rotation, is also generated by the dissimilar radii of the interfaces and possibly different interfacial parameters and resulting charge in the fluid. The dissimilar radii and interfacial parameters result in different double layer charge distribution when the inner cylinder is rotated, which along with the entrained charge creates the potential difference between cylinders. This measured potential, like the current, contains much information about the system and interfaces. However unlike the current, no charge must be transported through the interfaces and so somewhat less information is contained in the terminal voltage.

Figure 3-5 summarizes the dependence of the open circuit voltage and charge density as a function of temperature and rotation rate. The charge densities initially decrease with increasing temperature, but then increase for the highest temperature. This results from competing effects between the increase in double layer charge and increase in the oil conductivity with temperature. The terminal voltage appears to be decreasing with increasing temperature which is also due to the effects of the decreasing charge densities and changes in the double layers.

Figure 3-6 summarizes the terminal current and charge densities as a function of rotation rate and temperature. The charge densities again have a similar dependence as described for Figure 3-5. The terminal currents are increasing in magnitude with

temperature, this is also due to several temperature dependent properties such as the oil's conductivity increase and interfacial properties.

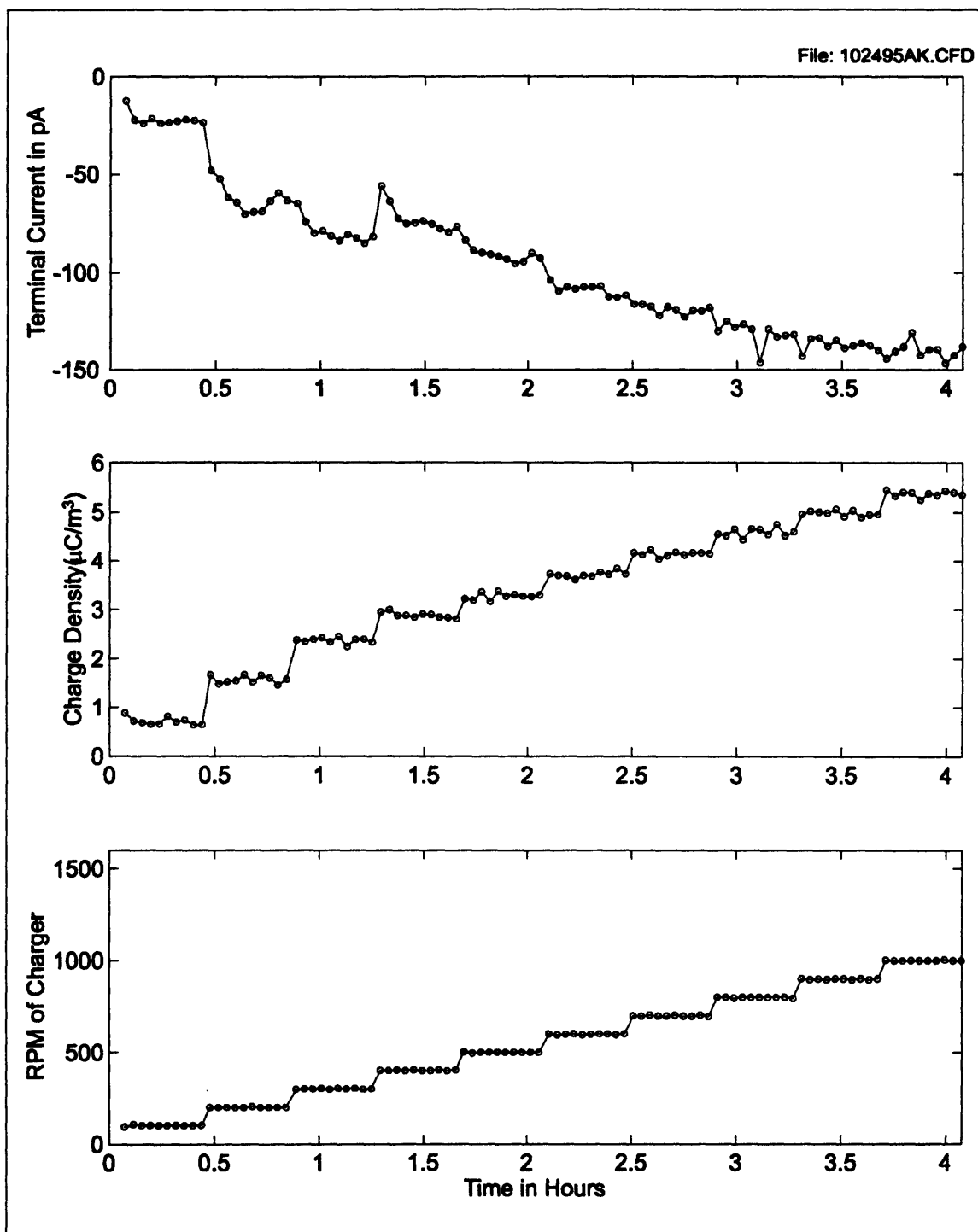


Figure 3-1: Measurement of terminal current and charge density at stepped rotation rates. The temperature of the oil was 45°C, while the conductivity and moisture of the oil were approximately 2.5 pS/m and 32 ppm respectively.

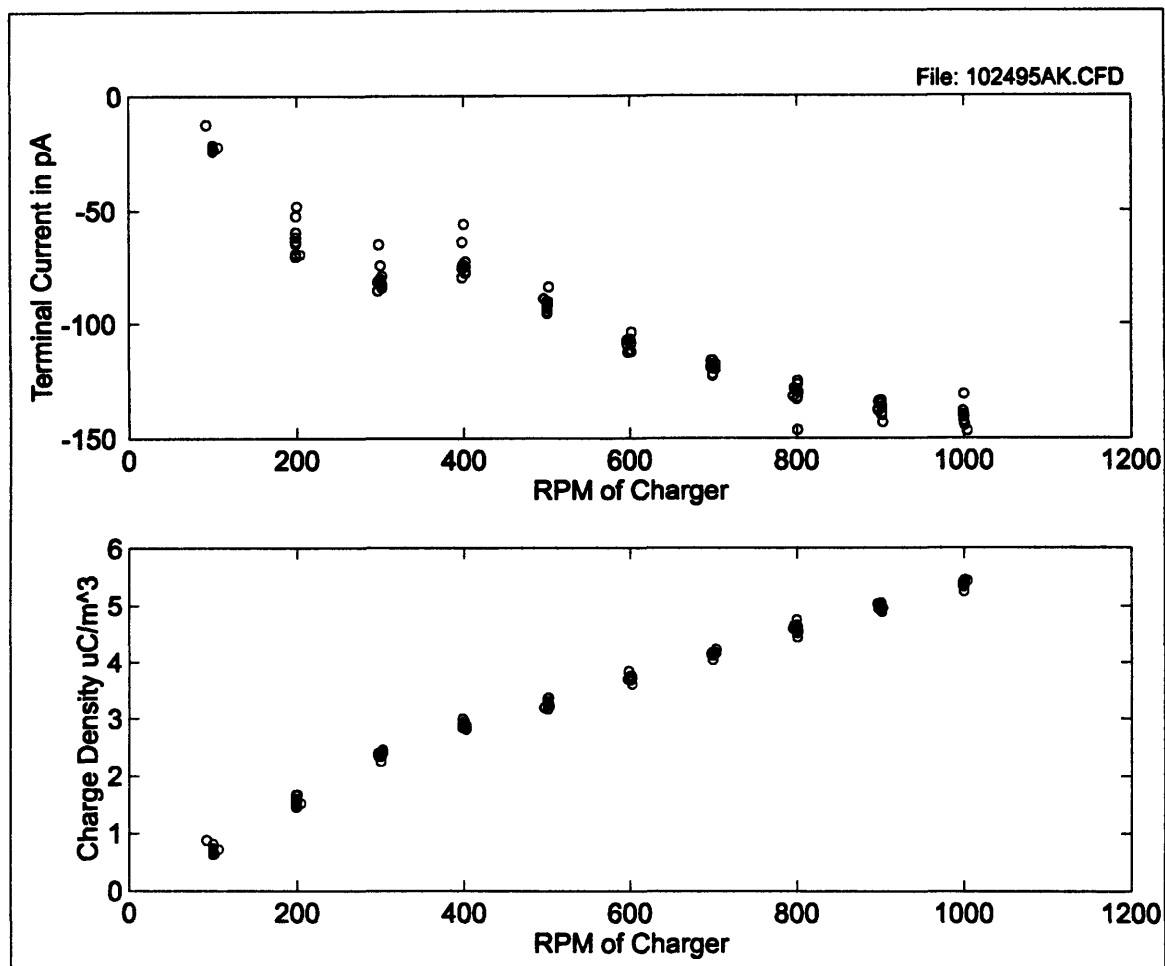


Figure 3-2: Summary of measurement data from Figure 3-1 demonstrating charge density and terminal current dependence on rotation. Increase in charge densities with rotation rate results from the decrease in the sublayer thickness at the interfaces, which allows more double layer charge to become mixed in the turbulent core region between cylinders.

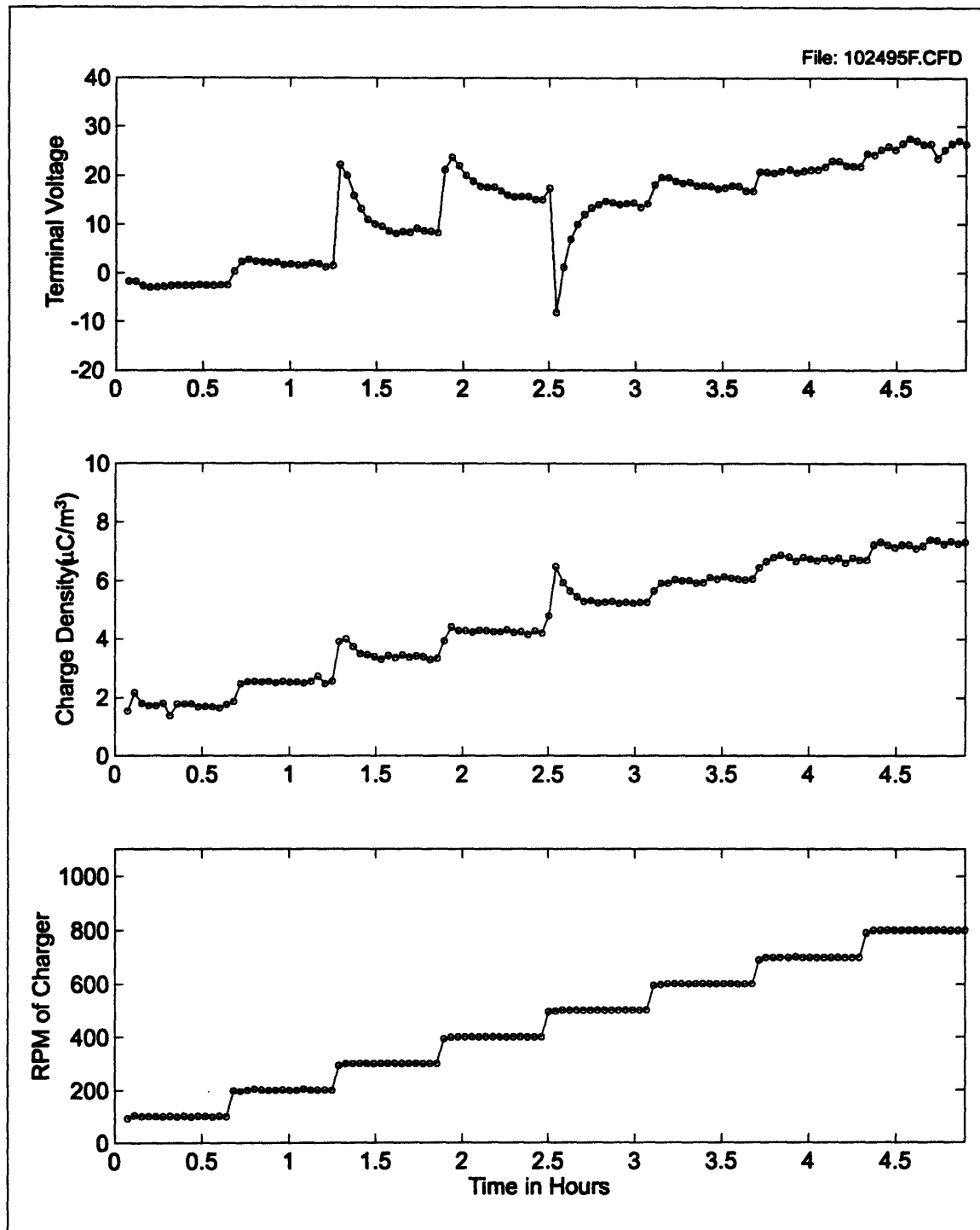


Figure 3-3: Measurement of terminal voltage and charge density at stepped rotation rates. The temperature of the oil was 15°C, while the conductivity and moisture of the oil were approximately 0.3 pS/m and 5 ppm, respectively.

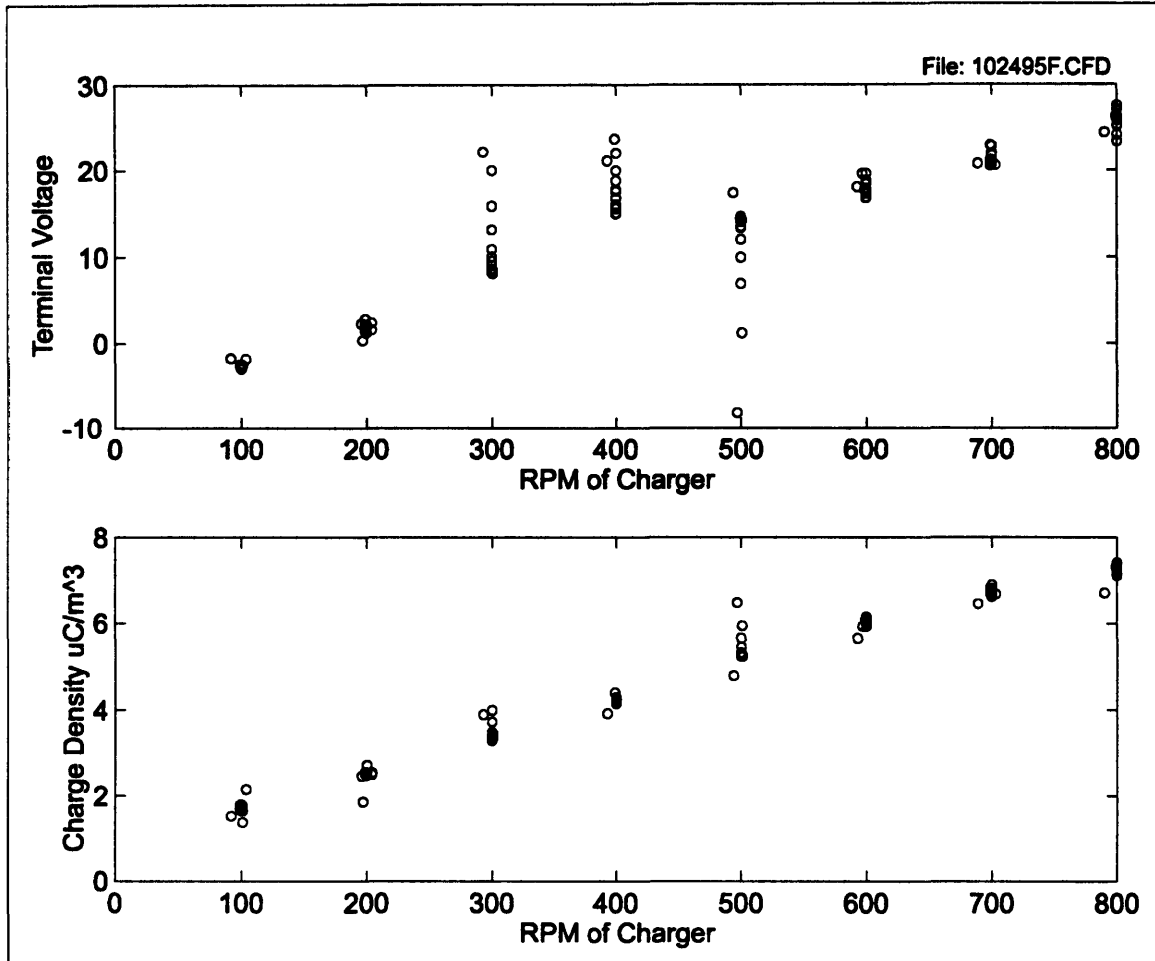


Figure 3-4: Summary of measurement data from Figure 3-3 demonstrating charge density and terminal voltage dependence on rotation.

Chapter 3: Preliminary Measurements

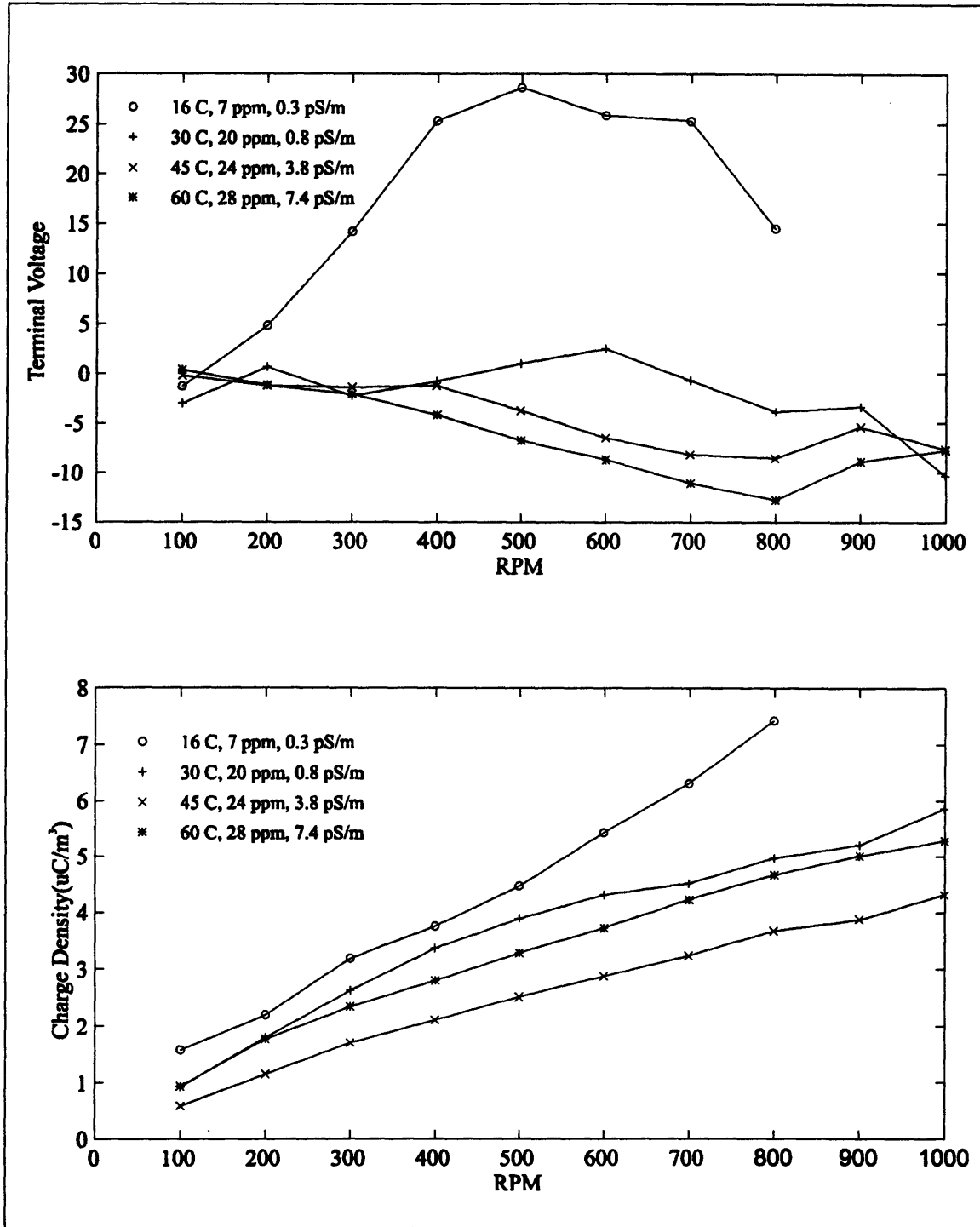


Figure 3-5: Summary of open circuit terminal voltage and charge density as functions of rotational rate and temperature. Competing effects between conductivity and interfacial parameters results in the non-monotonic variation of charge density as a function of temperature. Contributions to the terminal voltages are made by both inner and outer cylinder double layers and the bulk charge which are also dependent on competing effects.

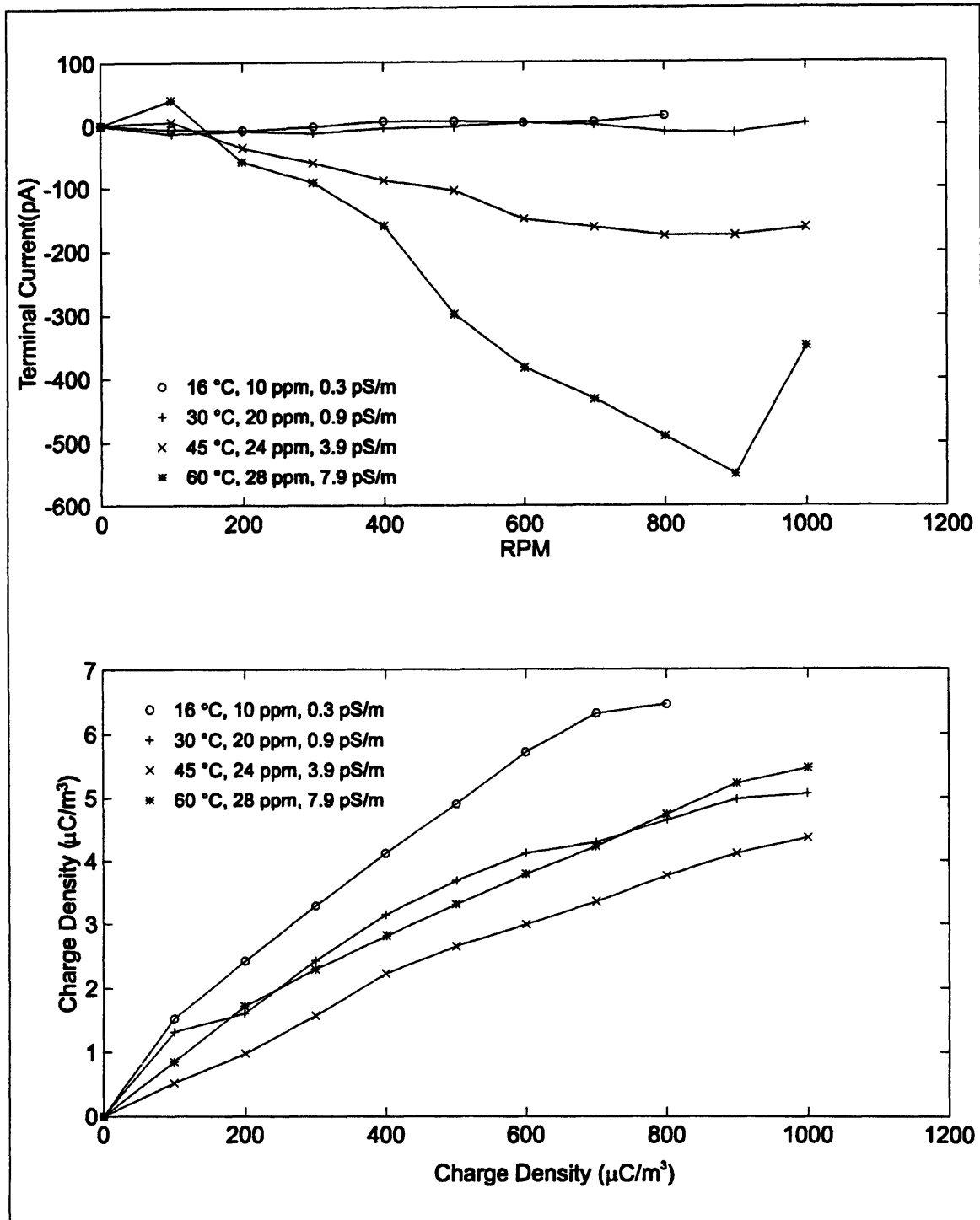


Figure 3-6: Summary of terminal short circuit current as a function of temperature and rotation rate. Charge densities are again non-monotonic as in Figure 3-5. Charge densities increase with rotation due to decreasing sublayer thickness at the interfaces allowing more charge to become entrained. The dominant effect on the terminal current as a function of temperature is the increase in conductivity which tends to reduce the equivalent series resistance of the CC and increase the currents.

Chapter 3: Preliminary Measurements

3.3 Applied Voltage

The following measurements were made using new Shell Diala A transformer oil with bare stainless steel cylinders. The cylinders were utilized as terminals to which both AC and DC voltages were applied, while the CC inner cylinder was turned at a constant rotational rate of 400 RPM.

Figure 3-7 and Figure 3-8 show the effects of applying various AC and DC voltages on the measured charge density. All applied voltages had a peak magnitude of 500 V and all AC voltages were sinusoidal. The application of a positive DC voltage resulted in the largest increase in charge density. Charge densities also increased with AC voltages, but the increase became unnoticeable as the frequency of the applied voltage increased. The negative DC voltage actually reduced the charge density.

The application of voltages to the terminals results in an additional electric field component in the radial direction in the space between cylinders. The geometry of this region forces this additional component to have a larger magnitude at the inner cylinder interface than at the outer cylinder. If it is then assumed that the net double layer charge densities at both interfaces are of the same polarity as the turbulent core charge densities, this behavior is reasonable. The application of a positive DC voltage (resulting in an additional electric field component in the positive radial direction) tends to increase the thickness of the double layer at the inner cylinder and decrease it at the outer cylinder. However, since the inner cylinder has a larger additional electric field component than the outer cylinder, the charge densities are increased. A similar argument can be made for the decrease of the charge densities with negative applied DC voltages, which tends to decrease the inner cylinder's double layer thickness more than the outer cylinder's is increased.

The effects of the AC applied voltages are reasonable if it is assumed that the positive and negative DC voltage effects can be combined into the bipolar sinusoidal waveform. When the sinusoid is in the positive part of the cycle, the inner double layer thickness is increased more than the outer is decreased and the trend is to increase the core charge density. However, during the negative part of the cycle, the inner cylinder double layer thickness is reduced more than the outer cylinder's is increased, which tends

to decrease the core charge density. From the DC measurements, using the same magnitude of voltage, it was observed that the amount by which charge densities are increased for positive voltages is greater than the amount by which they are decreased for negative voltages. If the total AC effect is considered to be a time average of the positive and negative voltage effects of the sinusoid, than an increase in charge density is reasonable as a result of the larger increase contribution from the positive part of the sinusoid. The reduction in the increase of the charge density with increasing frequency also seems reasonable, since the time allowed for the altered double layers to effect the core charge is decreased at higher frequencies.

Chapter 3: Preliminary Measurements

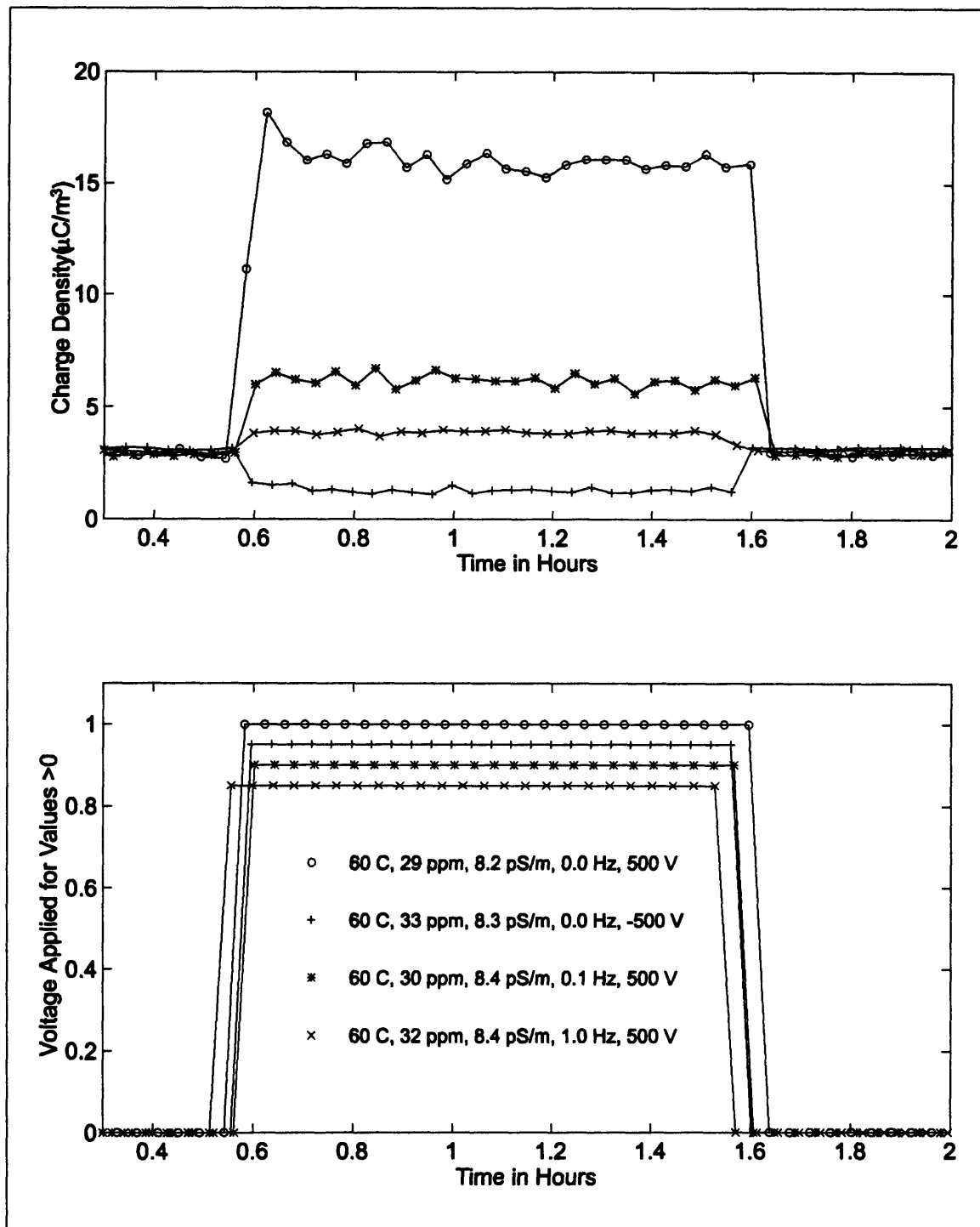


Figure 3-7: Effects of applied AC and DC voltages on measured charged density with CC rotational rate held constant at 400 RPM.

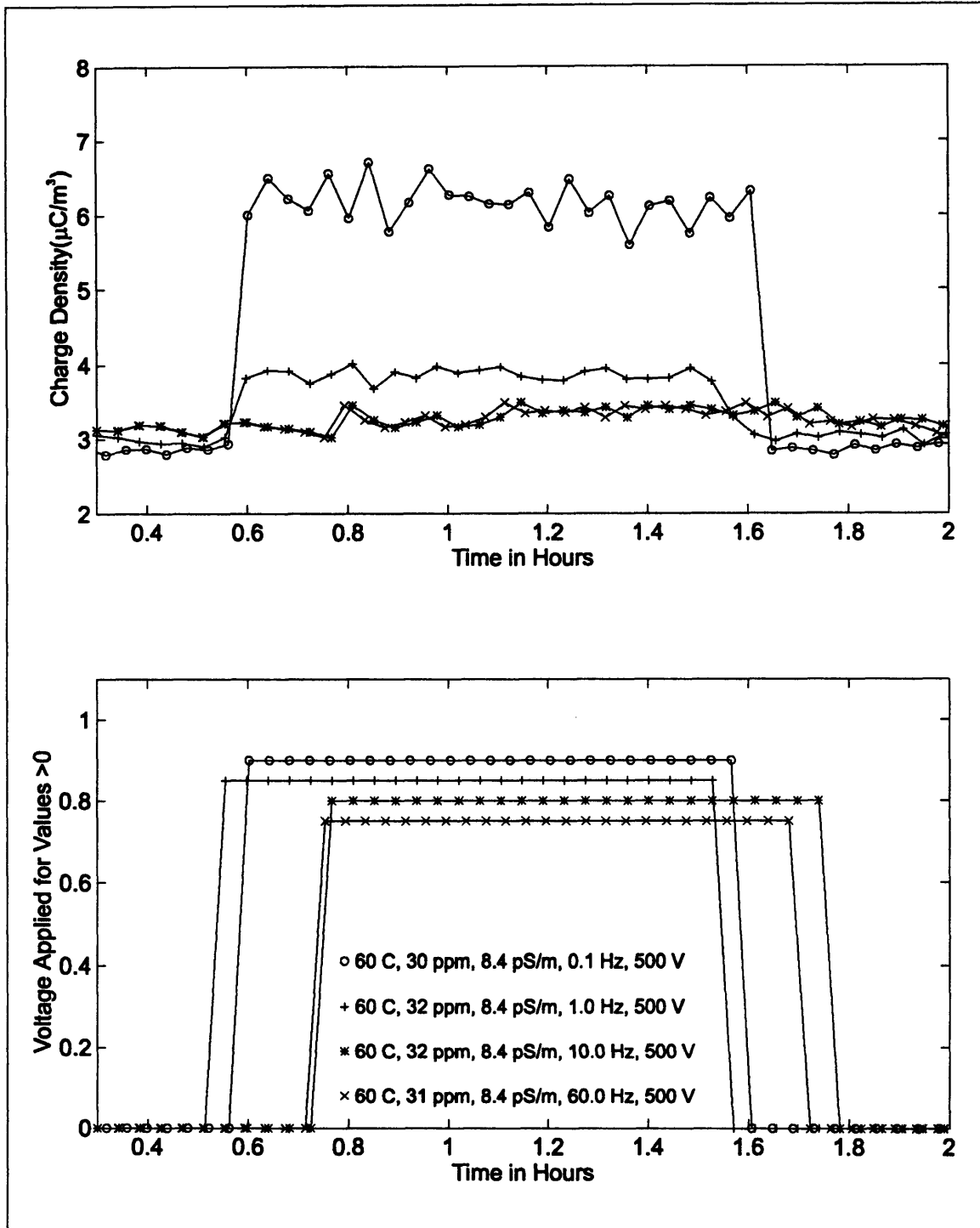


Figure 3-8: Effects of applied AC voltages as a function of frequency on measured charged density with CC rotational rate held constant at 400 RPM.

Chapter 3: Preliminary Measurements

4 Transient Behavior

4.1 Introduction

Most flow electrification experiments made in the Couette Facility concentrated on measuring parameters of the system under steady state conditions. However, many types of transient system responses were also observed. The transients measured were induced in several ways, including: rotation changes, applied voltages, and system cleaning. These responses are interesting because of the time constants associated with them, which tend to be much larger than apparent time constants in the system.

4.2 Initial System Conditioning

The first set of transient measurement were induced by cleaning of the system. Before these measurements were made, the CC was completely disassembled, all oil was removed and all surfaces were cleaned with organic solvents. In the final assembly a layer of oil of the same type with which the CC was to be filled was applied and mostly removed to reduce the potential of surface contamination. Both the CC chamber and the oil with which it was to be filled were vacuum dried for nearly one day. The oil was then loaded into the chamber from the reservoir and the temperature was reduced to 15°C before measurements were started.

Figure 4-1 shows the first set of measurements made on this system. The rotation rate was set to 400 RPM and held constant. However, the terminal voltage and charge density then change over the next several hours. Between 2 and 2.5 hours into the

Chapter 4: Transient Behavior

measurement an abrupt change in both parameters is also noticed. At this point the terminal voltage becomes so negative that the electrometer measuring the voltage saturates at approximately -200 V. Approximately 15 minutes after this change the experiment was stopped along with the rotation. Within several minutes the measurements were restarted as shown in Figure 4-2. The large charge densities and terminal voltages continue for approximately 45 minutes before the measured parameters become relatively stable. These transients are interesting because they have a very long time constant compared to known time constants of the system such as the relaxation time of the oil which is approximately 1 minute or the turbulent development time which is much less than one minute.

The exact cause of these transients is not known, but several hypotheses exist. The two sudden transients in the previous measurements are believed to be caused by sudden changes at each interface. The changes may have resulted from a surface deposition such as an oxide being worn away from the shear stresses created by the fluid. It may also be possible for this layer to be altered by an enhanced reaction due to the fluid mixing or the electrical potentials developed between cylinders when charge becomes entrained in the flow. Another type of surface deposition which may be responsible for this behavior could have resulted from the film of oil used to remove contamination during assembly. When the CC was dried under vacuum for an extended period of time, some of the low molecular weight components may have been removed, leaving a dense film at the interface.

This type of conditioning transient of the system is significant because many transformer failures occur very soon after they are installed or recommissioned after a repair.

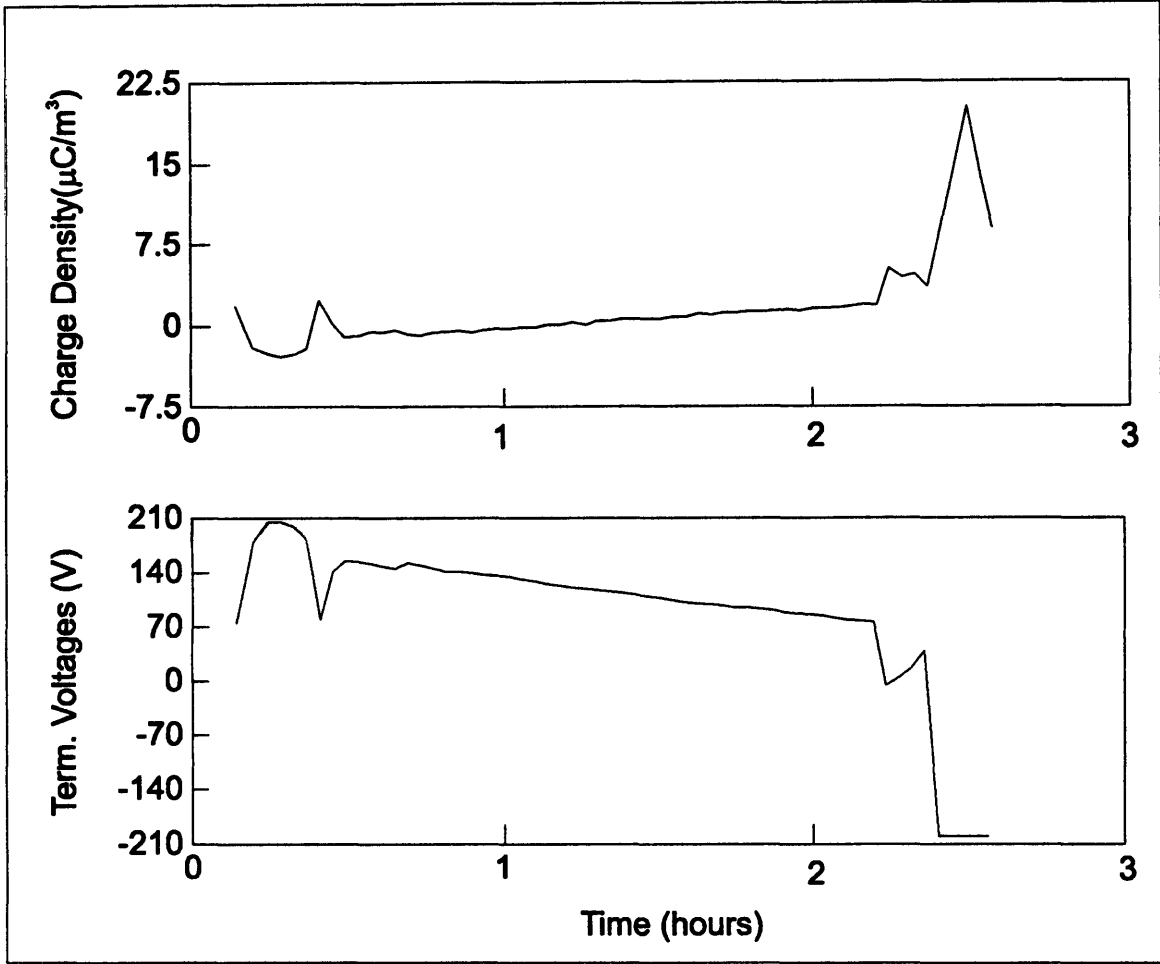


Figure 4-1: Initial conditioning transient observed during first measurements after cleaning and reassembly of the CC. The rotation rate was held at a constant 400 RPM, yet the terminal voltage and charge density continued to change for many hours. The measurements are continued in Figure 4-2.

Chapter 4: Transient Behavior

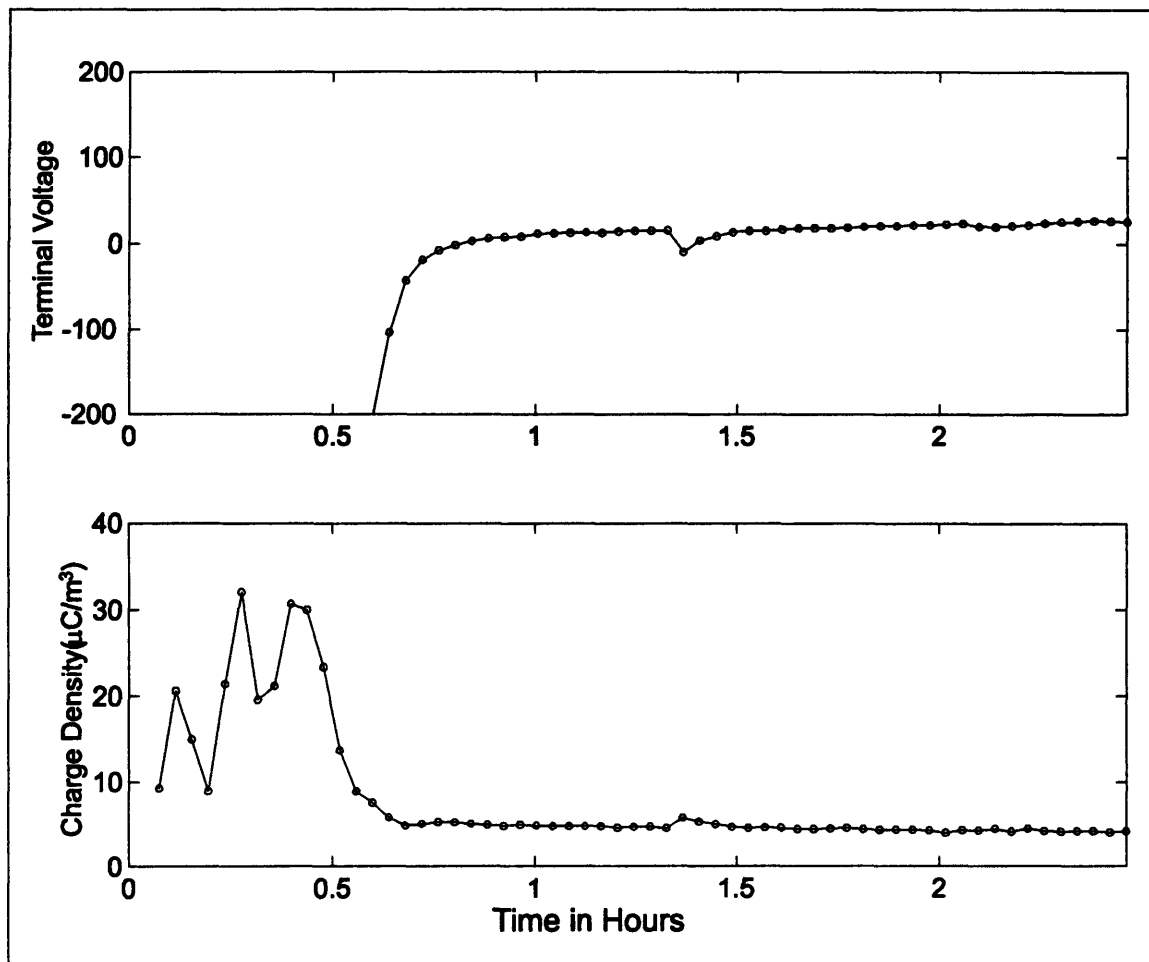


Figure 4-2: Continuation of measurements started in Figure 4-1. Rotation was stopped for several minutes between measurements while data acquisition was reset, but when the rotation was restarted for this measurement, the terminal voltage and charge density basically continued near the ending levels of Figure 4-1. The conditioning transient continues for approximately 45 minutes before the measured parameters reach a stable value.

4.3 Rotation Induced Transients

A second method which resulted in a transient in measured parameters was the stepping of the rotational rate. Figure 4-3 demonstrates the response of the terminal voltage and charge density to a step in the rotation from 100 to 400 RPM. The charge density is increased as a result of the step and shows only a slightly increasing trend over the next several hours. However, the terminal voltage shows a very large transient increase in voltage, which decays to a value lower than the 100 RPM voltage. The time constant of this response is on the order of several hours, which again does not compare to any known time constants of the system. One hypothesis is that during the step in rotation the increased shear stress at the inner cylinder altered the interface. The transient is then due to the recovery of the interface back to a steady state value. A second hypothesis is that the rapid increase in rotation resulted in a momentary reduction in the sublayer thickness as the fluid gained momentum. This reduced sublayer may have allowed additional double layer charge to be removed while the fluid was gaining momentum to reach its new velocity. This charge may have then become trapped possibly due to directional transport rates of charge through the interface.

Figure 4-4 demonstrates additional transients in the terminal voltage due to 100 RPM steps in rotation. The transients are again of longer duration than known time constants of the system.

Figure 4-5 shows transients in the terminal current due to steps of 100 RPM in the rotation rate. In these measurements the data points are several minutes apart and the transients only last for roughly one data point. This is reasonable based on the relaxation time constant of the oil.

Figure 4-6 again shows unexpectedly long transients in the terminal voltage and charge density with stepped rotation. However the transient which resulted from the 700 to 800 RPM step is much larger than other steps in the measurement. The transient in the voltage is also of the opposite polarity compared to the other transients. This indicates a very non-linear step response of the system.

Chapter 4: Transient Behavior

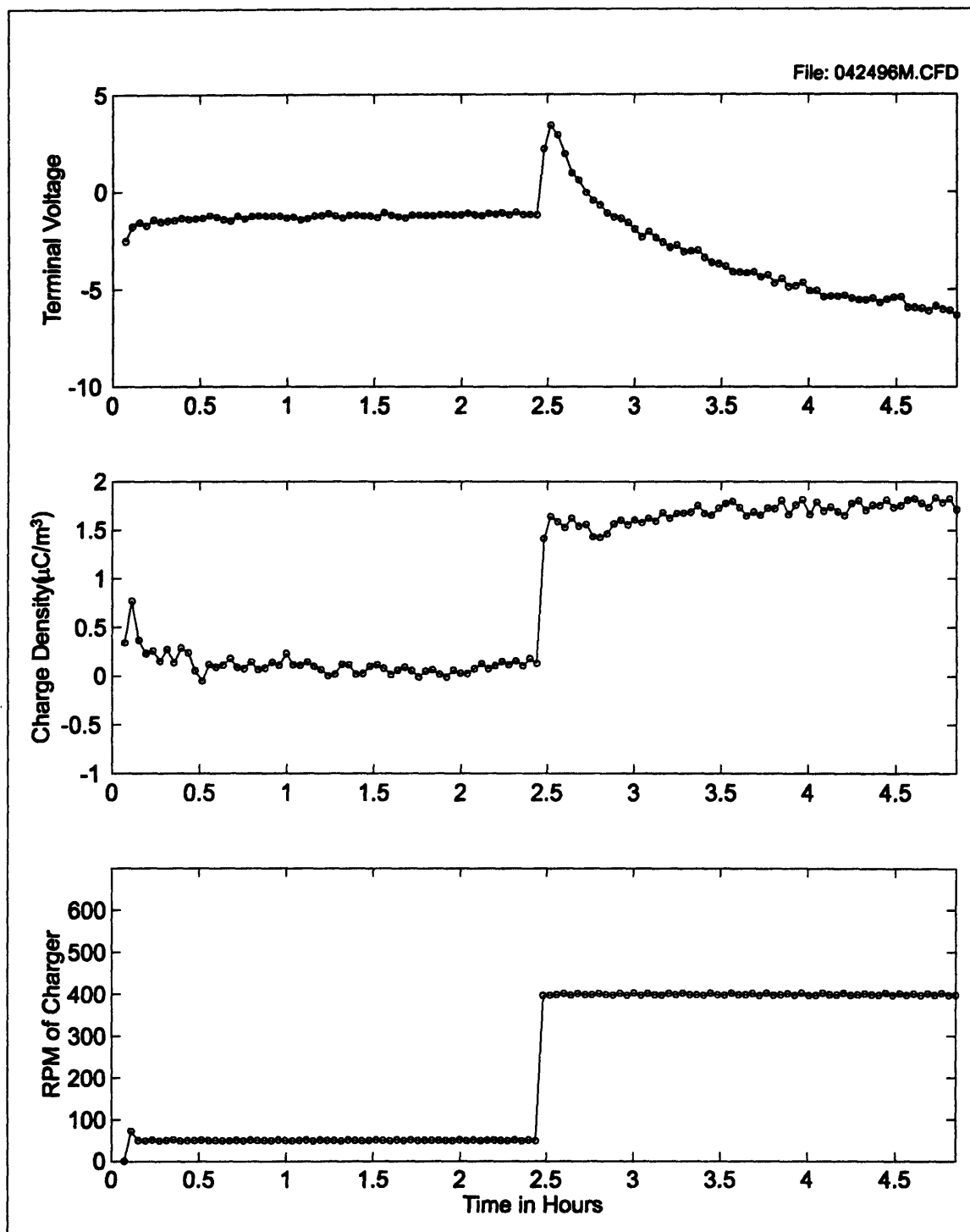


Figure 4-3: Transient induced by a step in the rotational rate. Since the terminal voltage time constant involved is not comparable to known time constants of the system, it is hypothesized that the momentary impulse in the shear stress on the inner cylinder may have altered the interface. A second hypothesis is that the rapid increase in rotation may have momentarily reduced the sublayer thickness allowing additional charge to be

removed from the double layer, reaction rates of charge across the surface may then result in a long time constant.

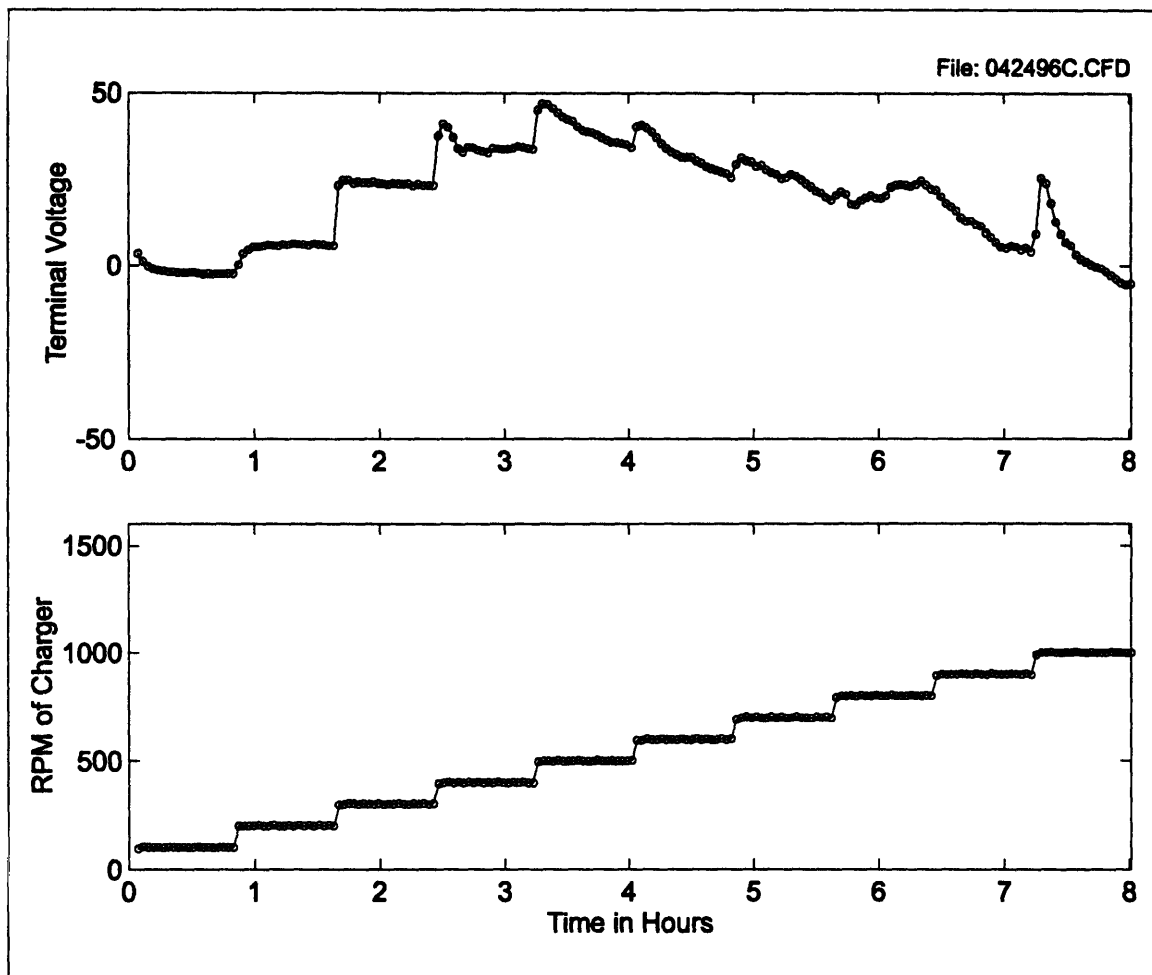


Figure 4-4: Transients observed in the terminal voltage due to steps in the rotational rate. Time constants of the transients are again longer than system time constants.

Chapter 4: Transient Behavior

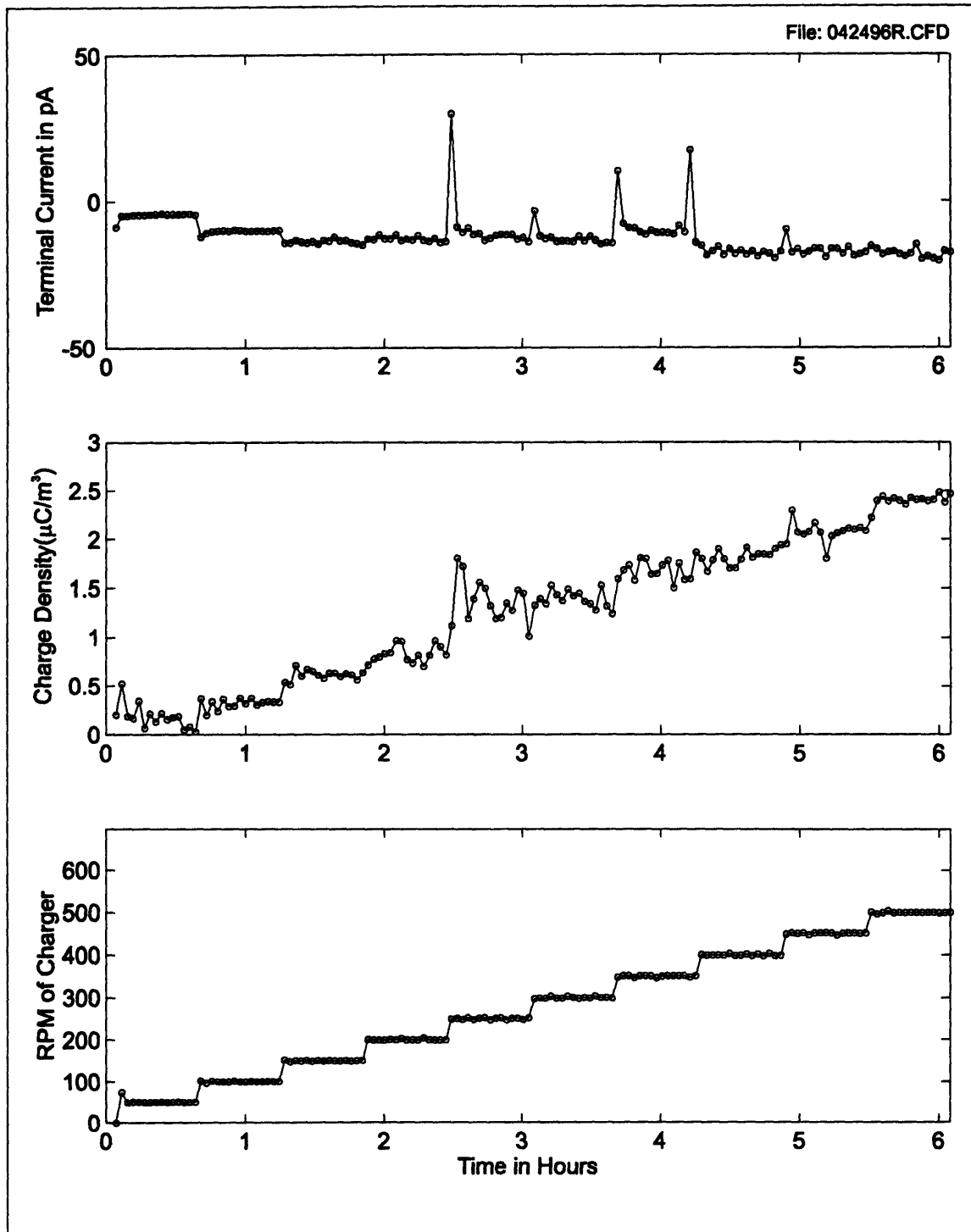


Figure 4-5: Transients observed in the terminal current due to steps in rotation. Time constants of the transients are on the order of the relaxation time of the oil as expected.

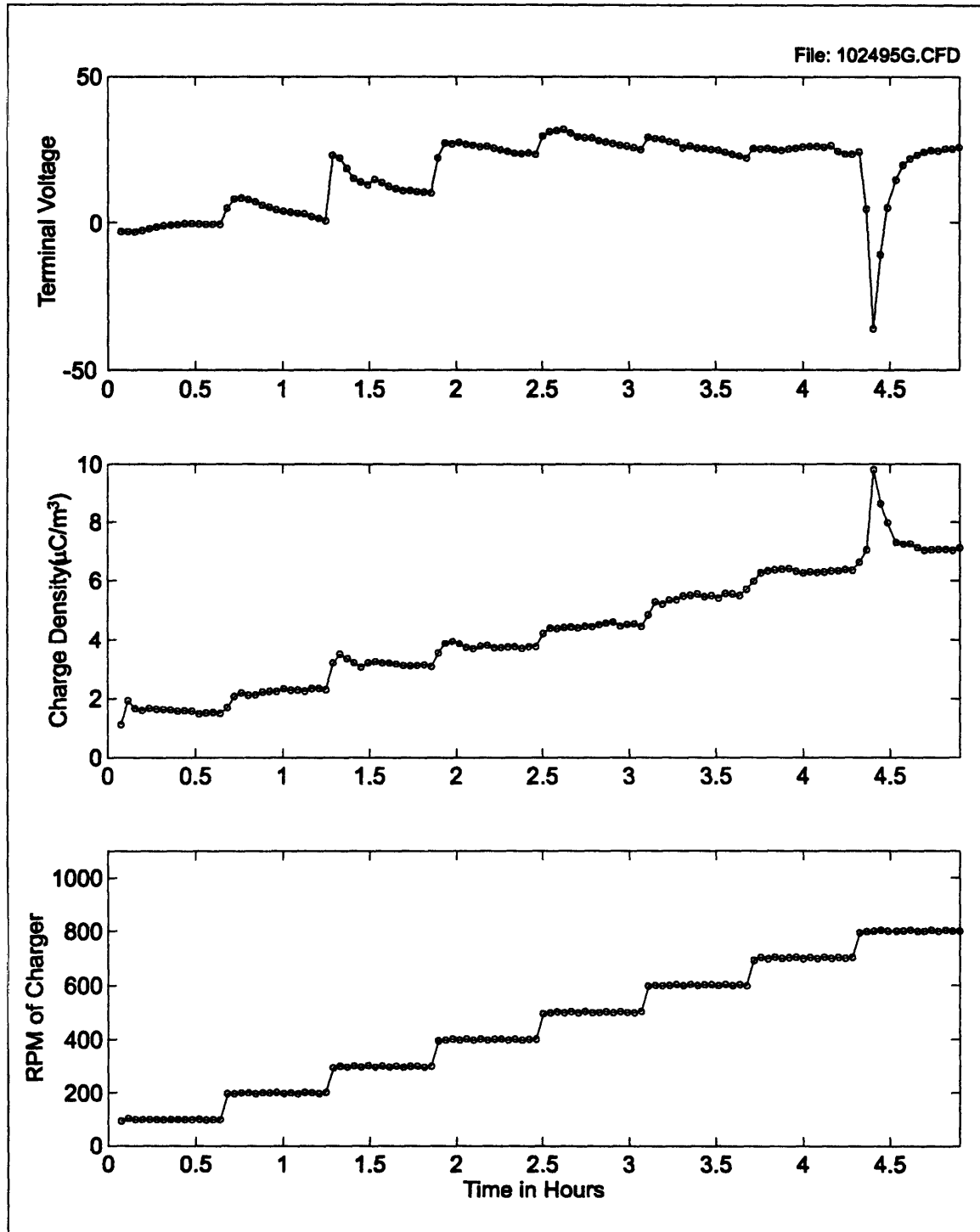


Figure 4-6: Transients in terminal voltage and charge density induced by steps in rotational rate. Notice that each step results in a small transient with relatively long time constant, however the step from 700 to 800 RPM resulted in a rather large negative transient in the terminal voltage and an associated transient in the charge density.

Chapter 4: Transient Behavior

4.4 Voltage Induced Transients

The third type of transient was generated by the application of voltages to the terminals of the CC. Transients due to applied voltages were created using two different methods. In the first method the voltage was applied with no rotation, while in the second method, the voltage was applied during rotation.

Figure 4-7 shows a baseline measurement for comparison with Figure 4-8 which was taken after a voltage was applied with no rotation. The baseline measurement only shows a short initial transient in voltage as the rotation in started. After the completion of the baseline measurement a 500V DC source was applied to the CC terminals for one hour. The voltage source was then disconnected and the system was allowed to relax for nearly ten minutes, which is approximately 60 times the relaxation time of the oil. Measurements were then started at a constant 400 RPM rotation rate as shown in Figure 4-8. When compared to the baseline data, the initial transient in this measurement can be seen to have a much larger time constant. The time constant of this transient is on the order of one hour, which is again much greater than the ten second relaxation time of the oil.

Two hypotheses as to the cause of this behavior have been made. This first hypothesis is that the applied voltage with no rotation results in the growth or removal of an oxide layer at one or both of the interfaces. The start of rotation then tends to restore the interface to its original state with a relatively long time constant. This restoration may be due to shear stresses or enhanced reaction caused by the increased diffusivity near the interfaces. A second hypothesis is that the voltage application may have altered the total charge in the double layer by enhancing the charge transport through the interface. When the voltage was then removed this charge may have then become “trapped” due to slower reverse transport rates resulting in the long transients.

Figure 4-9 and Figure 4-10 contain measurements for the application of voltages to the terminals and monitoring of the relaxation voltage under various rotational conditions. The applied voltage was 180 V DC and was applied for a duration of 10 minutes followed by a monitoring period of the relaxation voltage which lasted for 40 minutes. The first application in the measurements was made with no rotation, the second

application was made with a rotation rate of 400 RPM, the third was made with a rate of 800 RPM, and in the fourth application the rotation was stopped simultaneous to the start of relaxation voltage measurements.

Figure 4-11 compares the measured relaxation voltages under the previously described conditions. The relaxation voltages in these plots have been normalized by subtracting the asymptotic value in time and then dividing by the peak magnitude of the relaxation. The theoretical curve was based on the relaxation time constant of the oil based on its conductivity and dielectric constant.

The comparisons of the relaxation voltages with no rotation and with the rotation stopped show time constants which are near the theoretical. However when comparing the theoretical relaxation with that observed for both 400 and 800 RPM rotation rates, a second longer time constant is evident in the data. The source of this time constant in the system is unknown, but the same hypotheses made for the application of voltages with no rotation still hold.

Chapter 4: Transient Behavior

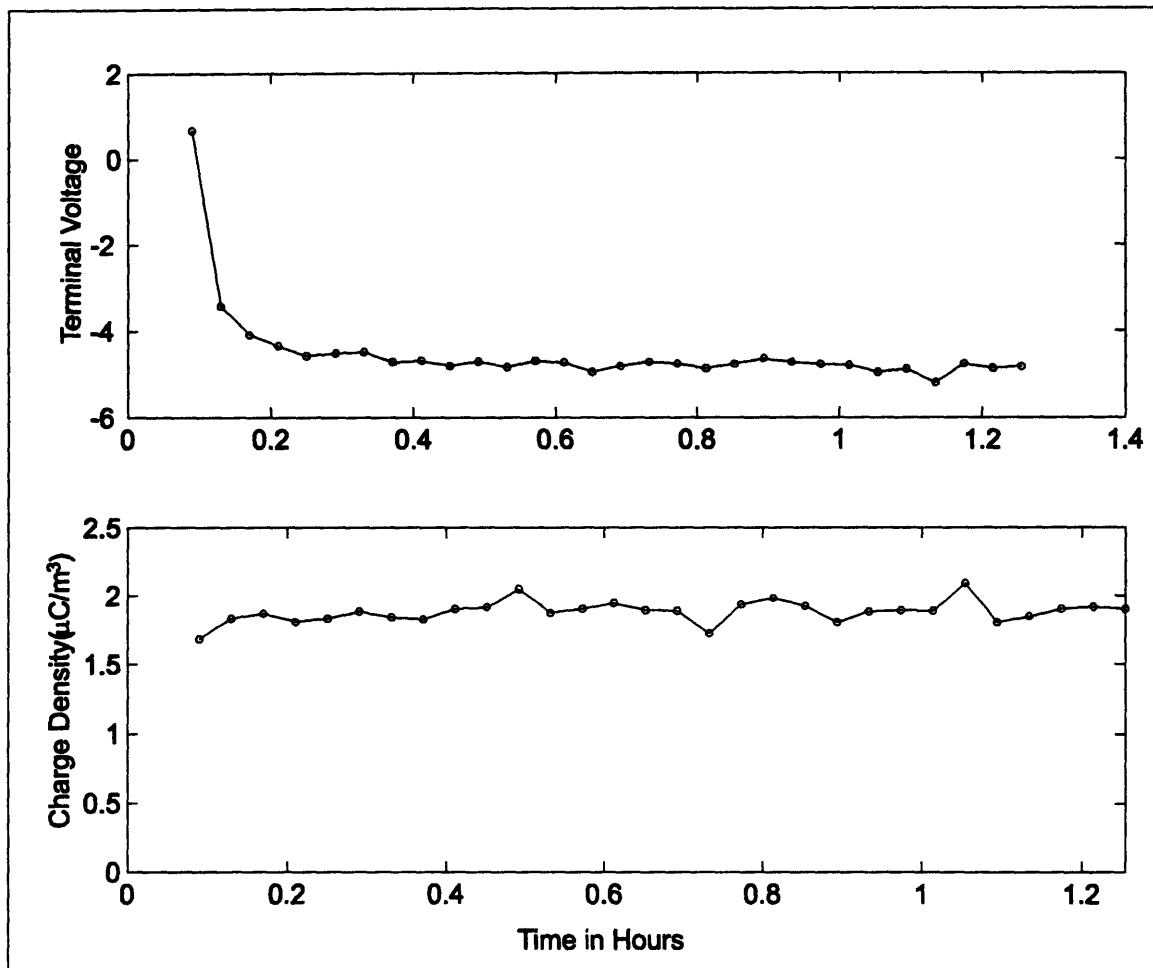


Figure 4-7: Baseline data of terminal voltage and charge density at constant rotation and temperature with no pre-stressing.

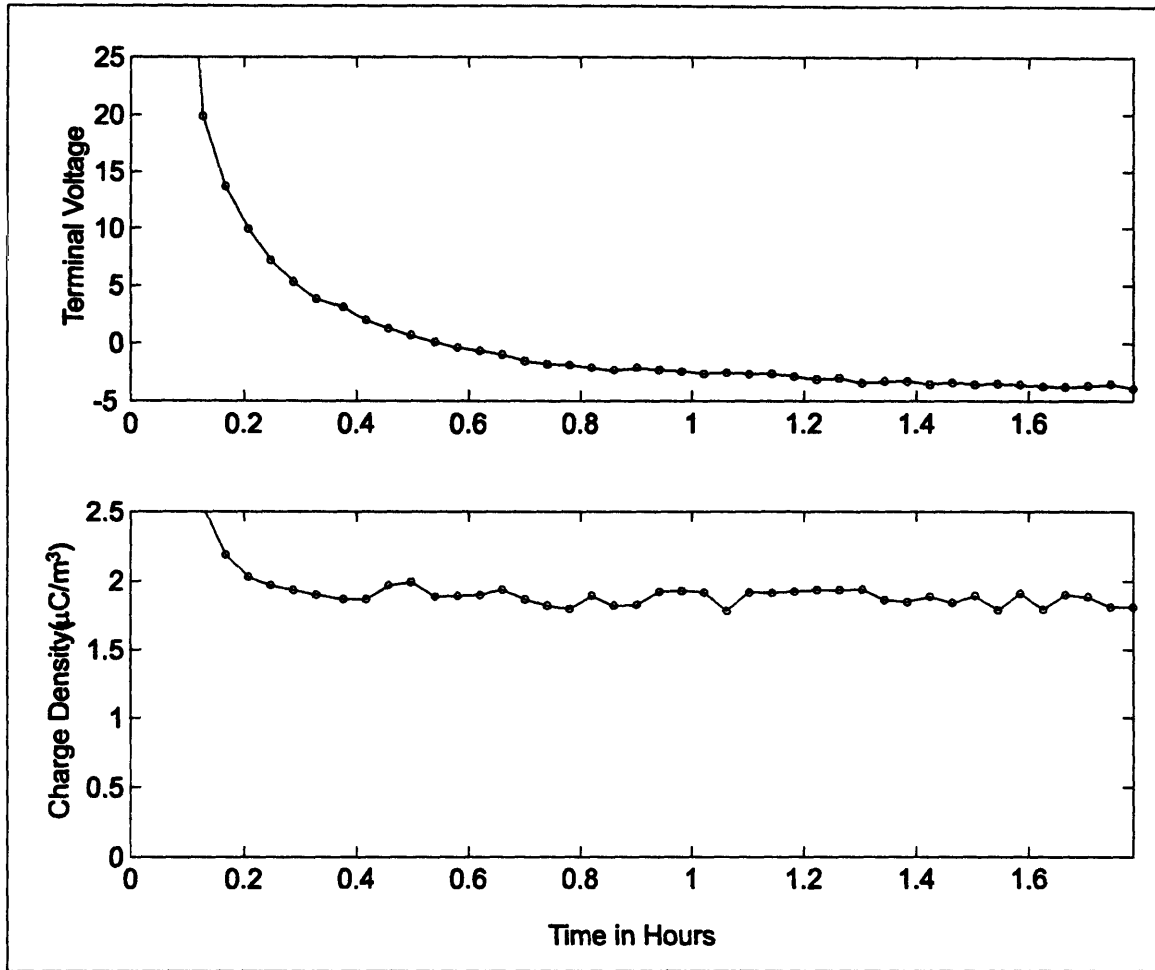


Figure 4-8: Terminal voltage and charge density after pre-stressing with a DC voltage. Before these measurements were started, 500 V was applied between terminals for one hour. The applied voltage was then disconnected and the charger was allowed to relax for ten minutes, which is nearly 600 times longer than the oil relaxation time. However when rotation is started a transient with a relatively long time constant is observed

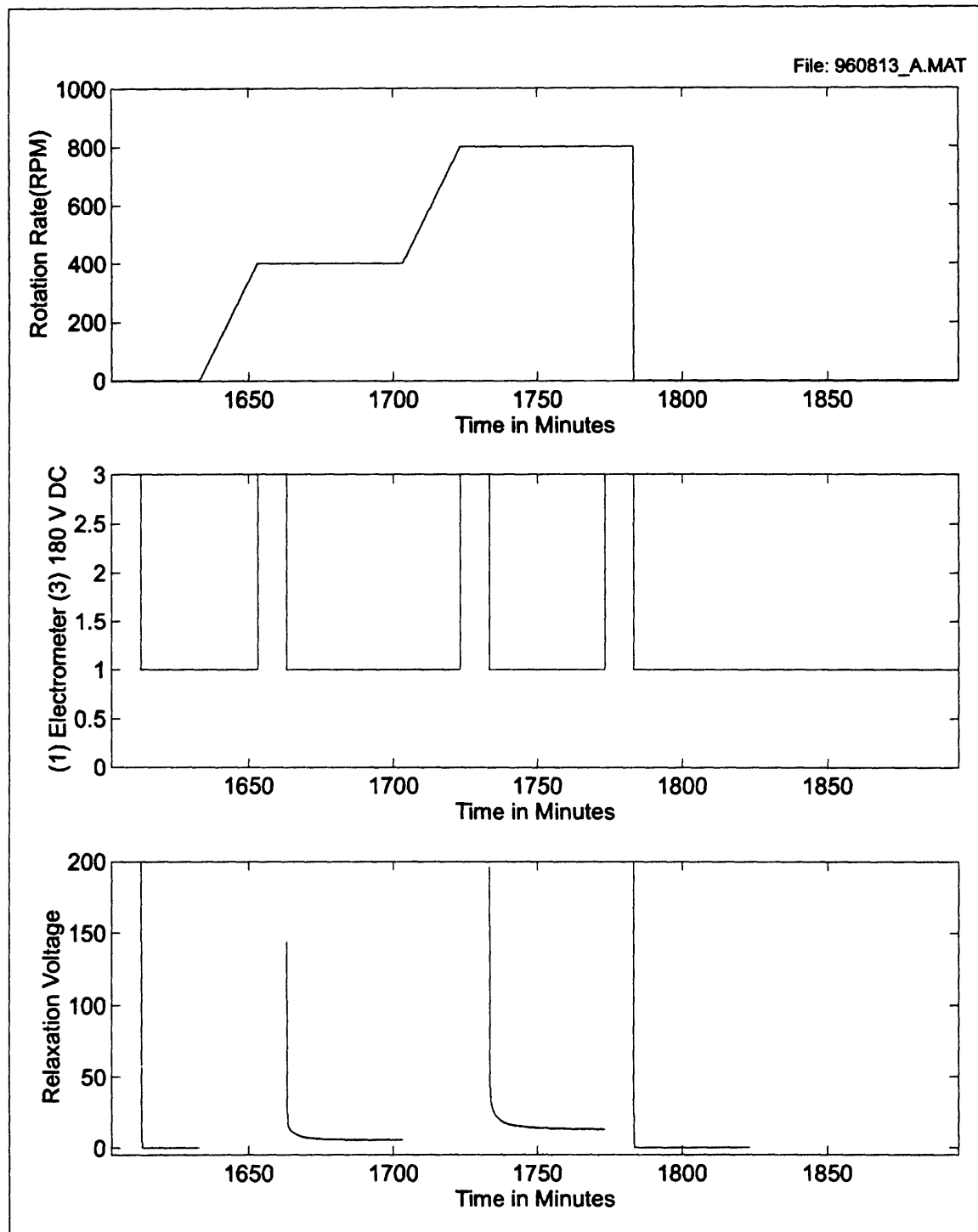


Figure 4-9: Measurements showing the relaxation of an applied terminal voltage of 180V for ten minutes. The application and relaxation was repeated four times in the measurement. The first was with no rotation, the second was with 400 RPM rotation, the third was with 800 RPM rotation, and in the fourth measurement the rotation was simultaneously stopped as the applied voltage was removed.

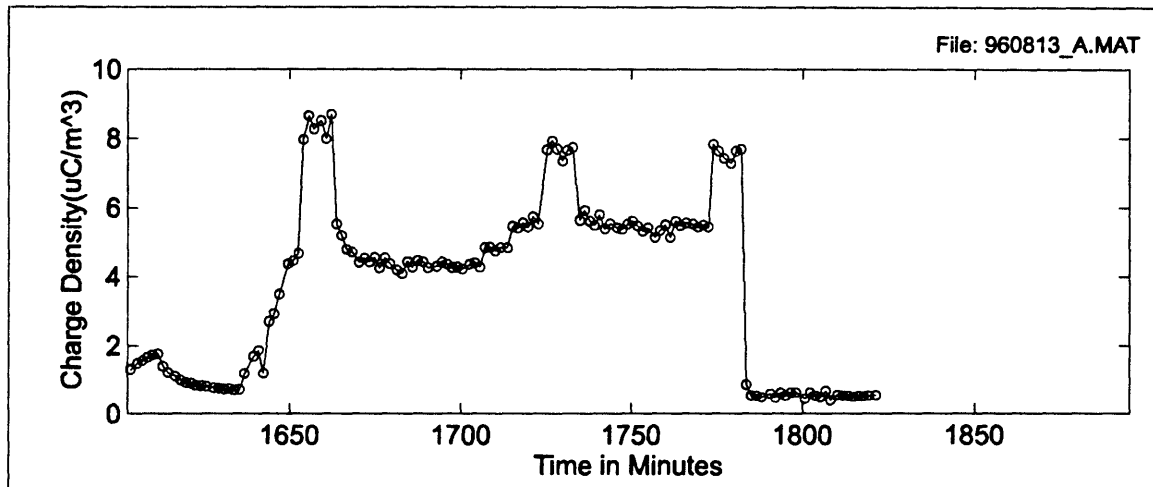


Figure 4-10: Charge densities during the application and relaxation of the terminal voltages in Figure 4-9.

Chapter 4: Transient Behavior

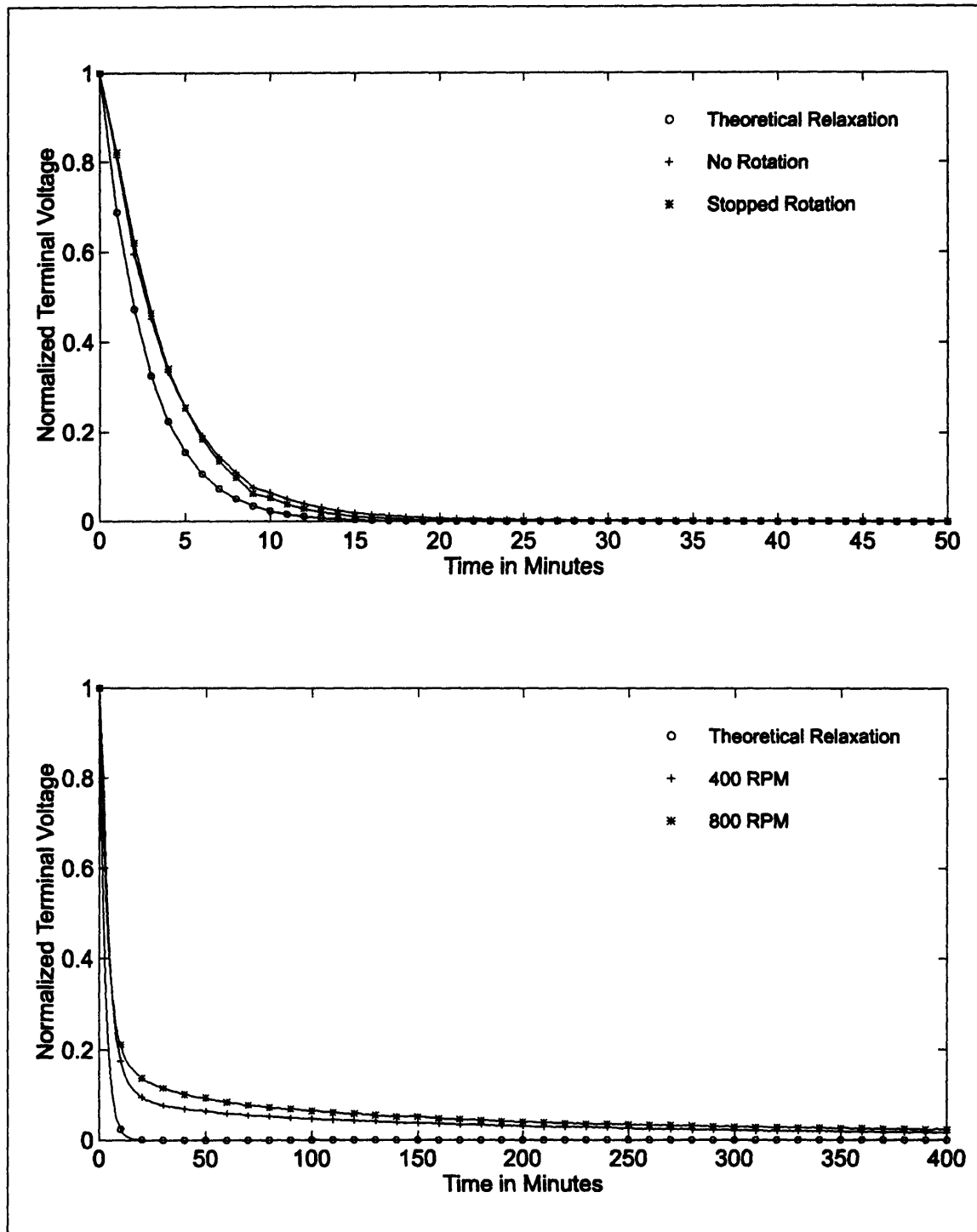


Figure 4-11: Comparison of terminal voltages under the four conditions of the measurement shown in Figure 4-9. The terminal voltages have been normalized by removing their final value and dividing by their peak magnitude. The terminal voltage with no rotation and with the rotation stopped match the decay based on only relaxation, while the decays with rotation contain a second longer time constant.

5 Fresh Oil Measurements

5.1 Introduction

In order to observe the differences and/or similarities in the electrification characteristics between new and aged oils, several measurements were made using fresh Shell Diala A transformer oil. These measurements were conducted with the inner and outer cylinders of the Couette charger left as bare stainless steel. The measurements include terminal parameters and charge densities at varied temperature and rotation with and without BTA added. The measurements can also be used to check the reproducibility of the characteristics for fresh oil based on several preliminary measurements.

5.2 Baseline Measurements

The first set of measurements were taken without BTA and consist of measurements of the terminal parameters as functions of rotation and temperature.

Figure 5-1 shows the measured voltage and charge densities for the open circuit terminal configuration at varied rotation and temperature. Here the terminal voltages tend to increase in magnitude with increasing rotation and also become more positive with increasing temperature. In comparison, the preliminary measurements (chapter 3) of the fresh oil also demonstrated a general increase in magnitude with rotation, however the voltages became more negative with increasing temperature. The charge densities in Figure 5-1 increased with rotation, but showed a decrease with increasing temperature until the 60°C measurement where the charge densities increase again. This behavior is very similar to the preliminary measurement's. The main difference is in the actual

Chapter 5: Fresh Oil Measurements

magnitude of the charge densities which vary by up to a factor of 2.5 times, potentially due to the differing conductivity of the oil.

Figure 5-2 shows the currents and charge density for the short circuit terminal conditions. The terminal currents are relatively small at the low temperatures and increase in magnitude with increasing temperature. The terminal currents also tend to become increasingly negative with increased rotation rate, which is similar to the behavior in the preliminary measurements. The actual magnitudes of currents between this and the preliminary measurement agree best at 60°C. The charge density behavior is comparable to the measurements during open circuit terminal conditions and also compares to preliminary measurements as the open circuit charge density did.

From these measurements some of the difficulties with comparisons between measurements, even with oils taken from the same oil drum, become obvious. The charge densities were most consistent in behavior but still showed variations in actual magnitude, which may be the result of differences in oil conductivity and moisture, along with changes in the interfaces between measurements due to cleaning, oxidation, etc. The terminal currents had some similarities, but matched best at 60°C. However the change in terminal voltage with temperature was actually the opposite between the fresh oil measurements and preliminary measurements.

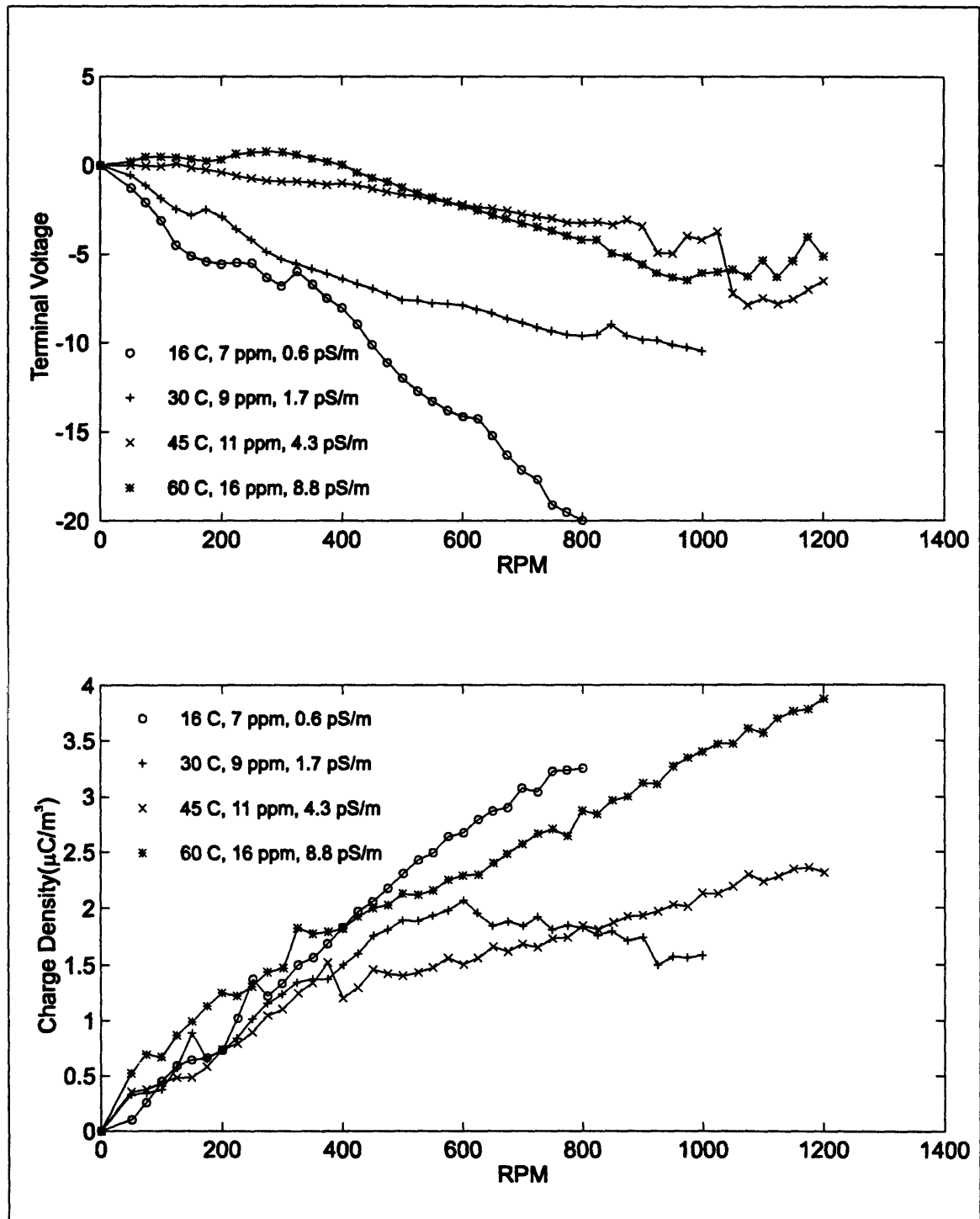


Figure 5-1: Dependence of terminal voltage and charge density on rotation and temperature for fresh Shell Diala A oil. Measurements were made using stepped rotation, values of terminal voltage and charge density were then averaged over each step.

Chapter 5: Fresh Oil Measurements

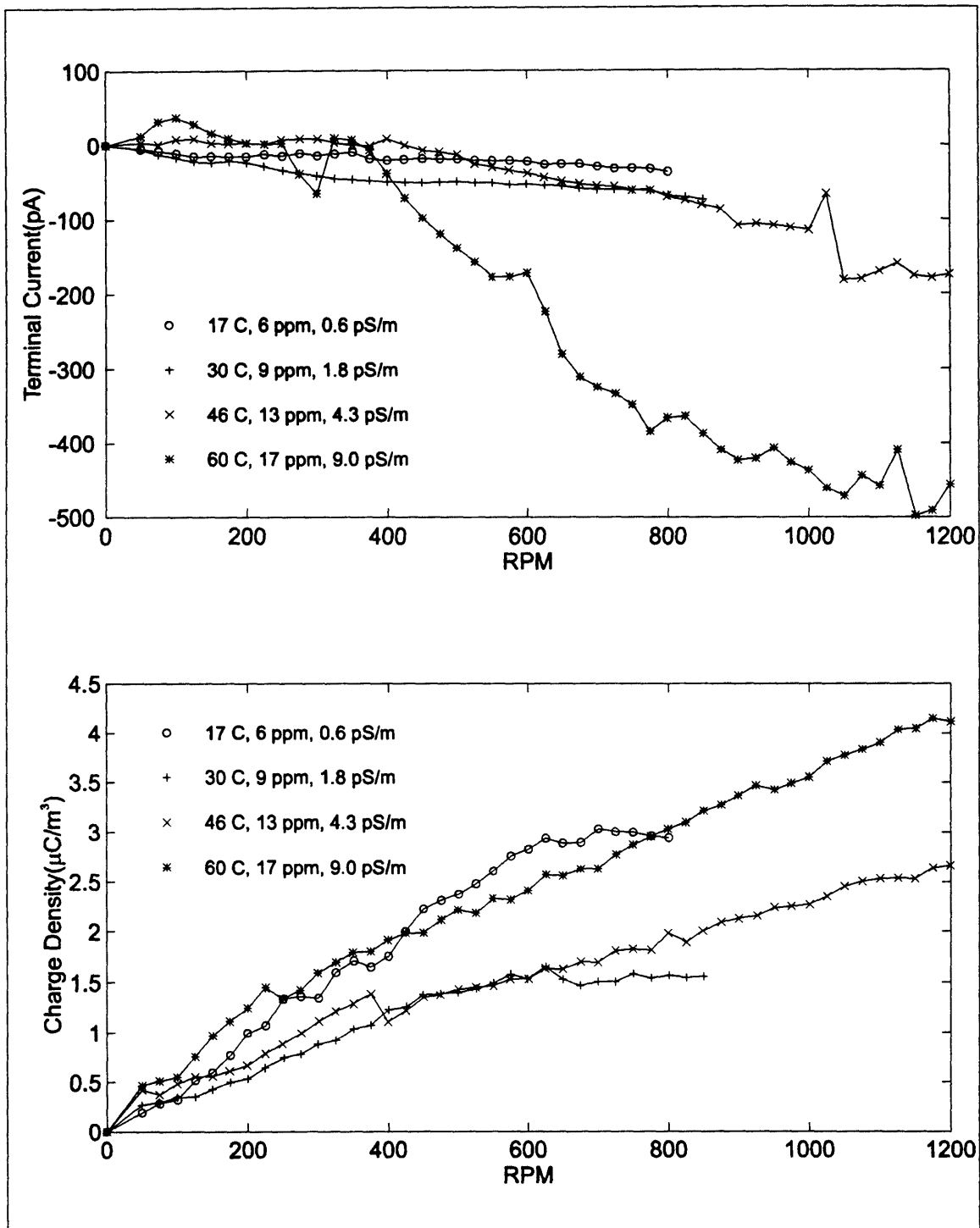


Figure 5-2: Dependence of terminal current and charge density on rotation and temperature for new Shell Diala A oil.

5.3 Addition of BTA

The next set of measurements demonstrate the effects of the addition of BTA to fresh Shell Diala A transformer oil. The additions were made in 5 ppm increments with the inner and outer stainless steel cylinders of the Couette charger left bare and the oil was at a temperature of 60°C. The BTA was added as a concentrate in oil through an injection port as described in Appendix A.

Figure 5-3 shows the first injection to bring the BTA concentration from 0 ppm to 5 ppm. The injection was made 1 hr. into the measurement and an immediate decrease in both the magnitude of the terminal current and the charge density is observed. The terminal current decreased by roughly 65%, while the charge density was reduced by roughly 75%. However the terminal current and charge density are then observed to increase again over time, reaching values between the preinjection values and values immediately following the injection. Also, the conductivity was observed to decrease over time following the injection, which has also been observed in [6].

Figure 5-4 contains the measurements for the second injection of BTA to bring the oil concentration from 5 ppm to 10 ppm. The magnitude of the terminal current and charge density again demonstrate an immediate decrease, but this time by only about 25%. The conductivity also dropped rather quickly at the time of injection and continued to decrease over the next several hours. As with the first injection, the terminal current and charge density again increased over time to values less than those measured before the second injection.

The third injection of BTA to raise the concentration from 10 ppm to 15 ppm is shown in Figure 5-5. The injection occurred approximately 1.75 hr. into the measurement and again immediate decreases in terminal current, charge density, and conductivity are observed. The decrease in terminal current was initially 70%, but the magnitude of the current increased rapidly over the next 15 minutes to roughly 20% of its preinjection value. The charge densities were reduced by about 20% after the injection. Both charge density and terminal current increased over the next several hours to values near the

Chapter 5: Fresh Oil Measurements

preinjection values. The conductivity, as in the two previous injections, also decreased in the several hours following the injection.

Figure 5-6 demonstrates two other effects related to flow electrification and the resulting change caused by the addition of BTA. In the figure, the offsets for both the conductivity cell and Absolute Charge Sensor are shown for each injection. The conductivity cell offset voltage is representative of the integral of the charge removed by the moving oil from the plates of the conductivity cell, which is constructed from an air capacitor. The ACS offset current represents several offset quantities in the charge measurement, but most importantly contains a component which is due to the streaming current from the charge sensor's probe tip. The cell offset voltage clearly demonstrates a reduction in the flow electrification on the conductivity cell with each injection of BTA. It is also observed, as in the charge densities and terminal currents, that the effects of each injection were reduced over time, and each successive injection resulted in a smaller offset over the 0 to 15 ppm range. The streaming current from the ACS probe showed an immediate reduction after the first injection, but also increases again with time. Further injections do not show a noticeable change in the streaming current off the probe tip.

Comparisons of the terminal current and charge density as functions of rotation and BTA concentration at 60°C are made in Figure 5-7. The general trend for the terminal current is a reduction in magnitude with increasing concentration at most rotation rates, however the 0 ppm curve does not fall at a larger current magnitude than the 5 ppm curve for rates less than 600 RPM. This is potentially due to the fact that these two measurements had the largest successive time spacing, allowing possible variation in the system. The charge densities also shown in the figure demonstrate a very smooth reduction with increasing concentration for all rotation rates above 300 RPMs.

The dependence of the oil's conductivity on BTA concentration is shown in Figure 5-8. The data points represent the conductivity of the oil many hours after the actual addition of BTA. The conductivity was not immediately measured after the BTA additions because the total conductivity reduction required many hours. The final concentration of 15 ppm BTA reduced the oil's conductivity by approximately 33%.

The reduction of the charge density and conductivity is interesting because normally one would expect an increase in relaxation time resulting from the decreased conductivity to allow the accumulation of larger charge densities. Since the charge densities still decreased, the double layer charge may have also been reduced such that the net effect was still a reduction in charge density.

Chapter 5: Fresh Oil Measurements

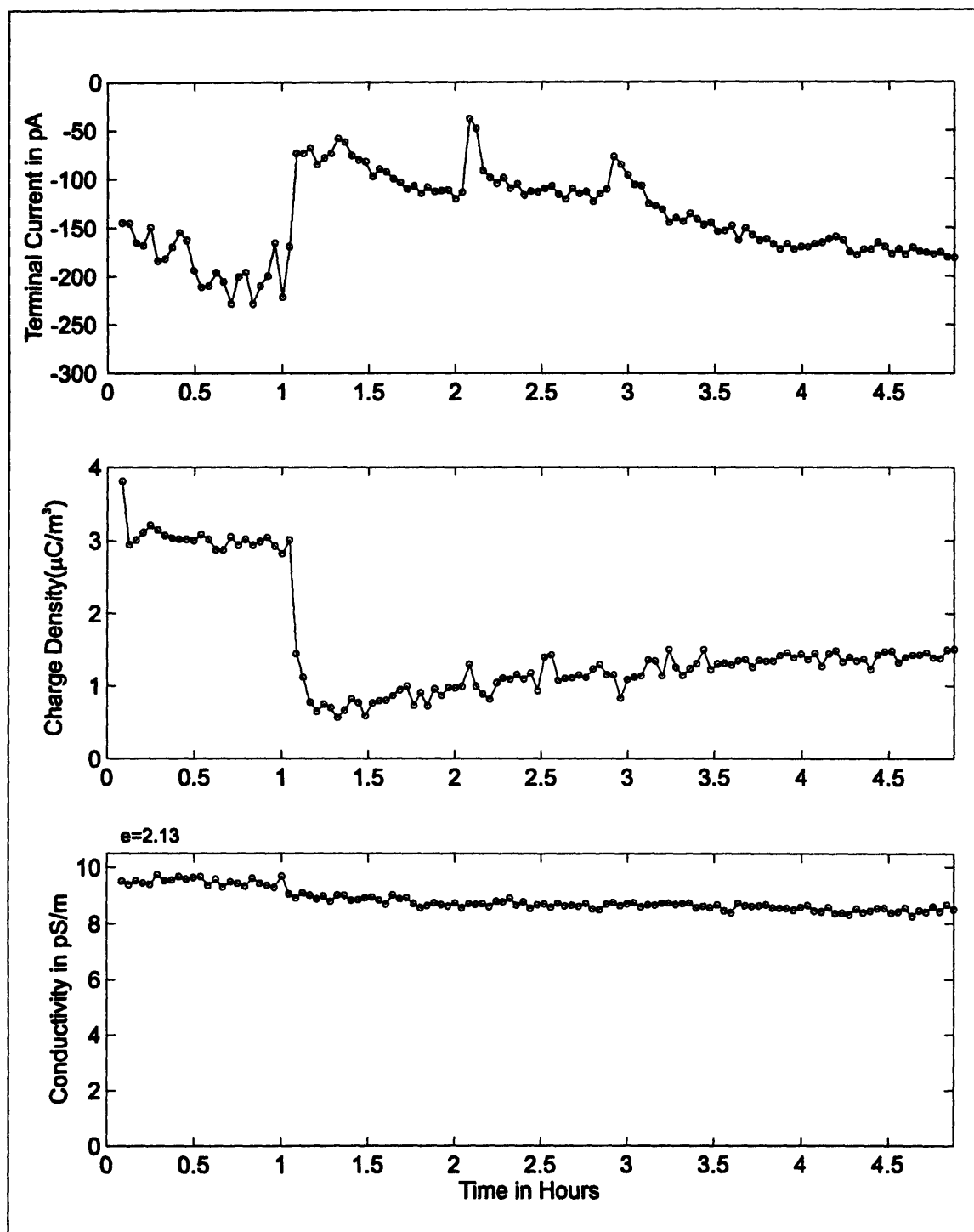


Figure 5-3: Addition of BTA at 1 hour into the measurement to raise the oil concentration from 0 ppm to 5 ppm.

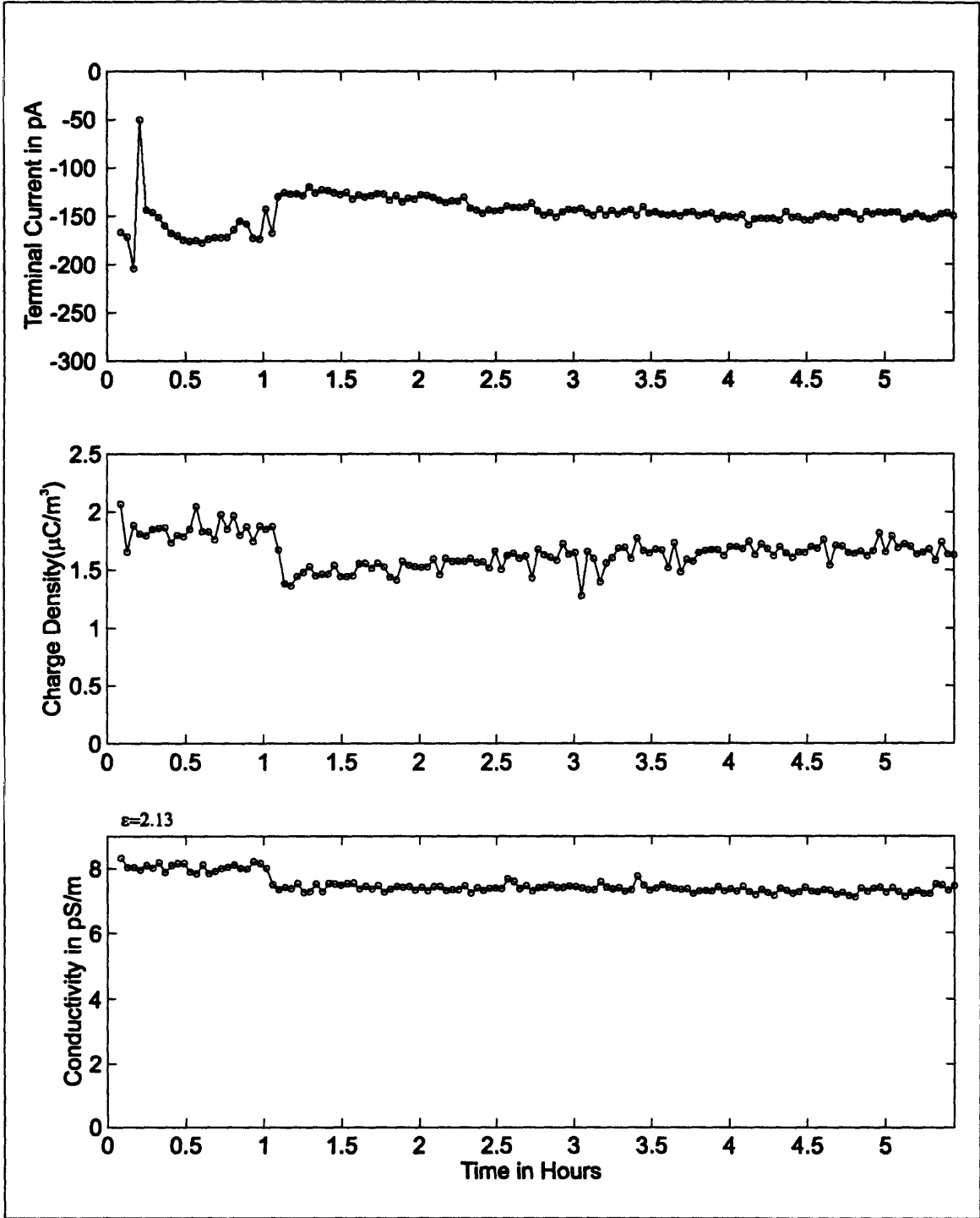


Figure 5-4: Addition of BTA at 1 hour into the measurement to raise the oil concentration from 5 ppm to 10 ppm.

Chapter 5: Fresh Oil Measurements

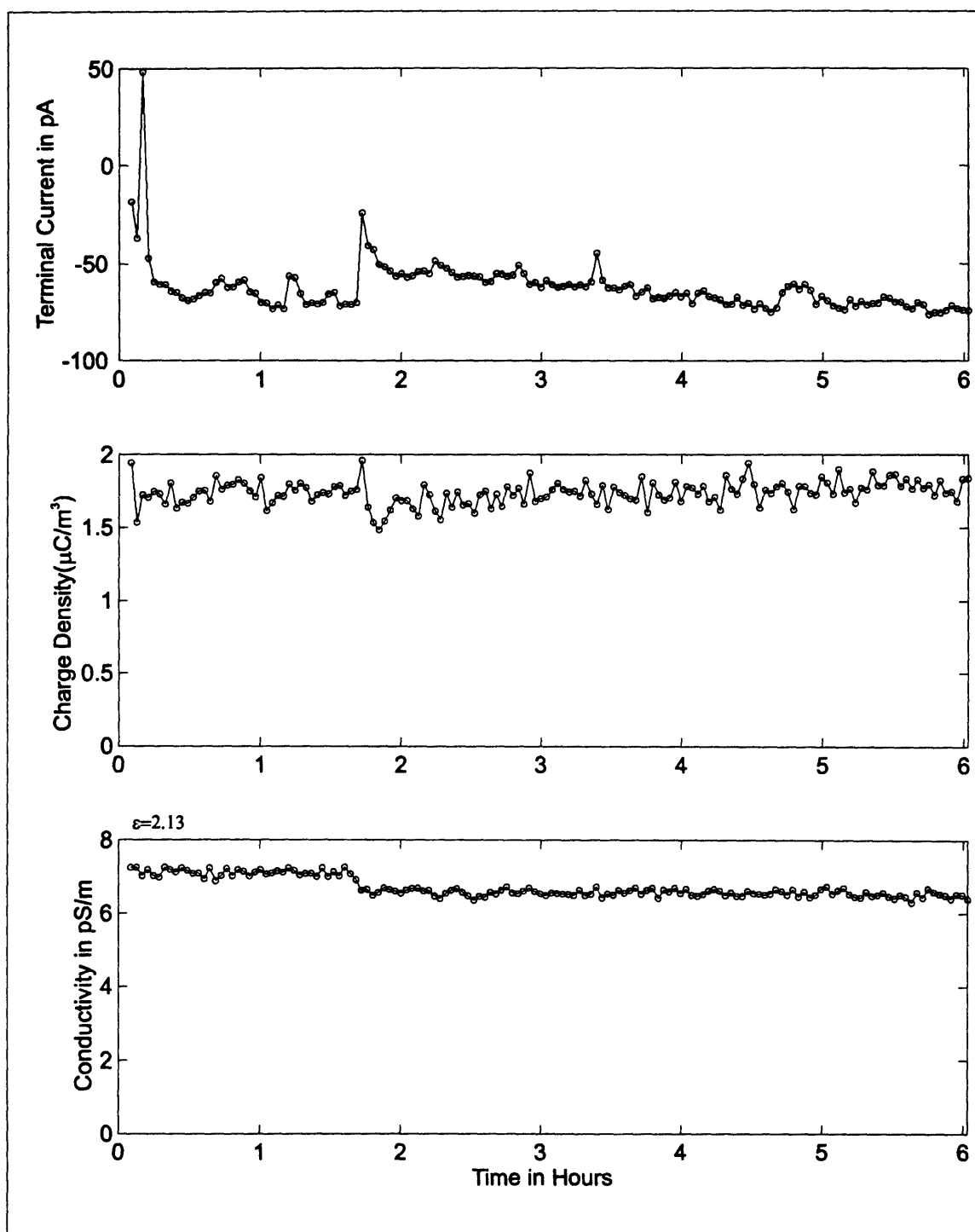


Figure 5-5: Addition of BTA at 1.75 hours into the measurement to raise the oil concentration from 10 ppm to 15 ppm.

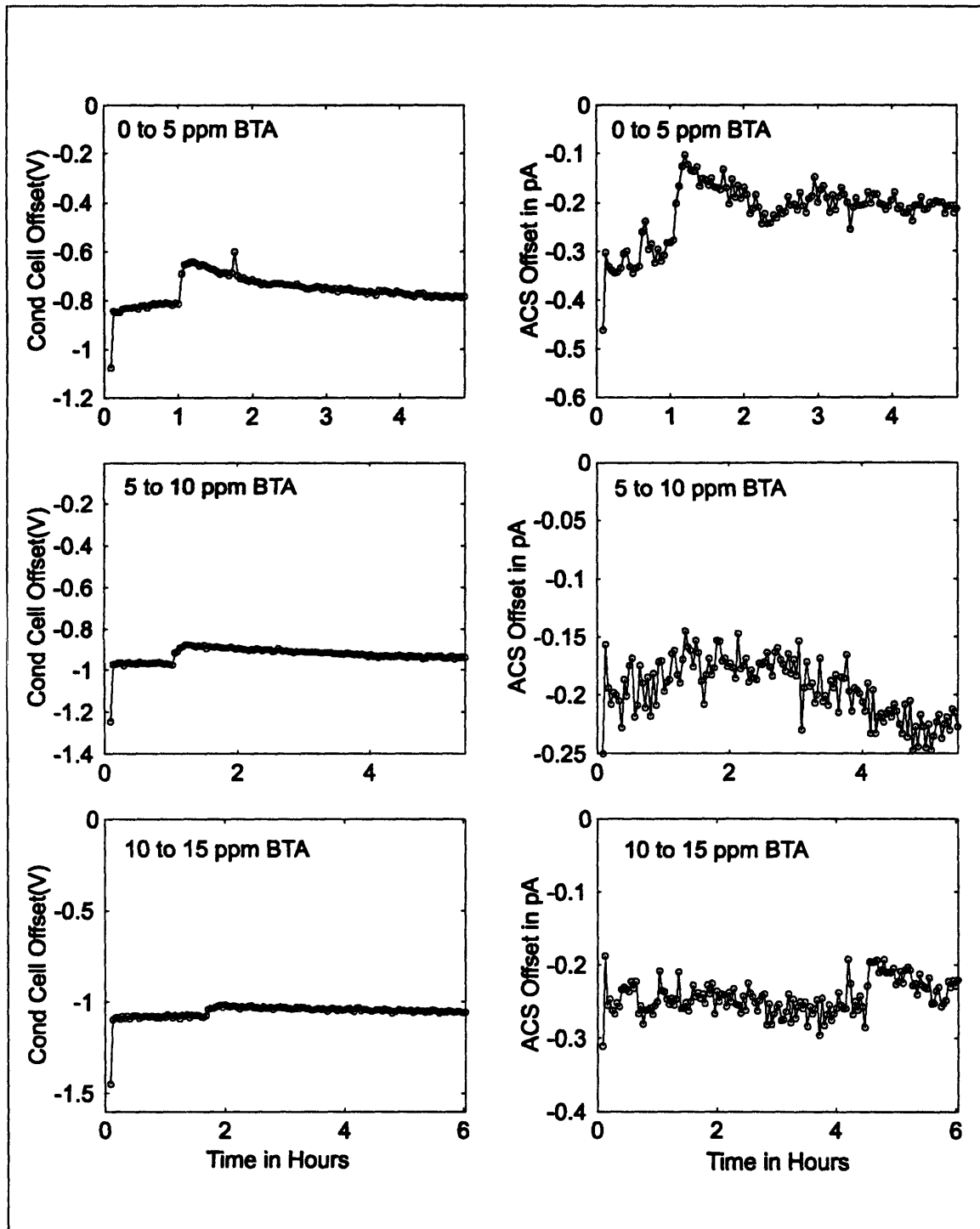


Figure 5-6: Effects of BTA addition on conductivity cell offset voltage and streaming current from the tip of the absolute charge sensor for each BTA addition.

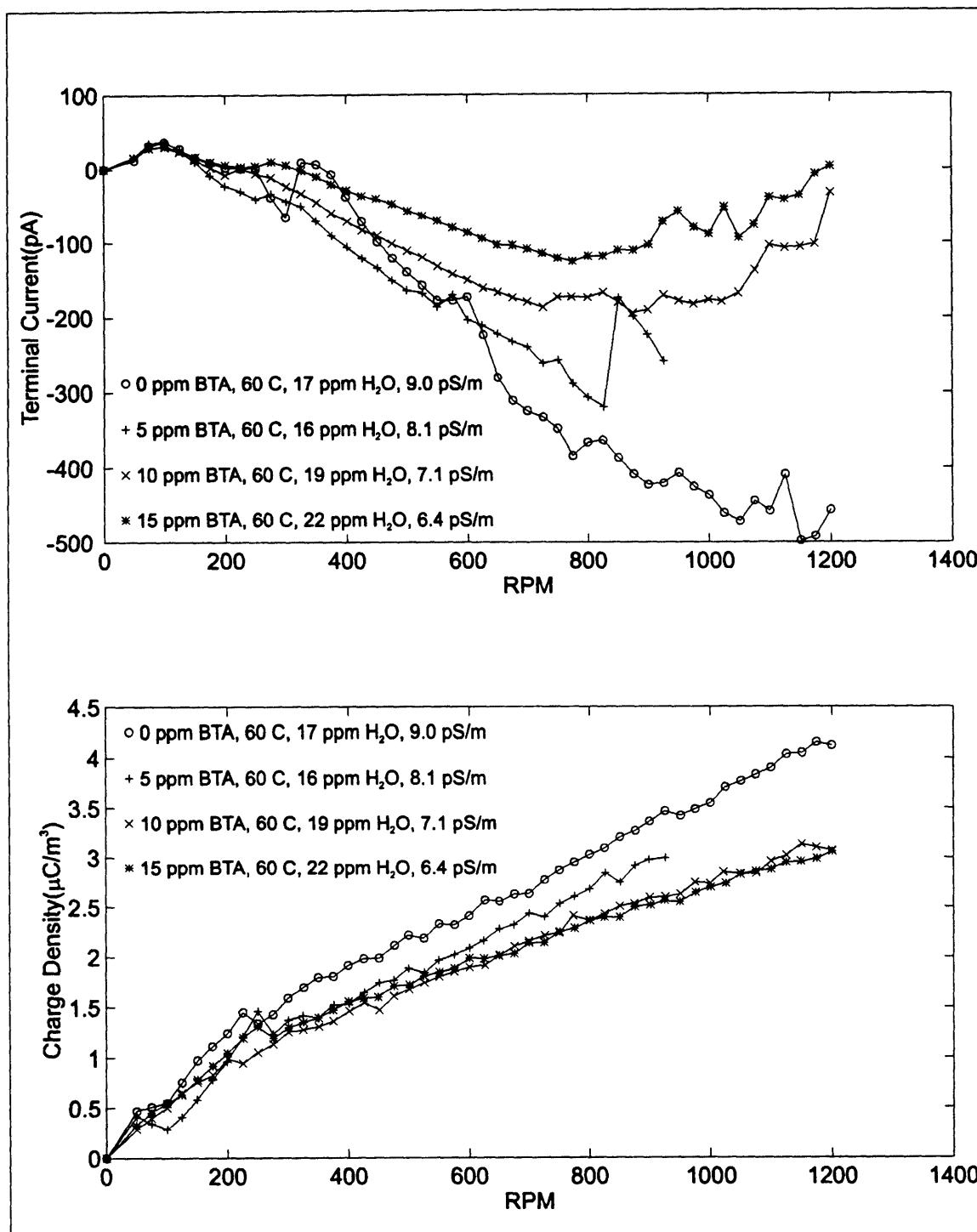


Figure 5-7: Effects of BTA on terminal current and charge density as a function of concentration and rotational rate.

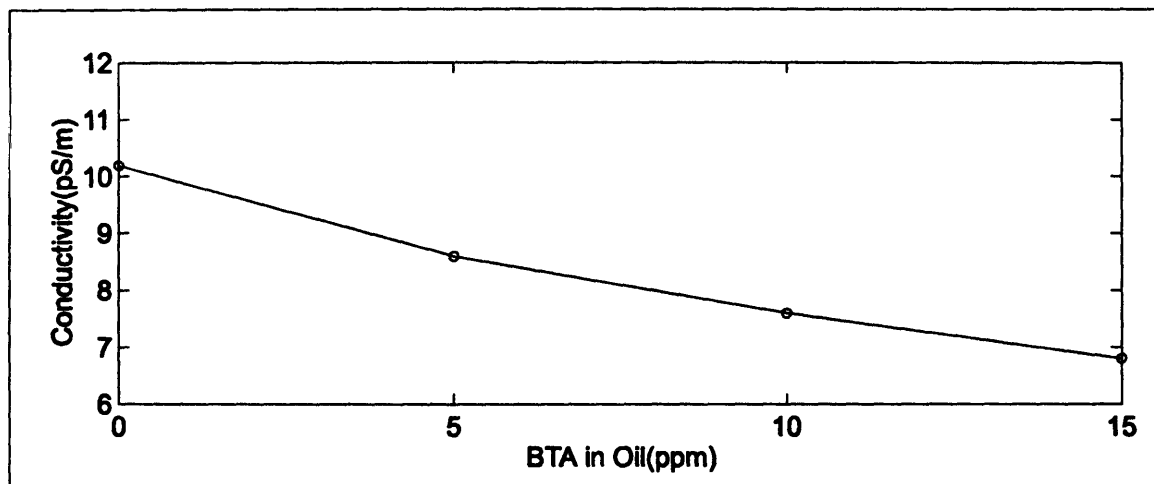


Figure 5-8: Effects of BTA on oil conductivity as a function of concentration.

Chapter 5: Fresh Oil Measurements

6 Aged Oil Measurements

6.1 Introduction

This chapter contains many measurements made on oil which was removed from a transformer that was in service at Texas Utilities. The measurements include temperature, rotational rate, applied AC, and applied DC dependencies of measured parameters including charge density and terminal voltages/currents, where appropriate. The measurements are then repeated with 15 ppm of BTA added and the measurements are compared to the 0 ppm values. Applicable measurements are then compared to measurements with the fresh Shell Diala A oil

6.2 Oil Drying

Before measurements with the used oil were started, it was first dried. The drying process is shown in Figure 6-1. The process was carried out in the reservoir where the moisture content and dielectric properties were measured. The charger was empty at this point and the moisture and conductivity in the figure also reflect this fact. The drying of the oil was accomplished by pulling a vacuum on the reservoir. The vacuum was started at 60 min. into the measurement and continued for approximately 80 min. until the rate of moisture removal slowed.

Figure 6-2 shows both the oil's conductivity dependence on moisture and the dielectric properties before and after the drying process as a function of frequency. From the top plot in the figure, the oil's conductivity appears to be nearly independent of moisture. The middle plot of the dielectric constant also shows virtually no change before

Chapter 6: Aged Oil Measurements

and after drying. The bottom plot of conductivity does however show a small change but this change could very easily be due to variations in temperature, since the reservoir oil is not actively being mixed.

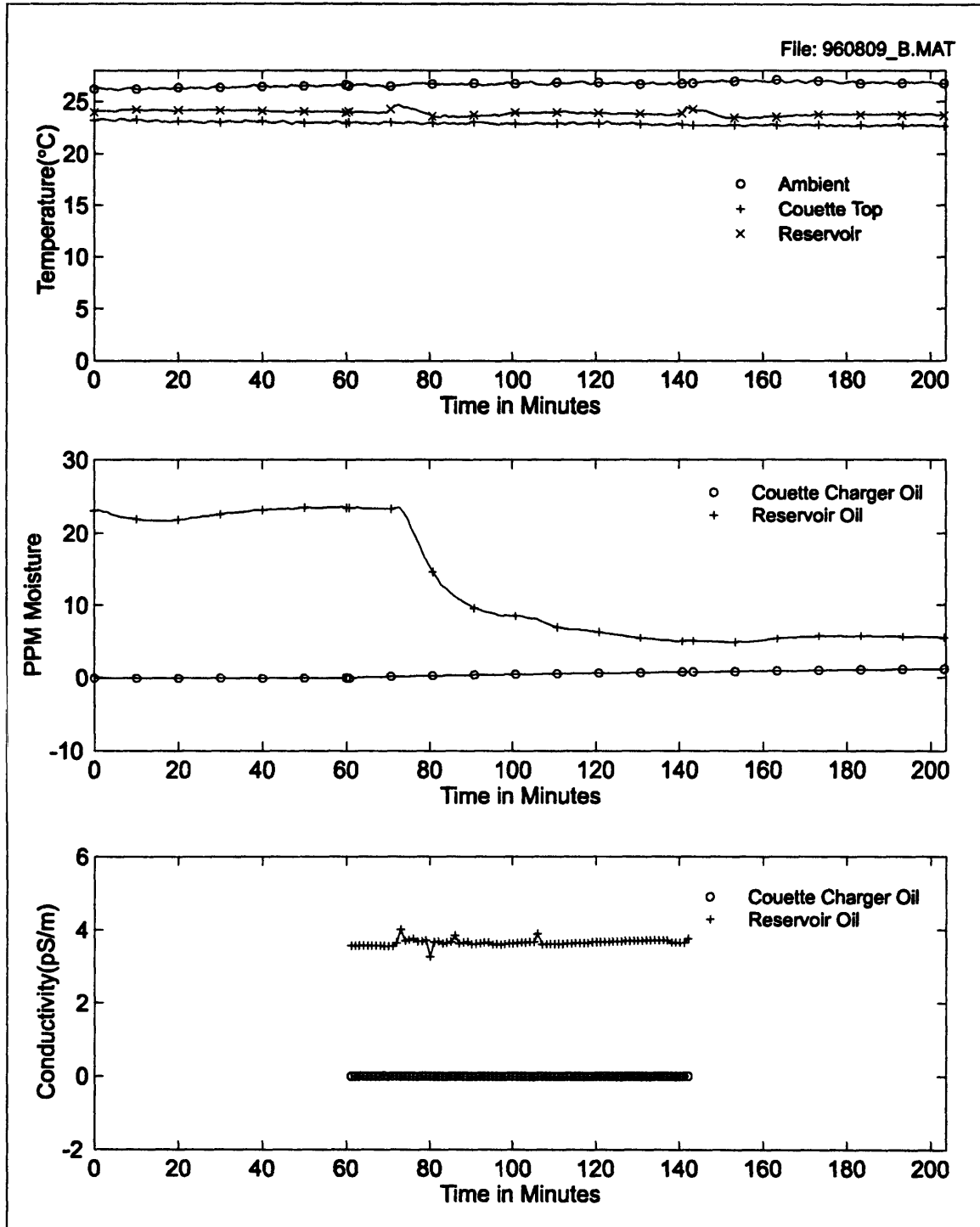


Figure 6-1: Drying process of aged transformer oil.

Chapter 6: Aged Oil Measurements

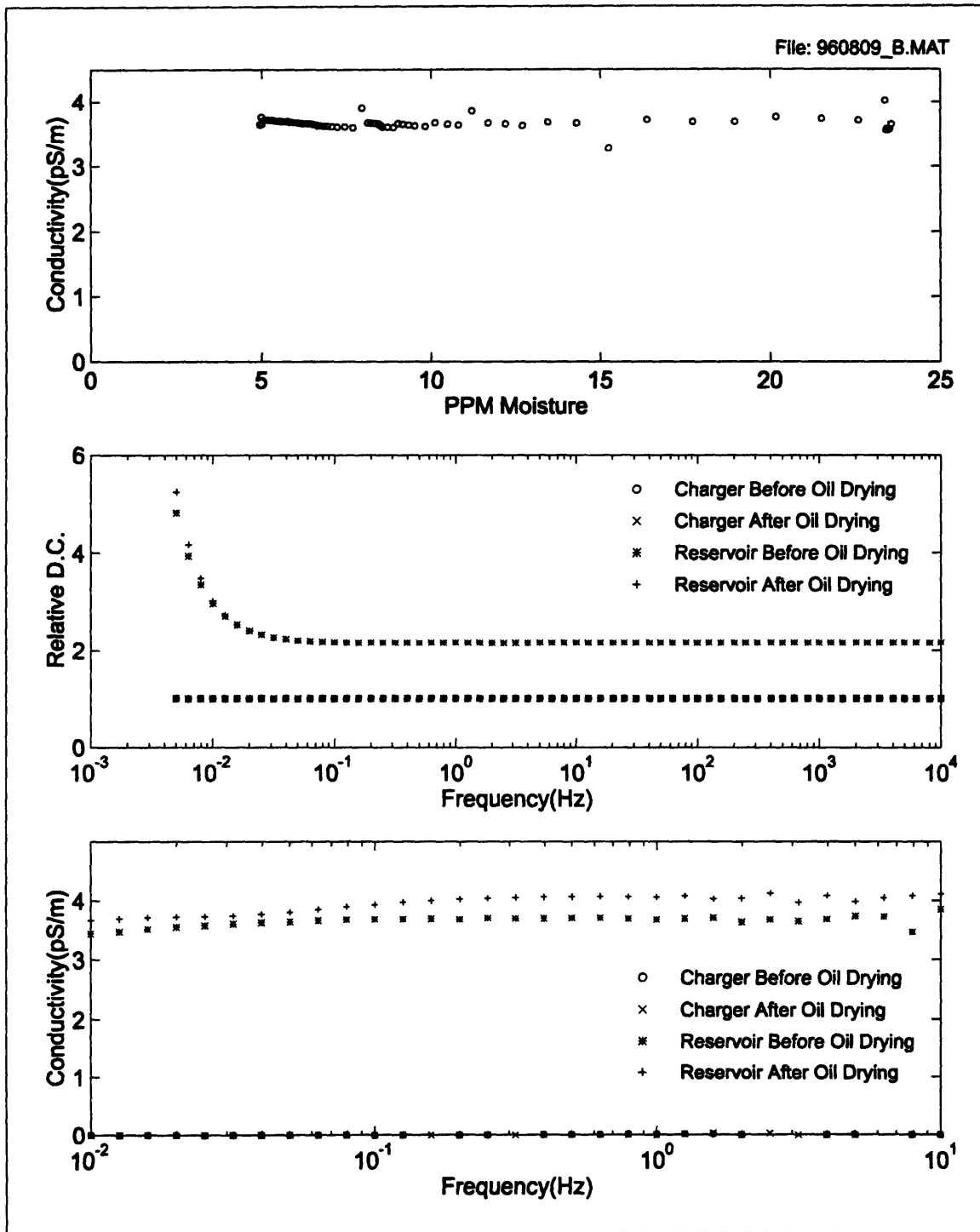


Figure 6-2: Summary of effects of oil drying on oil dielectric properties as functions of moisture and frequency.

6.3 Baseline Measurements

6.3.1 Rotation and Temperature Dependence

The next set of measurements demonstrate the rotation and temperature dependence of the short circuit terminal current, open circuit terminal voltage, and charge density. The technique used to measure the steady state values was altered from that used in previous chapters in order to provide more consistent values. Since long term transients had been observed with increasing the rotation rate in steps, it was not desirable to step the rotation, so rather a ramp was used to increase the rotational rate in the hope of avoiding the long duration transients. The actual steady state measurements were then made as the rotation rate was decreased in steps, which did not appear to generate long term transients possibly due to the slower changes in speed resulting from momentum of the inner cylinder and fluid, which created a coasting effect.

Figure 6-3 demonstrates a measurement using this technique. The data in the figure contains both open circuit and short circuit measurements. The charge density data is also shown in Figure 6-4. The voltages measured during the decreasing steps appears to be fairly steady as desired. The terminal currents show much fluctuation, especially at large rotational rates, but also have an apparently stable mean value at each step in the rate. The charge densities also appear to be stable at each step in rotation.

The baseline data for terminal current and voltage using this technique appear in Figure 6-5 and Figure 6-6 for the aged oil. In comparing the terminal voltages for the aged oil and the fresh oil it is noticed that the polarities of the voltages are opposite for most values. However comparison of the voltages between preliminary measurements and fresh oil measurements also demonstrated an opposite polarity, which means this variation may not be significant.

The terminal currents of the aged oil are also of opposite sign from those of the fresh oil and also opposite to preliminary measurements of fresh oil. The peak magnitude of the currents at 60°C for aged oil over all rotation rates was approximately 1200 pA, while in the fresh oil measurements the peak magnitude was 500 pA. The conductivity of

Chapter 6: Aged Oil Measurements

the aged oil was about 4 times larger at 60°C, which would partly contribute to the larger currents due to the lower effective impedance of the charger.

The measured charge densities of the aged oil exhibit several differences from the fresh oil measurements. The first major difference is in the magnitude of the charge densities, which are on the average 2 to 4 times larger than those of the fresh oil. This is significant because the conductivity is also many times larger in the aged oil, which results in a shorter relaxation time for the charge, and in general lower charge densities. Therefore the double layer charge is most likely larger in the case of the aged oil.

A second difference in the charge densities is in the dependence on rotation rate. In the fresh oil measurements the charge densities tend to increase with increasing rotation, while in the aged oil the charge densities seem to reach a saturation point at which increasing rotation causes minimal change in the charge density.

The third difference is in the temperature dependence of the charge densities. The fresh oil measurements demonstrate an initial decrease in charge with increasing temperature and end with an increase in charge with increasing temperature. However the aged oil measurements show charge densities which only increase with temperature. This most likely indicates that the dominant effect of increasing temperature in the case of the aged oil is to increase the charge in the double layer.

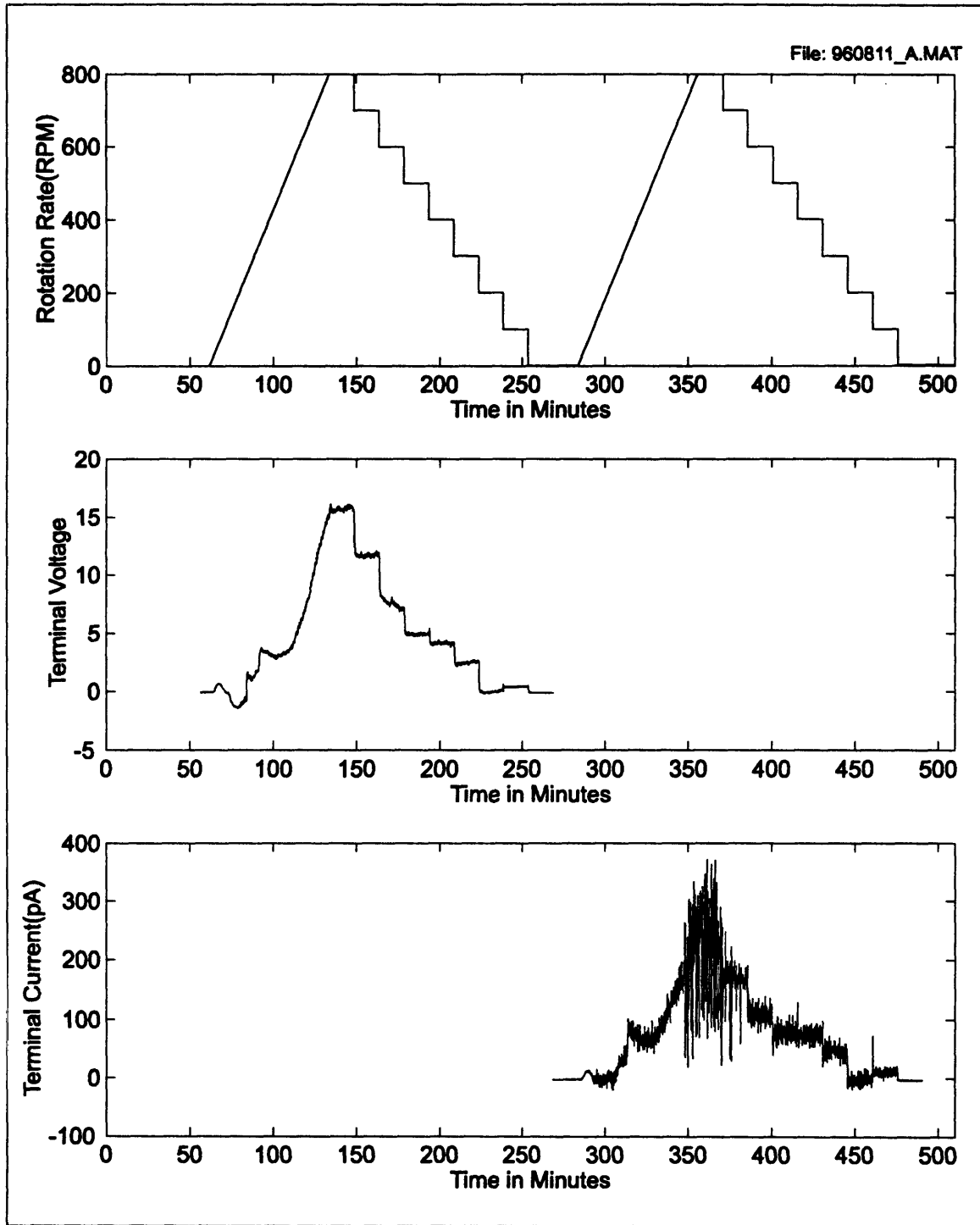


Figure 6-3: Measurements of terminal current and voltage with varied rotation.

Chapter 6: Aged Oil Measurements

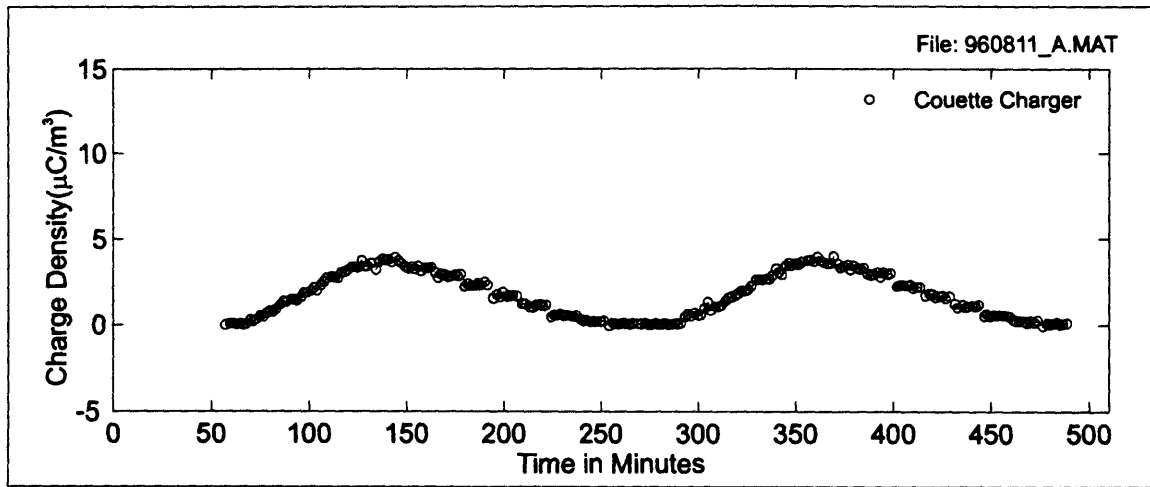


Figure 6-4: Measurement of charge density with varied rotation.

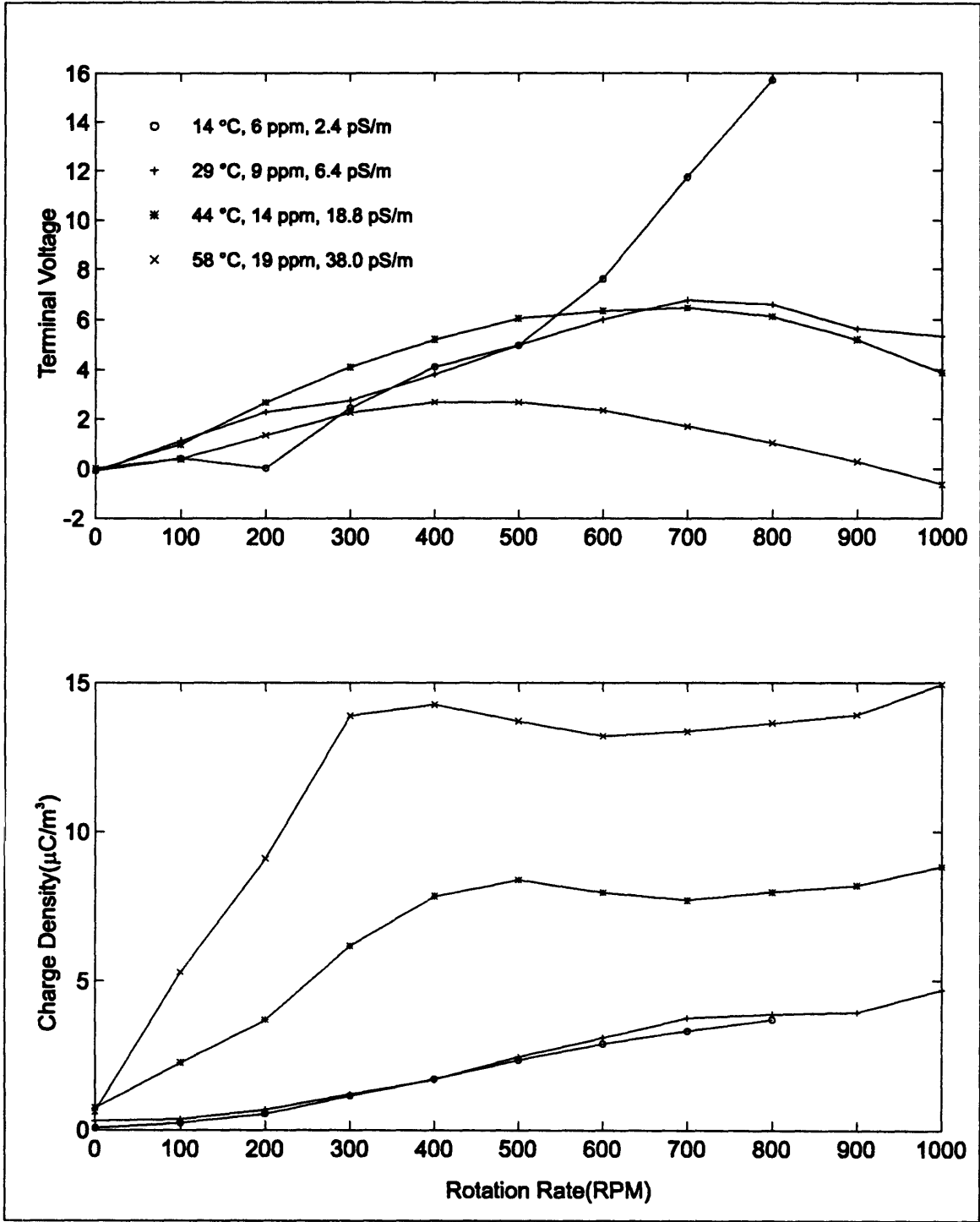


Figure 6-5: Summary of rotation and temperature dependence of terminal voltage and charge density for aged transformer oil.

Chapter 6: Aged Oil Measurements

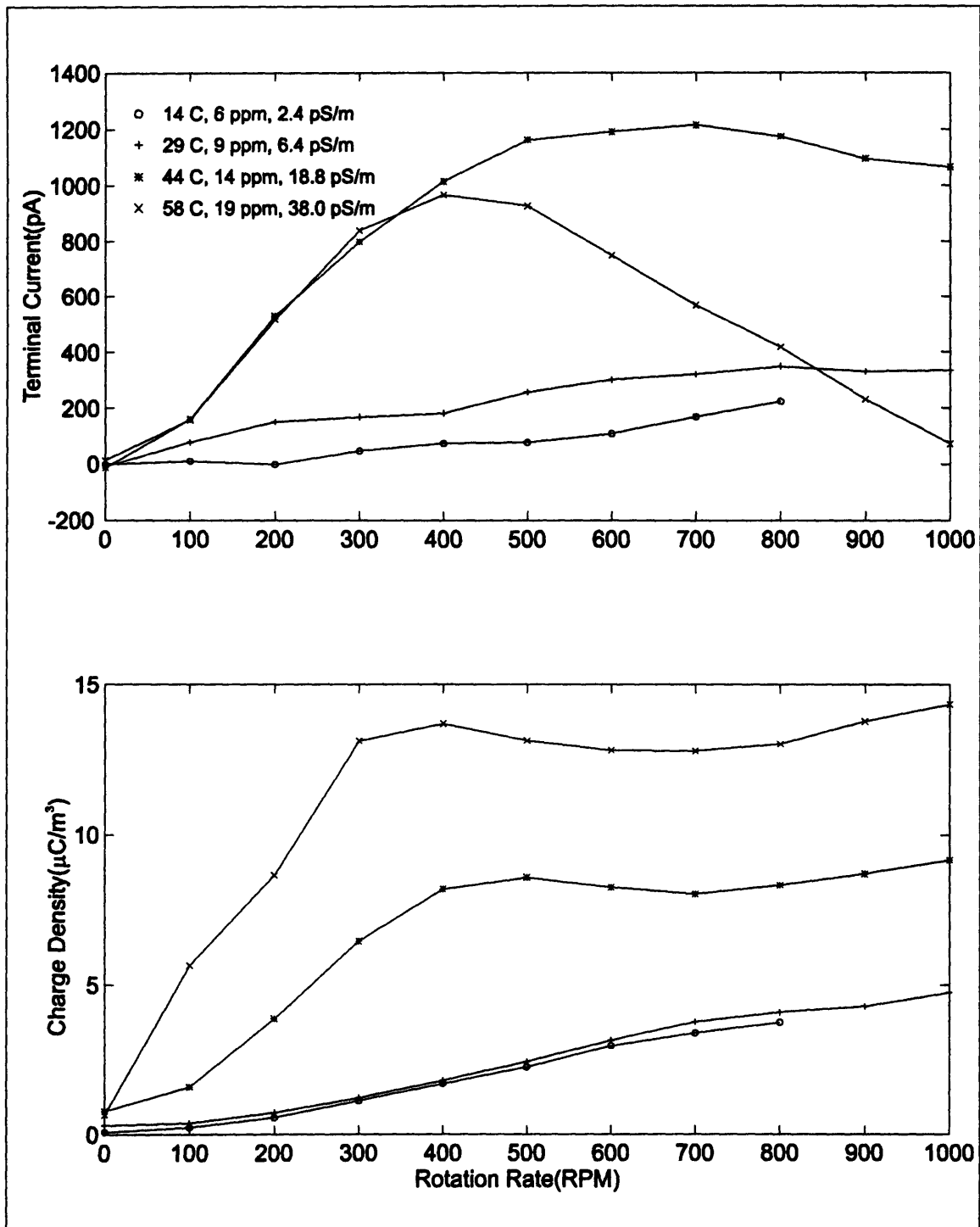


Figure 6-6: Summary of rotation and temperature dependence of terminal current and charge density for aged transformer oil.

6.3.2 Applied DC Voltage Dependence

The effects of applied DC voltages on the charge densities for the aged oil were measured to determine general trends and also to compare with charge densities measured with applied DC voltage after the addition of BTA to the aged oil later in this chapter. Static or quasistatic potentials are also encountered in real systems as part of the electric fields developed by charge accumulation due to flow.

Figure 6-7 demonstrates the technique used to measure the dependence of the charge density on applied DC voltage. The terminal voltage was swept between -500 V and +500 V in 100 V increments at a rotation rate of 400 RPM, the rotation rate was then increased to 800 RPM and the sweep was repeated starting at +500 V. This measurement was repeated at temperatures of 15°C, 30°C, 45°C, and 60°C.

Figure 6-8 summarizes the dependence of the charge densities on applied DC voltage and temperature for two rotational rates. Positive applied voltages result in an increase in charge density for all measurements except at 15°C, where a decrease is first observed. If the positive charge densities indicate net positive double layer charge densities, then this would indicate that the larger electric field at the inner cylinder helped to extend the double layer allowing more charge to become entrained.

In the case of the 15°C measurement, the charge density initially decreased and then increased as larger positive voltages were applied. Since the application of a positive voltage results in an electric field at the outer cylinder which tends to suppress the thickness of a positive double layer, this is also explainable. Although the electric field at the outer cylinder is weaker than at the inner, the contribution of charge suppression at the outer cylinder interface compared to the charge enhancement at the inner cylinder interface on the total charge density is still dependent on the associated sublayer thickness and also magnitude of charge in each double layer. So the dip in charge density of the 15°C measurement is reasonable. It might be also expected that positive charge densities should be increased with positive voltage when the voltage is large enough as it finally did in the 15°C measurement. This might be expected if the double layer thickness is comparable to the sublayer thickness because of its exponential nature. In this case the

Chapter 6: Aged Oil Measurements

suppression will most likely have a limited effect, because once the double layer is suppressed sufficiently, it will make a contribution. However, the potential enhancement with increasing voltage will remain due to the larger charge densities near the double layer boundary, which can be utilized in increasing the entrained charge.

This same argument of larger potential enhancements than suppressions can also be used to justify the final increase in charge density as the applied voltage becomes more and more negative. However, here the enhancement occurs at the outer cylinder interface rather than the inner.

The initial decreases in charge densities, for all but the 15°C measurement, with decreasing negative voltages can be attributed to the larger fields at the inner cylinder resulting in a more significant initial suppression of the double layer. The initial 15°C negative voltage behavior can be explained in the same way as the initial 15°C positive voltage behavior, which is that the total suppression/enhancement contributions from each interface are dependent on the sublayer thickness and double layer charge density magnitudes.

The temperature dependencies of the charge densities generally follow the same behavior of the baseline measurements with no applied voltage. The measured charge densities are observed to increase with increasing temperature for all measurements except at 15°C, where the charge densities are larger than at 30°C for negative applied voltages. The potential reasons for the initial behavior of the 15°C with decreasing negative voltage has been explained previously. The relative closeness of the charge densities at these two temperatures with no applied voltage allows different competing effects to cause this larger charge density for the 15°C over a range of negative voltages. Although it might be expected that as the voltage becomes more negative than in the measurements, the 30°C charge density should become larger than at 15°C as they are for positive applied voltages. However this may not occur if other effects not considered are dominating or if the outer interface, which is assumed to be enhanced by the applied voltage, has been altered in some way between 15°C and 30°C measurements.

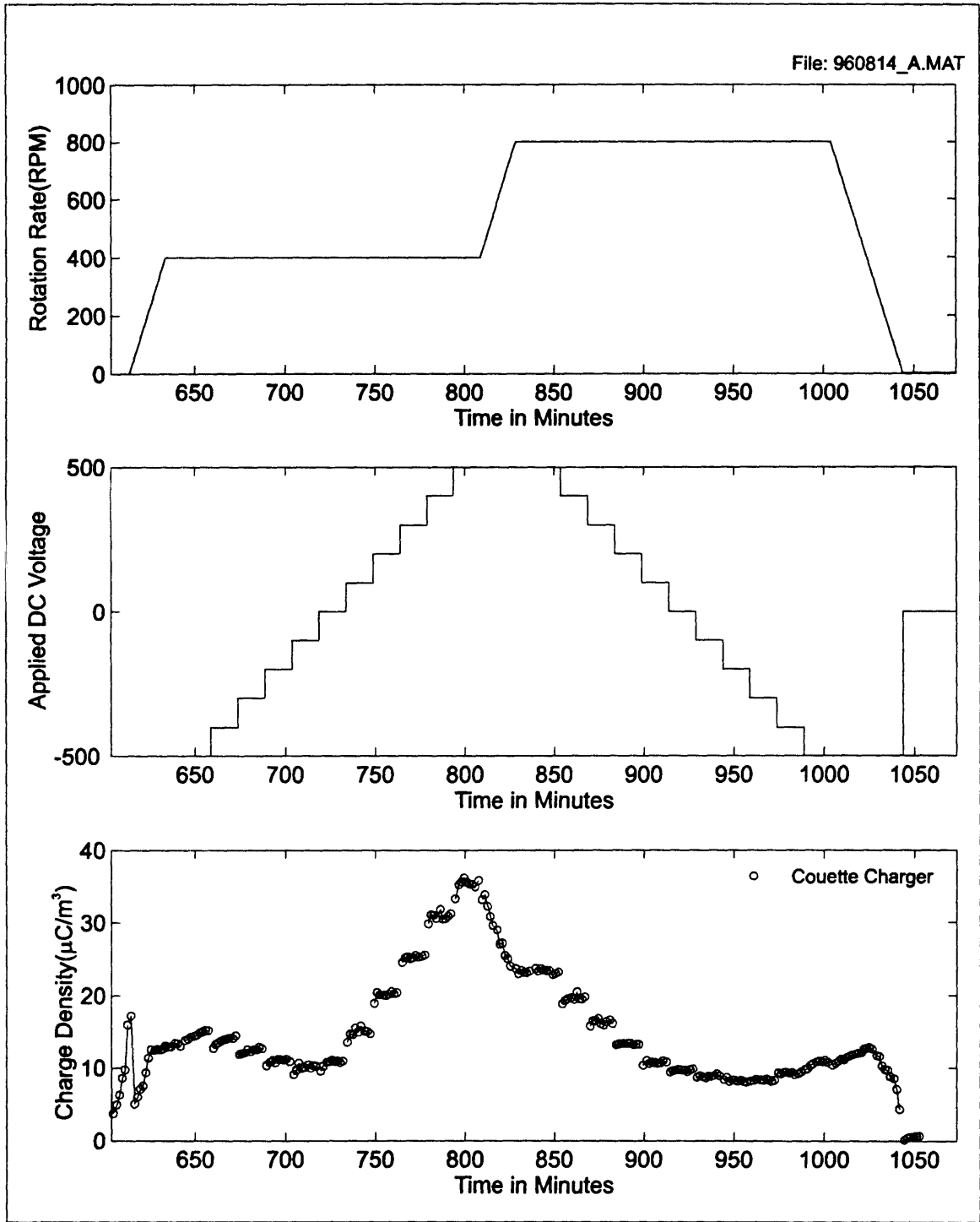


Figure 6-7: Effects of applied DC voltage on charge density.

Chapter 6: Aged Oil Measurements

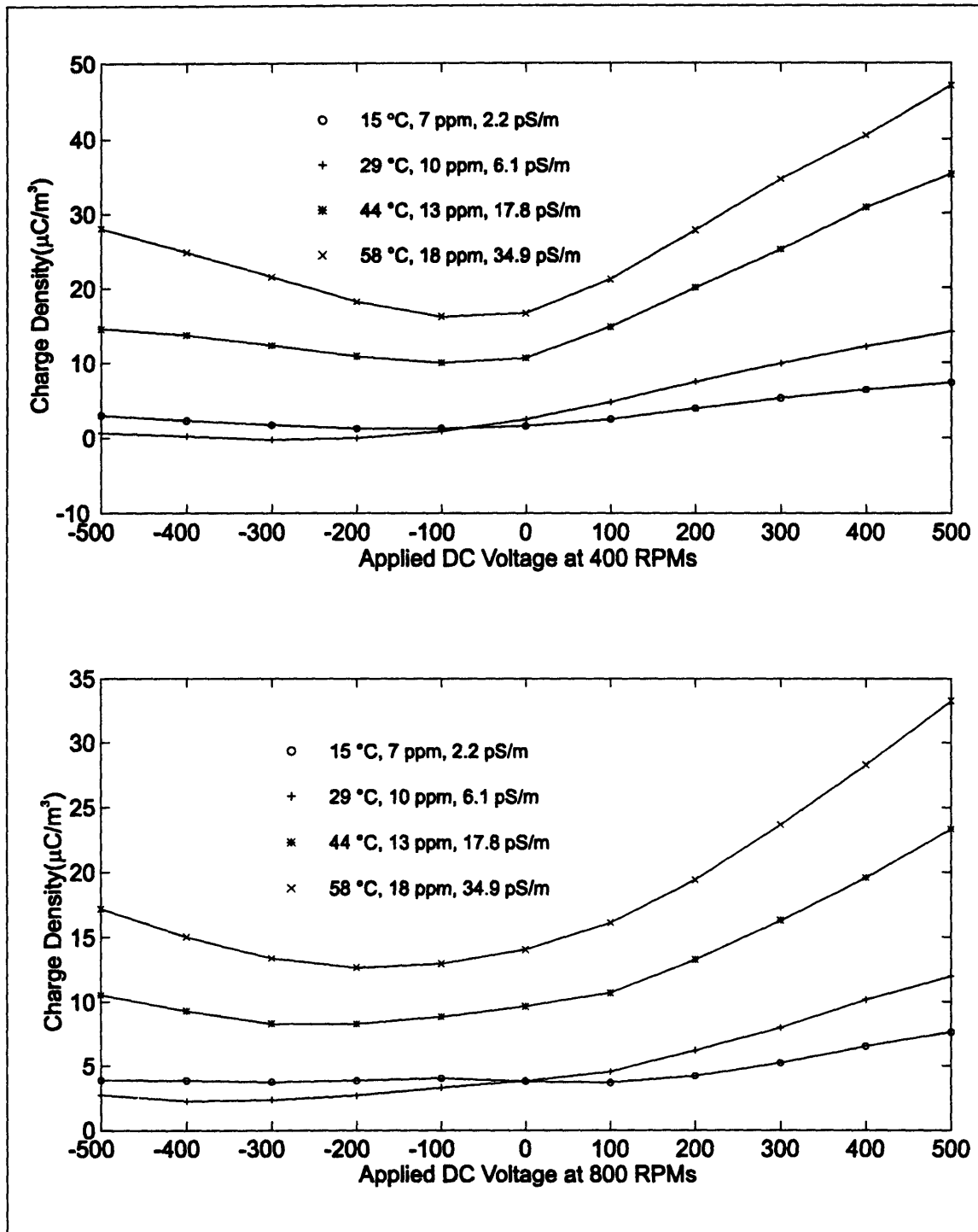


Figure 6-8: Summary of applied DC voltage on charge density for 400 and 800 RPM rotation at varied temperature.

6.3.3 Applied AC Voltage Dependence

In addition to static or quasistatic electric fields which result from charge accumulation in a transformer, AC electric fields are also present due to energization of the windings. Therefore measurements of the charge densities as a result of applied AC voltages were also made.

Figure 6-9 demonstrates measurements made at varied AC frequencies. The rotation of the CC was initially raised to 400 RPM. The frequency of the applied 500 V peak sinusoidal voltage was then varied logarithmically from .01 Hz to 60 Hz. Next the rotation was increased to 800 RPM and the frequency was again varied, starting with 60 Hz. From the measurements, it is observed that the charge densities are erratic at the low frequencies. This occurs because at these frequencies the charge densities are also varying with time at the same frequency as the applied voltage. The charge measurements which requires approximately one minute then tend to average different portions of the charge cycle resulting in a type of "aliasing". As the frequency increases, the charge measurement begins to smoothly average the charge density over many cycles. Also, the relaxation and diffusion characteristics of the system act as a low pass filter resulting in charge densities which have less variation in time with increasing frequency.

Figure 6-10 summarizes both the applied voltage frequency and temperature dependence of the charge densities at 400 and 800 RPM rotation rates. The charge densities are observed to increase with decreasing frequency as was seen in preliminary measurements. This is reasonable because time is required for the enhanced (depressed) double layer thickness, due to the field, to effect the bulk charge densities. Therefore the lower frequencies allow more time for the effects of the applied field to contribute to the bulk charge density.

The DC applied voltages can also be used to help justify the AC charge increases. In the DC case, positive voltages, especially above 250 V tended to increase the charge density significantly from its zero voltage value. In comparison, negative voltages had either small effects in reducing the charge or also increased it. Therefore if it is assumed that the AC effect should be just a weighted average of the effects at each point of the sinusoid, an increase is also reasonable.

Chapter 6: Aged Oil Measurements

Temperature effects again follow from zero applied voltage measurements, with the highest temperature resulting in the largest charge densities.

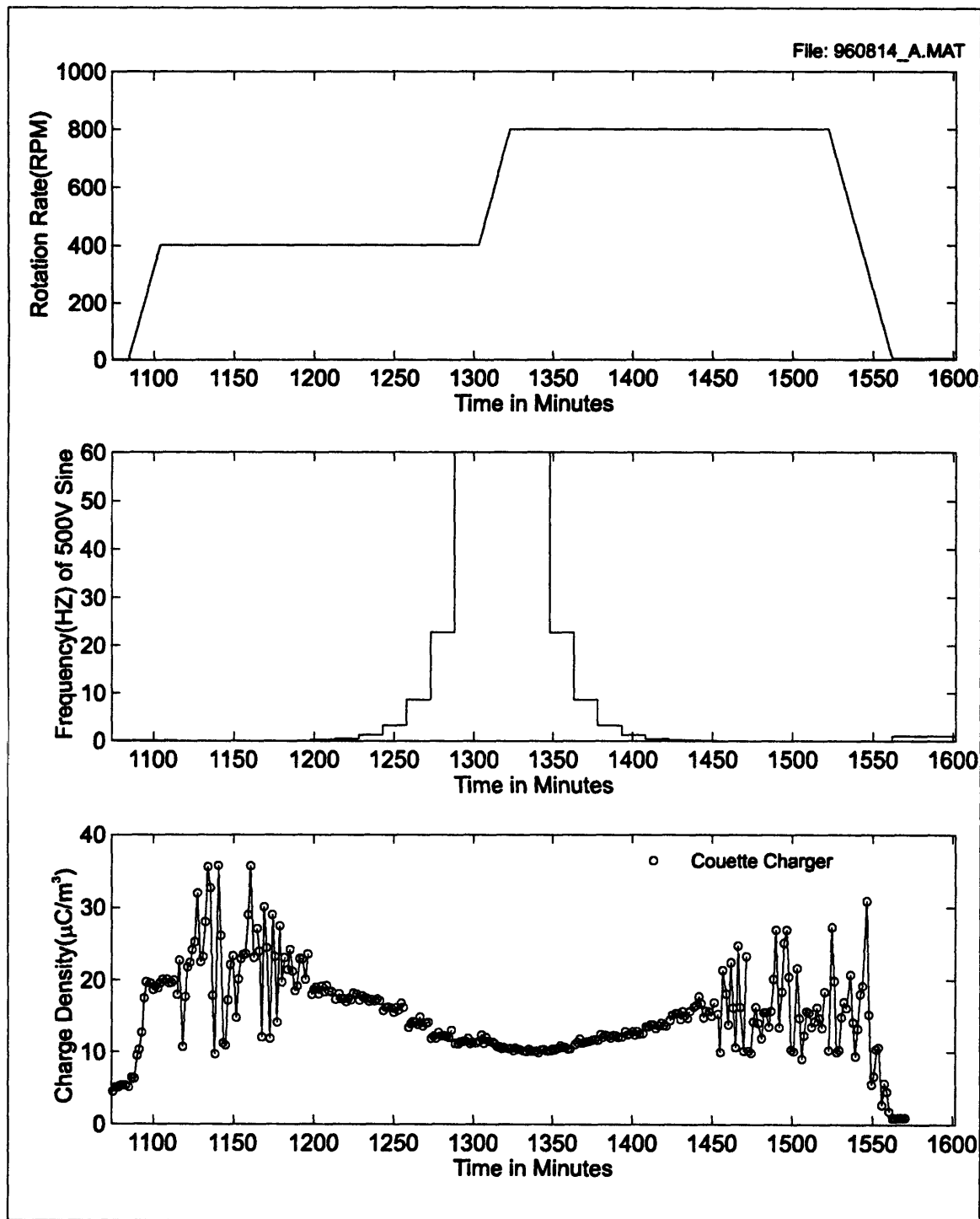


Figure 6-9: Effects of applied AC voltage frequency on charge density. The erratic behavior for low frequencies occurs as the frequency becomes comparable to the time required for a charge measurement.

Chapter 6: Aged Oil Measurements

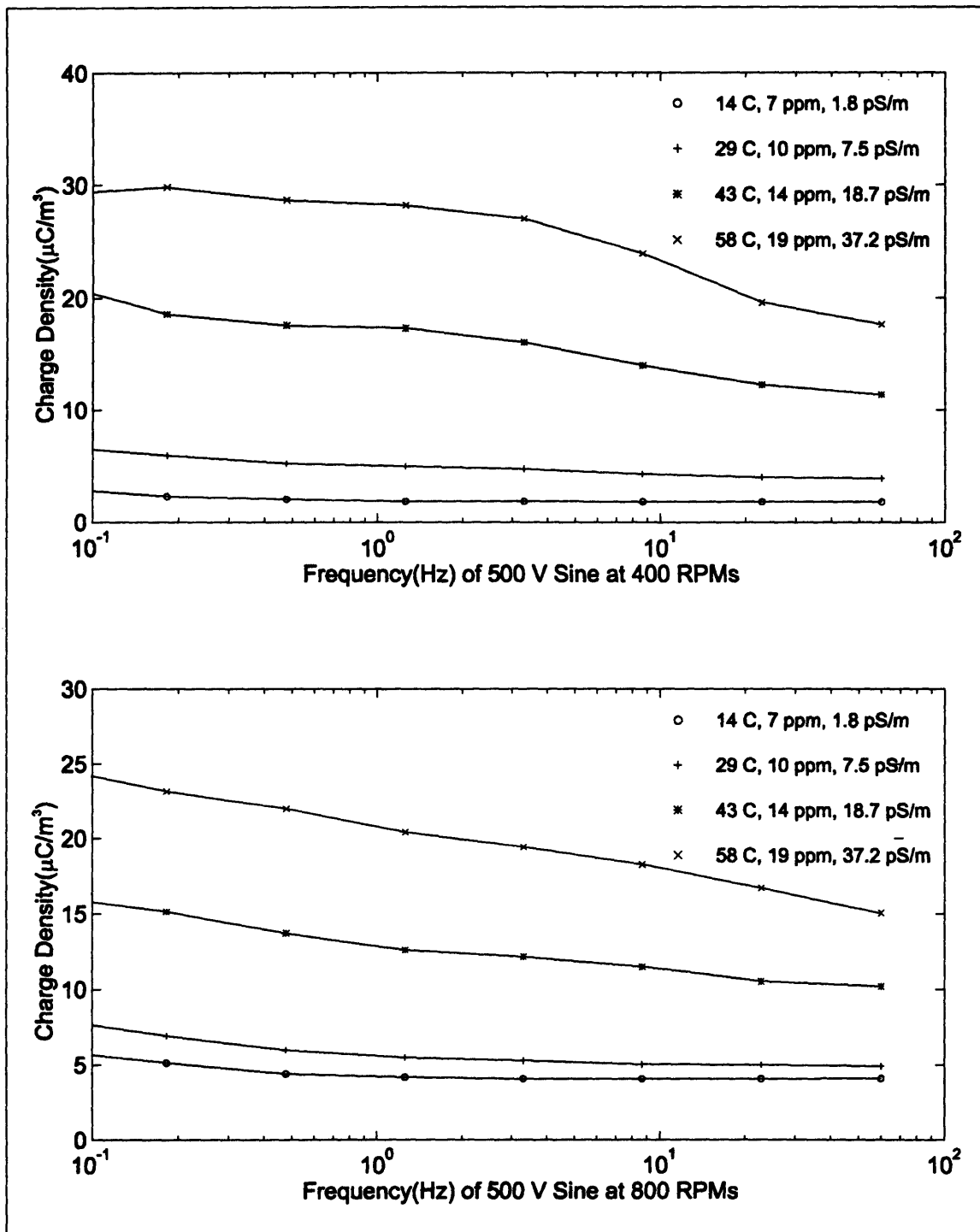


Figure 6-10: Summary of applied AC voltage effects on charge density for 400 and 800 RPM rotation at varied temperature.

6.4 Addition of BTA

In measurements of fresh Shell Diala A, the addition of BTA was observed to reduce charge densities and terminal currents, with the additional side effect of reducing the conductivity of the oil. In these measurements BTA is added to the Couette charger containing the aged oil in 5 ppm increments with the rotation constant at 800 RPM and the temperature at 60°C. These measurements will help to demonstrate the effectiveness of BTA on aged oil. Measurements later in this chapter compare all measured parameters before and after the addition of 15 ppm BTA.

Figure 6-11 and Figure 6-12 show the measurements made during the first injection of BTA. In the measurements a concentrated solution of aged oil containing BTA was introduced at 100 minutes to bring the total concentration of the oil in the Couette Charger to 5 ppm. The charge density decreased by roughly 12 % within several minutes after the injection, while the current changed almost immediately from -500pA to a positive value of 100 pA. The charge density then continued to decrease over the next six hours, while the terminal current returned to a negative value, which exceeded the magnitude of the value before the addition. The conductivity was also observed to decrease after the injection and continued to slowly decrease for many hours following the injection.

Figure 6-13 contains the measurement for the second injection of BTA (the terminal current does not appear in this measurement due to instrumentation problems). The charge density does not undergo a sudden decrease at the time of injection, but again a slow decrease is observed in the many following hours. The oil conductivity also decreases in the hours following the injection.

Chapter 6: Aged Oil Measurements

Figure 6-14 and Figure 6-15 show the measurements for the final injection of BTA to bring the concentration to 15 ppm. The terminal current again becomes positive immediately after the injection, but with a magnitude equal to that of the starting negative value. The charge density shows no abrupt change with the injection, but continues to slowly decrease over the measurement time. The terminal current decreases to a value slightly more negative than the starting value over the several hours following the injection. The conductivity of the oil also appeared to decrease over the time of the measurement.

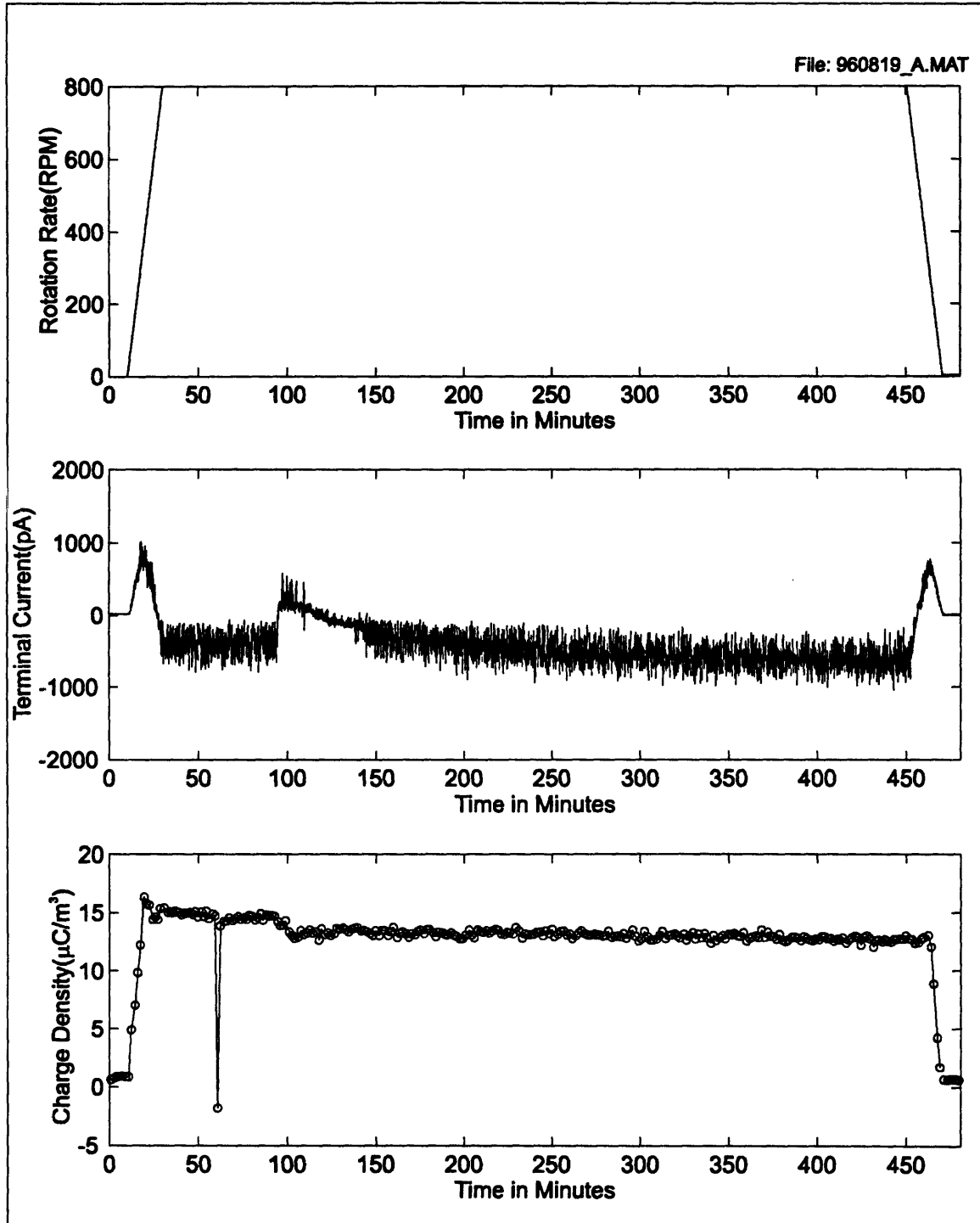


Figure 6-11: Addition of BTA in used transformer oil to bring concentration from 0 to 5 ppm.

Chapter 6: Aged Oil Measurements

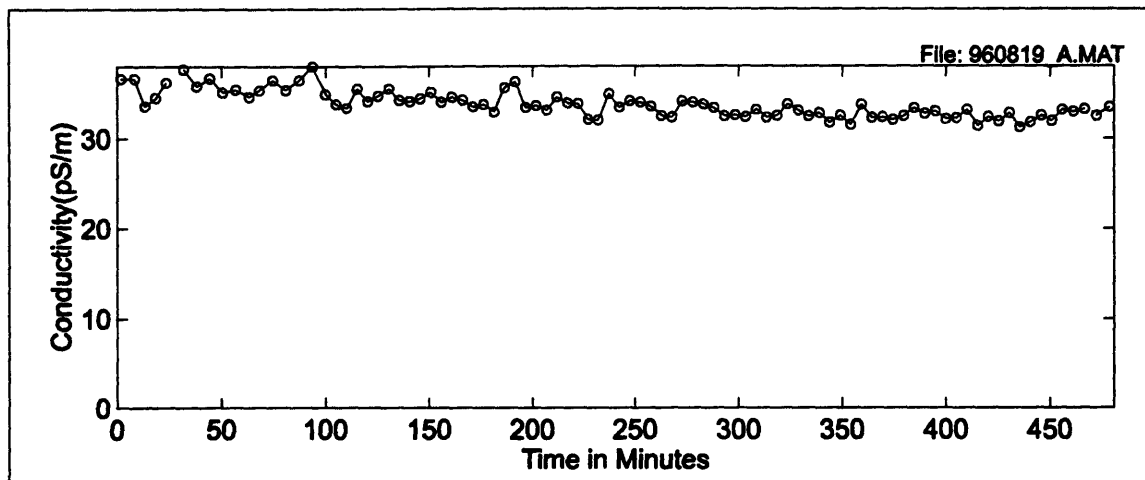


Figure 6-12: Addition of BTA in used transformer oil at approximately 100 minutes to bring concentration from 0 to 5 ppm.

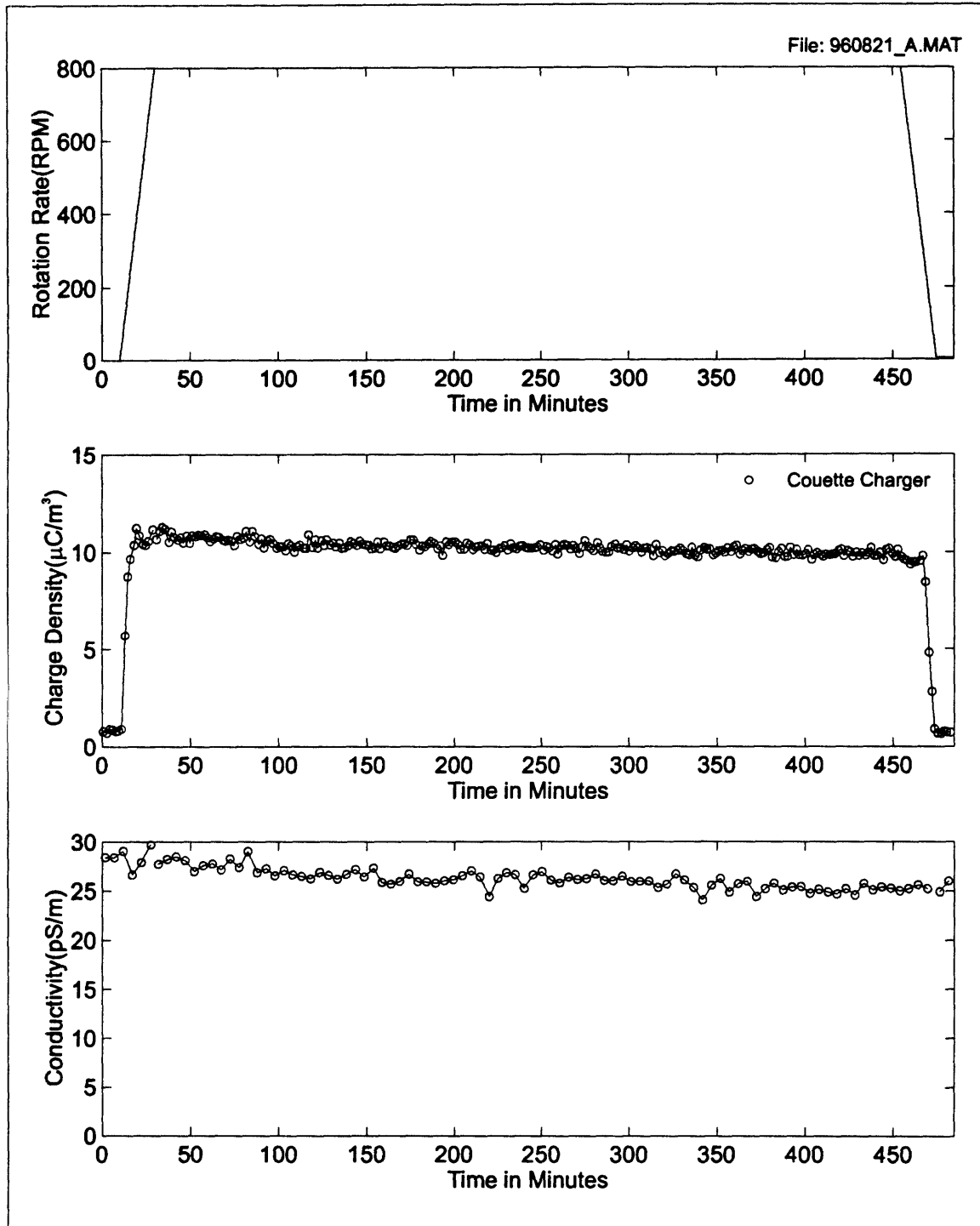


Figure 6-13: Addition of BTA in used transformer oil at approximately 100 minutes to bring concentration from 5 to 10 ppm.

Chapter 6: Aged Oil Measurements

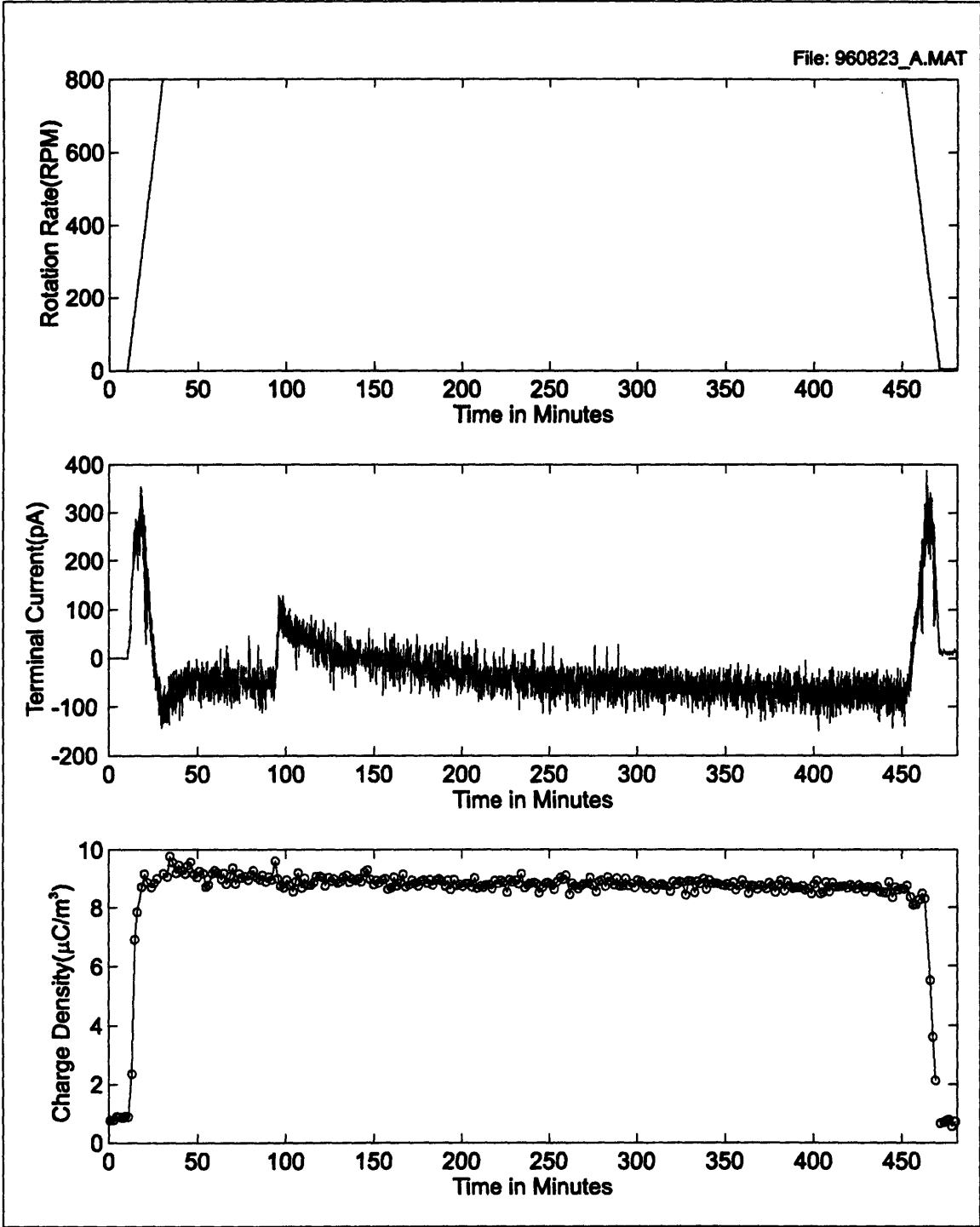


Figure 6-14: Addition of BTA in used transformer oil at approximately 100 minutes to bring concentration from 10 to 15 ppm.

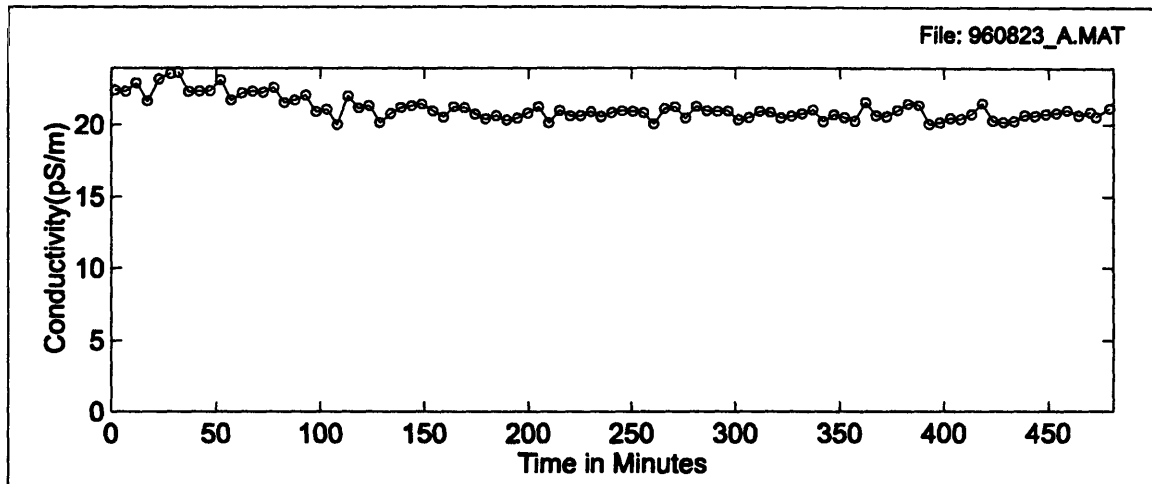


Figure 6-15: Addition of BTA in used transformer oil at approximately 100 minutes to bring concentration from 10 to 15 ppm.

6.5 Effects of BTA

6.5.1 Concentration Dependence

The following measurements summarize the effects of BTA on the charge densities and terminal parameters many hours after its addition at concentrations of 0, 5, 10, and 15 ppm. All measurements are at 60°C with bare stainless steel inner and outer cylinders.

Figure 6-16 compares the terminal current and charge density for each concentration. The first addition of BTA resulted in a decrease in the most positive value of voltage without BTA, but also resulted in a larger negative voltage at rotations approaching 1000 RPMs. However successive additions of BTA decreases both positive and negative magnitudes of the terminal voltage.

The charge densities are seen to decrease with increasing concentration of BTA. The largest decrease was caused by the addition of BTA which changed the concentration from 5 ppm to 10 ppm. Interestingly the measured conductivities are also decreasing significantly with increasing BTA concentration as can be seen in the legend of the figure. This effect is in complete contrast to typical conductivity enhancers, which reduce charge

Chapter 6: Aged Oil Measurements

accumulation in the fluid and on surfaces by decreasing the relaxation time of the charge by increasing the fluid conductivity.

Figure 6-17 compares the terminal currents and charge densities for increasing concentrations of BTA. Similar effects to those of the terminal voltage are observed in the current, including that of the first addition which resulted in a measured current with a larger peak magnitude than before the addition. Further additions again tended to reduce the terminal current, partly due to the lower impedance caused by the conductivity decrease. Charge density effects were basically the same as in the voltage measurements.

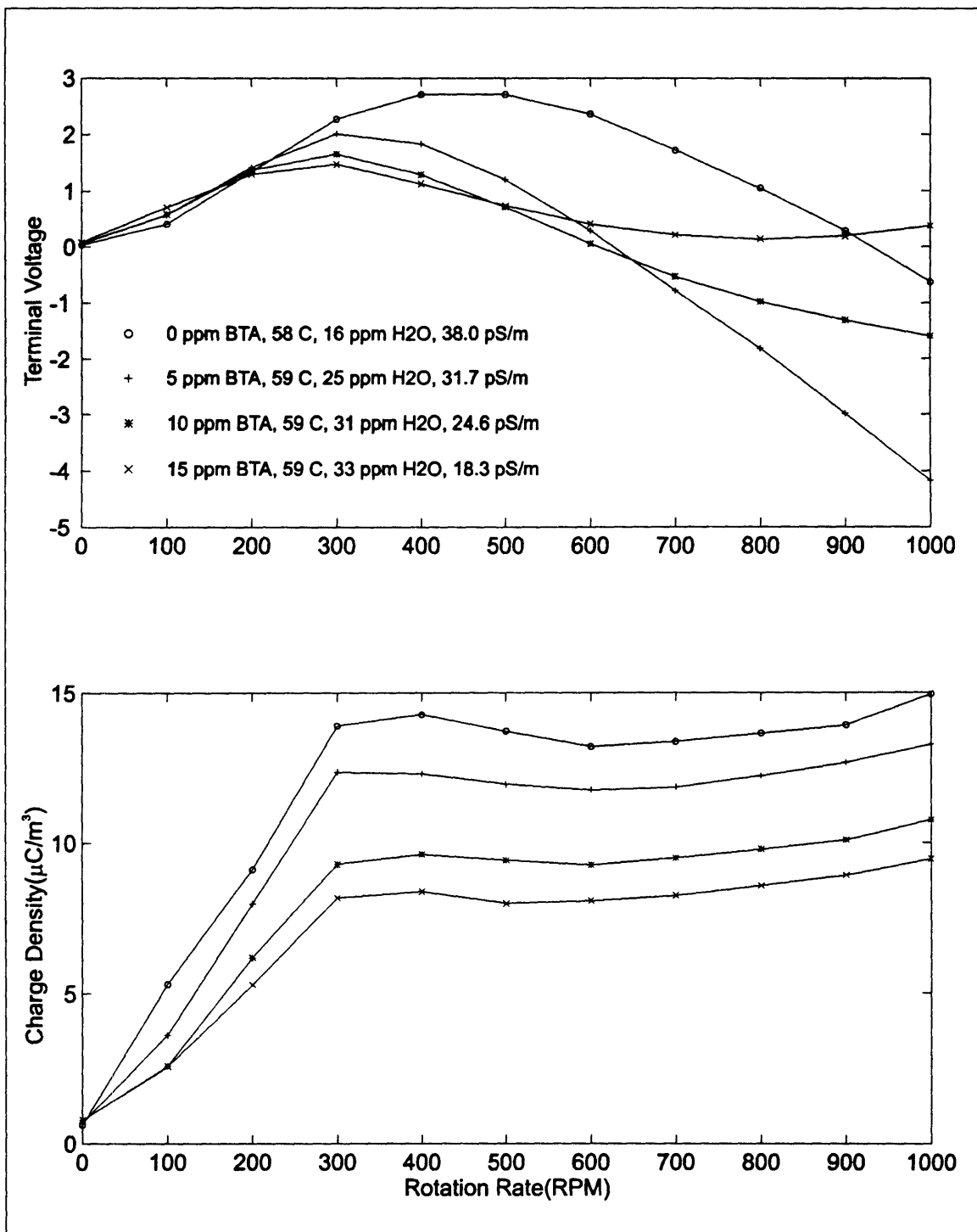


Figure 6-16: Summary of BTA effects as a function of concentration.

Chapter 6: Aged Oil Measurements

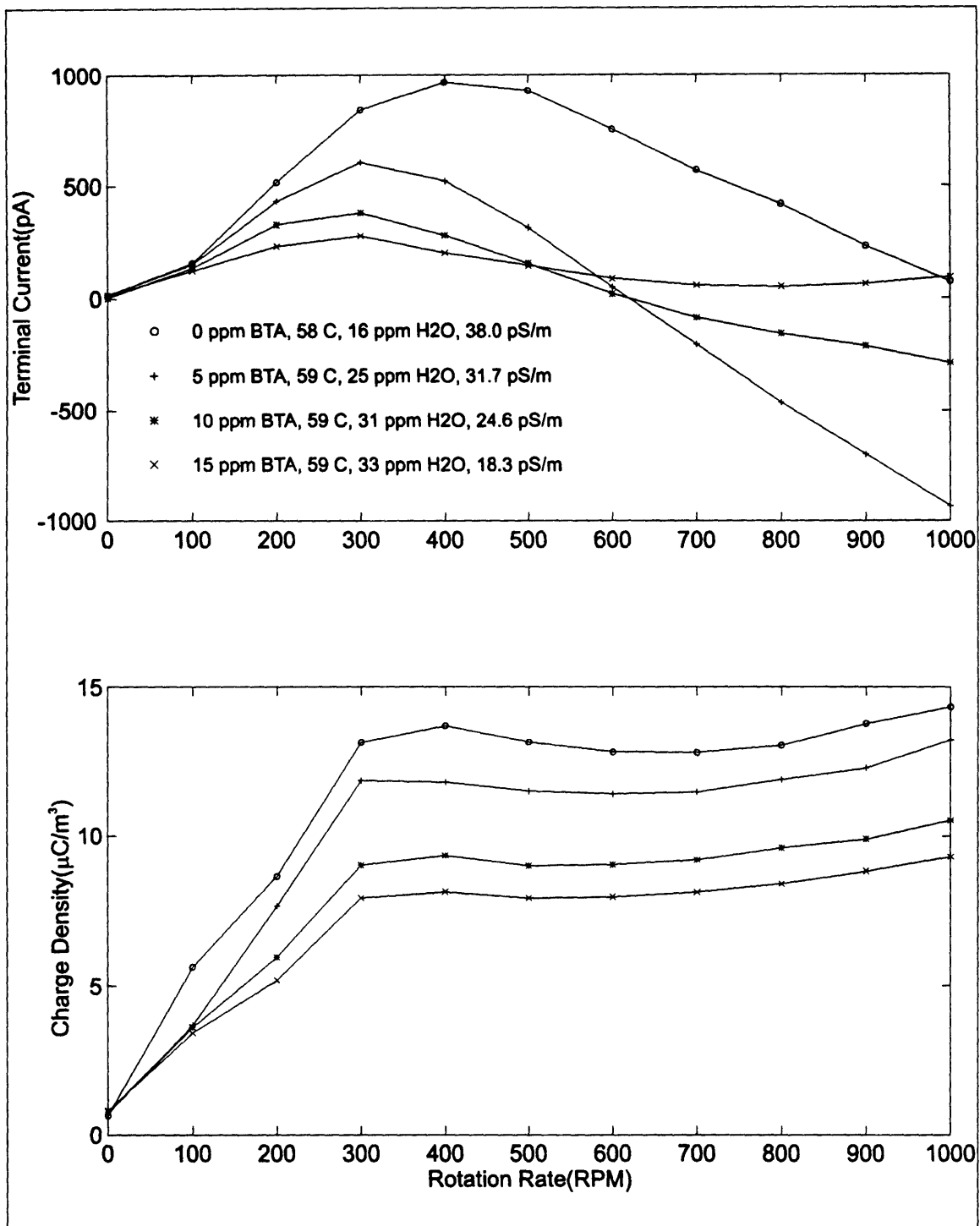


Figure 6-17: Summary of BTA effects as a function of concentration.

6.5.2 Rotation and Temperature Dependence

The measurements of this section demonstrate the temperature and rotational dependence of the charge density and terminal parameters for the aged transformer oil with 15 ppm of BTA. Comparisons are also made between measured quantities of the aged oil before and after the addition of BTA.

Figure 6-18 demonstrates the terminal voltage dependence of the aged oil with 15 ppm of BTA on temperature and rotation. The temperature trend is an increase in voltage between 15°C and 30°C followed by a decrease with increasing temperature. In the measurements without BTA the temperature trend was more dependent on the rotational rate. The voltage dependence without BTA generally decreased with increasing temperature at rates greater than approximately 500 RPM, while the voltage increased with increasing temperature to 45°C and then decreased with increased temperature at rates less than approximately 500 RPM.

The rotational dependence of the terminal voltage with 15 ppm BTA shows a general increase in voltage with increasing rate except at the highest temperature of 60°C. In this measurement the terminal voltage decreases after reaching 300 RPM. This initial increase in voltage followed by a decrease with increasing rate was observed at 45°C and somewhat at 30°C without BTA. Comparisons between terminal voltages with and without BTA at each temperature can be found in Figure 6-20. At 15°C the BTA measurement is generally less than without BTA, with a greater difference at higher rotation rates. The 30°C comparison shows similar voltages, however the trend for a decrease in voltage with increasing RPM for the measurement without BTA is apparent. The 45°C comparison shows the voltage of the BTA measurement to be less except at higher rotation rates where the decreasing trend without BTA is even more apparent.

Figure 6-19 contains the temperature and rotational dependence of the terminal current for the aged oil with 15 ppm BTA. The terminal currents are seen to increase with increasing temperature, except at 60°C, where the temperature dependence is also dependent on the rotation rate. The current for the 60°C measurement follows the increase with increasing temperature trend up until about 300 RPM after which the current

Chapter 6: Aged Oil Measurements

tends to decrease with increasing rotation. This is accompanied by a plateau of the charge densities also shown in the figure. The rotational trends of the current for all other temperatures besides 60°C have a simple increase with increasing rotation.

Figure 6-21 compares the terminal currents for the aged oil with and without BTA at several temperatures. In all cases the measurements with BTA show smaller terminal currents. The conductivity of the oil at each temperature is also reduced with BTA as shown in the legends, which is partially responsible for the decrease in current.

Figure 6-18 also contains the charge density dependence on temperature and rotation. The charge densities tend to increase with increasing temperature as observed without BTA. Figure 6-22 compares the charge densities with and without BTA as a function of RPM at several temperatures. At 15°C the charge densities were reduced with BTA by up to $1\mu\text{C}/\text{m}^3$. A mixed effect was observed at 30°C, where the lower rotational rates experience a slight increase of up to $.5\mu\text{C}/\text{m}^3$ and the higher rotational rates exhibited a decrease of up to $1\mu\text{C}/\text{m}^3$. However at the next higher temperature of 45°C, the charge density is significantly reduced with the addition of BTA. The measured charge densities are almost halved for rates above 400 RPMs. The greater effect of BTA at higher temperatures may be attributed to its dual effect on both interfacial parameters and conductivity. Since the change in these parameters by the BTA are competing to both raise and lower charge densities, the temperature dependence of these parameters is also important in determining whether the net effect is an increase or decrease.

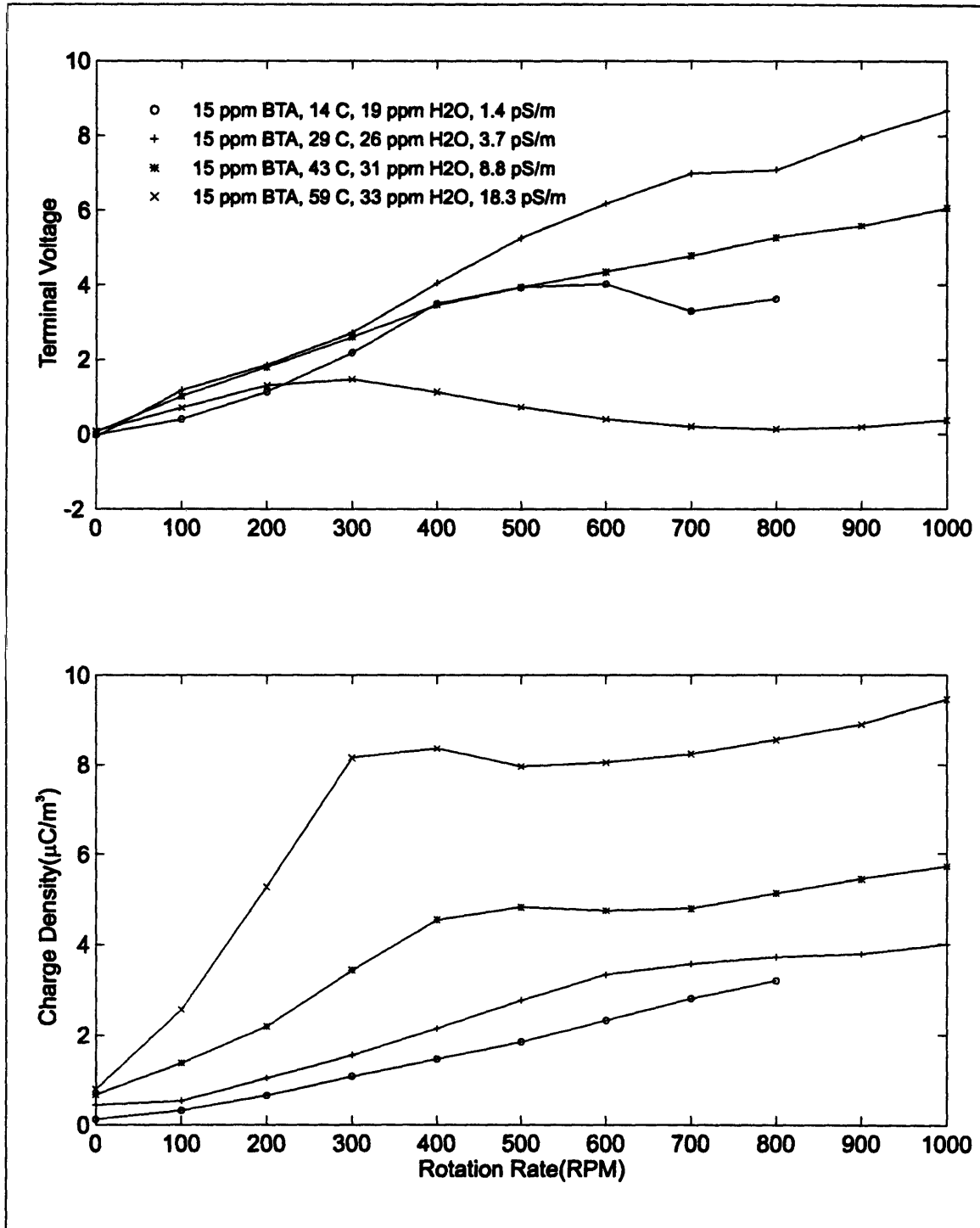


Figure 6-18: Temperature and rotation dependence of terminal voltage and charge density with 15 ppm BTA.

Chapter 6: Aged Oil Measurements

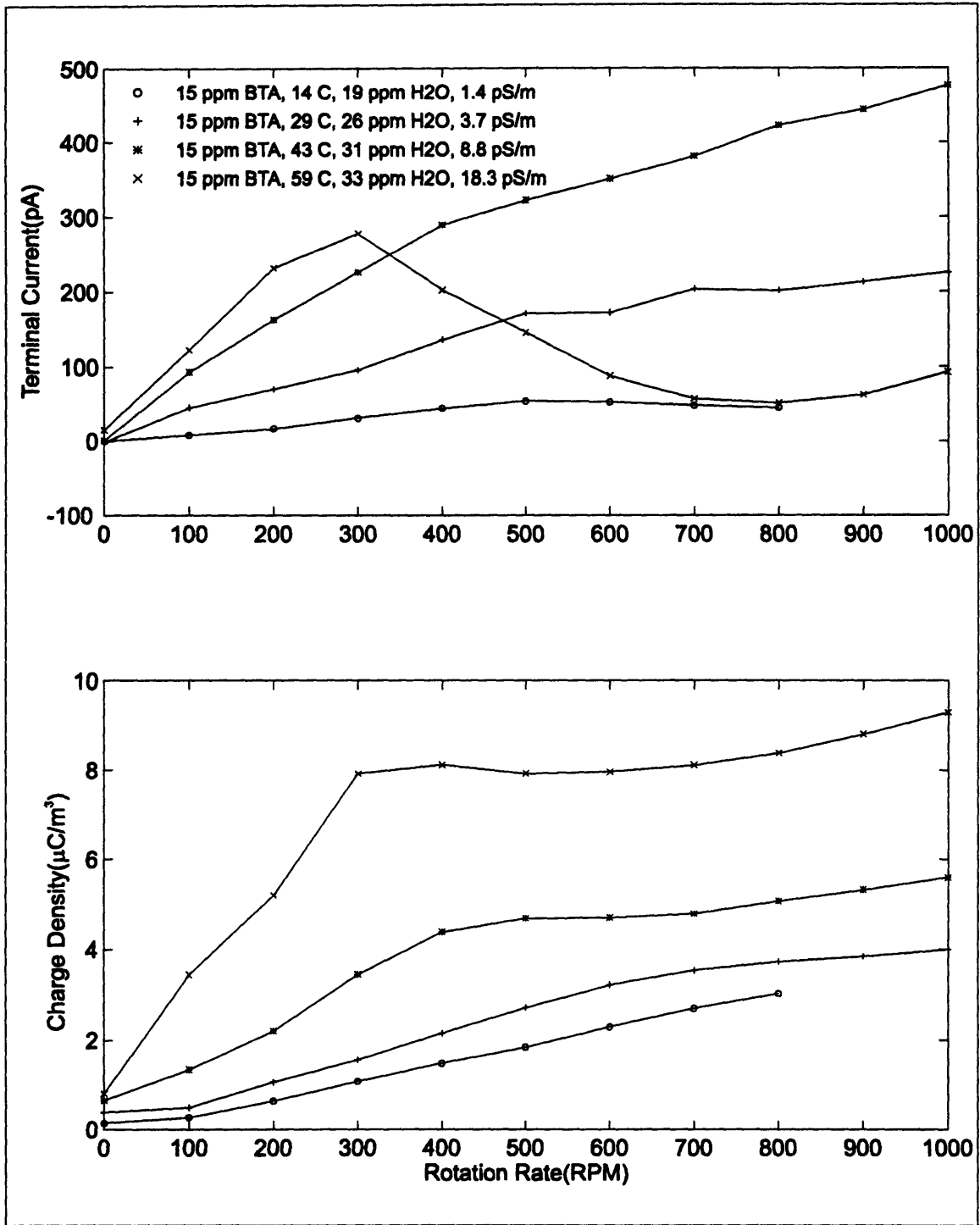


Figure 6-19: Temperature and rotation dependence of terminal current and charge density with 15 ppm BTA.

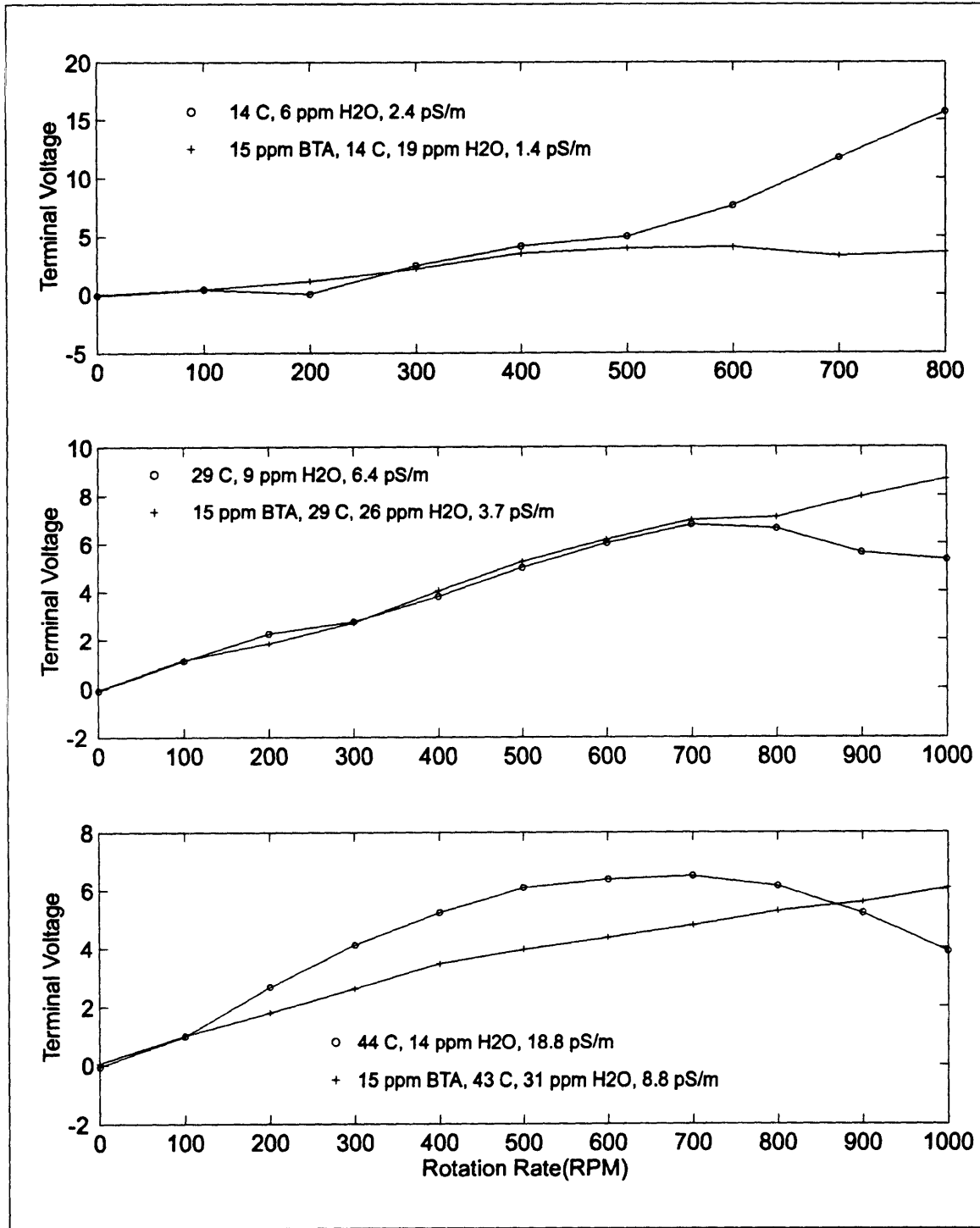


Figure 6-20: Comparison of terminal voltages with and without BTA at varied temperature.

Chapter 6: Aged Oil Measurements

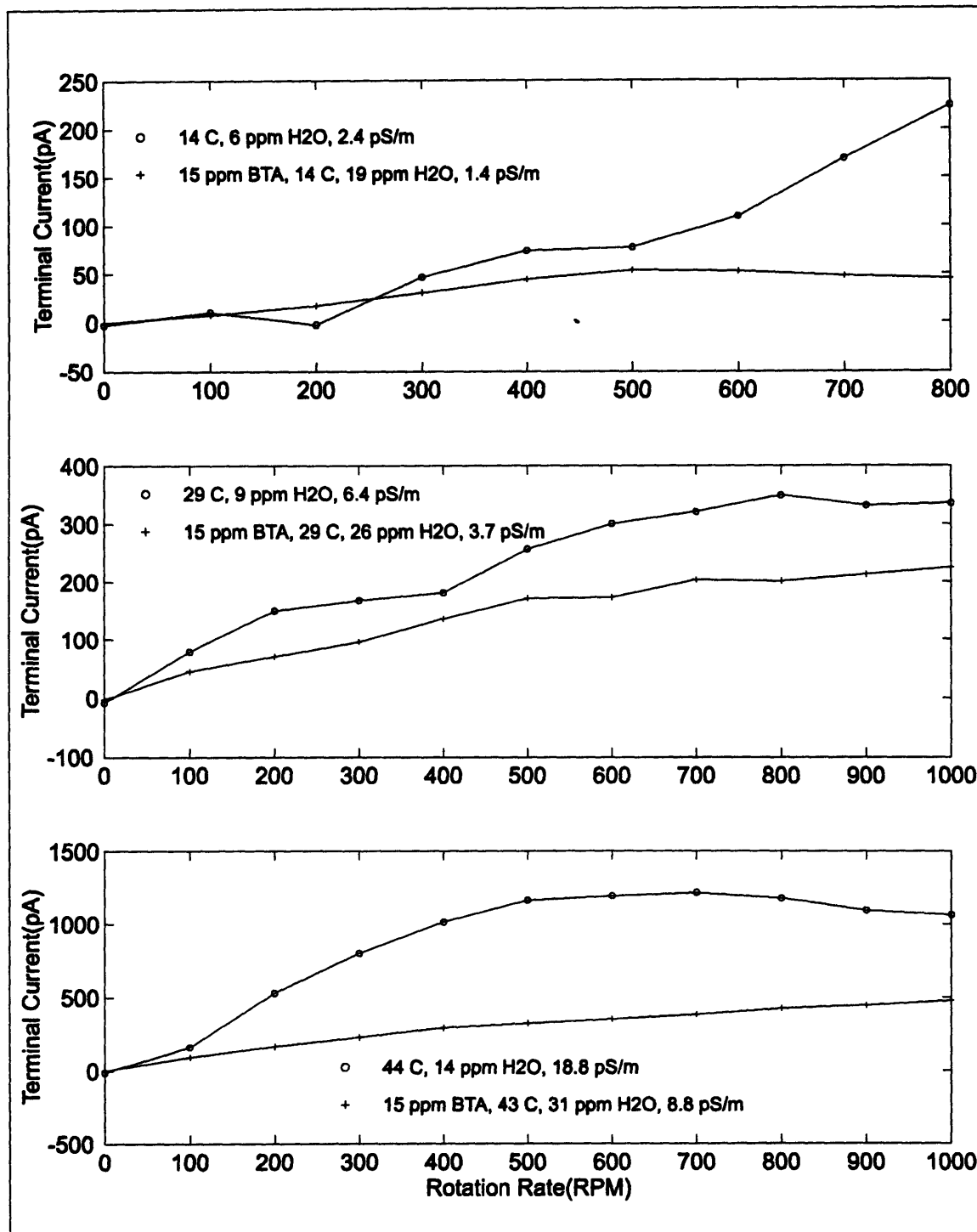


Figure 6-21: Comparison of terminal current with and without BTA at varied temperature.

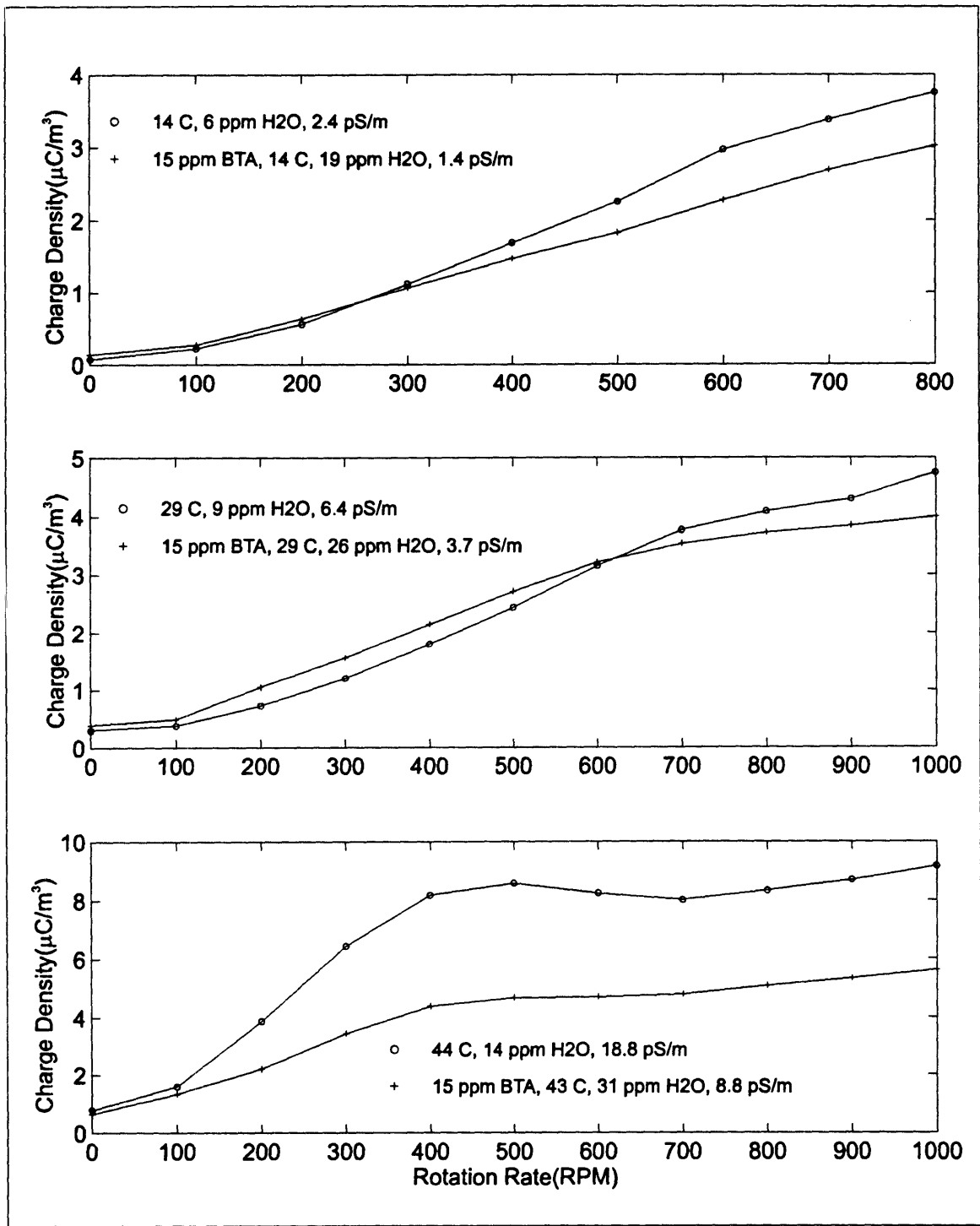


Figure 6-22: Comparison of charge density with and without BTA at varied temperature.

6.5.3 Applied DC Voltage

After the addition of 15ppm BTA, measurements of the effects on charge density by the application of a DC voltage to the CC terminals were repeated. Figure 6-23 demonstrates the charge density dependence on both voltage and temperature for both 400 and 800 RPM rotation rates. The charge densities again tend to increase with increasing temperature as they did with no applied voltage. The charge densities also tended to increase with temperature for the applied DC voltage measurement with no BTA, except for the temperature change between 15°C and 30°C with negative applied voltages. However it was argued that with increasing applied negative voltage the temperature dependence of the charge density would again be an increase in charge density with an increase in temperature. In these measurements the BTA most likely altered the system parameters such that this operating point with a reversed temperature dependence was not observed.

Figure 6-24 and Figure 6-25 compare the charge densities as a function of applied DC voltage with and without BTA at four temperatures. For the temperatures of 45°C and 60°C and the temperatures of 15°C and 30°C with positive applied voltage the charge densities were reduced with the addition of BTA. The two highest temperatures demonstrated the greatest reduction, where the charge densities were reduced by up to 50%. However for negative applied voltages at both 15°C and 30°C the charge densities were increased with the addition of BTA. Since the conductivity is also changed with the addition of BTA this phenomena is reasonable as the conductivity changes relaxation times and potentially the double layer thickness. However if the charge in the double layer is reduced with the addition of BTA it may be reasonable to expect a reduction in charge densities for larger negative voltages.

This would result from the lesser importance of the equilibrium double layer thickness as the applied voltages tend to add larger enhancements to the thickness. Although the reduced relaxation time of the oil with BTA could still result in a larger charge density, it was observed in these measurements that for positive applied voltages

this was not the case. Also, if it is assumed that the negative voltages are associated with the enhancement of the double layer thickness at the outer interface, because of the positive sign of the charge, then it is reasonable that the negative voltage might need to be larger than the positive voltage because of the weaker electric field at the outer cylinder than at the inner cylinder.

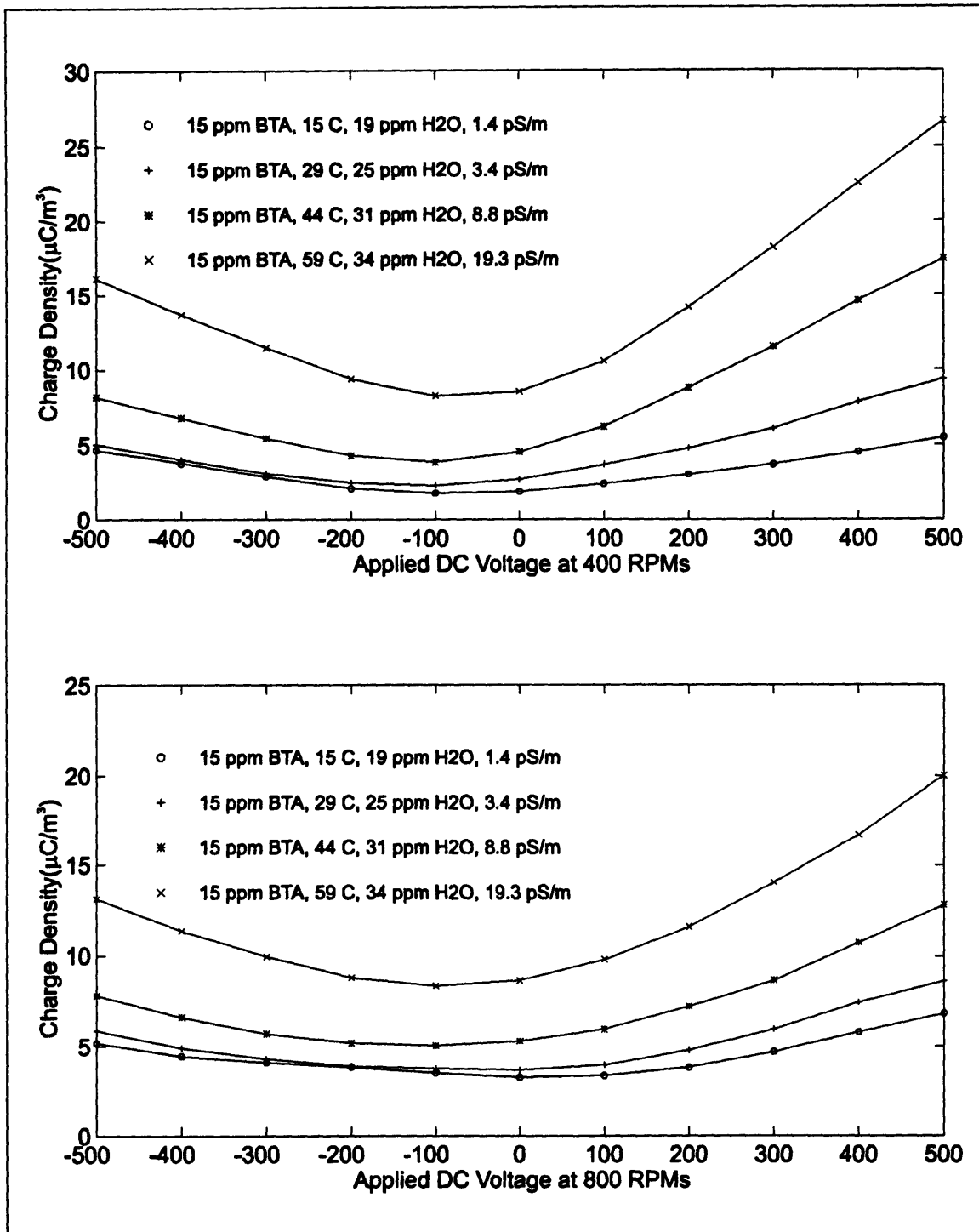


Figure 6-23: Temperature and applied DC voltage dependence on charge density with 15 ppm BTA.

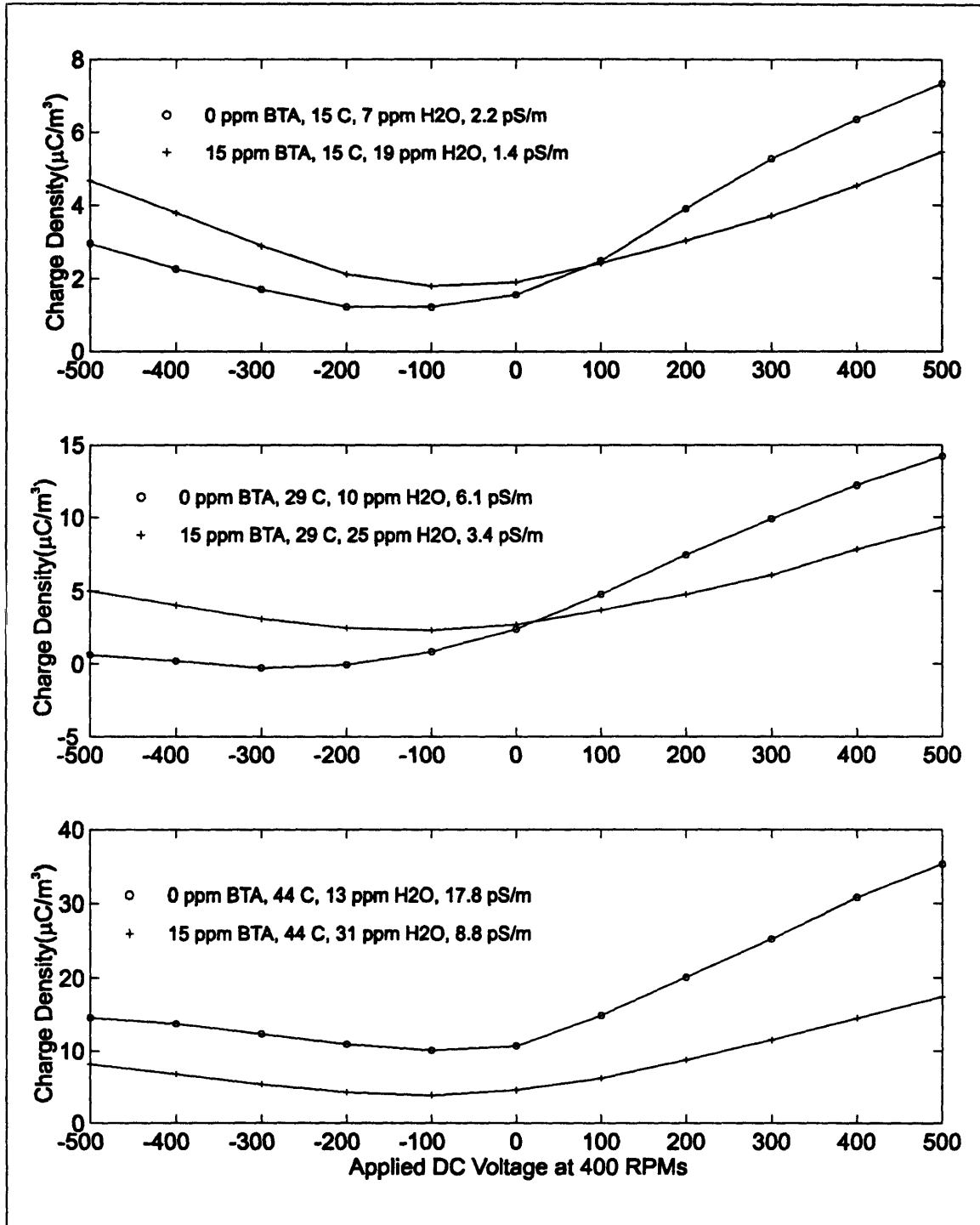


Figure 6-24: Comparison of charge density with and without BTA at varied applied DC voltage and temperature with the rotation rate at a constant 400 RPM.

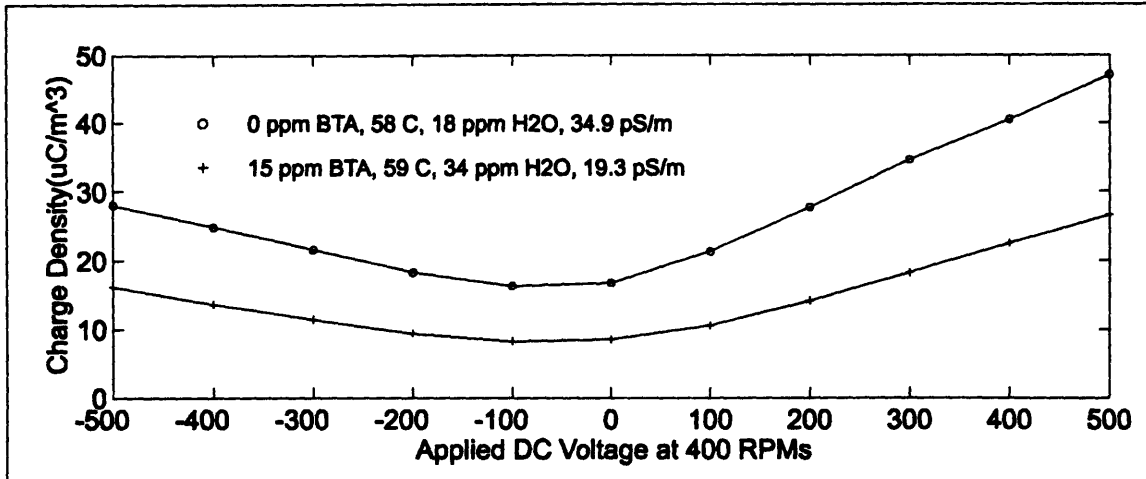


Figure 6-25: Comparison of charge density with and without BTA at varied applied DC voltage at 60°C with the rotation rate at a constant 400 RPM.

6.5.4 Applied AC Voltage

This section compares the charge density's dependence on applied AC voltages for the aged oil with 15ppm BTA with various oil temperatures and AC frequencies. Measurements with BTA are also compared to those without BTA at four temperatures.

Figure 6-26 compares the charge densities as functions of frequency at several temperatures for rotation rates of both 400 and 800 RPMs. The temperature dependence of the charge densities again repeats itself with higher temperatures resulting in larger densities as it has for both DC applied voltages and short circuit/open circuit measurements with BTA. The frequency dependence of the charge densities, which demonstrates an increase in charge density with decreasing frequency, matches the dependence observed without BTA.

Figure 6-27 and Figure 6-28 compare the charge densities in response to the applied AC voltages at 400 RPMs for four temperatures with and without BTA. Measurements at 30°C, 45°C, and 60°C show a reduction in charge density with the addition of BTA while the measurement at 15°C shows a slight increase. The increase in the 15°C measurement can be validated by observing the effects in the charge density response with the applied DC voltage at 15°C. In the DC measurement the BTA was

observed to increase the charge density for negative voltages, while decreasing it for positive voltages. If the AC charge density response is assumed to be an average of the DC response weighted by the applied AC sinusoid over one period and scaled by a factor which is inversely related to frequency then the slight increase is reasonable.

If this same argument for determining the comparative AC response is made for the other temperatures all agree except for the 30°C measurement. The DC charge response for the 30°C temperature demonstrates an almost equal amount of charge increase for negative applied voltages as decrease with positive applied voltages when BTA has been added. Based on previous arguments, this would indicate that the AC response with and without BTA should be nearly the same. However the AC charge densities appear to be significantly reduced with the addition of BTA. In observing the AC charge densities at the higher frequencies a difference with and without BTA is apparent. Since past measurements generally show the same charge density value at high frequency applied AC or open circuit/short circuit terminal constraints a discrepancy exists in comparing these two quantities for the 30°C measurements. This discrepancy is most likely due to a change in system parameters as a result of the time between measurements.

Chapter 6: Aged Oil Measurements

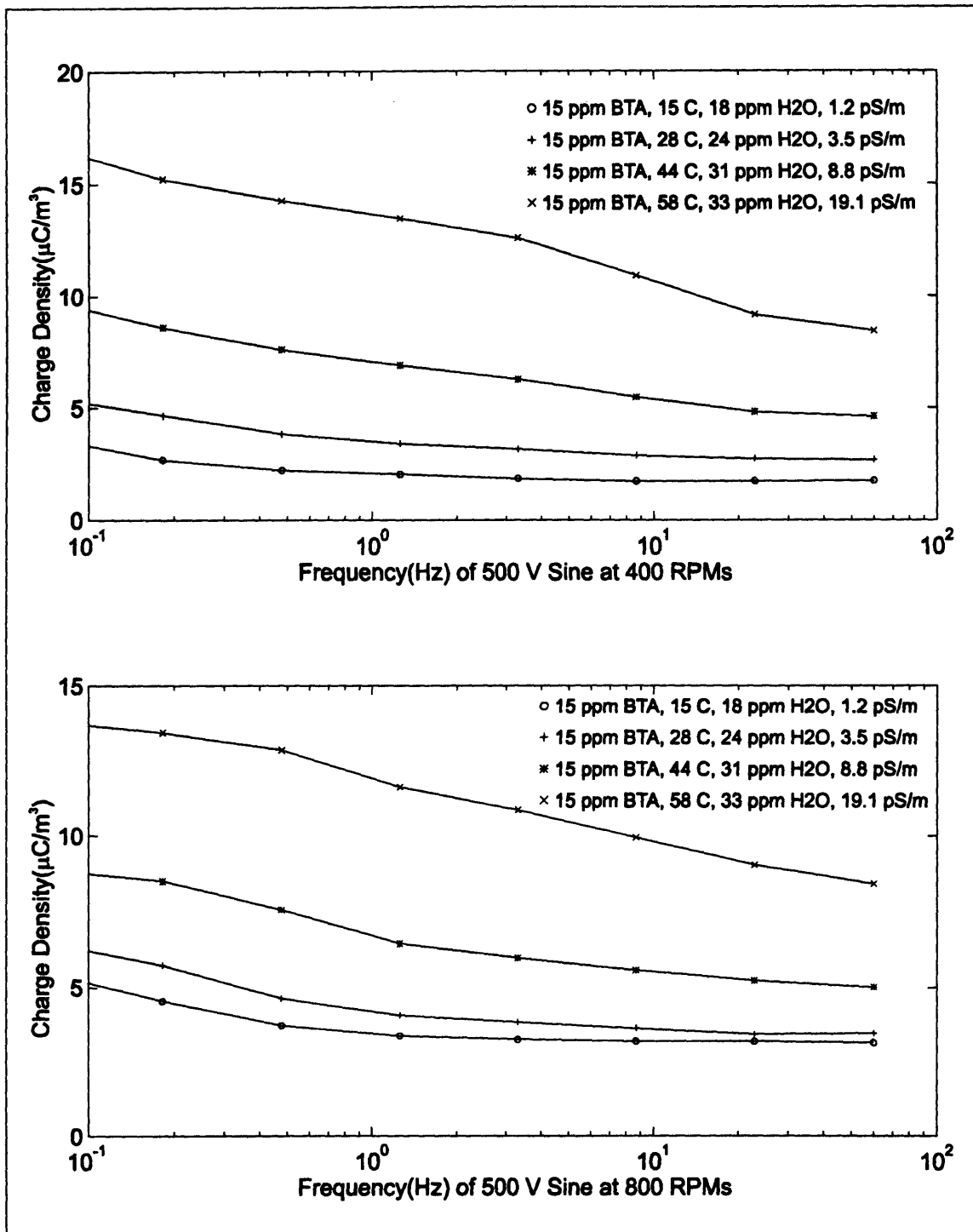


Figure 6-26: Temperature and applied AC voltage dependence on charge density with 15 ppm BTA.

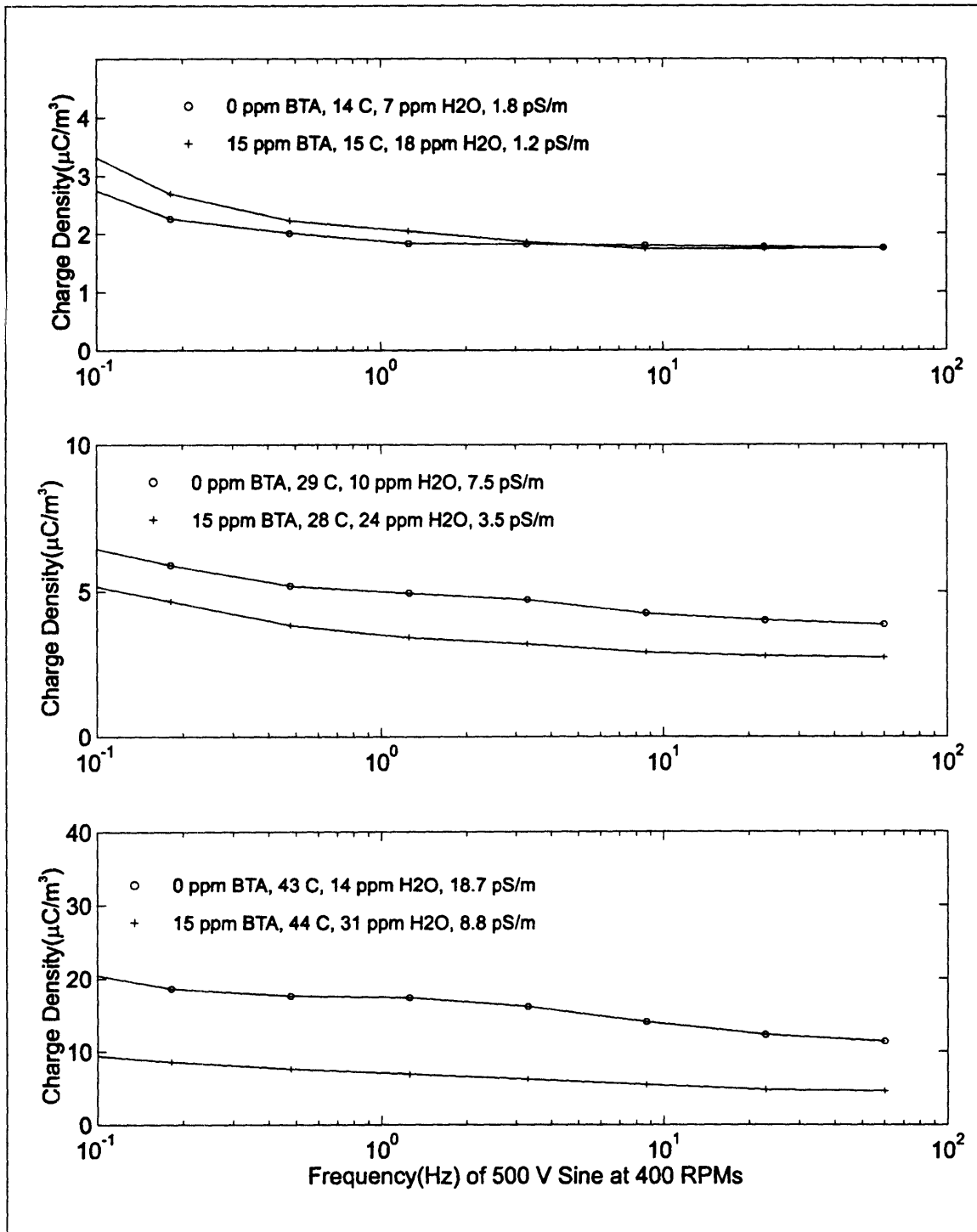


Figure 6-27: Comparison of charge density with and without BTA at varied applied AC voltage and temperature.

Chapter 6: Aged Oil Measurements

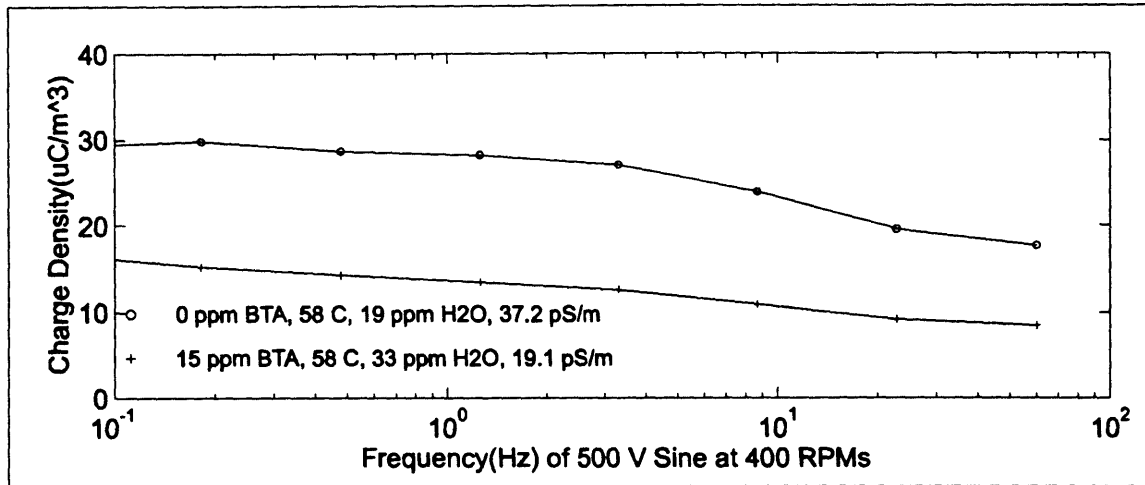


Figure 6-28: Comparison of charge density with and without BTA at varied applied AC voltage and temperature.

7 Conclusions

7.1 Transients

In chapter four several transient phenomena were observed as the result of both imposed and uncontrolled parameter changes. These transients were induced by cleaning of the system, step increases of the rotational rate, the application of DC prestresses while the system was at rest, and application of DC stresses while the inner cylinder was rotating.

The transient phenomena associated with the cleaning of the system proved to be the most interesting. Here large and abrupt changes in the charge density and terminal voltage of the Couette charger were observed in the first three to five hours after rotation was started for the very first measurements after loading with oil. The charge densities at times were 5 to 6 times larger than in measurements following the transient, while terminal voltages were at least ten times greater during the transient. This behavior is significant because many electrification related transformer failures occur shortly after installation or after the oil has been removed and replaced during servicing.

The other transient phenomena associated with rotation changes and electrical stressing of the Couette charger are significant because of the time constants which are observed. The time constants of both charge density and terminal parameters during many of these transients are seen to be much longer than known time constants of the system, including those of the dielectric relaxation and fluid dynamics. This may indicate that the relatively long time constants are associated with interfacial parameters or rates. Further

Chapter 7: Conclusions

investigation will require a more direct approach in observing and measuring interfacial properties.

7.2 Fresh and Aged Oils

Many measurements were made in this thesis using both fresh and aged oils. In chapter 3 preliminary measurements of fresh oil were made. When these were later compared with the fresh oil measurements of chapter 5 large differences were observed between the terminal voltages even under similar conditions. Since these oils were taken from the same barrel, it seems as though the history of the interface and handling of the oil can play a large role in determining the measured terminal voltage, even with an interface consisting of stainless steel and oil. However the terminal currents between these two sets of measurements were more comparable especially at the higher temperatures. The charge densities also showed some variation between measurements of fresh oil. For one measurement with fresh oil, the charge density over all temperatures at the highest rotation rates ranged from 1.5 to 4 mC/m³, while for the other the charge ranged from 4 to 6 mC/m³. Future experiments may require techniques which can create a more consistent interface, that will only change with changing oil properties.

Even though there are repeatability issues, measurements with aged oil provided currents and charge densities that were significantly larger than observed in fresh oil measurements. The maximum measured terminal currents at the temperature of 60° for the fresh oil had a magnitude of approximately 500pA, while the aged oil demonstrated a peak current of 1200pA. This may have been expected since the oil conductivity for the aged oil was approximately 4 times greater than that of the fresh oil. However the charge densities for the aged oil ranged from 5 to 15 μC/m³ over all temperatures, which has a significantly larger average and wider range than the fresh oil measurements. This is significant since the conductivity as previously stated was approximately 4 times greater than in the fresh oils, which would tend to reduce the bulk charge densities, indicating a significantly larger amount of charge in the double layer.

The effects of energization on charge densities were also studied for the aged oil. Applications of DC voltages between the Couette charger's inner and outer cylinders

resulted in both increases and decreases in charge density. However increases of the charge density were much larger than the decreases, being up to two times greater than with no applied voltage. The decreases were only observed with negative applied voltages. For many measurements, it was also observed that as the voltage became increasingly negative, the bulk charge densities were again increased rather than decreased. This effect of a slight decrease is most likely due to the difference in both sublayer thickness and electric field intensity at inner and outer cylinders due to the cylindrical geometry. Therefore in general it may be expected that applied voltages will increase the charge density.

Application of AC voltages were also demonstrated to increase the charge density in the aged oils. The charge density increase was very dependent on the frequency with lower frequencies giving larger increases. However most large power transformers are operated at a frequency near 50 or 60 Hz. In the measurement only small increases were observed at these frequencies, but based on observations for the DC applied voltages, it is likely that larger electric fields, that may be observed in a real transformer, would result in larger increases in charge density.

7.3 BTA Effects

BTA was added to both fresh oil in chapter 5 and aged oil in chapter 6. Concentrations of 5, 10, and 15 ppm were added at a temperature of 60°C. The addition of BTA was observed to have a positive effect on the reduction of both charge densities and terminal currents in most cases. Each addition of BTA to bring the oil concentration from 0 to 15ppm tended to lower both the charge density and terminal current in the fresh oil at 60°C. The aged oil also demonstrated reductions in charge density with each addition at 60°C. However the terminal current was observed to increase significantly for certain rotation rates after the first addition of 5 ppm, although further additions continued to reduce the terminal current. At a concentration of 15ppm and a temperature of 60°C the total reduction in charge density for the fresh oil was 25%, while the total reduction for the aged oil was 30%. At lower temperatures of 15°C and 30°C the addition of BTA in

Chapter 7: Conclusions

the aged oil resulted in only slight changes in charge density, including increases at certain rotation rates.

The addition of BTA in the aged transformer oil also reduced charge densities due to applied voltages. These reductions were comparable to the percent reductions observed at each temperature with no applied voltage. However two exceptions were observed at 15°C and 30°C with negative applied DC voltage. Under these conditions the charge density increased from the 0 ppm BTA value, although these increases only represented charge densities that were less than those of positive applied DC voltages with equal magnitude.

The conductivity of the oil was also significantly reduced by the addition of BTA. In the case of the fresh oil, 15ppm of BTA reduced the conductivity by 30%, while the conductivity of the aged oil was reduced by approximately 50%. This reduction in conductivity is beneficial in reducing ohmic losses in the oil and improving efficiency of a transformer, but the reduction of conductivity also increases the relaxation time of charge in the oil promoting electrification. However the addition of 15ppm BTA still generally resulted in much greater charge reductions than any observed increases.

Appendix A

BTA Addition

A.1 BTA Concentrate Preparation

A.1.1 BTA Concentration Calculations

The volume of concentrated BTA/Oil solution/suspension which must be added to the Couette Charger in order to achieve a desired concentration is dependent on the concentration of the concentrate and the total volume of oil in the Couette Charger. The symbols used in the following calculations of the concentrate concentration are defined as follows:

| | |
|-----------|---|
| D_{oil} | Density of Oil |
| K_{con} | Mass Fraction of BTA in Concentrated BTA Solution |
| M_{BTA} | Mass of BTA in Concentrated BTA Solution |
| V_{oil} | Volume of Oil in Concentrated BTA Solution |
| M_{oil} | Mass of Oil in Concentrated BTA Solution |

The mass fraction of BTA in the oil concentrate is defined as the total mass of BTA in the concentrate divided by the total mass of oil and BTA as in the following equation:

$$K_{con} = \frac{M_{BTA}}{M_{oil} + M_{BTA}} \quad (A.1)$$

To determine the total mass of BTA required to bring a desired volume of oil to a given concentration K_{con} , M_{oil} is replaced in the previous equation by its relation to density of the oil D_{oil} and its volume V_{oil} . Solving for the mass of BTA required yields the equation,

$$M_{BTA} = \frac{K_{con} M_{oil}}{(1 - K_{con})} = \frac{K_{con} V_{oil} D_{oil}}{(1 - K_{con})} \quad (A.2)$$

Appendix A: BTA Addition

The following symbols are used in determining the volume of concentrate needed to bring the CC to a given concentration:

| | |
|------------|---|
| V_{cc} | Volume of Oil in Couette Charger |
| V_{inj} | Volume of Oil Injected |
| K_{cc} | Mass Fraction of BTA in Couette Charger After Injection |
| K_{con} | Mass Fraction of BTA in Concentrated BTA Solution |
| M_{tot} | Total Mass of Oil in Couette Charger After Injection |
| M_{TBTA} | Total Mass of BTA to Achieve Concentration K_{cc} after Injection |

It is assumed that the injection volume of oil will increase the total volume of oil in which the BTA will be distributed when it is fully mixed, even though the CC is of fixed volume. This is because the CC is directly connected to the mini-reservoir in order to allow the injected volume of oil to be displaced, however this also allows BTA to diffuse into the mini-reservoir, making it part of the CC effective oil volume. Therefore the total mass of oil after injection is equal to the sum of the starting effective CC mass and the mass of oil injected. The total mass written in terms of the oil volumes is,

$$\underline{M_{tot} = D_{oil}(V_{cc} + V_{inj})} \quad (A.3)$$

The mass fraction of BTA in the CC effective volume can be written as

$$K_{cc} = \frac{M_{TBTA}}{M_{tot} + M_{TBTA}} \quad (A.4)$$

Substituting M_{tot} from equation A.3 and solving for M_{TBTA} yields an expression for the mass of the BTA required after the injection.

$$M_{BTA} = \frac{K_{cc} M_{tot}}{(1 - K_{cc})} = \frac{K_{cc}}{(1 - K_{cc})} D_{oil}(V_{cc} + V_{inj}) \quad (A.5)$$

Based on the concentration of the injected volume, the mass of BTA injected can also be determined as

$$M_{BTA} = \frac{K_{con}}{(1 - K_{con})} D_{oil} V_{inj} \quad (A.6)$$

Since the mass of BTA required for the given injection volume must equal the actual mass of BTA in the injected volume, by equating Eq. A.5 and Eq. A.6, we can then solve for the injection volume yielding

$$V_{inj} = \frac{\frac{K_{cc}}{(1-K_{cc})}V_{cc}}{\left(\frac{K_{con}}{(1-K_{con})} - \frac{K_{cc}}{(1-K_{cc})}\right)} = \frac{K_{cc}V_{cc}(1-K_{con})}{K_{con}(1-K_{cc}) - K_{cc}(1-K_{con})} \quad (A.7)$$

Using this expression we can determine the volume of concentrate required to achieve a desired concentration of BTA in the effective CC volume. If subsequent injections are to be made using the same concentrate concentration in order to further increase the BTA concentration in the CC, the required injection volume can be determined by subtracting the total volume of concentrate already injected from the total amount required to achieve the desired concentration.

A.1.2 BTA Solution/Suspension Preparation

The preparation of the BTA concentrate requires the drying and degassing of the oil being used along with the dissolving of the BTA into the oil. Preparation begins with determining the required amount of BTA for the amount of oil being prepared from Eq. A.2. The oil and BTA are then combined in a vacuum flask and allowed to dry and degas without heating for approximately one hour. A magnetic stirrer was also used to keep the oil well mixed while drying during this drying time. Next the flask was heated in a water bath with continued vacuum and stirring until the bath temperature reached approximately 95 °C or until all BTA had dissolved. The concentrate was then allowed to cool with both stirring and vacuum. If the BTA was being injected in a suspension form, the vacuum would be removed when cooled to room temperature, but the stirring would be continued in order to help maintain a uniform suspension. For cases where a solution was used, the injection oil was taken from the flask before BTA began precipitating from the solution.

A.2 Addition of BTA to the Couette Charger

The BTA concentrate was added to the charger through the injection port, which was connected to a teflon tube leading to the space near the gap between inner and outer

Appendix A: BTA Addition

cylinders. The valves were set to connect the CC to only the mini-reservoir, which contained a slight amount of oil. This minimized the amount of potential error in the BTA concentration caused by diffusion into the relatively large volume of the reservoir. Injections were made with the CC rotating, which allowed the concentrate to be rapidly mixed from the turbulence of the fluid flow and also allowed simultaneous observations of the effects on electrification.

Appendix B

Acquisition and System Control Software and Plotting Routines

B.1 Acquisition and Control Software

Data acquisition and control of all instruments in the Couette facility is accomplished by the use of a custom application which allows the user to tailor experiment events and data acquisition parameters to match the desired experiment. This flexible behavior is achieved by the software acting as an interpreter of a user designed schedule which contains high level commands. The schedule serves the purpose of instructing each instrument as to what their current activity should be, and also acts as a coordinator to synchronize events based on timing and individual instrument events which are signaled through a system of flags. The controlling code of each instrument is multitasked within the complete system of instruments allowing measurement and control of each instrument to be virtually independent of the others activities. The data taken by each instrument is then placed in a common textual file as the data is acquired in real time. After the completion of an experiment this textual file is then converted to a more efficient binary MAT file with the data of each instrument placed in a matrix which has a generic format and systematic name. This allows generic plotting and manipulation routines to be used for the data of any instrument, and also allows the arrangement of data from multiple instruments which is parametric in time.

B.1.1 Schedule Description

A schedule file for the Spin application serves the purpose of directing the parameters measured and set by each instrument. A schedule contains both commands which guide

Appendix B: Acquisition and System Control Software and Plotting Routines

the execution of the schedule itself and commands which are specific to each instrument. The commands to guide the schedule execution are referred to as scheduler commands and consist of commands to delay and direct execution based on time intervals, direct execution based on user or instrument events, and maintain looping counts. The commands which are used to control instruments are referred to as instrument commands.

Schedule Format:

The format of a schedule begins with a header line used to validate the file as follows:

```
{Couette Facility Schedule}
```

The actual schedule then begins. Each line of the schedule starts with a line number, which will be the basis for the sequence that the schedule is executed (unless instructions alter this normal flow). Following the line number is one of three symbols: a “:”, “!”, or a “/”. The “!” is used to designate the command following as a scheduler command, while a “:” indicates an instrument specific command is to follow. The “/” indicates that the following text is only a comment and is not to be executed in any way.

Scheduler commands are composed of a three letter mnemonic and an argument which may be empty and is contained in parentheses. They have the following form:

```
# !ccc(arg)
```

where,

is the line number, *ccc* is the command, and *arg* is the argument specific to the command.

Instrument commands have an additional parameter besides having a different symbol following the line number. This additional parameter is the instrument ID which allows

the command to be directed to the proper instrument in the case of the presence of more than one instrument of a given type. The generic format of an instrument command is as follows:

```
# :ccc i(arg)
```

where,

is the line number, *ccc* is the command, *arg* is the argument specific to the instrument and *i* is the ID of the instrument to which the command is being directed.

Comments have a simple format and have a line number only to fix their position within the schedule. Their format is:

```
# / any text
```

The schedule file is ended with a footer to indicate the end of all schedule lines for parsing purposes and is as follows:

```
{End Couette Facility Schedule}
```

Schedule Writing and Usage

Schedules should be written to work with a certain configuration of instruments as a result of the existence and ID of each instrument being part of the configuration parameters of the system and instruments in the system. Therefore the instruments should be configured for the desired experiment before writing of a schedule. Configuration is done through dialog boxes in the software configuration menus and is straight forward. It should also be noted that system configurations are loaded independently of the schedules and so before a schedule is run, it should be checked that the proper configuration is loaded. Also, before a schedule is run, a data file must be selected if the data from instruments is to be saved. By simply selecting the New... menu item under the Data menu, a file name can be chosen or the default name based on the current month, day, year and experiment count for the day can be used. The schedule can now be run by selecting the Run... menu item in the Schedule menu. While the schedule is running the textual data from each instrument can be viewed, along with information generated by both the scheduler in executing scheduler commands, and by the instruments as they receive and follow

Appendix B: Acquisition and System Control Software and Plotting Routines

commands. Also, while the schedule is running, its flow can be paused or stopped with the appropriate command in the Schedule menu. If the schedule is waiting for an event, it can be manually forced to continue with the Continue command in the Schedule menu. The status of the scheduler is indicated in the status bar of the application and when the execution of the schedule has stopped it will be indicated. The data can now be exported to its matrix form.

B.1.2 Scheduler Commands

This section describes commands used by the scheduler. Commands exist for creating delays, altering the flow of execution, and waiting for both user and instrument events. Commands also exist for maintaining counts and for setting time markers which can then also be used to make branching decisions.

Branching based on instrument events is accomplished using the FDE (flag directed execution) and WFF (command), these work in conjunction with commands sent to instruments which send flags under specified conditions (see instrument commands to determine specific flags). Each flag has an instrument name and ID associated with it which allows the determination of the instrument which sent the flag. A third number indicates which flag the instrument sent, allowing an instrument to specify one of many of its possible events or conditions has occurred. The scheduler maintains a record of flags it has received, and when a WFF or FDE command is encountered it continually checks this record until some condition becomes true. Since flags are not automatically removed, the commands CAF (clear all flags) and CSF (clear selected flags) are used to remove several or all flags as desired.

Syntax and Description

Delay Execution

Description:

Holds execution of schedule for delay indicated by hours, minutes and seconds.

!DLY(hh:mm:ss)

hh:mm:ss - hours, minutes, seconds to wait before continuing execution

Jump To Line

Description:

Continues execution at non-sequential line.

!JMP (line)

line - line number of destination

End

Description:

Stops scheduler, shuts down instruments, ends measurements.

!END ()

User Directed Execution

Description:

Prompts user to make choice and then continues execution at line based on user choice.

!UDE(hh:mm:ss,expiration line,message 1,message 2,message 3,message 4,
choice1,line1,...,choice N,line N)

hh:mm:ss - hours, minutes, seconds to wait before continuing execution

expiration line - line to continue execution upon expiration of wait interval

message1 ... message 4 - lines 1 to 4 of message text for user(a space must be left for each line if blank)

choice N - text of choice N

line N - line to continue execution at if choice N is made by user

Set Loop Counter

Description:

Sets loop counter with given name to given value

!SLC (Name,value)

Appendix B: Acquisition and System Control Software and Plotting Routines

Name - Single capital letter of counter(A-Z)

value - value to which loop counter is set

Increment Loop Counter

Description:

Increments Loop Counter with given name by given increment

!INC (Name,increment)

Name - Single capital letter of counter(A-Z)

increment - increment to add to loop counter

Decrement Loop Counter

Description:

Decrements loop counter with given name by given decrement

!DEC (Name, decrement)

Name - Single capital letter of counter(A-Z)

decrement - decrement to subtract from loop counter

CDE

Description:

Loop counter directed execution

!CDE (Name,condition,value, true line, false line)

Name - Single capital letter of counter(A-Z)

condition - >, <, =

value - value to which loop counter is compared

true line - line to continue executing if condition is true(zero indicates next line)

false line - line to continue executing if condition is false(zero indicates next line)

MTR

Description:

Marks current time with named tag for reference

!MTR (tag name)

tag name - Single capital letter(A-Z) indicating tag

TDE

Description:

Time directed execution

!TDE (tag name, hh:mm:ss, condition, true line, false line)

tag name - Single capital letter(A-Z) indicating tag, * is reference to absolute start time

hh:mm:ss - hour, minute, and second which is compared to elapsed time since marked time.

condition - > or <

true line - line to continue executing if condition is true(zero indicates next line)

false line - line to continue executing if condition is false(zero indicates next line)

WFT

Description:

Wait for Time

!WFT (tag name, hh:mm:ss)

tag name - Single capital letter(A-Z) indicating tag, * is reference to absolute start time

hh:mm:ss - elapsed time from tag at which point execution will continue

CAF

Description:

Clears all flags which instruments have sent.

Appendix B: Acquisition and System Control Software and Plotting Routines

!CAF ()

CSF

Description:

Clears specified flags which instruments have sent if present.

!CSF (NNN1, ID1, flag1 #,, NNNn, IDn, flagn #)

NNN - Three Letter Instrument Name

ID - Instrument ID

- flag number

Wait for Flags

Description:

Waits for All or One of N flags or expiration time before continuing execution

!WFF(hh:mm:ss, logic operation, MMM1, ID1, #1,, MMMn, IDn, #n)

logic operation - & to wait for all flags, | to wait for one flag

hh:mm:ss - hours, minutes, seconds to wait before continuing execution

MMM - Three Letter Instrument Name

ID - Instrument ID

- flag number

Flag Directed Execution

Description:

Waits for flags and continues execution based on flag signaled or defaults to default line if expiration time has expired.

!FDE(hh:mm:ss, default line, MMM1, ID1, #1, ln#1,, MMMn, IDn, #n, ln#n)

hh:mm:ss - hours, minutes, seconds to wait before continuing execution

MMM - Three Letter Instrument Name

ID - Instrument ID

- flag number

ln# - line to restart execution on

B.1.3 Instrument Commands

This section describes the commands for each instrument. Each description includes a list of commands for each instrument including a summary of the command and the parameters of the command(if any). A list of flags which may be sent as a result of the execution of the command is also included for each command.

Motor Commands

Set Speed

Description:

Immediately sets the speed of the motor to the new value;

:MOT id(SET,newspeed)

id - ID of motor

newspeed - new speed in units determined by calibration

STEP Speed

Description:

Steps from a starting speed to an ending speed in an specified number of steps and remaining at each speed for a specified duration

:MOT id(STEP,startspeed,endspeed,stepcount,hh:mm:ss)

id - ID of motor

startspeed - starting speed in units determined by calibration

endspeed - ending speed in units determined by calibration

stepcount - steps to take between start and end speed

hh:mm:ss - duration of each step

Flags:

MOT,id,1 - Sent after each step

MOT,id,2 - Sent upon reaching end of last step

Ramp Speed

Appendix B: Acquisition and System Control Software and Plotting Routines

Description:

Ramps from start speed to stop speed at the specified rate.

:MOT id(RAMP,startspeed,endspeed,rate)

id - ID of motor

startspeed - starting speed in units determined by calibration

endspeed - ending speed in units determined by calibration

stepcount - steps to take between start and end speed

hh:mm:ss - duration of each step

Flags:

MOT,id,2 - Sent upon reaching endspeed.

Pulse Speed

Description:

Pulses between two speeds, maintaining each for a specified time and continuing for a specified duration.

:MOT id(PULSE,speed1,hh1:mm1:ss1,speed2,hh2:mm2:ss2,hh:mm:ss)

id - ID of motor

speed1 - first speed of pulse in units determined by calibration

hh1:mm1:ss1 - duration of speed1

speed2 - second speed of pulse in units determined by calibration

hh2:mm2:ss2 - duration of speed2

hh:mm:ss - duration of pulsing

Flags:

MOT,id,2 - Sent upon reaching end of pulsing duration.

MOT,id,3 - Sent after each half cycle

MOT,id,4 - Sent after each full cycle

Terminal Switch Commands

Set Position

Description:

Immediately sets the position of the three position switch

:ZSW id(switchposition)

id - ID of switch

switchposition - new position 1,2, or 3

Bubbler Commands**Set State****Description:**

Immediately sets the state of the bubbler

:BUB id(state)

id - ID of bubbler

state - new state OFF, DRY, WET

Electrometer Commands**Change Electrometer Mode****Description:**

Selects the measurement mode of the electrometer: voltage, current, resistance, charge, new-charge. If measurement is in progress, measurement will continue in new mode.

:ELC id(M,m)

id - ID of electrometer

m - Mode of electrometer: V for voltage, A for current, R for resistance, C for charge, N for new charge measurement.

Take Single Measurement

Appendix B: Acquisition and System Control Software and Plotting Routines

Description:

Takes a single measurement of the specified quantity. If the electrometer is in a different mode, the mode will automatically change and remain in the specified state until changed by additional instructions.

:ELC id(S,m)

id - ID of electrometer

m - Type of measurement: V for voltage, A for current, R for resistance, C for charge, N for new charge measurement.

Take Repeated Measurements

Description:

Takes a repeated measurement of the specified quantity. If the electrometer is in a different mode, the mode will automatically change and remain in the specified state until changed by additional instructions.

:ELC id(R,m,hh:mm:ss)

id - ID of electrometer

m - Type of measurement: V for voltage, A for current, R for resistance, C for charge, N for new charge measurement.

hh:mm:ss - Time between each measurement

End Repeated Measurements

Description:

Ends a repeated measurement and leaves the electrometer in the current(not Amps) mode.

:ELC id(E)

id - ID of electrometer

Wavetek Commands

Set

Description:

Immediately set the output of the amplifier to the specified waveform at the specified frequency, amplitude and offset based on units calibration.

:WAV id(SET,DC,offset)
:WAV id(SET,SIN,amplitude,offset,frequency(HZ))
:WAV id(SET,ISIN, amplitude,offset,frequency(HZ))
:WAV id(SET,COS, amplitude,offset,frequency(HZ))
:WAV id(SET,ICOS, amplitude,offset,frequency(HZ))
:WAV id(SET,TRI, amplitude,offset,frequency(HZ))
:WAV id(SET,SQR, amplitude,offset,frequency(HZ))
:WAV id(OFF)

id - ID of electrometer

amplitude - peak amplitude of waveform

offset - offset of waveform

frequency - >2.4uHz and < 100,000 Hz

Flags:

none.

STEPS

Description:

Steps amplitude of waveform.

:WAV id(STEPS,SIN,start amplitude, stop amplitude, steps, hh:mm:ss
,offset,frequency(HZ))

:WAV id(STEPS, ISIN,start amplitude, stop amplitude, steps, hh:mm:ss
,offset,frequency(HZ))

:WAV id(STEPS, COS,start amplitude, stop amplitude, steps, hh:mm:ss
,offset,frequency(HZ))

:WAV id(STEPS, ICOS,start amplitude, stop amplitude, steps, hh:mm:ss
,offset,frequency(HZ))

Appendix B: Acquisition and System Control Software and Plotting Routines

:WAV id(STEPA, TRI,start amplitude, stop amplitude, steps, hh:mm:ss ,offset,frequency(HZ))

:WAV id(STEPA, SQR,start amplitude, stop amplitude, steps, hh:mm:ss ,offset,frequency(HZ))

id - ID of electrometer

start amplitude - peak amplitude of step start

stop amplitude - peak amplitude of step end

offset - offset of waveform

frequency - $>2.4\mu\text{Hz}$ and $< 100,000 \text{ Hz}$

hh:mm:ss - duration of each step

steps - number of transitions

Flags:

WAV,id,1 - Sent upon reaching end of current step.

WAV,id,2 - Sent upon reaching end of all steps.

STEPO

Description:

Steps offset of waveform.

:WAV id(STEPO,DC,start offset, stop offset, steps, hh:mm:ss)

:WAV id(STEPO,SIN,start offset, stop offset, steps, hh:mm:ss , amplitude,frequency(HZ))

:WAV id(STEPO, ISIN,start offset, stop offset, steps, hh:mm:ss , amplitude,frequency(HZ))

:WAV id(STEPO, COS,start offset, stop offset, steps, hh:mm:ss , amplitude,frequency(HZ))

:WAV id(STEPO, ICOS,start offset, stop offset, steps, hh:mm:ss , amplitude,frequency(HZ))

:WAV id(STEPO, TRI,start offset, stop offset, steps, hh:mm:ss , amplitude,frequency(HZ))

:WAV id(STEPO, SQR,start offset, stop offset, steps, hh:mm:ss , amplitude,frequency(HZ))

id - ID of electrometer

start offset - peak amplitude of step start

stop offset - peak amplitude of step end

amplitude - offset of waveform

frequency - >2.4uHz and < 100,000 Hz

hh:mm:ss - duration of each step

steps - number of transitions

Flags:

WAV,id,1 - Sent upon reaching end of current step.

WAV,id,2 - Sent upon reaching end of all steps.

SWEEPF

Description:

Sweeps through range of frequencies using the minimum number of cycles and minimum duration to determine the actual length of time at each frequency.

:WAV id(SWEEPF,SIN,start frequency, stop frequency, steps, lin/log, min num periods, hh:mm:ss , amplitude, offset)

:WAV id(SWEEPF, ISIN,start frequency, stop frequency, steps, lin/log, min num periods, hh:mm:ss , amplitude, offset)

:WAV id(SWEEPF, COS,start frequency, stop frequency, steps, lin/log, min num periods, hh:mm:ss , amplitude, offset)

:WAV id(SWEEPF, ICOS,start frequency, stop frequency, steps, lin/log, min num periods, hh:mm:ss , amplitude, offset)

:WAV id(SWEEPF, TRI,start frequency, stop frequency, steps, lin/log, min num periods, hh:mm:ss , amplitude, offset)

:WAV id(SWEEPF, SQR,start frequency, stop frequency, steps, lin/log, min num periods, hh:mm:ss , amplitude, offset)

Appendix B: Acquisition and System Control Software and Plotting Routines

id - ID of electrometer

start frequency - starting frequency $>2.4\mu\text{Hz}$ and $< 100,000 \text{ Hz}$

stop frequency - ending frequency $>2.4\mu\text{Hz}$ and $< 100,000 \text{ Hz}$

amplitude - amplitude of waveform

hh:mm:ss - minimum duration of each step

steps - number of transitions

min num periods - minimum number of periods in each step

lin/log - LIN for linear step spacing in frequency LOG for logarithmically spaced steps

Flags:

WAV,id,1 - Sent upon reaching end of current step.

WAV,id,2 - Sent upon reaching end of all steps.

Absolute Charge Sensor Commands

Purge Bellows

Description:

Purges the Bellows the specified number of times. Purging begins when the current GPM frequency is done. If GPM measurements are simultaneously being taken, the next purging if $n>1$ will be when the GPM has again finished.

:ACS id(P,n)

id - ID of controller box of ACS

n - number of times to purge

Flags:

ACS,id,1 - Sent after each purge.

ACS,id,2 - Sent after n purgings.

Single Charge Measurement

Description:

Starts a single charge density measurement when the GPM completes the current frequency measurement.

:ACS id(S)

id - ID of controller box of ACS

Flags:

ACS,id,3 - Sent after measurement complete

Repeated Charge Measurement**Description:**

Starts repeated charge density measurement when the GPM completes the current frequency measurement.

:ACS id(R, hh:mm:ss)

id - ID of controller box of ACS

hh:mm:ss - Repeat rate of Measurements. The true repeat rate will be slower if this is less than the actual time of the measurement or a GPM measurement is simultaneously being taken.

Flags:

ACS,id,3 - Sent after each measurement is complete.

End ACS Function**Description:**

Immediately stops any measurement or purging of the ACS.

:ACS id(E)

id - ID of controller box of ACS

Gain and Phase Measurement Commands

Single Measurement at Single Frequency

Description:

Start a single measurement at a single frequency, data is generated for specified GPM channels which must also be enabled.

:GPM id(S,freq.,1,2,3,4)

id - ID of controller box of GPM

freq - log of frequency of measurement

1,2,3,4 - enter zero for no measurement on channel, any non-zero value for a measurement;

Flags:

GPM,id,1 - Sent after measurement is complete.

Single Frequency Sweep

Description:

Start a single frequency sweep over the specified range, data is generated for specified GPM channels which must also be enabled.

:GPM id(W,start,stop,1,2,3,4)

id - ID of controller box of GPM

start - log of starting frequency of measurement

stop - log of ending frequency of measurement

1,2,3,4 - enter zero for no measurement on channel, any non-zero value for a measurement;

Flags:

GPM,id,1 - Sent after measurement is complete.

GPM,id,2 - Sent after sweep is complete.

Repeated Measurement at Single Frequency

Description:

Start a repeated measurement at a single frequency, data is generated for specified GPM channels which must also be enabled.

:GPM id(R,hh:mm:ss,freq.,1,2,3,4)

id - ID of controller box of GPM

hh:mm:ss - interval to repeat measurements; if the measurement time is larger or ACS measurement are simultaneously being taken the true interval may be longer.

freq - log of frequency of measurement

1,2,3,4 - enter zero for no measurement on channel, any non-zero value for a measurement;

Flags:

GPM,id,1 - Sent after measurement is complete.

Repeated Frequency Sweep**Description:**

Start a single frequency sweep over the specified range, data is generated for specified GPM channels which must also be enabled.

:GPM id(M,hh:mm:ss,start,stop,1,2,3,4)

id - ID of controller box of GPM

hh:mm:ss - interval to repeat measurements; if the measurement time is larger or ACS measurement are simultaneously being taken the true interval may be longer.

start - log of starting frequency of measurement

stop - log of ending frequency of measurement

1,2,3,4 - enter zero for no measurement on channel, any non-zero value for a measurement;

Flags:

GPM,id,1 - Sent after measurement is complete.

GPM,id,2 - Sent after each sweep is complete

End GPM Function**Description:**

Immediately stops any measurement GPM.

Appendix B: Acquisition and System Control Software and Plotting Routines

:GPM id(E)

id - ID of controller box of ACS

Thermocouple Commands

Take Single Temperature Measurement and Specify Flag Conditions

Description:

Take a single temperature measurement.

:TEM id(S,condition 1, condition 1 temp, condition 2, condition 2 temp)

id - ID of thermocouple

condition 1 - either < or > any other character to ignore

condition 1 temp - temperature to compare to measured using specified condition.

condition 2 - either < or > any other character to ignore

condition 2 temp - temperature to compare to measured using specified condition

Flags:

TEM,id,1 - Sent if > condition is true.

TEM,id,2 - Sent if < condition is true.

Take Repeated Temperature Measurements and Specify Flag Conditions

Description:

Take repeated temperature measurements.

:TEM id(R,hh:mm:ss,condition 1, condition 1 temp, condition 2, condition 2 temp)

id - ID of thermocouple

hh:mm:ss - repeat rate of temperature measurements

condition 1 - either < or > any other character to for no condition

condition 1 temp - temperature to compare to measured using specified condition.

condition 2 - either < or > any other character for no condition

condition 2 temp - temperature to compare to measured using specified condition

Flags:

TEM,id,1 - Sent if > condition is true.

TEM,id,2 - Sent if < condition is true.

End Repeated Temperature Measurements

Description:

Take repeated temperature measurements.

:TEM id(E)

id - ID of thermocouple

Moisture Meter Commands

Take Single Moisture Measurement and Specify Flag Conditions

Description:

Take a single Moisture measurement and check measurement against specified flag conditions if any and send flag.

:MST id(S,condition comparison quantity,condition 1, condition 1 quantity, condition 2, condition 2 quantity)

id - ID of thermocouple

condition comparison quantity - R for relative saturation, P for PPM if instrument is configured for a mode generating PPM quantities, any other character for no condition.

condition 1 - either < or > any other character to ignore

condition 1 quantity - quantity to compare to measured using specified condition.

condition 2 - either < or > any other character to ignore

condition 2 quantity - quantity to compare to measured using specified condition

Flags:

MST,id,1 - Sent if > condition is true.

MST,id,2 - Sent if < condition is true.

Take Repeated Moisture Measurements and Specify Flag Conditions

Description:

Appendix B: Acquisition and System Control Software and Plotting Routines

Take repeated moisture measurements check conditions for each measurement made if any are specified and send flags if true.

:MST id(R, hh:mm:ss condition comparison quantity, condition 1, condition 1 quantity, condition 2, condition 2 quantity)

id - ID of thermocouple

hh:mm:ss - repeat rate of temperature measurements

condition comparison quantity - R for relative saturation, P for PPM if instrument is configured for a mode generating PPM quantities, any other character for no condition.

condition 1 - either < or > any other character to ignore

condition 1 quantity - quantity to compare to measured using specified condition.

condition 2 - either < or > any other character to ignore

condition 2 quantity - quantity to compare to measured using specified condition

Flags:

MST,id,1 - Sent if > condition is true.

MST,id,2 - Sent if < condition is true.

End Repeated Moisture Measurements

Description:

Take repeated temperature measurements.

:MST id(E)

id - ID of thermocouple

B.1.4 Software Module Descriptions

The Spin application was written in the C++ programming language and was specifically designed for the Windows operating system using Borland's OWL(Object Windows Language extension to C++). Following is a list of module files along with a brief description of the functionality included with the classes and functions contained within. Note that due to the size of the source code in these files, they do not appear in this thesis.

| File Names | Functional Description of Contents |
|-----------------------------|---|
| atod.h, atod.cpp | access of the analog to digital converter and multiplexer |
| bubbler.h, bubbler.cpp | control and configuration of apparatus to add and remove moisture from oil |
| comm.h, comm.cpp | access of serial communication ports |
| ctrlbox.h,ctrlbox.cpp | parameters and control of ACS,GPM instruments |
| cboxmold.h, cboxmold.cpp | configuration of ACS,GPM instruments |
| dac.h, dac.cpp | access of digital to analog converters |
| data.h, data.cpp | abstract data class for all instruments |
| datafile.h, datafile.cpp | searching of data file for data from specific instrument |
| dio.h, dio.cpp | access to digital IO ports |
| elcmeter.h, elcmeter.cpp | control and configuration of electrometer instrument |
| facility.h, facitily.cpp | management of instruments including directing of commands, collection of : data, flags, and information, and the distribution of processing time. |
| flags.h, flags.cpp | instrument flags and associated containers |
| gpib.h, gpib.cpp | access to GPIB interface |
| hizswch.h, hizswch.cpp | control and configuration of automatic selector switch with high cross channel impedance. |
| infowin.h, infowin.cpp | window displaying scrollable text information |
| infoque.h, infoque.cpp | information que cotainer |
| instruct.h, instruct.cpp | scheduler, instrument instruction class |
| instmold.h, instmold.cpp | abstract classes for instruments molds, used to configure and create instruments |
| instplst.h, instplst.cpp | Template class for loading, saving, and accessing instrument configurations |
| mmeter.h, mmeter.cpp | measurement and configuration of moisture instruments. |
| motor.h, motor.cpp | control and configuration of motors and pumps |
| notedata.h, notedata.cpp | class for storing experiment notes |
| notedlg.h, notedlg.cpp | dialog for creating experiment notes |
| paramf.h, paramf.cpp | storing of generic parameters to a file |
| schedule.h, schedule.cpp | loading, saving, and accessing of schedule |
| schdler.h, schdler.cpp | execution of schedule |
| sec2hms.h, sec2hms.cpp | conversion of seconds to hours, min, and seconds |
| spinwin.h, spinwin.cpp | main application and main window |
| tcpl.h, tcpl.cpp | measurement and configuration of thermocouples |
| usrqdlg.h, usrrqdlg.cpp | user request dialog for getting user input to direct schedule execution |
| wavetek.h, wavetek.cpp | control and configuration of arbitrary waveform generator |
| spinwin.rc, spinwin.rh | resource script and header file for icons, dialogs, and menus |

Appendix B: Acquisition and System Control Software and Plotting Routines

B.1.5 Experiment Schedules

This section contains the schedules used to acquire much of the data in this thesis. A short summary of the measurements made appears before the actual schedule.

Schedule: loading.sch

This schedule was used to monitor the loading process of the oil into the reservoir. Throughout the schedule, temperature and moisture of the reservoir and CC are measured. Before the oil is loaded, a full frequency sweep is made of the dielectric cells. The user is prompted for the start of the oil loading and the dielectric properties are measured at a single frequency. When the user indicates loading is complete, a full frequency sweep of the oil dielectric properties are made.

{Couette Facility Schedule}

```
10 :TEM 1(R,00:01:00,*,0,*,0)
20 :TEM 2(R,00:01:00,*,0,*,0)
30 :TEM 3(R,00:01:00,*,0,*,0)
40 :TEM 4(R,00:01:00,*,0,*,0)
45 :TEM 5(R,00:01:00,*,0,*,0)
50 :MST 1(R,00:01:00,*,*,0,*,0)
60 :MST 2(R,00:01:00,*,*,0,*,0)
65 :MST 3(R,00:01:00,*,*,0,*,0)
70 :GPM 1(W,4.0,-2.3,0,2,0,4)
80 !WFF(02:00:00,&,GPM,1,2)
90 !CAF()
100 !UDE (20:00:00,110,Ready to Load Oil?, , , ,Yes,110)
110 :GPM 1(R,00:01:00,-1.0,0,2,0,4)
120 !UDE (20:00:00,130,Done Loading Oil?, , , ,Yes,130)
130 :GPM 1(W,4.0,-2.3,0,2,0,4)
140 !WFF(02:00:00,&,GPM,1,2)
400 !END()
```

{End Couette Facility Schedule}

Schedule: drying.sch

This schedule was used to monitor the drying process of the oil. All temperatures and moistures are measured. A full frequency sweep is made of the dielectric cells before

drying and after drying. After the first sweep is completed, the used is prompted to indicate the beginning of drying. The conductivity is then monitored at a single frequency during the drying process. The user is again prompted to indicate the end of the drying process.

{Couette Facility Schedule}

```
10 :TEM 1(R,00:01:00,* ,0,* ,0)
20 :TEM 2(R,00:01:00,* ,0,* ,0)
30 :TEM 3(R,00:01:00,* ,0,* ,0)
40 :TEM 4(R,00:01:00,* ,0,* ,0)
45 :TEM 5(R,00:01:00,* ,0,* ,0)
50 :MST 1(R,00:01:00,* ,* ,0,* ,0)
60 :MST 2(R,00:01:00,* ,* ,0,* ,0)
65 :MST 3(R,00:01:00,* ,* ,0,* ,0)
70 :GPM 1(W,4.0,-2.3,0,2,0,4)
80 !WFF(02:00:00,&,GPM,1,2)
90 !CAF()
100 !UDE (20:00:00,110,Ready to Dry Oil?, , , ,Yes,110)
110 :GPM 1(R,00:01:00,-1.0,0,2,0,4)
111 :TEM 1(R,00:01:00,* ,0,* ,0)
112 :TEM 2(R,00:01:00,* ,0,* ,0)
113 :TEM 3(R,00:01:00,* ,0,* ,0)
114 :TEM 4(R,00:01:00,* ,0,* ,0)
115 :TEM 5(R,00:01:00,* ,0,* ,0)
116 :MST 1(R,00:01:00,* ,* ,0,* ,0)
117 :MST 2(R,00:01:00,* ,* ,0,* ,0)
118 :MST 3(R,00:01:00,* ,* ,0,* ,0)
120 !UDE (20:00:00,130,Done Drying Oil?, , , ,Yes,130)
130 :GPM 1(W,4.0,-2.3,0,2,0,4)
131 :TEM 1(R,00:01:00,* ,0,* ,0)
132 :TEM 2(R,00:01:00,* ,0,* ,0)
133 :TEM 3(R,00:01:00,* ,0,* ,0)
134 :TEM 4(R,00:01:00,* ,0,* ,0)
135 :TEM 5(R,00:01:00,* ,0,* ,0)
136 :MST 1(R,00:01:00,* ,* ,0,* ,0)
137 :MST 2(R,00:01:00,* ,* ,0,* ,0)
138 :MST 3(R,00:01:00,* ,* ,0,* ,0)
140 !WFF(02:00:00,&,GPM,1,2)
400 !END()
{End Couette Facility Schedule}
```

Appendix B: Acquisition and System Control Software and Plotting Routines

Schedule: group1.sch

This schedule performs several electrification measurements. All temperatures and moistures are measured, except for the reservoir's throughout the experiments. The first set of measurements made are of the terminal's open circuit voltage, short circuit current, and charge density at varied rotation. The rotation is initially ramped up to 1000 RPM and then stepped back down to zero. The second measurement is of the charge density as a function of applied voltages (-500 V to 500V) for 400 and 800 RPM rotation rates. The third measurement is of the charge density as a function of an applied AC voltage (500 V peak, .01Hz to 60 Hz) at both 400 and 800 RPM. The fourth set of measurements is of the open circuit decay of the terminal voltage after an applied DC voltage. Measurements with no rotation, constant 400 RPM rotation, constant 800 RPM rotation, and a measurement which stops rotation at the start of the open circuit voltage measurement. A full frequency sweep of dielectric properties is also made before and after all measurements.

{Couette Facility Schedule}

```
10 :TEM 1(R,00:01:00,*,0,*,0)
20 :TEM 2(R,00:01:00,*,0,*,0)
30 :TEM 3(R,00:01:00,*,0,*,0)
40 :TEM 4(R,00:01:00,*,0,*,0)
50 :MST 1(R,00:01:00,*,*,0,*,0)
60 :MST 2(R,00:01:00,*,*,0,*,0)
70 :GPM 1(W,4.0,-2.3,0,0,0,4)
80 !WFF(02:00:00,&,GPM,1,2)
90 !CAF()
100 :ACS 1(R,00:01:00)
110 :GPM 1(R,00:05:00,-1.0,0,0,0,4)
120 :ELC 1(R,V,00:00:05)
130 !DLY(00:05:00)
140 :MOT 1(RAMP,0,1000,11.1)
150 !WFF(02:00:00,&,MOT,1,2)
160 :MOT 1(STEP,1000,0,10,00:15:00)
170 !CAF()
172 :ACS 1(R,00:01:00)
175 :ELC 1(R,V,00:00:05)
180 !FDE(01:00:00,195,MOT,1,2,195,MOT,1,1,170)
```

195 !CAFQ
197 :ACS 1(R,00:01:00)
200 :ELC 1(R,A,00:00:05)
210 !DLY(00:15:00)
230 :MOT 1(RAMP,0,1000,11.1)
240 !WFF(02:00:00,&,MOT,1,2)
250 :MOT 1(STEP,1000,0,10,00:15:00)
260 !CAFQ
265 :ACS 1(R,00:01:00)
270 :ELC 1(R,A,00:00:05)
280 !FDE(01:00:00,285,MOT,1,2,285,MOT,1,1,260)
285 !CAFQ
290 :ELC 1(E)
300 :ACS 1(E)
310 !DLY(00:20:00)
320 // Start Applied Voltage Experiment
322 :TEM 1(R,00:01:00,*,0,*,0)
323 :TEM 2(R,00:01:00,*,0,*,0)
324 :TEM 3(R,00:01:00,*,0,*,0)
325 :TEM 4(R,00:01:00,*,0,*,0)
326 :MST 1(R,00:01:00,*,*,0,*,0)
327 :MST 2(R,00:01:00,*,*,0,*,0)
330 :ACS 1(R,00:01:00)
340 :GPM 1(R,00:10:00,-1.0,0,0,0,4)
350 :ZSW 1(3)
360 :WAV 1(SET,DC,-500)
370 !DLY(00:10:00)
375 :ACS 1(R,00:01:00)
380 :MOT 1(RAMP,0,400,20)
390 !WFF(01:00:00,&,MOT,1,2)
400 !CAFQ
420 !DLY(00:10:00)
430 :WAV 1(STEPO,DC,-500,500,10,00:15:00)
440 !CAFQ
450 :ACS 1(R,00:01:00)
460 !FDE(01:00:00,470,WAV,1,2,470,WAV,1,1,440)
470 !CAFQ
480 :ACS 1(R,00:01:00)
490 :MOT 1(RAMP,400,800,20)
500 !WFF(01:00:00,&,MOT,1,2)
510 !DLY(00:10:00)
520 :WAV 1(STEPO,DC,500,-500,10,00:15:00)
530 !CAFQ
540 :ACS 1(R,00:01:00)
550 !FDE(01:00:00,560,WAV,1,2,560,WAV,1,1,530)

Appendix B: Acquisition and System Control Software and Plotting Routines

```
560 !CAF()
570 :ACS 1(R,00:01:00)
580 :MOT 1(RAMP,800,0,-20)
590 !WFF(01:00:00,&,MOT,1,2)
600 !CAF()
605 :ACS 1(R,00:01:00)
610 :WAV 1(SET,DC,0)
620 !DLY(00:10:00)
630 :ZSW 1(1)
640 :ACS 1(E)
650 !DLY(00:20:00)
660 // Sweep Applied Voltage Frequency
670 :TEM 1(R,00:01:00,*,0,*,0)
680 :TEM 2(R,00:01:00,*,0,*,0)
690 :TEM 3(R,00:01:00,*,0,*,0)
700 :TEM 4(R,00:01:00,*,0,*,0)
710 :MST 1(R,00:01:00,*,*,0,*,0)
720 :MST 2(R,00:01:00,*,*,0,*,0)
730 :ACS 1(R,00:01:00)
740 :GPM 1(R,00:10:00,-1.0,0,0,0,4)
750 :ZSW 1(3)
760 :WAV 1(SET,SIN,500,0,0.1)
770 !DLY(00:10:00)
780 :ACS 1(R,00:01:00)
790 :MOT 1(RAMP,0,400,20)
800 !WFF(01:00:00,&,MOT,1,2)
810 !CAF()
830 !DLY(00:10:00)
840 :WAV 1(SWEEPF,SIN,0.01,60,9,LOG,30,00:15:00,500,0)
850 !CAF()
860 :ACS 1(R,00:01:00)
870 !FDE(01:00:00,880,WAV,1,2,880,WAV,1,1,850)
880 !CAF()
890 :ACS 1(R,00:01:00)
900 :MOT 1(RAMP,400,800,20)
910 !WFF(01:00:00,&,MOT,1,2)
920 !DLY(00:10:00)
930 :WAV 1(SWEEPF,SIN,60,0.01,9,LOG,30,00:15:00,500,0)
940 !CAF()
950 :ACS 1(R,00:01:00)
960 !FDE(01:00:00,970,WAV,1,2,970,WAV,1,1,940)
970 !CAF()
980 :ACS 1(R,00:01:00)
990 :MOT 1(RAMP,800,0,-20)
1000 !WFF(01:00:00,&,MOT,1,2)
```

1010 !CAF()
1020 :ACS 1(R,00:01:00)
1030 :WAV 1(SET,DC,0)
1040 !DLY(00:10:00)
1050 :ZSW 1(1)
1060 :ACS 1(E)
1070 !DLY(00:30:00)
1080 // Start Relaxation Experiment
1090 :TEM 1(R,00:01:00,*,0,*,0)
1100 :TEM 2(R,00:01:00,*,0,*,0)
1110 :TEM 3(R,00:01:00,*,0,*,0)
1120 :TEM 4(R,00:01:00,*,0,*,0)
1130 :MST 1(R,00:01:00,*,*,0,*,0)
1140 :MST 2(R,00:01:00,*,*,0,*,0)
1150 :ACS 1(R,00:01:00)
1160 :GPM 1(R,00:10:00,-1.0,0,0,0,4)
1170 :ZSW 1(3)
1180 :WAV 1(SET,DC,180)
1185 :ELC 1(M,V)
1190 !DLY(00:10:00)
1200 :ELC 1(R,V,00:00:01)
1210 :ZSW 1(1)
1220 !DLY(00:20:00)
1230 :ELC 1(E)
1240 :MOT 1(RAMP,0,400,20)
1250 !WFF(01:00:00,&,MOT,1,2)
1260 !CAF()
1270 :ZSW 1(3)
1280 :WAV 1(SET,DC,180)
1290 !DLY(00:10:00)
1300 :ZSW 1(1)
1305 :ELC 1(R,V,00:00:01)
1310 !DLY(00:40:00)
1320 :ELC 1(E)
1330 :MOT 1(RAMP,400,800,20)
1340 !WFF(01:00:00,&,MOT,1,2)
1350 !CAF()
1360 :ZSW 1(3)
1370 :WAV 1(SET,DC,180)
1380 !DLY(00:10:00)
1390 :ZSW 1(1)
1400 :ELC 1(R,V,00:00:01)
1410 !DLY(00:40:00)
1420 :ELC 1(E)
1425 :WAV 1(SET,DC,180)

Appendix B: Acquisition and System Control Software and Plotting Routines

```
1426 :ZSW 1(3)
1427 !DLY(00:10:00)
1428 :ELC 1(R,V,00:00:01)
1430 :ZSW 1(1)
1435 :MOT 1(SET,0)
1440 !DLY(00:40:00)
1442 :WAV 1(SET,DC,0)
1445 :ELC 1(E)
1455 :ACS 1(E)
1460 !DLY(00:20:00)
1470 // Take Full Frequency Sweep of CC
1480 :GPM 1(W,4.0,-2.3,0,0,0,4)
1490 !WFF(02:00:00,&,GPM,1,2)
1500 :TEM 1(E)
1510 :TEM 2(E)
1520 :TEM 3(E)
1530 :TEM 4(E)
1540 :MST 1(E)
1550 :MST 2(E)
1560 !END()
```

{End Couette Facility Schedule}

B.2 Data Plotting and Manipulation

Acquired data is initially placed in a textual format in a file with a .cfid extension. The data in this file is unorganized in the fact that each line of data may be from a different instrument. The environment chosen for the manipulation and plotting of this data was the Matlab mathematical software package. In order to get this potentially large quantity of data into the Matlab environment the .cfid file is first exported to a MAT file, which allows the data to be easily loaded as a number of matrices containing data from each instrument. Section B.2.1 describes the matrices which result when the MAT file is loaded. A number of Matlab scripts have been developed which are used to plot data from any instrument and assist in creating formatted pages of plots for each experiment.

B.2.1 Exported MAT File Contents

Instrument Name and ID Format

nnniName = [[*name1*],[*name2*],...[*namen*]]

where *nnn* is instrument type mnemonic, and *name1 ...*, are the names of the instruments

nnnID = [id1 id2 ... idn]

where, *nnn* is instrument type mnemonic, and *id1..* are the Ids corresponding to the names in the name matrix.

Temporal Data Format

Data which is continuous from start to stop

Matrix Name: *nnniT*

where, *nnn* is name of data, *i* is the ID of instrument

Format of Matrix:

[[*time1 y1 y2 yn*], [*time2 y1 y2 yn*], ... [*time3 y1 y2 yn*]]

where time is in seconds and *y*'s are data dependent

Single Data Points

Matrix Name: *nnniTS*

where, *nnn* is name of data, *i* is the ID of instrument

Format of Matrix:

[[*time1 y1 y2 yn*], [*time2 y1 y2 yn*], ... [*time3 y1 y2 yn*]]

where time is in seconds and *y*'s are data dependent

Groups of Data

Matrix Name: *nnniTr*

where, *nnn* is name of data,

i is the ID of instrument and

r is the group number(sequential starting with first measurement group)

Format of Matrix:

[[*time1 y1 y2 yn*], [*time2 y1 y2 yn*], ... [*time3 y1 y2 yn*]]

where time is in seconds and *y*'s are data dependent

Exported Matrixes Generated for Scheduler and Each Instrument Type

Scheduler

StartTime = [hh mm ss]

RunTime = [hh mm ss]

Appendix B: Acquisition and System Control Software and Plotting Routines

StartDate = [yy mm dd]

Motor

Name and ID:

MOTName
MOTID

Temporal Data:

Data Name: MOT
y = 1; Motor Speed

High Impedance Switch

Name and ID:

ZSWName
ZSWID

Temporal Data:

Data Name: ZSW
y = 1; Switch Position 1,2,3

Bubbler

Name and ID:

BUBName
BUBID

Temporal Data:

Data Name: BUB
y = 1; Bubbler State(0=off,1=dry,2=wet)

Electrometer

Name and ID:

ELCName

ELCID

Temporal Data:

Electrometer Mode

Data Name: ELC

y = 1; Mode(0=voltage, 1=current, 2=resistance, 3=charge)

Voltage

Data Name: ELV

y = 1; Voltage

Current

Data Name: ELA

y = 1; Current

Resistance

Data Name: ELR

y = 1; Resistance

Charge

Data Name: ELQ

y = 1; Voltage

Wavetek

Name and ID:

WAVName

WAVID

Temporal Data:

Data Name: WAV

y=1; function(dc=0,sin=1,cos=2isin=3,icos=4,tri=5,sqr=6)

y=2; amplitude(always 0 for dc)

y=3; offset

y=4; frequency(always 1 for dc)

Appendix B: Acquisition and System Control Software and Plotting Routines

ACS

Name and ID:

ACSName

ACSID

Temporal Data:

Data Name: PRG

y=1; purge state(0=done,1=purging)

Data Name: ACS

y=1; Charge Density($\mu\text{C}/\text{m}^3$)

y=2; Offset(pA)

y=3; Current(pA)

y=4; Scale Factor

y=5; Overload Count

y=6; ACS Error

GPM

Name and ID:

GPMName

GPMID

Temporal Data:

channel 1

Data Name: G1P

y=1; Frequency in Hz

y=2; Gain(dB)

y=3; Phase(def)

y=4; Offset(V)

y=5; Amplification

y=6; Conductance(S)

y=7; Capacitance(F)

y=8; Relative D.C.

y=9; Conductivity(S/m)

channel 2

Data Name: G2P

y=1; Frequency in Hz

y=2; Gain(dB)

y=3; Phase(def)

y=4; Offset(V)

y=5; Amplification

y=6; Conductance(S)

y=7; Capacitance(F)

y=8; Relative D.C.

y=9; Conductivity(S/m)

channel 3

Data Name: G3P

y=1; Frequency in Hz

y=2; Gain(dB)

y=3; Phase(def)

y=4; Offset(V)

y=5; Amplification

y=6; Conductance(S)

y=7; Capacitance(F)

y=8; Relative D.C.

y=9; Conductivity(S/m)

channel 4

Data Name: G4P

y=1; Frequency in Hz

y=2; Gain(dB)

y=3; Phase(def)

y=4; Offset(V)

y=5; Amplification

y=6; Conductance(S)

y=7; Capacitance(F)

y=8; Relative D.C.

y=9; Conductivity(S/m)

Thermocouple

Name and ID:

TEMName

TEMID

Appendix B: Acquisition and System Control Software and Plotting Routines

Temporal Data:

Data Name: TEM

y=1; Temperature in degrees C

Moisture Meter

Name and ID:

MSTName

MSTID

Temporal Data:

Data Name: MST

y=1; %rS

y=2; PPM

y=3; Temperature in degrees C

B.2.2 Matlab Data Manipulation and Utility Scripts

| Script or Function Name | Description |
|-------------------------|---|
| getmat.m | Loads MAT file chosen with open dialog box |
| modleg.m | Modifies formatting of legend |
| newpage.m | Sets up a new page for the plotting of data |
| stamp.m | Adds title and data file information to page |
| timeplot.m | Plots instrument data as a function of time |
| paraplot.m | Plots data from two instruments which is parametric in time |
| ptplot.m | Used by paraplot.m |
| prnplot.m | Prompts for printing of all or several of plotted pages |

getmat.m

% Script Allowing User to select MAT file which is then loaded.

%

% Parameters:

% DataPath

% Path to start selection in

% Get Mat File Name

```

[filename pathname] = uigetfile(DataPath,'Plot Couette Data');

if (filename==0)
    error('Error Opening Data File!')
end

% Load MAT File
eval(['load ' pathname filename])

% Calculate End Seconds for User Use
EndSeconds = RunTime(1) * 3600 + RunTime(2) * 60 + RunTime(3);

% Make Stamps for File, Date, and Time
DateStamp = ['Date: ' num2str(StartDate(2)) '-' num2str(StartDate(3)) '-'
num2str(rem(StartDate(1),100))];
TimeStamp = ['Time: ' num2str(StartTime(1)) ':' sprintf('%02.2d',StartTime(2))];
FileStamp = ['File: ' filename];

```

newpage.m

% Script to Create New Figure Page

```

% Create Page Counter
if (~exist('PageCount'))
    PageCount = 0;
end

```

```

% Increment Page Count
PageCount = PageCount + 1;

```

```

% Creat New Page
F(PageCount) = figure('PaperPosition',[.25 .75 8 9.5],'NumberTitle','off','Name',['Couette
Data: ' num2str(PageCount)]);

```

stamp.m

% Script to Stamp Figure Page with Heading, Date, Time, and File information

% For correct positioning, current Plot must be lower left before calling.

```

text('String',['Couette Data: Page '
num2str(PageCount)],'FontSize',19,'HorizontalAlignment','center',...
'Units','Inches','Position',[3 8.5])

```

Appendix B: Acquisition and System Control Software and Plotting Routines

```
text('String',DateStamp,'FontSize',10,'HorizontalAlignment','left',...  
'Units','Inches','Position',[5 8.20])
```

```
text('String',TimeStamp,'FontSize',10,'HorizontalAlignment','left',...  
'Units','Inches','Position',[5 8.05])
```

```
text('String',FileStamp,'FontSize',10,'HorizontalAlignment','left',...  
'Units','Inches','Position',[5 7.90])
```

timeplot.m

```
% Script for plotting one or more temporal data types
```

```
% Parameters:
```

```
% Repeated = [r1 r2... rx]
```

```
% rx = 0 for don't plot, rx=-1 to plot all repeated, rx>0 to plot one repeat group
```

```
% Single = [s1 s2...dc]
```

```
% sx = 0 for don't plot single points, sx!=0 to plot
```

```
% Standard = [n1 n2...nx]
```

```
% nx = 0 for dont plot standart data, nx!=0 to plot
```

```
% DataName = [[nnn1],[nnn2],...[nnnx]];
```

```
% if only 1 plot type is specified all ids are assumed of that name
```

```
% PlotIDs = [id1 id2 ... idx];
```

```
% IDs of instruments to plot corresponding to data type
```

```
% y = [y1 y2 .. yn]
```

```
% y's to plot for each corresponding ID and DataType
```

```
% TimeUnits = p
```

```
% where p = 'h' for hour, 'm' for minutes, p='s' for seconds
```

```
% EnforceZero
```

```
% flag to determine whether y axis starts at zero if all data is above or below y=0
```

```
% TimeAxisStart
```

```
% starting time of axis in seconds, ignored if < 0
```

```
% TimeAxisStop
```

```
% stopping time of axis in seconds, ignored if < 0
```

```
% YUnitPrefix
```

```
% scaling of y axis, M-Mega,k-kilo,m-milli,u-mirco,n-nano,p-pico
```

```
% MarkerDensity = [m1 m2 ... mx]
```

```
% where mx = 1 indicates a marker for every Value, mx = 0 indicates no markers, mx  
> 1 number of points between markers
```

```
% NoLegend
```

```
% flags whether or not legend is displayed
```

```
% Note Axis of first specified ID will be used for plot
```

```
% Enlarge figure for proper legend positioning
```

```
% Set Time Scale Factor
```

```
if (exist('TimeUnits'))  
    if (TimeUnits == 'h')  
        TimeScale = 3600;  
    elseif (TimeUnits == 'm')  
        TimeScale = 60;  
    else  
        TimeScale = 1;  
    end  
else  
    TimeScale = 1;  
end
```

```
% Y Axis Scaling
```

```
if (exist('YUnitPrefix'))  
    if (YUnitPrefix == 'M')  
        YScale = 1e6;  
    elseif (YUnitPrefix == 'k')  
        YScale = 1e3;  
    elseif (YUnitPrefix == 'm')  
        YScale = 1e-3;  
    elseif (YUnitPrefix == 'u')  
        YScale = 1e-6;  
    elseif (YUnitPrefix == 'n')  
        YScale = 1e-9;  
    elseif (YUnitPrefix == 'p')  
        YScale = 1e-12;  
    else  
        YScale = 1;  
    end  
else  
    YScale = 1;  
end
```

```
% Check number of DataNames compared to IDs
```

```
if (length(IDs) > size(DataName,1))  
    for currentIDnum = 2:length(IDs)  
        DataName(currentIDnum,:) = DataName(1,:);  
    end  
end
```

Appendix B: Acquisition and System Control Software and Plotting Routines

```
    end
end

% Check number of y values compared to IDs
if (length(IDs) > length(y))
    for currentIDnum = 2:length(IDs)
        y(currentIDnum) = y(1);
    end
end

% Check number of Single values compared to IDs
if (exist('Single'))
    if (length(IDs) > length(Single))
        for currentIDnum = 2:length(IDs)
            Single(currentIDnum) = Single(1);
        end
    end
end

% Check number of Repeat values compared to IDs
if (exist('Repeated'))
    if (length(IDs) > length(Repeated))
        for currentIDnum = 2:length(IDs)
            Repeated(currentIDnum) = Repeated(1);
        end
    end
end

% Check number of Standard values compared to IDs
if (exist('Standard'))
    if (length(IDs) > length(Standard))
        for currentIDnum = 2:length(IDs)
            Standard(currentIDnum) = Standard(1);
        end
    end
end

% Check number of MarkerDensity values compared to IDs
if (exist('MarkerDensity'))
    if (length(IDs) > length(MarkerDensity))
        for currentIDnum = 2:length(IDs)
            MarkerDensity(currentIDnum) = MarkerDensity(1);
        end
    end
end
```



```

else
    MarkerDensity = ones(length(IDs),1);
end

% Check for No Legend
if (~exist('NoLegend'))
    NoLegend = 0;
end

% Save Initial Position info
pos = get(gcf,'Position');

% Enlarge figure to allow location of legend
set(gcf,'Position',[0 0 1000 700]);

% Plot Data for Each ID

marker = ['o+x*o+x*o+x*o+x*o+x*o+x*'];

for currentIDnum = 1:length(IDs)

% Check if plot single is flagged
if (exist('Single'))
    if (S(currentIDnum))

        % Check for existence of single ('NNNidTS')
        if (exist([DataName(currentIDnum,:) num2str(IDs(currentIDnum)) 'TS']))
            plot(eval([DataName(currentIDnum,:)
num2str(IDs(currentIDnum)) 'TS(:,1)']/TimeScale,eval([DataName(currentIDnum,:)
num2str(IDs(currentIDnum))
'TS(:,y(currentIDnum)+1)']/YScale,marker(currentIDnum),'MarkerSize',4)
            hold on;
        end
    end
end

end

% Check if plot multiple is flagged
if (exist('Repeated'))
    if (Repeated(currentIDnum)<0)
        % Check for existence of Multiple ('NNNidT1'...)

```

Appendix B: Acquisition and System Control Software and Plotting Routines

```

        Rnum = 1;
        Temp = [DataName(currentIDnum,:) num2str(IDs(currentIDnum)) 'T'
num2str(Rnum)];
        while (exist(Temp))
            plot(eval([Temp '(:,1)']/TimeScale,eval([Temp
'(:,y(currentIDnum)+1)']/YScale)
            hold on;
            if (MarkerDensity(currentIDnum))
                plot(eval([Temp
'(1:MarkerDensity(currentIDnum):size(eval(Temp),1),1)']/TimeScale,eval([Temp
'(1:MarkerDensity(currentIDnum):size(eval(Temp),1),y(currentIDnum)+1)']/YScale,mark
er(currentIDnum),'MarkerSize',4)
                end
            Rnum = Rnum + 1;
            Temp = [DataName(currentIDnum,:) num2str(IDs(currentIDnum))
'T' num2str(Rnum)];
        end

        elseif (Repeated(currentIDnum)>0)
            Temp = [DataName(currentIDnum,:) num2str(IDs(currentIDnum)) 'T'
num2str(Repeated(currentIDnum))];
            if (exist(Temp))
                plot(eval([Temp '(:,1)']/TimeScale,eval([Temp
'(:,y(currentIDnum)+1)']/YScale)
                hold on;
                if (MarkerDensity(currentIDnum))
                    plot(eval([Temp
'(1:MarkerDensity(currentIDnum):size(eval(Temp),1),1)']/TimeScale,eval([Temp
'(1:MarkerDensity(currentIDnum):size(eval(Temp),1),y(currentIDnum)+1)']/YScale,mark
er(currentIDnum),'MarkerSize',4)
                    end
                end
            end
        end

end

% Check for Contiuous ('NNNidT')
if (exist('Standard'))
    if (Standard(currentIDnum))
        Temp = [DataName(currentIDnum,:) num2str(IDs(currentIDnum)) 'T'];
        if (exist(Temp))
            plot(eval([Temp '(:,1)']/TimeScale,eval([Temp
'(:,y(currentIDnum)+1)']/YScale)
            hold on;
            if (MarkerDensity(currentIDnum))

```

```

                                plot(eval([Temp
'(1:MarkerDensity(currentIDnum):size(eval(Temp),1),1)']/TimeScale,eval([Temp
'(1:MarkerDensity(currentIDnum):size(eval(Temp),1),y(currentIDnum)+1)']/YScale,mark
er(currentIDnum),'MarkerSize',4)
                                end
                                end
                                end
                                end
                                end %loop

hold off

% Adjust Axis
ax = axis;
new_ax = ax;

% Adjust Y Axis
if (exist('EnforceZero'))
    if (EnforceZero)
        if ((new_ax(3) > 0) & (new_ax(4) > 0))
            new_ax = [ax(1) ax(2) 0 ax(4)];
        elseif ((new_ax(3) < 0) & (new_ax(4) < 0))
            new_ax = [ax(1) ax(2) ax(3) 0];
        end
    end
end

% Adjust Time Axis
if (exist('TimeAxisStart'))
    if (TimeAxisStart >= 0)
        new_ax = [TimeAxisStart/TimeScale new_ax(2) new_ax(3) new_ax(4)];
    end
end
if (exist('TimeAxisStop'))
    if (TimeAxisStop >= 0)
        new_ax = [new_ax(1) TimeAxisStop/TimeScale new_ax(3) new_ax(4)];
    end
end

% Make Axis Adjustments
axis(new_ax);

% Add Y Axis Label
if (exist([DataName(currentIDnum,:) num2str(IDs(1)) 'A']))

```

Appendix B: Acquisition and System Control Software and Plotting Routines

```
%Prefix
if (exist('YUnitPrefix'))
    if (YUnitPrefix == 'M')
        prefix = 'Mega';
    elseif (YUnitPrefix == 'k')
        prefix = 'Kilo ';
    elseif (YUnitPrefix == 'm')
        prefix = 'Milli ';
    elseif (YUnitPrefix == 'u')
        prefix = 'Micro ';
    elseif (YUnitPrefix == 'n')
        prefix = 'Nano ';
    elseif (YUnitPrefix == 'p')
        prefix = 'Pico ';
    else
        prefix = "";
    end
else
    prefix = "";
end
error("");
ylabel([prefix eval([DataName(currentIDnum,:) num2str(IDs(1)) 'A(y(1)+1,:)'])]);
end

% Add Time Axis
if (exist('TimeUnits'))
    if (TimeUnits == 'h')
        ylabel('Time in Hours');
    elseif (TimeUnits == 'm')
        xlabel('Time in Minutes');
    else
        xlabel('Time in Seconds');
    end
else
    xlabel('Time in Seconds');
end

% Check if Legend should be added

if (~NoLegend)
    % Add Legend
    legendEmpty = 1;
    legendCount = 0;
```

```

% Create Legend String
a= ['legend('];

for CurrentIDnum = 1:length(IDs)
    if (exist([DataName(currentIDnum,:) num2str(IDs(CurrentIDnum)) 'L']))
        if (~legendEmpty)
            a = [ a ',';];
        end
        legendEmpty = 0;
        legendCount= legendCount + 1;
        a = [a "" marker(CurrentIDnum) "" ""
deblank(eval([DataName(CurrentIDnum,:) num2str(IDs(CurrentIDnum)) 'L(y(1),:)])) """);
    end
end

a = [ a ')];

if (~legendEmpty)
    lg = eval(a);
    set(lg,'Box','off','FontSize',10,'Visible','off');
    ch=get(lg,'Children');

    for objectnum = 1:2:(2*legendCount-1)
        set(ch(objectnum),'MarkerSize',4)
        set(ch(objectnum +1),'FontSize',10)
    end
end

end

%Restore figure size
set(gcf,'Position',pos);

% Clear Parameter Variables for Next Time
clear Repeated Single Standard DataName PlotIDs y TimeUnits EnforceZero
TimeAxisStart TimeAxisStop YUnitPrefix MarkerDensity NoLegend

```

paraplot.m

% Script for Creating Plots of Data which is Parametric in Time

```

% XName = [xname];
%     where xname is the Data Name for the X Axis
% YName = [yname];
%     where yname is the Data Name for the y Axis

```

Appendix B: Acquisition and System Control Software and Plotting Routines

```
% XID = id;
%   where id is the ID of the X Data
% YID = id;
%   where id is the ID of the Y Data
% Xy = y
%   where y is the y column number for the X data
% Yy = y
%   where y is the y column number for the Y data
% XStandard
%   flag to use standard data from X Data
% YStandard
%   flag to use standard data from Y Data
% XSingle
%   flag to use single data from X Data
% YSingle
%   flag to use single data from Y Data
% XRepeated = [r1 r2...rx]
%   repeated X data groups to use, r1 = -1 indicates use all, r1 =0 indicates none
% YRepeated = [r1 r2...rx]
%   repeated Y data groups to use, r1 = -1 indicates use all, r1 =0 indicates none
% StartSeconds
%   minimum time to use for parametric data
% StopSeconds
%   maximum time to use for parametric data
% Interpolate
%   Indicates which Data to Interpolate either 'X' or 'Y', Data must be monotonic
% MakeLogPlot
%   'X' for Log X axis, 'Y' Log Y axis, 'N' for None, 'B' for Both
% Marker
%   marker to use for symbols, 'o', '+', 'x', '*'
% EnforceYZero
%   flag for forcing 0 if data is single signed
% EnforceXZero
%   flag for Forcing 0 if data is single signed
% YUnitPrefix
%   scaling of y axis, M-Mega,k-kilo,m-milli,u-mirco,n-nano,p-pico
% XUnitPrefix
%   scaling of y axis, M-Mega,k-kilo,m-milli,u-mirco,n-nano,p-pico

% Check Existance of Parameters
if (~exist('XStandard'))
    XStandard = 0;
end

if (~exist('YStandard'))
```

```

        YStandard = 0;
end

if (~exist('XSingle'))
    XSingle = 0;
end

if (~exist('YSingle'))
    YSingle = 0;
end

if (~exist('XRepeated'))
    XRepeated = 0;
end

if (~exist('YRepeated'))
    YRepeated = 0;
end

if (~exist('MakeLogPlot'))
    MakeLogPlot = 'N';
end

if (~exist('EnforceXZero'))
    EnforceXZero = 0;
end

if (~exist('EnforceYZero'))
    EnforceYZero = 0;
end

% Y Axis Scaling
if (exist('YUnitPrefix'))
    if (YUnitPrefix == 'M')
        YScale = 1e6;
    elseif (YUnitPrefix == 'k')
        YScale = 1e3;
    elseif (YUnitPrefix == 'm')
        YScale = 1e-3;
    elseif (YUnitPrefix == 'u')
        YScale = 1e-6;
    elseif (YUnitPrefix == 'n')
        YScale = 1e-9;
    elseif (YUnitPrefix == 'p')
        YScale = 1e-12;
    end
end

```

Appendix B: Acquisition and System Control Software and Plotting Routines

```
        else
            YScale = 1;
        end
    else
        YScale = 1;
    end

% X Axis Scaling
if (exist('XUnitPrefix'))
    if (XUnitPrefix == 'M')
        XScale = 1e6;
    elseif (XUnitPrefix == 'k')
        XScale = 1e3;
    elseif (XUnitPrefix == 'm')
        XScale = 1e-3;
    elseif (XUnitPrefix == 'u')
        XScale = 1e-6;
    elseif (XUnitPrefix == 'n')
        XScale = 1e-9;
    elseif (XUnitPrefix == 'p')
        XScale = 1e-12;
    else
        XScale = 1;
    end
else
    XScale = 1;
end

% Times
if (~exist('StartSeconds'))
    StartSeconds = 0;
end

if (~exist('StopSeconds'))
    StopSeconds = EndSeconds;
end

if (~exist('Marker'))
    Marker = 'o';
end

% Deteremine Interpolate Name
if (exist('Interpolate'))
    if (Interpolate == 'X')
```



```

        InterpID = XID;
        SourceID = YID;
        InterpName = XName;
        SourceName = YName;
        StandardSource = YStandard;
        StandardInterp = XStandard;
        InterpY = Xy;
        SourceY = Yy;
        SingleInterp = XSingle;
        SingleSource = YSingle;
        RepeatedInterp = XRepeated;
        RepeatedSource = YRepeated;
    else
        Interpolate == 'Y';
        InterpName = YName;
        SourceName = XName;
        InterpID = YID;
        SourceID = XID;
        StandardSource = XStandard;
        StandardInterp = YStandard;
        InterpY = Yy;
        SourceY = Xy;
        SingleInterp = YSingle;
        SingleSource = XSingle;
        RepeatedInterp = YRepeated;
        RepeatedSource = XRepeated;
    end
else
    Interpolate == 'Y';
    InterpName = Yname;
    SourceName = XName;
    InterpID = YID;
    SourceID = XID;
    StandardSource = XStandard;
    StandardInterp = YStandard;
    InterpY = Yy;
    SourceY = Xy;
    SingleInterp = YSingle;
    SingleSource = XSingle;
    RepeatedInterp = YRepeated;
    RepeatedSource = XRepeated;
end

```

```

% Set Plot Scaling to Auto

```

Appendix B: Acquisition and System Control Software and Plotting Routines

```
axis('auto')
```

```
% Plot Source Standard vs. All Interp
```

```
if (StandardSource)
```

```
    % Make Standard Name
```

```
    FullSource = [SourceName num2str(SourceID) 'T'];
```

```
    if (exist(FullSource))
```

```
        % Standard Interp
```

```
        FullInterp = [InterpName num2str(InterpID) 'T'];
```

```
        if (exist(FullInterp) & StandardInterp)
```

```
            ptpplot;
```

```
        end
```

```
        % Single Interp
```

```
        FullInterp = [InterpName num2str(InterpID) 'TS'];
```

```
        if (exist(FullInterp) & SingleInterp)
```

```
            ptpplot;
```

```
        end
```

```
        % Repeated Interp
```

```
        if (RepeatedInterp(1) == -1)
```

```
            % Plot All Repeated
```

```
            Rnum = 1;
```

```
            FullInterp = [InterpName num2str(InterpID) 'T' num2str(Rnum)];
```

```
            while (exist(FullInterp))
```

```
                ptpplot;
```

```
                Rnum = Rnum + 1;
```

```
                FullInterp = [InterpName num2str(InterpID) 'T'
```

```
num2str(Rnum)];
```

```
            end
```

```
        elseif (RepeatedInterp(1) ~= 0)
```

```
            for (Rnum = RepeatedInterp)
```

```
                FullInterp = [InterpName num2str(InterpID) 'T'
```

```
num2str(Rnum)];
```

```
                if (exist(FullInterp))
```

```
                    ptpplot;
```

```
                end
```

```
            end
```

```
        end
```

```
    end
```

```
end
```

```

% Single Source Data
if (SingleSource)

    % Make Single Name
    FullSource = [SourceName num2str(SourceID) 'TS'];
    if (exist(FullSource))

        % Standard Interp
        FullInterp = [InterpName num2str(InterpID) 'T'];
        if (exist(FullInterp) & StandardInterp)
            ptplot;
        end

        % Single Interp
        FullInterp = [InterpName num2str(InterpID) 'TS'];
        if (exist(FullInterp) & SingleInterp)
            ptplot;
        end

        % Repeated Interp
        if (RepeatedInterp(1) == -1)
            % Plot All Repeated
            Rnum = 1;
            FullInterp = [InterpName num2str(InterpID) 'T' num2str(Rnum)];
            while (exist(FullInterp))
                ptplot;
                Rnum = Rnum + 1;
                FullInterp = [InterpName num2str(InterpID) 'T'
num2str(Rnum)];
            end

            elseif (RepeatedInterp(1) ~= 0)
                for (Rnum = RepeatedInterp)
                    FullInterp = [InterpName num2str(InterpID) 'T'
num2str(Rnum)];

                    if (exist(FullInterp))
                        ptplot;
                    end
                end
            end
        end
    end
end
end

```

Appendix B: Acquisition and System Control Software and Plotting Routines

```
% All Repeated Source Data
if (RepeatedSource(1) == -1)

    % Look for Sequential Repeated Data
    Rnum = 1;
    FullSource = [SourceName num2str(SourceID) 'T' num2str(Rnum)];
    while (exist(FullSource))

        % Standard Interp
        FullInterp = [InterpName num2str(InterpID) 'T'];
        if (exist(FullInterp) & StandardInterp)
            ptplot;
        end

        % Single Interp
        FullInterp = [InterpName num2str(InterpID) 'TS'];
        if (exist(FullInterp) & SingleInterp)
            ptplot;
        end

        % Repeated Interp
        if (RepeatedInterp(1) == -1)
            % Plot All Repeated
            Rnum = 1;
            FullInterp = [InterpName num2str(InterpID) 'T' num2str(Rnum)];
            while (exist(FullInterp))
                ptplot;
                Rnum = Rnum + 1;
                FullInterp = [InterpName num2str(InterpID) 'T'
num2str(Rnum)];
            end

            elseif (RepeatedInterp(1) ~= 0)
                for (Rnum = RepeatedInterp)
                    FullInterp = [InterpName num2str(InterpID) 'T'
num2str(Rnum)];
                    if (exist(FullInterp))
                        ptplot;
                    end
                end
            end

        % Next Sequential
        Rnum = Rnum + 1;
    end
end
```

```

        FullSource = [SourceName num2str(SourceID) 'T' num2str(Rnum)];

    end

% List of Repeated
elseif (RepeatedSource(1))

    for (Rnum = RepeatedSource)
        FullSource = [SourceName num2str(SourceID) 'T' num2str(Rnum)];

        if (exist(FullSource))

            % Standard Interp
            FullInterp = [InterpName num2str(InterpID) 'T'];
            if (exist(FullInterp) & StandardInterp)
                ptplot;
            end

            % Single Interp
            FullInterp = [InterpName num2str(InterpID) 'TS'];
            if (exist(FullInterp) & SingleInterp)
                ptplot;
            end

            % Repeated Interp
            if (RepeatedInterp(1) == -1)
                % Plot All Repeated
                Rnum = 1;
                FullInterp = [InterpName num2str(InterpID) 'T'
num2str(Rnum)];

                while (exist(FullInterp))
                    ptplot;
                    Rnum = Rnum + 1;
                    FullInterp = [InterpName num2str(InterpID) 'T'
num2str(Rnum)];
                end

            elseif (RepeatedInterp(1) ~= 0)
                for (Rnum = RepeatedInterp)
                    FullInterp = [InterpName num2str(InterpID) 'T'
num2str(Rnum)];

                    if (exist(FullInterp))
                        ptplot;
                    end
                end
            end
        end
    end
end

```

Appendix B: Acquisition and System Control Software and Plotting Routines

```

                                end
                            end
                        end
                    end

% Label Axis
if (exist([XName num2str(XID) 'A']))

    %Prefix
    if (exist('XUnitPrefix'))
        if (XUnitPrefix == 'M')
            prefix = 'Mega';
        elseif (XUnitPrefix == 'k')
            prefix = 'Kilo ';
        elseif (XUnitPrefix == 'm')
            prefix = 'Milli ';
        elseif (XUnitPrefix == 'u')
            prefix = 'Micro ';
        elseif (XUnitPrefix == 'n')
            prefix = 'Nano ';
        elseif (XUnitPrefix == 'p')
            prefix = 'Pico ';
        else
            prefix = "";
        end
    else
        prefix = "";
    end

    xlabel([prefix eval([XName num2str(XID) 'A(Xy+1,:)'])]);
end
```

```

% Y Axis Label
if (exist([YName num2str(YID) 'A']))
    %Prefix
    if (exist('YUnitPrefix'))
        if (YUnitPrefix == 'M')
            prefix = 'Mega';
        elseif (YUnitPrefix == 'k')
            prefix = 'Kilo ';
        elseif (YUnitPrefix == 'm')
            prefix = 'Milli ';
        end
    end
end
```

```

        elseif (YUnitPrefix == 'u')
            prefix = 'Micro ';
        elseif (YUnitPrefix == 'n')
            prefix = 'Nano ';
        elseif (YUnitPrefix == 'p')
            prefix = 'Pico ';
        else
            prefix = "";
        end
    else
        prefix = "";
    end

    ylabel([prefix eval(['YName num2str(YID) 'A(Yy+1,:)'])]);
end

```

```

% Adjust Y Axis
if ((MakeLogPlot ~= 'B') & (MakeLogPlot ~= 'Y'))
    if (EnforceYZero)
        ax = axis;
        if ((ax(3) > 0) & (ax(4) > 0))
            axis([ax(1) ax(2) 0 ax(4)])
        elseif ((ax(3) < 0) & (ax(4) < 0))
            axis([ax(1) ax(2) ax(3) 0])
        end
    end
end
end

```

```

% Adjust X Axis
if ((MakeLogPlot ~= 'B') & (MakeLogPlot ~= 'X'))
    if (EnforceXZero)
        ax = axis;
        if ((ax(1) > 0) & (ax(2) > 0))
            axis([0 ax(2) ax(3) ax(4)])
        elseif ((ax(1) < 0) & (ax(2) < 0))
            axis([ax(1) 0 ax(3) ax(4)])
        end
    end
end
end

```

Appendix B: Acquisition and System Control Software and Plotting Routines

```
% Clean Up
clear XName YName XID YID Xy Yy XStandard TStandard XSingle YSingle
XRepeated YRepeated StartSeconds StopSeconds Interpolate MakeLogPlot Marker
clear EnforceXZero EnforceYZero YUnitPrefix XUnitPrefix
```

ptplot.m

```
% Sub-Sript ptplot.m Used by paratplt.m
```

```
% Calculates Maximum Overlap in Time which is in the Range of StartSeconds and
StopSeconds of the Parametric Data,
% picks times from Source and Interpolates for Y Values in Interp, then plots.
```

```
% Global Variables
```

```
% FullSource
%   full Source Matrix Name
% FullInterp
%   full Interpolation Matrix Name
% InterpY
%   y column of Interpolation Data
% SourceY
%   y column of Source Data
% StartSeconds
%   minimum Time
% StopSeconds
%   maximum Time
% Interpolate
%   Axis of Interpolate Data 'X' or 'Y'
% MakeLogPlot
%   'X' for Log X axis, 'Y' Log Y axis, 'N' for None, 'B' for Both
% Marker
%   marker to use for symbols, 'o', '+', 'x', '*'
% XScale
%   Scale Divisor for X axis
% YScale
%   Scale Divisor for Y axis
```

```
% Set Marker Size
MarkerSize = 3;
```

```
% Determine Max Time
```



```

maxtime = min([max(eval([FullSource '(:,1)'])) max(eval([FullInterp '(:,1)']))
StopSeconds]);

% Determine Min Time
mintime = max([min(eval([FullSource '(:,1) '])) min(eval([FullInterp '(:,1)']))
StartSeconds]);

% Determine Source Index in Range and in Overlap
source_index = find((eval([FullSource '(:,1) ']) >= mintime ) & (eval([FullSource '(:,1)'])
<= maxtime));

% Determine X and Y Data in Range and Overlap
source_data = eval([FullSource '(source_index,SourceY+1)']);

% Put Interpolation Data in Matrix
InterpMatrix(:,1) = eval([FullInterp '(:,1)']);
InterpMatrix(:,2) = eval([FullInterp '(:,InterpY+1)']);

% Check if Almost Monotonic  $X_n = X_{n+1}$ 
nonmon_index = find((InterpMatrix(2:size(InterpMatrix,1),1) -
InterpMatrix(1:size(InterpMatrix,1)-1,1)) == 0);
delta = 0.05;

% Remove All Steps
while (~isempty(nonmon_index))

    % Make Monotonic by Slightly Perturbing  $X_n$  and  $X_{n+1}$  depending on Increasing
order or decreasing order
    if (InterpMatrix(1,1) > InterpMatrix(size(InterpMatrix,1),1))
        % Decreasing Order
        InterpMatrix(nonmon_index,1) = InterpMatrix(nonmon_index,1) + delta;
        InterpMatrix(nonmon_index+1,1) = InterpMatrix(nonmon_index+1,1) -
delta;
    elseif (InterpMatrix(1,1) < InterpMatrix(size(InterpMatrix,1),1))
        % Increasing Order
        InterpMatrix(nonmon_index,1) = InterpMatrix(nonmon_index,1) - delta;
        InterpMatrix(nonmon_index+1,1) = InterpMatrix(nonmon_index+1,1) +
delta;
    end

    delta =delta/2;
    nonmon_index = find((InterpMatrix(2:size(InterpMatrix,1),1) -
InterpMatrix(1:size(InterpMatrix,1)-1,1)) == 0);
end

```

Appendix B: Acquisition and System Control Software and Plotting Routines

```
interp_data = interp1(InterpMatrix(:,1),InterpMatrix(:,2),eval([FullSource
'(source_index,1)']));

% Plot
if (Interpolate == 'X')
    if (MakeLogPlot == 'N')

        plot(interp_data/XScale,source_data/YScale,Marker,'MarkerSize',MarkerSize)
            hold on
    elseif (MakeLogPlot == 'Y')

        semilogy(interp_data/XScale,source_data/YScale,Marker,'MarkerSize',MarkerSize
)
            hold on
    elseif (MakeLogPlot == 'X')

        semilogx(interp_data/XScale,source_data/YScale,Marker,'MarkerSize',MarkerSize
)
            hold on
    else

        loglog(interp_data/XScale,source_data/YScale,Marker,'MarkerSize',MarkerSize)
            hold on
    end
else
    if (MakeLogPlot == 'N')

        plot(source_data/XScale,interp_data/YScale,Marker,'MarkerSize',MarkerSize)
            hold on
    elseif (MakeLogPlot == 'Y')

        semilogy(source_data/XScale,interp_data/YScale,Marker,'MarkerSize',MarkerSize
)
            hold on
    elseif (MakeLogPlot == 'X')

        semilogx(source_data/XScale,interp_data/YScale,Marker,'MarkerSize',MarkerSize
)
            hold on
    else

        loglog(source_data/XScale,interp_data/YScale,Marker,'MarkerSize',MarkerSize)
            hold on
    end
end
end
```

```
% Clean Up
clear source_index interp_data source_data maxtime mintime nonmon_index InterpMatrix
delta
```

prnplot.m

```
% Script to Print Plots
```

```
% Prompt for Print All
```

```
resp = input('Print All Plots(y/n): ','s');
```

```
if ((resp == 'y') | (resp == 'Y'))
```

```
    %Mark All for Print
```

```
    prnt = ones(1,PageCount);
```

```
else
```

```
    % Check Which to Print
```

```
    prnt = zeros(1,PageCount);
```

```
    resp = input('Print Some Plots(y/n): ','s');
```

```
    if ((resp == 'y') | (resp == 'Y'))
```

```
        for plotcount = 1:PageCount
```

```
            resp = input(['Print Plot ' num2str(plotcount) '(y/n): ','s']);
```

```
            if ((resp == 'y') | (resp == 'Y'))
```

```
                % Mark for Print
```

```
                prnt(plotcount) = 1;
```

```
            end
```

```
        end
```

```
    end
```

```
end
```

```
% Print Marked Plots
```

```
for plotcount = 1:PageCount
```

```
    if (prnt(plotcount))
```

```
        figure(F(plotcount));
```

```
        print
```

```
    end
```

```
end
```

B.2.3 Plotting and Analysis Scripts for Experiment Schedules

| Script or Function Name | Description |
|--------------------------------|--|
| loading.m | Plots data from schedule: loading |
| drying.m | Plots data from schedule: drying |
| group1.m | Plots data from schedule: group1 |
| gp1ext.m | Plots summary of terminal voltage, terminal current, |

Appendix B: Acquisition and System Control Software and Plotting Routines

| | |
|-----------|--|
| | charge density, and calculates interfacial parameters for schedule: group1 |
| ifpest.m | Calculates interfacial parameters |
| rlxanal.m | Plots normalized open circuit voltage decay following applied voltage for schedule: group1 |

loading.m

```
% Plot schedule: loading
```

```
% Close All Clear All
```

```
close all;
```

```
clear all;
```

```
% Get MAT File
```

```
DataPath = 'F:\darrell\couette\software\matexp~1\*.mat';
```

```
getmat;
```

```
% Plot Data
```

```
% Page 1
```

```
newpage;
```

```
% Top
```

```
subplot(3,1,1);
```

```
DataName = 'TEM';
```

```
IDs = [2 4 5];
```

```
y = 1;
```

```
Repeated = -1;
```

```
EnforceZero = 1;
```

```
TimeAxisStart = 0;
```

```
TimeAxisStop = EndSeconds;
```

```
TimeUnits = 'm';
```

```
MarkerDensity = [10 10 10];
```

```
timeplot;
```

```
% Middle
```

```
subplot(3,1,2);
```

```
DataName = 'MST';
```

```
IDs = 1:3;
```

```
y = 1;
```

```
Repeated = -1;
```

```
EnforceZero = 1;
```

```
TimeAxisStart = 0;
```

```
TimeAxisStop = EndSeconds;  
TimeUnits = 'm';  
MarkerDensity = 10;  
timeplot;
```

```
% Bottom  
subplot(3,1,3);  
DataName = 'MST';  
IDs = 2:3;  
y = 2;  
Repeated = -1;  
EnforceZero = 1;  
TimeAxisStart = 0;  
TimeAxisStop = EndSeconds;  
TimeUnits = 'm';  
MarkerDensity = 10;  
timeplot;
```

```
stamp;
```

```
% Page 2  
newpage;
```

```
% Middle  
subplot(3,1,2);
```

```
% Couette Charger and Reservoir Conductivity  
DataName = [['G4P'];['G2P']];  
IDs = [1 1];  
y = 9;  
Repeated = 2;  
EnforceZero = 1;  
TimeAxisStart = 0;  
TimeAxisStop = EndSeconds;  
TimeUnits = 'm';  
YUnitPrefix = 'p';
```

```
timeplot;  
ylabel('Conductivity(pS/m)')
```

Appendix B: Acquisition and System Control Software and Plotting Routines

```
% Bottom
subplot(3,1,3);

% Couette Charger and Reservoir D.C.
DataName = [['G4P'];['G2P'];];
IDs = [1 1];
y = 8;
Repeated = 2;
EnforceZero = 1;
TimeAxisStart = 0;
TimeAxisStop = EndSeconds;
TimeUnits = 'm';
timeplot;

stamp;

% Page 3
newpage;

% Middle
subplot(3,1,2);

% Dielectric Constant

% Couette Before
XName = 'G4P';
XID = 1;
Xy = 1;
XRepeated = 1;

YName = 'G4P';
YID = 1;
Yy = 8;
YRepeated = 1;

Interpolate = 'Y';
MakeLogPlot = 'X';
EnforceYZero = 1;
Marker = 'o';
paratplt;

% Couette After
XName = 'G4P';
```

```

XID = 1;
Xy = 1;
XRepeated = 3;

YName = 'G4P';
YID = 1;
Yy = 8;
YRepeated = 3;

Interpolate = 'Y';
MakeLogPlot = 'X';
Marker = 'x';
EnforceYZero = 1;
paratplt;

% Reservoir Before
XName = 'G2P';
XID = 1;
Xy = 1;
XRepeated = 1;

YName = 'G2P';
YID = 1;
Yy = 8;
YRepeated = 1;

Interpolate = 'Y';
MakeLogPlot = 'X';
EnforceYZero = 1;
Marker = '*';
paratplt;

%Reservoir After
XName = 'G2P';
XID = 1;
Xy = 1;
XRepeated = 3;

YName = 'G2P';
YID = 1;
Yy = 8;
YRepeated = 3;

Interpolate = 'Y';
MakeLogPlot = 'X';

```

Appendix B: Acquisition and System Control Software and Plotting Routines

```
Marker = '+';  
EnforceYZero = 1;  
paratplt;
```

```
% Add Legend  
modleg(legend('o','Charger Before Oil Loading','x','Charger After Oil  
Loading','*','Reservoir Before Oil Loading','+','Reservoir After Oil Loading'))
```

```
% Bottom
```

```
% Conductivity  
subplot(3,1,3)
```

```
% Charger Before  
XName = 'G4P';  
XID = 1;  
Xy = 1;  
XRepeated = 1;
```

```
YName = 'G4P';  
YID = 1;  
Yy = 9;  
YRepeated = 1;
```

```
Interpolate = 'Y';  
MakeLogPlot = 'X';  
EnforceYZero = 1;  
YUnitPrefix = 'p';  
Marker = 'o';  
paratplt;
```

```
% Charger After  
XName = 'G4P';  
XID = 1;  
Xy = 1;  
XRepeated = 3;
```

```
YName = 'G4P';  
YID = 1;  
Yy = 9;  
YRepeated = 3;
```



```
Interpolate = 'Y';  
MakeLogPlot = 'X';  
Marker = 'x';  
EnforceYZero = 1;  
YUnitPrefix = 'p';
```

```
% Reservoir Before  
XName = 'G2P';  
XID = 1;  
Xy = 1;  
XRepeated = 1;
```

```
YName = 'G2P';  
YID = 1;  
Yy = 9;  
YRepeated = 1;
```

```
Interpolate = 'Y';  
MakeLogPlot = 'X';  
EnforceYZero = 1;  
YUnitPrefix = 'p';  
Marker = '*';  
paratplt;
```

```
% Reservoir After  
XName = 'G2P';  
XID = 1;  
Xy = 1;  
XRepeated = 3;
```

```
YName = 'G2P';  
YID = 1;  
Yy = 9;  
YRepeated = 3;
```

```
Interpolate = 'Y';  
MakeLogPlot = 'X';  
Marker = '+';  
EnforceYZero = 1;  
YUnitPrefix = 'p';
```

```
paratplt;
```

```
% Axis Mods
```

Appendix B: Acquisition and System Control Software and Plotting Routines

```
ylabel('Conductivity(pS/m)')  
axis([10^(-2) 10^1 0 5])  
modleg(legend('o','Charger Before Oil Loading','x','Charger After Oil  
Loading','*','Reservoir Before Oil Loading','+','Reservoir After Oil Loading'))
```

```
stamp;
```

```
% Check for Print  
prnplt;
```

```
drying.m
```

```
% Plot schedule: loading
```

```
% Close All Clear All  
close all;  
clear all;
```

```
% Get MAT File  
DataPath = 'F:\darrell\couette\software\matexp~1\*.mat';  
getmat;
```

```
% Plot Data
```

```
% Page 1  
newpage;
```

```
% Top  
subplot(3,1,1);  
DataName = 'TEM';  
IDs = [2 4 5];  
y = 1;  
Repeated = -1;  
EnforceZero = 1;  
TimeAxisStart = 0;  
TimeAxisStop = EndSeconds;  
TimeUnits = 'm';  
MarkerDensity = [10 10 10];  
timeplot;
```

```
% Middle
subplot(3,1,2);
DataName = 'MST';
IDs = 1:3;
y = 1;
Repeated = -1;
EnforceZero = 1;
TimeAxisStart = 0;
TimeAxisStop = EndSeconds;
TimeUnits = 'm';
MarkerDensity = 10;
timeplot;
```

```
% Bottom
subplot(3,1,3);
DataName = 'MST';
IDs = 2:3;
y = 2;
Repeated = -1;
EnforceZero = 1;
TimeAxisStart = 0;
TimeAxisStop = EndSeconds;
TimeUnits = 'm';
MarkerDensity = 10;
timeplot;
```

```
stamp;
```

```
% Page 2
newpage;
```

```
% Middle
subplot(3,1,2);
```

```
% Middle
subplot(3,1,2);
```

```
% Couette Charger and Reservoir Conductivity
DataName = [['G4P'];['G2P'];];
IDs = [1 1];
```

Appendix B: Acquisition and System Control Software and Plotting Routines

```
y = 9;
Repeated = 2;
EnforceZero = 1;
TimeAxisStart = 0;
TimeAxisStop = EndSeconds;
TimeUnits = 'm';
YUnitPrefix = 'p';

timeplot;
ylabel('Conductivity(pS/m)')

% Bottom
subplot(3,1,3);

% Couette Charger and Reservoir D.C.
DataName = [['G4P'];['G2P'];];
IDs = [1 1];
y = 8;
Repeated = 2;
EnforceZero = 1;
TimeAxisStart = 0;
TimeAxisStop = EndSeconds;
TimeUnits = 'm';
timeplot;

stamp;

% Page 3
newpage;

% Top
subplot(3,1,1)

% Conductivity vs. Moisture
XName = 'MST';
XID = 3;
Xy = 2;
XRepeated = 2;

YName = 'G2P';
YID = 1;
Yy = 9;
YRepeated = 2;
```

```
YUnitPrefix = 'p';
Interpolate = 'X';
EnforceYZero = 1;
Marker = 'o';
paratplt;

ylabel('Conductivity(pS/m)')
```

```
% Middle
subplot(3,1,2);
```

```
% Dielectric Constant
```

```
% Couette Before
XName = 'G4P';
XID = 1;
Xy = 1;
XRepeated = 1;
```

```
YName = 'G4P';
YID = 1;
Yy = 8;
YRepeated = 1;
```

```
Interpolate = 'Y';
MakeLogPlot = 'X';
EnforceYZero = 1;
Marker = 'o';
paratplt;
```

```
% Couette After
XName = 'G4P';
XID = 1;
Xy = 1;
XRepeated = 3;
```

```
YName = 'G4P';
YID = 1;
Yy = 8;
YRepeated = 3;
```

```
Interpolate = 'Y';
```

Appendix B: Acquisition and System Control Software and Plotting Routines

```
MakeLogPlot = 'X';  
Marker = 'x';  
EnforceYZero = 1;  
paratplt;
```

```
% Reservoir Before  
XName = 'G2P';  
XID = 1;  
Xy = 1;  
XRepeated = 1;
```

```
YName = 'G2P';  
YID = 1;  
Yy = 8;  
YRepeated = 1;
```

```
Interpolate = 'Y';  
MakeLogPlot = 'X';  
EnforceYZero = 1;  
Marker = '*';  
paratplt;
```

```
%Reservoir After  
XName = 'G2P';  
XID = 1;  
Xy = 1;  
XRepeated = 3;
```

```
YName = 'G2P';  
YID = 1;  
Yy = 8;  
YRepeated = 3;
```

```
Interpolate = 'Y';  
MakeLogPlot = 'X';  
Marker = '+';  
EnforceYZero = 1;  
paratplt;
```

```
% Add Legend  
modleg(legend('o','Charger Before Oil Drying','x','Charger After Oil Drying','*','Reservoir  
Before Oil Drying','+','Reservoir After Oil Drying'))
```

```

% Bottom

% Conductivity
subplot(3,1,3)

% Charger Before
XName = 'G4P';
XID = 1;
Xy = 1;
XRepeated = 1;

YName = 'G4P';
YID = 1;
Yy = 9;
YRepeated = 1;

Interpolate = 'Y';
MakeLogPlot = 'X';
EnforceYZero = 1;
YUnitPrefix = 'p';
Marker = 'o';
paratplt;

% Charger After
XName = 'G4P';
XID = 1;
Xy = 1;
XRepeated = 3;

YName = 'G4P';
YID = 1;
Yy = 9;
YRepeated = 3;

Interpolate = 'Y';
MakeLogPlot = 'X';
Marker = 'x';
EnforceYZero = 1;
YUnitPrefix = 'p';

% Reservoir Before
XName = 'G2P';
XID = 1;

```

Appendix B: Acquisition and System Control Software and Plotting Routines

```
Xy = 1;  
XRepeated = 1;
```

```
YName = 'G2P';  
YID = 1;  
Yy = 9;  
YRepeated = 1;
```

```
Interpolate = 'Y';  
MakeLogPlot = 'X';  
EnforceYZero = 1;  
YUnitPrefix = 'p';  
Marker = '*';  
paratplt;
```

```
% Reservoir After  
XName = 'G2P';  
XID = 1;  
Xy = 1;  
XRepeated = 3;
```

```
YName = 'G2P';  
YID = 1;  
Yy = 9;  
YRepeated = 3;
```

```
Interpolate = 'Y';  
MakeLogPlot = 'X';  
Marker = '+';  
EnforceYZero = 1;  
YUnitPrefix = 'p';
```

```
paratplt;
```

```
% Axis Mods  
ylabel('Conductivity(pS/m)')  
axis([10-2 101 0 5])  
modleg(legend('o','Charger Before Oil Drying','x','Charger After Oil Drying','*','Reservoir  
Before Oil Drying','+','Reservoir After Oil Drying'))
```

```
stamp;
```

```
% Check for Print
```



```

prnplt;

group1.m
% Schedule: group1

% Close All Clear All
close all;
clear all;

% Get MAT File
DataPath = 'F:\darrell\couette\software\matexp~1\*.mat';
getmat;

% Plot Data for Voltage and Current Measurements
experiment1start = 0;
experiment1end = max(TEM1T1(:,1));

% Page 1
newpage;

% Top
subplot(3,1,1);
DataName = 'MOT';
IDs = 1;
y = 1;
Standard = 1;
EnforceZero = 1;
TimeAxisStart = 0;
TimeAxisStop = EndSeconds;
TimeUnits = 'm';
MarkerDensity = 0;
NoLegend = 1;
TimeAxisStop = experiment1end;

timeplot;
ylabel('Rotation Rate(RPM)');

% Middle
subplot(3,1,2);
DataName = 'ELV';
IDs = 1*ones(1,12);
y = 1;
Repeated = 1:12;

```

Appendix B: Acquisition and System Control Software and Plotting Routines

```
EnforceZero = 1;  
TimeAxisStart = 0;  
TimeAxisStop = experiment1end;  
TimeUnits = 'm';  
MarkerDensity = 0;  
NoLegend = 1;
```

```
timeplot;  
ylabel('Terminal Voltage');
```

```
% Bottom  
subplot(3,1,3);  
DataName = 'ELA';  
IDs = 1;  
y = 1;  
Repeated = -1;  
EnforceZero = 1;  
TimeAxisStart = 0;  
TimeAxisStop = experiment1end;  
TimeUnits = 'm';  
YUnitPrefix = 'p';  
MarkerDensity = 0;  
NoLegend = 1;
```

```
timeplot;  
ylabel('Terminal Current(pA)');
```

```
stamp;
```

```
% Page 2  
newpage;
```

```
% Top  
subplot(3,1,1);  
DataName = 'ACS';  
IDs = 1;  
y = 1;  
Repeated = -1;  
EnforceZero = 1;  
TimeAxisStart = 0;  
TimeAxisStop = experiment1end;  
TimeUnits = 'm';  
timeplot;
```

```
% Middle
subplot(3,1,2);
DataName = 'TEM';
IDs = [1 4];
y = 1;
Repeated = 1;
EnforceZero = 1;
TimeAxisStart = 0;
TimeUnits = 'm';
MarkerDensity = [10 10];
timeplot;
```

```
% Bottom
subplot(3,1,3);
DataName = 'MST';
IDs = 2;
y = 2;
Repeated = 1;
EnforceZero = 1;
TimeAxisStart = 0;
TimeUnits = 'm';
MarkerDensity = 10;
timeplot;
```

```
stamp;
```

```
% Page 3
newpage;
```

```
% Top
subplot(3,1,1);
DataName = 'G4P';
IDs = 1;
y = 9;
Repeated = 2;
EnforceZero = 1;
TimeAxisStart = 0;
TimeAxisStop = experiment1end;
TimeUnits = 'm';
YUnitPrefix = 'p';
timeplot;
ylabel('Conductivity(pS/m)')
```

```
% Middle
```

Appendix B: Acquisition and System Control Software and Plotting Routines

```
subplot(3,1,2);
DataName = 'TEM';
IDs = [2 3];
y = 1;
Repeated = 1;
EnforceZero = 1;
TimeAxisStart = 0;
TimeAxisStop = experiment1end;
TimeUnits = 'm';
MarkerDensity = [10 10];
timeplot;
```

```
% Bottom
subplot(3,1,3);
DataName = 'MST';
IDs = 1;
y = 1;
Repeated = 1;
EnforceZero = 1;
TimeAxisStart = 0;
TimeAxisStop = experiment1end;
TimeUnits = 'm';
timeplot;
```

```
stamp;
```

```
% Page 4
newpage;
```

```
% Top
subplot(3,1,1);
```

```
% Ramped
XName = 'MOT';
XID = 1;
Xy = 1;
XStandard = 1;
```

```
YName = 'ELV';
YID = 1;
Yy = 1;
YRepeated = 1;
```

```
Interpolate = 'X';
paratplt;
```

```
% Stepped
XName = 'MOT';
XID = 1;
Xy = 1;
XStandard = 1;

YName = 'ELV';
YID = 1;
Yy = 1;
YRepeated = 2:12;

Interpolate = 'X';
Marker = '+';
paratplt;
modleg(legend('o','Ramped Rotation','+','Stepped Rotation'))
Ylabel('Terminal Voltage')
```

```
% Middle
subplot(3,1,2);
XName = 'MOT';
XID = 1;
Xy = 1;
XStandard = 1;
```

```
YName = 'ELA';
YID = 1;
Yy = 1;
YRepeated = 1;
YUnitPrefix = 'p';
```

```
Interpolate = 'X';
paratplt;
```

```
XName = 'MOT';
XID = 1;
Xy = 1;
XStandard = 1;
```

```
YName = 'ELA';
YID = 1;
Yy = 1;
YRepeated = 2:12;
```

Appendix B: Acquisition and System Control Software and Plotting Routines

```
YUnitPrefix = 'p';
```

```
Interpolate = 'X';
```

```
Marker = '+';
```

```
paratplt;
```

```
modleg(legend('o','Ramped Rotation','+','Stepped Rotation'))
```

```
Ylabel('Terminal Current(pA)')
```

```
% Bottom
```

```
subplot(3,1,3);
```

```
XName = 'MOT';
```

```
XID = 1;
```

```
Xy = 1;
```

```
XStandard = 1;
```

```
YName = 'ACS';
```

```
YID = 1;
```

```
Yy = 1;
```

```
YRepeated = 1:24;
```

```
Interpolate = 'X';
```

```
paratplt;
```

```
stamp;
```

```
% Page 5
```

```
newpage;
```

```
% Top Left Gain
```

```
subplot(3,2,1)
```

```
DataName = 'G4P';
```

```
IDs = 1;
```

```
y = 2;
```

```
Repeated = 2;
```

```
EnforceZero = 1;
```

```
TimeUnits = 'm';
```

```
timeplot;
```

```
ax = axis;  
axis([ax(1) ax(2) (ax(3)-5) 0])
```

```
% Top Right GPM Phase  
subplot(3,2,2)
```

```
DataName = 'G4P';  
IDs = 1;  
y = 3;  
Repeated = 2;  
EnforceZero = 1;  
TimeUnits = 'm';  
timeplot;  
ax = axis;  
%axis([ax(1) ax(2) (ax(3)-5) 0])
```

```
% Middle Left GPM Offset  
subplot(3,2,3)
```

```
DataName = 'G4P';  
IDs = 1;  
y = 4;  
Repeated = 2;  
EnforceZero = 1;  
TimeUnits = 'm';  
timeplot;  
ax = axis;  
%axis([ax(0) ax(1) (ax(3)-5) 0])
```

```
% Middle Right ACS Offset  
subplot(3,2,4)  
DataName = 'ACS';  
IDs = 1;  
y = 2;  
Repeated = -1;  
EnforceZero = 1;  
TimeUnits = 'm';  
TimeAxisStart = 0;  
TimeAxisStop = experiment1end;  
timeplot;  
ax = axis;  
%axis([ax(0) ax(1) (ax(3)-5) 0])
```

Appendix B: Acquisition and System Control Software and Plotting Routines

```
% Bottom Right ACS Current
```

```
subplot(3,2,6)
```

```
DataName = 'ACS';
```

```
IDs = 1;
```

```
y = 3;
```

```
Repeated = -1;
```

```
EnforceZero = 1;
```

```
TimeUnits = 'm';
```

```
TimeAxisStart = 0;
```

```
TimeAxisStop = experiment1end;
```

```
timeplot;
```

```
ax = axis;
```

```
%axis([ax(0) ax(1) (ax(3)-5) 0])
```

```
% Bottom Left ACS Overshoot
```

```
subplot(3,2,5)
```

```
DataName = 'ACS';
```

```
IDs = 1;
```

```
y = 5;
```

```
Repeated = -1;
```

```
EnforceZero = 1;
```

```
TimeUnits = 'm';
```

```
TimeAxisStart = 0;
```

```
TimeAxisStop = experiment1end;
```

```
timeplot;
```

```
ax = axis;
```

```
%axis([ax(0) ax(1) (ax(3)-5) 0])
```

```
stamp;
```

```
% Applied Voltage Experiment
```

```
Experiment2Start = min(TEM1T2(:,1));
```

```
Experiment2End = max(TEM1T2(:,1));
```

```
% Page 6
```

```
newpage;
```



```

% Top
subplot(3,1,1);
DataName = 'MOT';
IDs = 1;
y = 1;
Standard = 1;
EnforceZero = 1;
TimeAxisStart = 0;
TimeAxisStop = EndSeconds;
TimeUnits = 'm';
MarkerDensity = 0;
NoLegend = 1;
TimeAxisStart = Experiment2Start;
TimeAxisStop = Experiment2End;

```

```

timeplot;
ylabel('Rotation Rate(RPM)');

```

```

% Middle
subplot(3,1,2);
DataName = 'WAV';
IDs = 1;
y = 3;
Standard = 1;
EnforceZero = 1;
TimeAxisStart = Experiment2Start;
TimeAxisStop = Experiment2End;
TimeUnits = 'm';
MarkerDensity = 0;
NoLegend = 1;

```

```

timeplot;
ylabel('Applied DC Voltage');

```

```

% Bottom
subplot(3,1,3);
DataName = 'ACS';
IDs = 1;
y = 1;
Repeated = -1;
EnforceZero = 1;
TimeAxisStart = Experiment2Start;

```

Appendix B: Acquisition and System Control Software and Plotting Routines

```
TimeAxisStop = Experiment2End;  
TimeUnits = 'm';  
timeplot;
```

```
stamp;
```

```
% Page 7  
newpage;
```

```
% Top  
subplot(3,1,1);  
DataName = 'G4P';  
IDs = 1;  
y = 9;  
Repeated = 3;  
EnforceZero = 1;  
TimeAxisStart = Experiment2Start;  
TimeAxisStop = Experiment2End;  
TimeUnits = 'm';  
YUnitPrefix = 'p';  
timeplot;  
ylabel('Conductivity(pS/m)')
```

```
% Middle  
subplot(3,1,2);  
DataName = 'TEM';  
IDs = [1 4];  
y = 1;  
Repeated = 2;  
EnforceZero = 1;  
TimeAxisStart = Experiment2Start;  
TimeAxisStop = Experiment2End;  
TimeUnits = 'm';  
MarkerDensity = [10 10];  
timeplot;
```

```
% Bottom  
subplot(3,1,3);  
DataName = 'MST';  
IDs = 2;  
y = 2;  
Repeated = 2;
```

```
EnforceZero = 1;
TimeAxisStart = Experiment2Start;
TimeAxisStop = Experiment2End;
TimeUnits = 'm';
MarkerDensity = 10;
timeplot;

stamp;
```

```
% Page 8
newpage;
```

```
% TOP
subplot(3,1,1);
DataName = 'TEM';
IDs = [2 3];
y = 1;
Repeated = 2;
EnforceZero = 1;
TimeAxisStart = Experiment2Start;
TimeAxisStop = Experiment2End;
TimeUnits = 'm';
MarkerDensity = [10 10];
timeplot;
```

```
% Middle
subplot(3,1,2);
DataName = 'MST';
IDs = 1;
y = 1;
Repeated = 2;
EnforceZero = 1;
TimeAxisStart = Experiment2Start;
TimeAxisStop = Experiment2End;
TimeUnits = 'm';
timeplot;
```

```
% Bottom
subplot(3,1,3)
XName = 'WAV';
XID = 1;
```

Appendix B: Acquisition and System Control Software and Plotting Routines

```
Xy = 3;  
XStandard = 1;
```

```
YName = 'ACS';  
YID = 1;  
Yy = 1;  
YRepeated = 27:37;
```

```
Interpolate = 'X';
```

```
EnforceYZero = 1;  
Marker = 'o';  
paratplt;
```

```
XName = 'WAV';  
XID = 1;  
Xy = 3;  
XStandard = 1;
```

```
YName = 'ACS';  
YID = 1;  
Yy = 1;  
YRepeated = 39:49;
```

```
Interpolate = 'X';
```

```
EnforceYZero = 1;  
Marker = '+';  
paratplt;
```

```
modleg(legend('o','400 RPM','+','800 RPM'))  
xlabel('Applied DC Voltage')
```

```
stamp
```

```
% Page 9  
newpage;
```

```
% Top Left Gain  
subplot(3,2,1)
```

```
DataName = 'G4P';  
IDs = 1;
```

```

y = 2;
Repeated = 3;
EnforceZero = 1;
TimeUnits = 'm';
timeplot;
ax = axis;
axis([ax(1) ax(2) (ax(3)-5) 0])

```

```

% Top Right GPM Phase
subplot(3,2,2)

```

```

DataName = 'G4P';
IDs = 1;
y = 3;
Repeated = 3;
EnforceZero = 1;
TimeUnits = 'm';
timeplot;
ax = axis;
%axis([ax(1) ax(2) (ax(3)-5) 0])

```

```

% Middle Left GPM Offset
subplot(3,2,3)

```

```

DataName = 'G4P';
IDs = 1;
y = 4;
Repeated = 3;
EnforceZero = 1;
TimeUnits = 'm';
timeplot;
ax = axis;
%axis([ax(0) ax(1) (ax(3)-5) 0])

```

```

% Middle Right ACS Offset
subplot(3,2,4)
DataName = 'ACS';
IDs = 1;
y = 2;
Repeated = -1;
EnforceZero = 1;
TimeUnits = 'm';
TimeAxisStart = Experiment2Start;

```

Appendix B: Acquisition and System Control Software and Plotting Routines

```
TimeAxisStop = Experiment2End;  
timeplot;  
ax = axis;  
%axis([ax(0) ax(1) (ax(3)-5) 0])
```

```
% Bottom Right ACS Current  
subplot(3,2,6)
```

```
DataName = 'ACS';  
IDs = 1;  
y = 3;  
Repeated = -1;  
EnforceZero = 1;  
TimeUnits = 'm';  
TimeAxisStart = Experiment2Start;  
TimeAxisStop = Experiment2End;  
timeplot;  
ax = axis;  
%axis([ax(0) ax(1) (ax(3)-5) 0])
```

```
% Bottom Left ACS Overshoot  
subplot(3,2,5)
```

```
DataName = 'ACS';  
IDs = 1;  
y = 5;  
Repeated = -1;  
EnforceZero = 1;  
TimeUnits = 'm';  
TimeAxisStart = Experiment2Start;  
TimeAxisStop = Experiment2End;  
timeplot;  
ax = axis;  
%axis([ax(0) ax(1) (ax(3)-5) 0])
```

```
stamp;
```

```
% Applied Voltage Sweep
```

```
Experiment3Start = min(TEM1T3(:,1));  
Experiment3End = max(TEM1T3(:,1));
```

```
% Page 10  
newpage;
```

```
% Top  
subplot(3,1,1);  
DataName = 'MOT';  
IDs = 1;  
y = 1;  
Standard = 1;  
EnforceZero = 1;  
TimeAxisStart = 0;  
TimeAxisStop = EndSeconds;  
TimeUnits = 'm';  
MarkerDensity = 0;  
NoLegend = 1;  
TimeAxisStart = Experiment3Start;  
TimeAxisStop = Experiment3End;
```

```
timeplot;  
ylabel('Rotation Rate(RPM)');
```

```
% Middle  
subplot(3,1,2);  
DataName = 'WAV';  
IDs = 1;  
y = 4;  
Standard = 1;  
EnforceZero = 1;  
TimeAxisStart = Experiment3Start;  
TimeAxisStop = Experiment3End;  
TimeUnits = 'm';  
MarkerDensity = 0;  
NoLegend = 1;
```

```
timeplot;  
ylabel('Frequency(HZ) of 500V Sine');
```

```
% Bottom
```

Appendix B: Acquisition and System Control Software and Plotting Routines

```
subplot(3,1,3);
DataName = 'ACS';
IDs = 1;
y = 1;
Repeated = -1;
EnforceZero = 1;
TimeAxisStart = Experiment3Start;
TimeAxisStop = Experiment3End;
TimeUnits = 'm';
timeplot;
```

```
stamp;
```

```
% Page 11
```

```
newpage;
```

```
% Top
```

```
subplot(3,1,1);
DataName = 'G4P';
IDs = 1;
y = 9;
Repeated = 4;
EnforceZero = 1;
TimeAxisStart = Experiment3Start;
TimeAxisStop = Experiment3End;
TimeUnits = 'm';
YUnitPrefix = 'p';
timeplot;
ylabel('Conductivity(pS/m)')
```

```
% Middle
```

```
subplot(3,1,2);
DataName = 'TEM';
IDs = [1 4];
y = 1;
Repeated = 3;
EnforceZero = 1;
TimeAxisStart = Experiment3Start;
TimeAxisStop = Experiment3End;
TimeUnits = 'm';
MarkerDensity = [10 10];
timeplot;
```



```
% Bottom
subplot(3,1,3);
DataName = 'MST';
IDs = 2;
y = 2;
Repeated = 3;
EnforceZero = 1;
TimeAxisStart = Experiment3Start;
TimeAxisStop = Experiment3End;
TimeUnits = 'm';
MarkerDensity = 10;
timeplot;
```

```
stamp;
```

```
% Page 12
newpage;
```

```
% TOP
subplot(3,1,1);
DataName = 'TEM';
IDs = [2 3];
y = 1;
Repeated = 3;
EnforceZero = 1;
TimeAxisStart = Experiment3Start;
TimeAxisStop = Experiment3End;
TimeUnits = 'm';
MarkerDensity = [10 10];
timeplot;
```

```
% Middle
subplot(3,1,2);
DataName = 'MST';
IDs = 1;
y = 1;
Repeated = 3;
EnforceZero = 1;
TimeAxisStart = Experiment3Start;
TimeAxisStop = Experiment3End;
TimeUnits = 'm';
```

Appendix B: Acquisition and System Control Software and Plotting Routines

```
timeplot;
```

```
% Bottom
```

```
subplot(3,1,3)
```

```
XName = 'WAV';
```

```
XID = 1;
```

```
Xy = 4;
```

```
XStandard = 1;
```

```
YName = 'ACS';
```

```
YID = 1;
```

```
Yy = 1;
```

```
YRepeated = 54:63;
```

```
Interpolate = 'X';
```

```
EnforceYZero = 1;
```

```
Marker = 'o';
```

```
MakeLogPlot = 'X';
```

```
paratplt;
```

```
XName = 'WAV';
```

```
XID = 1;
```

```
Xy = 4;
```

```
XStandard = 1;
```

```
YName = 'ACS';
```

```
YID = 1;
```

```
Yy = 1;
```

```
YRepeated = 65:74;
```

```
Interpolate = 'X';
```

```
EnforceYZero = 1;
```

```
Marker = '+';
```

```
MakeLogPlot = 'X';
```

```
paratplt;
```

```
modleg(legend('o','400 RPM','+','800 RPM'))
```

```
xlabel('Frequency(Hz) of 500 V Sine')
```

```
stamp
```

```
% Page 13
```

```
newpage;
```

```
% Top Left Gain
```

```
subplot(3,2,1)
```

```
  DataName = 'G4P';
```

```
  IDs = 1;
```

```
  y = 2;
```

```
  Repeated = 4;
```

```
  EnforceZero = 1;
```

```
  TimeUnits = 'm';
```

```
  timeplot;
```

```
  ax = axis;
```

```
  axis([ax(1) ax(2) (ax(3)-5) 0])
```

```
% Top Right GPM Phase
```

```
subplot(3,2,2)
```

```
  DataName = 'G4P';
```

```
  IDs = 1;
```

```
  y = 3;
```

```
  Repeated = 4;
```

```
  EnforceZero = 1;
```

```
  TimeUnits = 'm';
```

```
  timeplot;
```

```
  ax = axis;
```

```
  %axis([ax(1) ax(2) (ax(3)-5) 0])
```

```
% Middle Left GPM Offset
```

```
subplot(3,2,3)
```

```
  DataName = 'G4P';
```

```
  IDs = 1;
```

```
  y = 4;
```

```
  Repeated = 4;
```

```
  EnforceZero = 1;
```

```
  TimeUnits = 'm';
```

```
  timeplot;
```

```
  ax = axis;
```

```
  %axis([ax(0) ax(1) (ax(3)-5) 0])
```

Appendix B: Acquisition and System Control Software and Plotting Routines

```
% Middle Right ACS Offset
subplot(3,2,4)
DataName = 'ACS';
IDs = 1;
y = 2;
Repeated = -1;
EnforceZero = 1;
TimeUnits = 'm';
TimeAxisStart = Experiment3Start;
TimeAxisStop = Experiment3End;
timeplot;
ax = axis;
%axis([ax(0) ax(1) (ax(3)-5) 0])
```

```
% Bottom Right ACS Current
subplot(3,2,6)

DataName = 'ACS';
IDs = 1;
y = 3;
Repeated = -1;
EnforceZero = 1;
TimeUnits = 'm';
TimeAxisStart = Experiment3Start;
TimeAxisStop = Experiment3End;
timeplot;
ax = axis;
%axis([ax(0) ax(1) (ax(3)-5) 0])
```

```
% Bottom Left ACS Overshoot
subplot(3,2,5)

DataName = 'ACS';
IDs = 1;
y = 5;
Repeated = -1;
EnforceZero = 1;
TimeUnits = 'm';
TimeAxisStart = Experiment3Start;
TimeAxisStop = Experiment3End;
timeplot;
ax = axis;
%axis([ax(0) ax(1) (ax(3)-5) 0])
```

```
stamp;
```

```
% Relaxation Experiments
```

```
Experiment4Start = min(TEM1T4(:,1));  
Experiment4End = max(TEM1T4(:,1));
```

```
% Page 14
```

```
newpage;
```

```
% Top
```

```
subplot(3,1,1);  
DataName = 'MOT';  
IDs = 1;  
y = 1;  
Standard = 1;  
EnforceZero = 1;  
TimeAxisStart = 0;  
TimeAxisStop = EndSeconds;  
TimeUnits = 'm';  
MarkerDensity = 0;  
NoLegend = 1;  
TimeAxisStart = Experiment4Start;  
TimeAxisStop = Experiment4End;
```

```
timeplot;
```

```
ylabel('Rotation Rate(RPM)');
```

```
% Middle
```

```
subplot(3,1,2);  
DataName = 'ZSW';  
IDs = 1;  
y = 1;  
Standard = 1;  
EnforceZero = 1;  
TimeAxisStart = Experiment4Start;  
TimeAxisStop = Experiment4End;  
TimeUnits = 'm';  
MarkerDensity = 0;  
NoLegend = 1;
```

Appendix B: Acquisition and System Control Software and Plotting Routines

```
timeplot;  
ylabel('(1) Electrometer (3) 180 V DC');
```

```
% Bottom  
subplot(3,1,3);  
DataName = 'ELV';  
IDs = 1;  
y = 1;  
Repeated = -1;  
EnforceZero = 1;  
TimeAxisStart = Experiment4Start;  
TimeAxisStop = Experiment4End;  
TimeUnits = 'm';  
MarkerDensity = 0;  
NoLegend = 1;
```

```
timeplot;  
ylabel('Relaxation Voltage');
```

```
stamp;
```

```
% Page 15  
newpage;
```

```
% Top  
subplot(3,1,1);  
DataName = 'ACS';  
IDs = 1;  
y = 1;  
Repeated = -1;  
EnforceZero = 1;  
TimeAxisStart = Experiment4Start;  
TimeAxisStop = Experiment4End;  
TimeUnits = 'm';  
timeplot;
```

```
% Middle
subplot(3,1,2);
DataName = 'G4P';
IDs = 1;
y = 9;
Repeated = 5;
EnforceZero = 1;
TimeAxisStart = Experiment4Start;
TimeAxisStop = Experiment4End;
TimeUnits = 'm';
YUnitPrefix = 'p';
timeplot;
ylabel('Conductivity(pS/m)')
```

```
% Bottom
subplot(3,1,3);
DataName = 'TEM';
IDs = [1 4];
y = 1;
Repeated = 4;
EnforceZero = 1;
TimeAxisStart = Experiment4Start;
TimeAxisStop = Experiment4End;
TimeUnits = 'm';
MarkerDensity = [10 10];
timeplot;
```

```
stamp;
```

```
% Page 16
newpage;
```

```
% Top
subplot(3,1,1);
DataName = 'MST';
IDs = 2;
y = 2;
Repeated = 4;
EnforceZero = 1;
```

Appendix B: Acquisition and System Control Software and Plotting Routines

```
TimeAxisStart = Experiment4Start;  
TimeAxisStop = Experiment4End;  
TimeUnits = 'm';  
MarkerDensity = 10;  
timeplot;
```

```
% Middle  
subplot(3,1,2);  
DataName = 'TEM';  
IDs = [2 3];  
y = 1;  
Repeated = 4;  
EnforceZero = 1;  
TimeAxisStart = Experiment4Start;  
TimeAxisStop = Experiment4End;  
TimeUnits = 'm';  
MarkerDensity = [10 10];  
timeplot;
```

```
% Bottom  
subplot(3,1,3);  
DataName = 'MST';  
IDs = 1;  
y = 1;  
Repeated = 4;  
EnforceZero = 1;  
TimeAxisStart = Experiment4Start;  
TimeAxisStop = Experiment4End;  
TimeUnits = 'm';  
timeplot;
```

```
stamp;
```

```
% Page 17  
newpage;
```

```
% Top Left Gain  
subplot(3,2,1)
```

```
DataName = 'G4P';  
IDs = 1;  
y = 2;
```



```
Repeated = 5;  
EnforceZero = 1;  
TimeUnits = 'm';  
timeplot;  
ax = axis;  
axis([ax(1) ax(2) (ax(3)-5) 0])
```

```
% Top Right GPM Phase  
subplot(3,2,2)
```

```
DataName = 'G4P';  
IDs = 1;  
y = 3;  
Repeated = 5;  
EnforceZero = 1;  
TimeUnits = 'm';  
timeplot;  
ax = axis;  
%axis([ax(1) ax(2) (ax(3)-5) 0])
```

```
% Middle Left GPM Offset  
subplot(3,2,3)
```

```
DataName = 'G4P';  
IDs = 1;  
y = 4;  
Repeated = 5;  
EnforceZero = 1;  
TimeUnits = 'm';  
timeplot;  
ax = axis;  
%axis([ax(0) ax(1) (ax(3)-5) 0])
```

```
% Middle Right ACS Offset  
subplot(3,2,4)  
DataName = 'ACS';  
IDs = 1;  
y = 2;  
Repeated = 77;  
EnforceZero = 1;  
TimeUnits = 'm';  
timeplot;  
ax = axis;
```

Appendix B: Acquisition and System Control Software and Plotting Routines

```
%axis([ax(0) ax(1) (ax(3)-5) 0])
```

```
% Bottom Right ACS Current  
subplot(3,2,6)
```

```
DataName = 'ACS';  
IDs = 1;  
y = 3;  
Repeated = 77;  
EnforceZero = 1;  
TimeUnits = 'm';  
timeplot;  
ax = axis;  
%axis([ax(0) ax(1) (ax(3)-5) 0])
```

```
% Bottom Left ACS Overshoot  
subplot(3,2,5)
```

```
DataName = 'ACS';  
IDs = 1;  
y = 5;  
Repeated = 77;  
EnforceZero = 1;  
TimeUnits = 'm';  
timeplot;  
ax = axis;  
%axis([ax(0) ax(1) (ax(3)-5) 0])
```

```
stamp;
```

```
% Page 18  
newpage;
```

```
% Middle
```

```

subplot(3,1,2);

XName = 'G4P';
XID = 1;
Xy = 1;
XRepeated = 1;

YName = 'G4P';
YID = 1;
Yy = 8;
YRepeated = 1;

Interpolate = 'Y';
MakeLogPlot = 'X';
EnforceYZero = 1;
paratplt;

XName = 'G4P';
XID = 1;
Xy = 1;
XRepeated = 6;

YName = 'G4P';
YID = 1;
Yy = 8;
YRepeated = 6;

Interpolate = 'Y';
MakeLogPlot = 'X';
Marker = 'x';
EnforceYZero = 1;

paratplt;

% Add Legend
modleg(legend('o','Pre-Experiment Measurement','x','Post-Experiment Measurement'))

% Bottom
subplot(3,1,3)
XName = 'G4P';
XID = 1;
Xy = 1;
XRepeated = 1;

```

Appendix B: Acquisition and System Control Software and Plotting Routines

```
YName = 'G4P';
YID = 1;
Yy = 9;
YRepeated = 1;

Interpolate = 'Y';
MakeLogPlot = 'X';
EnforceYZero = 1;
YUnitPrefix = 'p';
paratplt;

XName = 'G4P';
XID = 1;
Xy = 1;
XRepeated = 6;

YName = 'G4P';
YID = 1;
Yy = 9;
YRepeated = 6;

Interpolate = 'Y';
MakeLogPlot = 'X';
Marker = 'x';
EnforceYZero = 1;
YUnitPrefix = 'p';

paratplt;

% Axis Mods
ylabel('Conductivity(pS/m)')
ax = axis;
axis([10^(-2) 10^1 ax(3) ax(4)])
modleg(legend('o','Pre-Experiment Measurement','x','Post-Experiment Measurement'))

stamp;

% Check for Print
prnplt;

gp1ext.m
% Extraction of Parameters for Estimation from group1b
```

```

% Close All Clear All
close all;
clear all;

% Get MAT File
DataPath = 'D:\darrell\couette\software\matexp~1\*.mat';
getmat;

% Make Data Matrix
Data = zeros(11,4);
Data(:,1) = (0:100:1000)';

for step = 2:12
    Data(13-step,2) = mean(eval(['ELV1T' num2str(step) '(:,2)']));
    Data(13-step,3) = mean(eval(['ELA1T' num2str(step) '(:,2)']));
    Data(13-step,4) = mean(eval(['ACS1T' num2str(step) '(:,2)']));
end

newpage;
subplot(3,1,1)
plot(Data(:,1),Data(:,2))
hold on
plot(Data(:,1),Data(:,2),'o','MarkerSize',4)
xlabel('Rotation Rate(RPM)')
ylabel('Terminal Voltage')

subplot(3,1,2)
plot(Data(:,1),Data(:,3)/1e-12)
hold on
plot(Data(:,1),Data(:,3)/1e-12,'o','MarkerSize',4)
xlabel('Rotation Rate(RPM)')
ylabel('Terminal Current(pA)')

subplot(3,1,3)
plot(Data(:,1),Data(:,4))
hold on
plot(Data(:,1),Data(:,4),'o','MarkerSize',4)
xlabel('Rotation Rate(RPM)')
ylabel('Charge Density(uC/m^3)')

stamp;

```

Appendix B: Acquisition and System Control Software and Plotting Routines

% Calculate Interfacial Parameters Rates

% Find Average Conductivity

Conductivity = mean(G4P1T2(:,10))

Temperature = mean(TEM4T1(:,2))

ifpest(Data, Temperature, Conductivity)

ifpest.m

function ifpest(Data, Temperature, Conductivity)

% Estimation of Interfacial Electrification Parameters

% Matrix of Data for Estimation

% Data(:,1) = Rotation in RPM

% Data(:,2) = Voc

% Data(:,3) = Isc

% Data(:,4) = P0

% Remove Zero Rotation

Data = Data(2:9,:);

% Convert Charge to actual Colombs

Data(:,4) = Data(:,4) * 1e-6;

% Geometric Factors

R1 = .0762

R2 = .1016

a = R1

H = .4064

% Oil Properties

DC = 2.17 * 8.85e-12

V = 3.956e-10 * exp(0.2725/(8.6167e-5*(Temperature+273.15)))

Nu = 886 * V

b = (2e-11)/Nu

q = 1

Dm = b*((8.6167e-5)*(Temperature+273.15))/q

T2 = DC/Conductivity

% Sublayer

Re = (2 * Data(:,1))*(2*pi/60) * a^2/V

Cf = 2*0.079 * Re.^(-0.3)

Sc = V/Dm

delta = 3.3 ./((Sc^0.356).*Re.*Cf)

% Double Layer

DebyeL = ((Dm*DC/Conductivity)^0.5)

% Normalizations

NR1 = R1/R2

Na = a/R2

NR2 = R2/R2

NVoc = Data(:,2)/(Dm/b)

NIsc = Data(:,3)/(pi*H*Conductivity*Dm/b)

Np0 = Data(:,4)/(Conductivity/b)

NDebyeL = DebyeL/R2

Ndelta = delta

NSig1 = Inf

NT1 = 0

% Calculate P1 and P2

P1 = (NVoc*NDebyeL/log(Na)) - (Np0*(Na^2 + (1 - Na^2)/(2*log(Na)))/(2*NDebyeL))

P2 = (-NVoc*NDebyeL/log(Na)) + (Np0*(1 + (1 - Na^2)/(2*log(Na)))/(2*NDebyeL))

% Case 1

p1w = mean((P1 .* sinh(Na*Ndelta/NDebyeL))/Na)

P1calc = Na*p1w./sinh(Na*Ndelta/NDebyeL)

C1I1 = sum(((P1 - P1calc)./P1calc).^2)

p2w = mean(P2 .* sinh(Ndelta/NDebyeL))

P2calc = p2w./sinh(Ndelta/NDebyeL)

C1I2 = sum(((P2 - P2calc)./P2calc).^2)

% Case 2

E1K1 = mean(P1 .* cosh(Na*Ndelta/NDebyeL)/Na)

P1calc = E1K1*Na./cosh(Na*Ndelta/NDebyeL)

C2I1 = sum(((P1 - P1calc)./P1calc).^2)

E2K2 = mean(P2 .* cosh(Ndelta/NDebyeL))

P2calc = E2K2./cosh(Ndelta/NDebyeL)

C2I2 = sum(((P2 - P2calc)./P2calc).^2)

Appendix B: Acquisition and System Control Software and Plotting Routines

```
% Case 3
%Interface 1
ZK1 = fmins('case3Er1',[1 1],[0 1e-6 1e-6 4 5 6 7 8 9 10 11 12 13 5000
],[,],Na,sinh(Na*Ndelta/NDebyeL),cosh(Na*Ndelta/NDebyeL),P1)
ZK1(1)
ZK1(2)
C3I1 = case3Er1(ZK1,Na,sinh(Na*Ndelta/NDebyeL),cosh(Na*Ndelta/NDebyeL),P1)

%Interface 2
ZK2 = fmins('case3Er1',[1 1],[0 1e-6 1e-6 4 5 6 7 8 9 10 11 12 13 5000
],[,],1,sinh(Ndelta/NDebyeL),cosh(Ndelta/NDebyeL),P2)
ZK2(1)
ZK2(2)
C3I2 = case3Er1(ZK2,1,sinh(Ndelta/NDebyeL),cosh(Ndelta/NDebyeL),P2)

% Determine Best Case

% Interface 1
if ((ZK1(2) > 100) | (ZK1(2) < .01))
    if (C1I1 < C2I1)
        Interface1Case = 1
    else
        Interface1Case = 2
    end
else
    Interface1Case = 3
end

% Interface 2
if ((ZK2(2) > 100) | (ZK2(2) < .01))
    if (C1I2 < C2I2)
        Interface2Case = 1
    else
        Interface2Case = 2
    end
else
    Interface2Case = 3
end

% Calculate P3, P4 assume change in charge density with voltage is zero
P3 = -1 + (log(Na/NR1)/(NSig1*log(Na))) + (NVoc./NIsC).*(-2/log(Na))
```


P4 = P3

```
% Calculate K1
if (Interface1Case == 1)
    % Case 1
    K1 = (1./(P3.*sinh(Na.*Ndelta./NDebyeL).*NDebyeL))
    % Use only Positive Rates
    K1 = mean(K1(find(K1>0),1))
elseif (Interface1Case == 2)
    % Case 2
    Kr1 = (P3.*cosh(Na.*Ndelta./NDebyeL) - NT1 + 1)
    Kr1 = mean(Kr1(find(Kr1>0),1))
elseif (Interface1Case == 3)
    % Case 3
    % Use only + Reaction Rates
    Kr1 = (P3.*ZK1(2).*(sinh(Na.*Ndelta./NDebyeL) +
(1./ZK1(2)).*cosh(Na.*Ndelta./NDebyeL)) - NT1 + 1)
    Kr1 = mean(Kr1(find(Kr1>0),1))
end
```

```
% Calculate K2
if (Interface2Case == 1)
    % Case 1
    K2 = (1./(P4.*sinh(Ndelta./NDebyeL).*NDebyeL))
    % Use only Positive Rates
    K2 = mean(K2(find(K2>0),1))

elseif (Interface2Case == 2)
    % Case 2
    Kr2 = (P4.*cosh(Ndelta./NDebyeL) + 1)
    Kr2 = mean(Kr2(find(Kr2>0),1))
elseif (Interface2Case == 3)
    % Case 3
    % Use only Positive Rates
    Kr2 = (P4.*ZK2(2).*(sinh(Ndelta./NDebyeL) +
(1./ZK2(2)).*cosh(Ndelta./NDebyeL)) + 1)
    Kr2 = mean(Kr2(find(Kr2>0),1))
end
```

Appendix B: Acquisition and System Control Software and Plotting Routines

```
% Display Results
disp('Analysis Results:')
disp(' ');
disp('Interface 1 (Inner Cylinder):')
disp([' Case: ' num2str(Interface1Case)])

if (Interface1Case == 1)
    % Case 1
    disp(['Wall Charge Density: ' num2str(p1w*Conductivity/b)])
    disp(['Reaction Velocity: ' num2str(K1*Dm/R2)])
elseif (Interface1Case == 2)
    % Case 2
    kr1 = 1/(Kr1*T2);
    xixfkr = (E1K1*Kr1)*Conductivity*DebyeL*T2/b;
    disp(['Effective CD*Forwarded Rate/Reverse Rate: ' num2str(xixfkr)])
    disp(['Reverse Reaction Velocity: ' num2str(kr1)])

elseif (Interface1Case == 3)
    % Case 3
    disp(['Effective Charge Density(Xi): ' num2str(ZK1(1)*Conductivity/b)])
    kr1 = 1/(Kr1*T2);
    kf1 = ZK1(2)*kr1*DebyeL;
    disp(['Forward Reaction Velocity: ' num2str(kf1)])
    disp(['Reverse Reaction Velocity: ' num2str(kr1)])
end

disp(' ');
disp('Interface 2 (Outer Cylinder):')
disp([' Case: ' num2str(Interface2Case)])

if (Interface2Case == 1)
    % Case 1
    disp(['Wall Charge Density: ' num2str(p2w*Conductivity/b)])
    disp(['Reaction Velocity: ' num2str(K2*Dm/R2)])
elseif (Interface2Case == 2)
    % Case 2
    kr2 = 1/(Kr2*T2);
    xixfkr = (E2K2*Kr2)*Conductivity*DebyeL*T2/b;
    disp(['Effective CD*Forwarded Rate/Reverse Rate: ' num2str(xixfkr)])
    disp(['Reverse Reaction Velocity: ' num2str(kr2)])

elseif (Interface2Case == 3)
    % Case 3
    disp(['Effective Charge Density(Xi): ' num2str(ZK1(1)*Conductivity/b)])
    kr2 = 1/(Kr2*T2);
```

```

kf2 = ZK2(2)*kr2*DebyeL;
disp(['Forward Reaction Velocity: ' num2str(kf1)])
disp(['Reverse Reaction Velocity: ' num2str(kr1)])
end

```

rlxanal.m

```

% Analysis of Applied Voltage to Open Circuit Measurements

```

```

% Make Relaxation Exponential Comparison

```

```

Conductivity = mean(G4P1T5(:,10))

```

```

DC = mean(G4P1T5(:,9))*8.85e-12

```

```

Relax(:,1) = (0:(40*60))';

```

```

Relax(:,2) = exp(-Relax(:,1)/(DC/Conductivity));

```

```

% Make Normalized Plot

```

```

VRPM0(:,1) = ELV1T11(:,1) - min(ELV1T11(:,1));

```

```

VRPM0(:,2) = ELV1T11(:,2) -

```

```

min(ELV1T11((size(ELV1T11,1)/2):size(ELV1T11,1),2));

```

```

VRPM0(:,2) = VRPM0(:,2) / max(VRPM0(:,2));

```

```

VRPM400(:,1) = ELV1T12(:,1) - min(ELV1T12(:,1));

```

```

VRPM400(:,2) = ELV1T12(:,2) -

```

```

min(ELV1T12((size(ELV1T12,1)/2):size(ELV1T12,1),2));

```

```

VRPM400(:,2) = VRPM400(:,2) / max(VRPM400(:,2));

```

```

VRPM800(:,1) = ELV1T13(:,1) - min(ELV1T13(:,1));

```

```

VRPM800(:,2) = ELV1T13(:,2) -

```

```

min(ELV1T13((size(ELV1T13,1)/2):size(ELV1T13,1),2));

```

```

VRPM800(:,2) = VRPM800(:,2) / max(VRPM800(:,2));

```

```

VRPM800S(:,1) = ELV1T14(:,1) - min(ELV1T14(:,1));

```

```

VRPM800S(:,2) = ELV1T14(:,2) -

```

```

min(ELV1T14((size(ELV1T14,1)/2):size(ELV1T14,1),2));

```

```

VRPM800S(:,2) = VRPM800S(:,2) / max(VRPM800S(:,2));

```

```

% Plot

```

```

figure;

```

```

plot(VRPM0(:,1),VRPM0(:,2))

```

```

hold on

```

```

plot(VRPM400(:,1),VRPM400(:,2),'+', 'MarkerSize',3)

```

Appendix B: Acquisition and System Control Software and Plotting Routines

```
plot(VRPM800(:,1),VRPM800(:,2))
plot(VRPM800S(:,1),VRPM800S(:,2))
plot(Relax(:,1),Relax(:,2))
```

```
axis([0 400 0 1])
```

```
% Estimate Pwall
```

```
clear Data400
```

```
Data400(:,2) = ELV1T12(:,2);
```

```
Data400(:,1) = 400 * ones(size(ELV1T12,1),1);
```

```
ChargeIndex = find((ACS1T73(:,1) > ELV1T12(1,1)) & (ACS1T73(:,1) < ELV1T12(size(ELV1T12,1),1)));
```

```
Data400(:,4) = mean(ACS1T73(ChargeIndex,2))*ones(size(ELV1T12,1),1);
```

```
[pw1400 pw2400] = ifpest2(Data400,15,Conductivity);
```

```
clear Data800
```

```
Data800(:,2) = ELV1T13(:,2);
```

```
Data800(:,1) = 800 * ones(size(ELV1T13,1),1);
```

```
ChargeIndex = find((ACS1T73(:,1) > ELV1T13(1,1)) & (ACS1T73(:,1) < ELV1T13(size(ELV1T13,1),1)));
```

```
Data800(:,4) = mean(ACS1T73(ChargeIndex,2))*ones(size(ELV1T13,1),1);
```

```
[pw1800 pw2800] = ifpest2(Data800,15,Conductivity);
```

```
figure
```

```
plot(ELV1T12(:,1)-ELV1T12(1,1),pw1400,ELV1T12(:,1)-ELV1T12(1,1),pw2400)
```

```
hold on
```

```
plot(ELV1T12(:,1)-ELV1T12(1,1),pw1400,'o',ELV1T12(:,1)-
```

```
ELV1T12(1,1),pw2400,'o','MarkerSize',3)
```

```
plot(ELV1T13(:,1)-ELV1T13(1,1),pw1800,ELV1T13(:,1)-ELV1T13(1,1),pw2800)
```

```
ax = axis;
```

```
axis([5*(DC/Conductivity) ax(2) 0 .005])
```

Appendix C

Recovery Voltage Simulation

C.1 Recovery Voltage Measurement

Recovery voltage measurement constitutes another means for characterizing the behavior of a two terminal device in the time domain. Recovery voltage measurements are generally made on distributed systems which lie physically between two or more conductors that can be utilized as terminals. Some such examples are transformers where the primary and secondary windings can be used as terminals, and coaxial cables for which inner and outer conductors can be used.

The technique of recovery voltage measurement involves three stages. The first stage is a charging stage in which a DC voltage is applied for a predetermined length of time τ_c . The second stage is the partial discharging of the system by application of a short circuit (or equivalently 0 V) for a time τ_d . The actual recovery voltage is then measured as the open circuit voltage response following the discharge period. The shape of this voltage response in most dielectric systems is a rise from zero volts at the time of open circuit to a peak value, which is then followed by a decay back to zero volts. The recovery voltage curve is typically characterized by its peak voltage value and the elapsed time from the open circuit condition at which this peak occurred. By varying the charging time τ_c and discharging time τ_d a signature of the system can be developed.

The exact method for analyzing the recovery voltage depends on the exact application. In some circumstances the response can be modeled by the geometry and physics of polarization and charge transport in the system. In other cases the system may be too complex to model, in which case comparisons with previous measurements are used as a means of detecting trends in the system. The goal here is to predict recovery

Appendix C: Recovery Voltage Simulation

voltage measurements for systems of known geometry and material properties for which the dielectric spectrums have been determined.

C.2 Recovery Voltage for a Second Order RC Network

As a starting point for the study of recovery voltage responses for a system, a simple lumped element, second order RC network was chosen as shown in Figure C-1. The lumped system is useful because its response is well defined and constant with time, which allows easy comparison between actual measurements and theoretical results. Recovery voltage measurements were first made on the networks for comparison with closed form solutions. Once the measurement technique was verified, attempts were then made to determine the response from only spectral data.

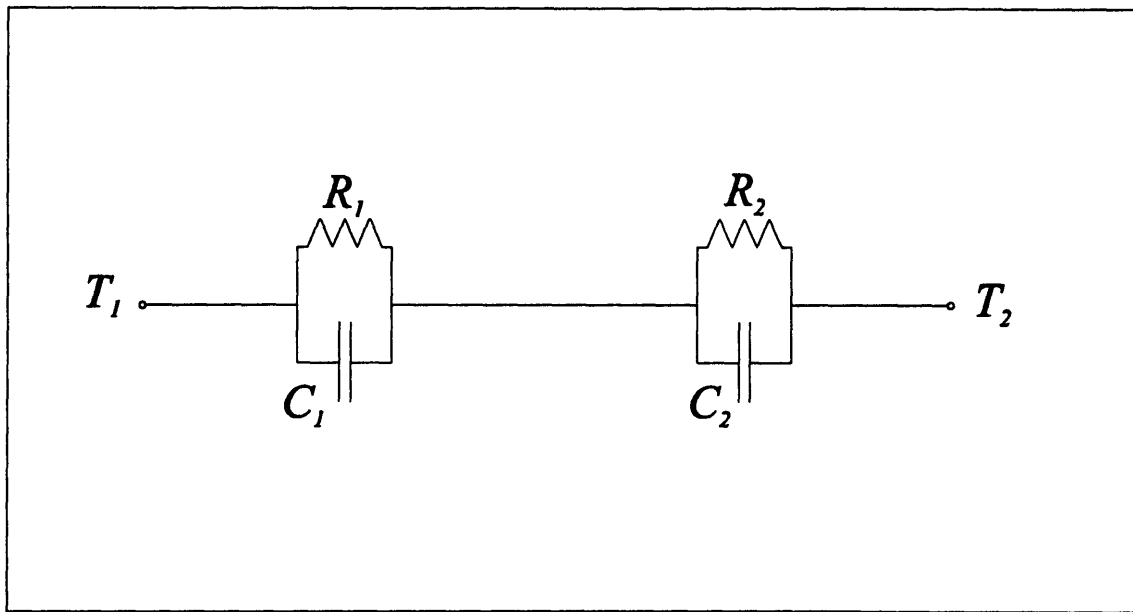


Figure C-1: Second order RC network used for initial recovery voltage measurements.

C.2.1 Measurements

Recovery voltage measurements were made with the Tettex Automatic Recovery Voltage Meter Type 5461. In the measurements the charging voltage was set at 200 V and the ratio of charging time to discharge time was kept at two. Measurements at several charging durations were made on two networks with different capacitor and resistor values. A typical recovery voltage response is shown in Figure C-2. The measured peak

voltage and time of peak for each network using different charging intervals appear in Table C-1 through Table C-4.

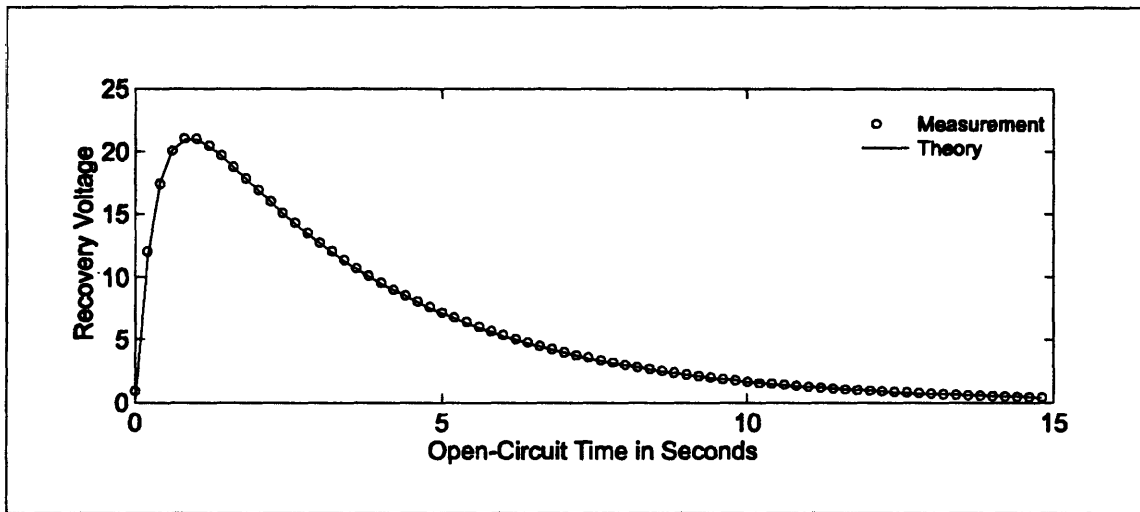


Figure C-2: Comparison of measured recovery voltage and theoretical recovery voltage for network with $R_1=1.05 \text{ M}\Omega$, $R_2=10.3 \text{ M}\Omega$, $C_1 =330\text{nF}$, and $C_2=335\text{nF}$. The charging voltage was 200 V, while the charging time was .5 seconds and the discharging time was .25 seconds.

| T_c (s) | Measured | Theoretical | % Deviation |
|-----------|------------|-------------|-------------|
| | V_{peak} | V_{peak} | |
| 0.020 | 1.84 | 1.75 | 5.1 |
| 0.050 | 4.24 | 4.18 | 1.5 |
| 0.100 | 7.79 | 7.72 | 0.9 |
| 0.200 | 13.2 | 13.23 | -0.2 |
| 0.500 | 21.0 | 21.06 | -0.3 |
| 1.000 | 20.7 | 20.64 | 0.3 |
| 2.000 | 11.5 | 11.31 | 1.7 |
| 5.000 | 1.19 | 1.11 | 7.5 |
| 10.00 | 0.050 | 0.02 | 133.6 |
| 20.00 | --- | --- | --- |
| 50.00 | --- | --- | --- |

Table C-1: Comparison of measured and theoretical values for peak value of recovery voltage for network with $R_1=1.05 \text{ M}\Omega$, $R_2=10.3 \text{ M}\Omega$, $C_1 =330\text{nF}$, and $C_2=335\text{nF}$ using a 200 V charging voltage.

Appendix C: Recovery Voltage Simulation

| T_c (s) | Measured | Theoretical | % Deviation |
|-----------|----------------|----------------|-------------|
| | T_{peak} (s) | T_{peak} (s) | |
| 0.020 | 0.896 | 0.885 | 1.2 |
| 0.050 | 0.896 | 0.885 | 1.2 |
| 0.100 | 0.896 | 0.885 | 1.2 |
| 0.200 | 0.895 | 0.885 | 1.1 |
| 0.500 | 0.892 | 0.885 | 0.8 |
| 1.000 | 0.888 | 0.885 | 0.3 |
| 2.000 | 0.896 | 0.885 | 1.2 |
| 5.000 | 0.890 | 0.885 | 0.5 |
| 10.00 | 1.59 | 0.885 | 79.6 |
| 20.00 | --- | --- | --- |
| 50.00 | --- | --- | --- |

Table C-2: Comparison of measured and theoretical values of recovery voltage peak time for network with $R_1=1.05\text{ M}\Omega$, $R_2=10.3\text{ M}\Omega$, $C_1=330\text{ nF}$, and $C_2=335\text{ nF}$ using a 200 V charging voltage.

| T_c (s) | Measured | Theoretical | % Deviation |
|-----------|------------|-------------|-------------|
| | V_{peak} | V_{peak} | |
| 0.020 | 0.231 | 0.18 | 28.7 |
| 0.050 | 0.507 | 0.44 | 14.6 |
| 0.100 | 0.956 | 0.86 | 10.6 |
| 0.200 | 1.77 | 1.65 | 7.3 |
| 0.500 | 3.82 | 3.59 | 6.5 |
| 1.000 | 6.04 | 5.70 | 5.9 |
| 2.000 | 7.70 | 7.31 | 5.3 |
| 5.000 | 5.57 | 5.33 | 4.5 |
| 10.00 | 1.87 | 1.79 | 4.4 |
| 20.00 | 0.194 | 0.170 | 14.0 |
| 50.00 | --- | --- | --- |

Table C-3: Comparison of measured and theoretical values for peak value of recovery voltage for network with $R_1=9.96\text{ M}\Omega$, $R_2=10.2\text{ M}\Omega$, $C_1=317\text{ nF}$, and $C_2=103\text{ nF}$ using a 200 V charging voltage.

| T_c (s) | Measured | Theoretical | % Deviation |
|-----------|----------------|----------------|-------------|
| | T_{peak} (s) | T_{peak} (s) | |
| 0.020 | 1.29 | 1.733 | -25.5 |
| 0.050 | 1.59 | 1.733 | -8.2 |
| 0.100 | 1.59 | 1.733 | -8.2 |
| 0.200 | 1.69 | 1.733 | -2.5 |
| 0.500 | 1.69 | 1.733 | -2.5 |
| 1.000 | 1.68 | 1.733 | -3.0 |
| 2.000 | 1.69 | 1.733 | -2.5 |
| 5.000 | 1.69 | 1.733 | -2.5 |
| 10.00 | 1.69 | 1.733 | -2.5 |
| 20.00 | 1.68 | 1.733 | -3.0 |
| 50.00 | --- | --- | --- |

Table C-4: Comparison of measured and theoretical values of recovery voltage peak time for network with $R_1=9.96 \text{ M}\Omega$, $R_2=10.2 \text{ M}\Omega$, $C_1 =317\text{nF}$, and $C_2=103\text{nF}$ using a 200 V charging voltage.

C.2.2 Comparison with Theory

The theoretical recovery voltage responses can be determined using standard circuit techniques. In the solution, the network voltage has been expressed as the sum of the voltage across each pair of RC elements such that

$$v_i(t) = v_1(t) + v_2(t) \quad (\text{C.1})$$

The solutions for the voltages $v_1(t)$ and $v_2(t)$ are divided into three intervals, the charging interval, the discharging interval, and the recovery interval, which are denoted with the superscripts c, d, and r respectively. The solutions for charging interval $0 < t < \tau_c$ are

$$v_1^c(t) = \frac{R_2 C_2 - \tau_{eq}}{R_2 C_{eq}} V_c \exp(-t/\tau_{eq}) + \frac{R_{eq}}{R_2} V_c \quad (\text{C.2})$$

$$v_2^c(t) = \frac{R_1 C_1 - \tau_{eq}}{R_1 C_{eq}} V_c \exp(-t/\tau_{eq}) + \frac{R_{eq}}{R_1} V_c \quad (\text{C.3})$$

where,

$$R_{eq} \equiv \frac{R_1 R_2}{R_1 + R_2} \quad (\text{C.4})$$

Appendix C: Recovery Voltage Simulation

$$C_{eq} \equiv C_1 + C_2 \quad (C.5)$$

$$\tau_{eq} \equiv C_{eq} R_{eq} \quad (C.6)$$

and V_c is the charging voltage. The solutions for the discharging interval $\tau_c < t < (\tau_c + \tau_d)$ are

$$v_1^d = \frac{-Q_w}{C_1 + C_2} \exp(-(t - \tau_c)/\tau_{eq}) \quad (C.7)$$

$$v_2^d = \frac{Q_w}{C_1 + C_2} \exp(-(t - \tau_c)/\tau_{eq}) \quad (C.8)$$

where,

$$Q_w = -v_1^c(\tau_c^-)C_1 + v_2^c(\tau_c^-)C_2 \quad (C.9)$$

Finally, the solutions for the recovery period $(\tau_c + \tau_d) < t$ are

$$v_1^r = \frac{-Q_w}{C_1 + C_2} \exp(-\tau_d/\tau_{eq}) \exp(-(t - \tau_c - \tau_d)/(R_1 C_1)) \quad (C.10)$$

$$v_2^r = \frac{-Q_w}{C_1 + C_2} \exp(-\tau_d/\tau_{eq}) \exp(-(t - \tau_c - \tau_d)/(R_2 C_2)) \quad (C.11)$$

where

$$Q_w = -v_1^c(\tau_c^-)C_1 + v_2^c(\tau_c^-)C_2 \quad (C.12)$$

Since the time of the peak and magnitude of the peak for the recovery period are also of interest they were calculated as

$$\tau_{peak} = \frac{R_1 R_2 C_1 C_2}{R_2 C_2 - R_1 C_1} \ln\left(\frac{R_2 C_2}{R_1 C_1}\right) \quad (C.13)$$

where τ_{peak} is the time of peak referenced from the start of the recovery interval, and

$$V_{peak} = \frac{Q_{oc}}{C_1 + C_2} \exp(-\tau_d / \tau_{eq}) \left[\exp(-\tau_{peak} / (R_2 C_2)) - \exp(-\tau_{peak} / (R_1 C_1)) \right] \quad (C.14)$$

The measured and theoretical values for the time of peak and magnitude of the peak are compared in Table C-1 through Table C-4. The values match fairly well except for some of the shortest charging times and some of the longest. These errors are most likely due to the impedance of the recovery voltage meter, which was discovered to have a significant series resistance.

C.2.3 Simulation of Recovery Voltage

The recovery voltage for the RC network has so far been measured experimentally and determined using time domain circuit analysis techniques. Next the recovery voltage will be determined from its impedance spectrum. At this point that may seem redundant, but the ultimate goal is to be able to predict the recovery voltage from a spectral measurement of a distributed system. Using the network allows us a simple method of determining an impedance spectrum over all frequencies, while also giving a closed form response for comparison.

The difficulty in the task of determining the recovery voltage from the impedance spectrum lies in the incorporation of initial conditions into the recovery stage of the measurement. This was easily accomplished when the circuit was known and the charge on the capacitors could be used to set the state when the terminal constraint changed from an applied voltage to an open circuit. This is also equivalent to having the differential equations governing the system in closed form. However, our knowledge of the system is assumed to be limited to a sampled impedance spectrum, which is the transfer function between voltage and current for the system. Attempts could have been made to recover the differential equations from this sampled response, but a second more simplistic solution to the problem was devised.

The technique for determining the recovery voltage is based on the causality of the system, which is basically that the present state of the system is only dependent on present and past inputs. Since the systems we are dealing with are real physical systems comprised of dielectrics this assumption should obviously be reasonable. Now consider

Appendix C: Recovery Voltage Simulation

having the knowledge of the current flowing into the system for all time. Determining the voltage would be a matter of convolution with the admittance of the system in the time domain or multiplication in the frequency domain. But, determining the current for all time would generally require us to know the voltage for all time including the recovery period, which is unknown. However, in this case we already know the current for $t \geq (\tau_c + \tau_d)$ which is the open circuit current of zero. So all we are left to determine is the current for $t < (\tau_c + \tau_d)$. Now the causality of the system allows us to determine the current for $t < (\tau_c + \tau_d)$ by knowledge of only the voltage for $t < (\tau_c + \tau_d)$, which is composed of the charging voltage for $0 < t < \tau_c$ and the discharging voltage of zero for $\tau_c < t < \tau_d$.

Simulations using this technique were carried out numerically using the FFT and IFFT. Each step in determining the recovery voltage for the second-order RC network appears in Figure C-3 through Figure C-6. This simulation uses a charging voltage of 200 V, a charging time of 0.5 seconds and a discharging time of 0.25 seconds. The resistors and capacitors of the network are the same as those used in the networks of Table C-2 and Table C-1.

The measured peak and time of peak in the simulated recovery voltage match the closed form solution well. The simulated peak voltage was 21.03 V while the analytical solution was 21.06 V. The time of peak for the simulation was .883 s while the analytical value was .885 s.

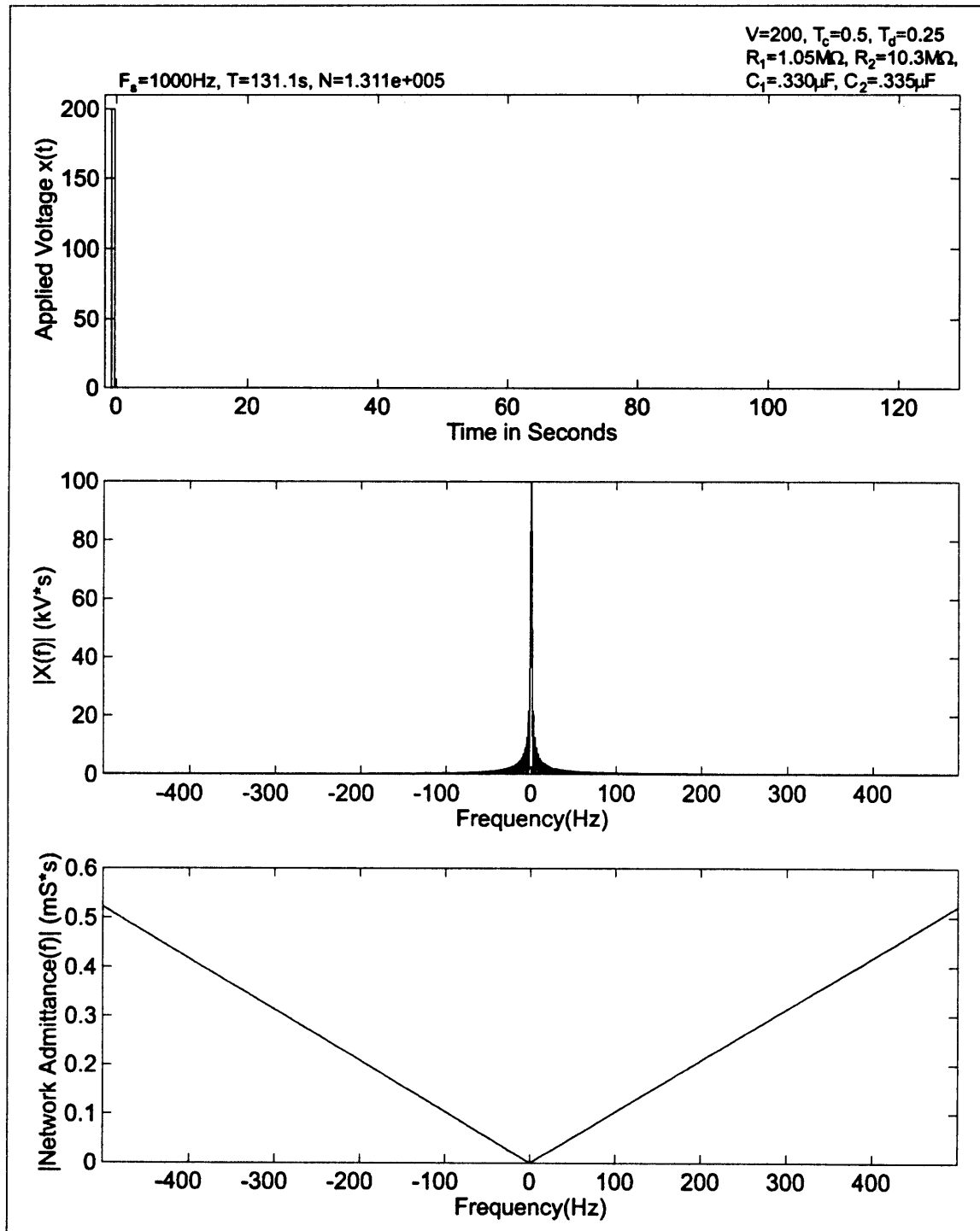


Figure C-3: Simulation of recovery voltage. Top) Applied voltage, recovery voltage is unknown and is therefore set to zero. Middle) FFT of applied voltage. Bottom) Magnitude of admittance as a function of frequency for RC network.

Appendix C: Recovery Voltage Simulation

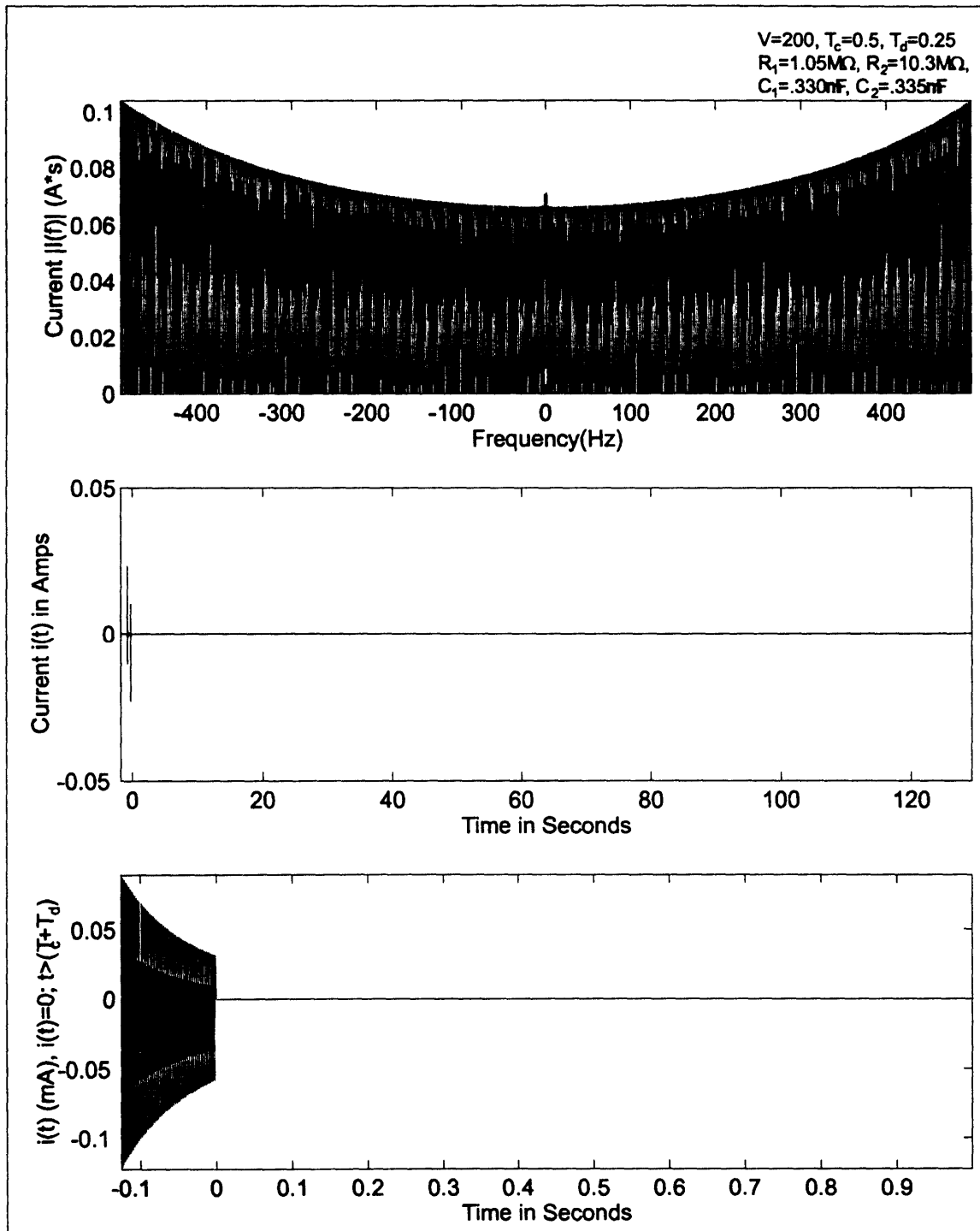


Figure C-4: Simulation of recovery voltage. Top) FFT of current flowing into RC network due to applied voltage. Middle) IFFT of current. Bottom) Current after imposing open circuit conditions at recovery period.

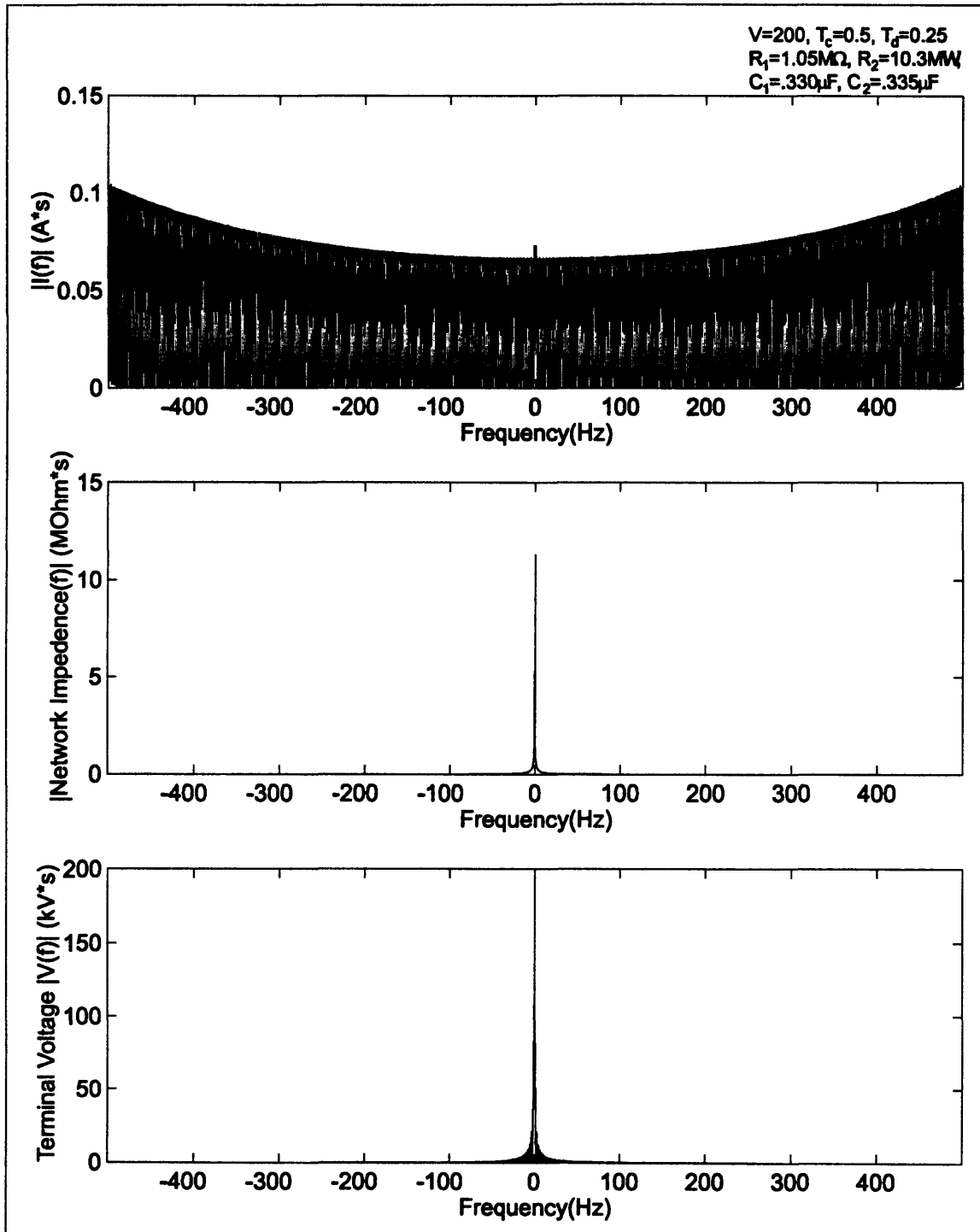


Figure C-5: Simulation of recovery voltage. Top) FFT of current after imposing zero current for recovery stage. Middle) Magnitude of network impedance. Bottom) FFT of network voltage after imposing open circuit condition for recovery period.

Appendix C: Recovery Voltage Simulation

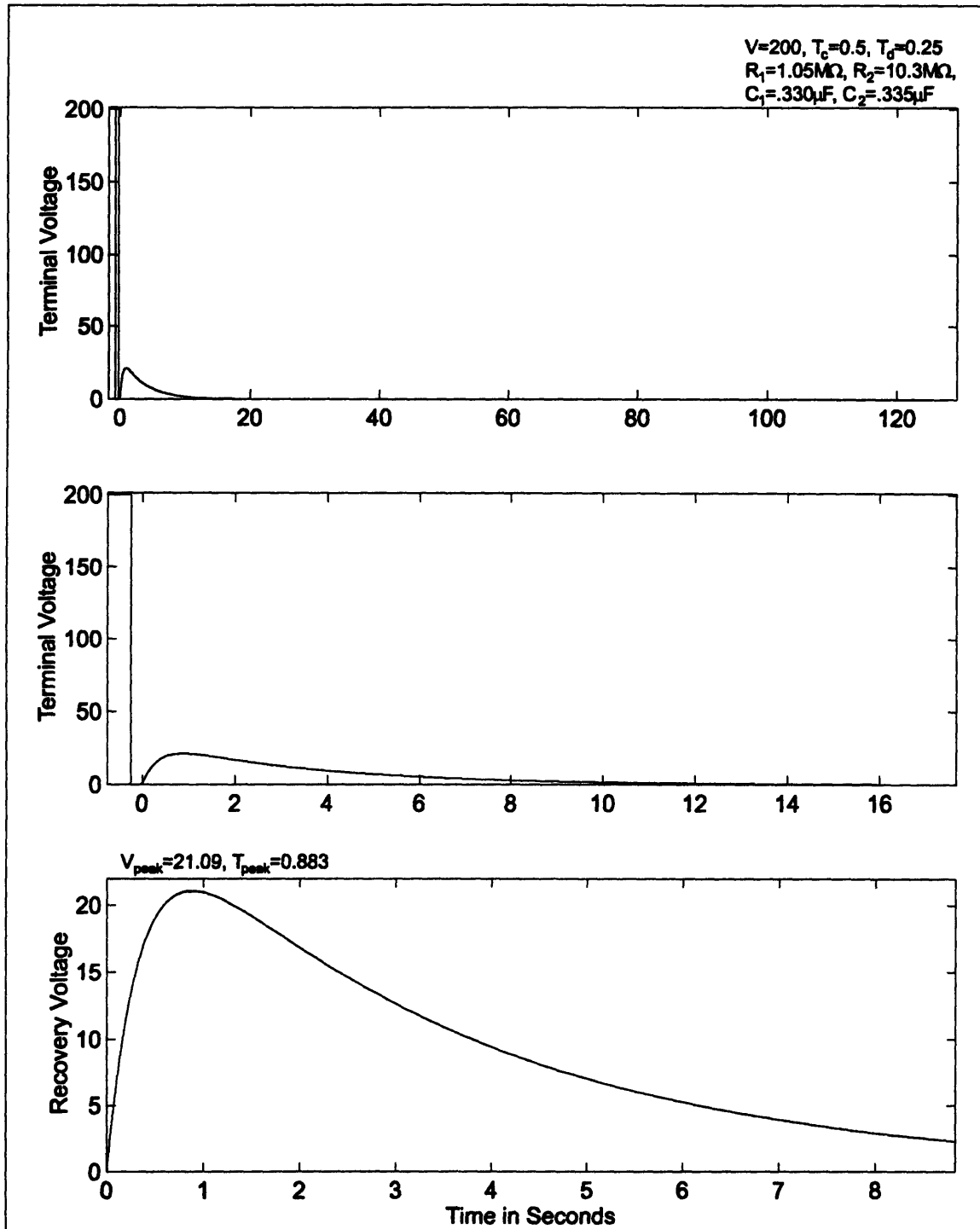


Figure C-6: Simulation of recovery voltage. Top) Applied and recovery voltage after IFFT. Middle) Applied and recovery voltage. Bottom) Simulated recovery voltage.

C.3 Recovery Voltage for a Pressboard/Oil System

Prediction of the recovery voltage for a distributed system could be carried out using one of two methods. The first method would be to measure the impedance spectrum of the distributed system and then use this spectrum to simulate or predict the recovery voltage. The second method, which is applicable where the geometry and dielectric spectrum of each component of the system is well known, is to calculate the total system impedance from a system model.

The system for which predictions will be made is the Couette charger with pressboard covering the inner and outer cylinders and oil filling the gap between cylinders. Since the geometry and dielectric properties are fairly well known, the second method will be applied. The model for the system will consist of a series impedance for each layer of material in the system. The value of the impedance can easily be determined from the dielectric constant, conductivity, inner radius of the layer, outer radius of the layer, and the height of the layer as follows

$$\hat{Z}(\omega) = \frac{\ln(r_o/r_i)}{2\pi h(\sigma + j\omega\epsilon)} \quad (\text{C.15})$$

where r_o and r_i are the outer and inner radius respectively, h is the height, σ is the conductivity, and ϵ is the dielectric constant. Since three layers exist, three series impedances are necessary, one for the pressboard on the inner cylinder, one for the oil, and one for the pressboard on the outer cylinder. The dielectric constant of the oil will be assumed as $2.2\epsilon_0$, while the conductivity will be independently measured. The dielectric properties of the pressboard are somewhat more complex because of its dispersive nature. The conductivity and dielectric constant of the pressboard are functions of frequency, which are also dependent on the temperature and moisture of the pressboard. The expression for the total impedance of the system is

$$\hat{Z}(\omega) = \frac{\ln(r_{pbi}/r_i)}{2\pi h(\sigma_{pb}(\omega, T, M) + j\omega\epsilon_{pb}(\omega, T, M))} + \frac{\ln(r_{pbo}/r_{pbi})}{2\pi h(\sigma_{oil} + j\omega 2.2\epsilon_0)} + \frac{\ln(r_o/r_{pbo})}{2\pi h(\sigma_{pb}(\omega, T, M) + j\omega\epsilon_{pb}(\omega, T, M))} \quad (\text{C.16})$$

Appendix C: Recovery Voltage Simulation

where r_i is the inner cylinder radius, r_{pbi} is the outer radius of the inner cylinder pressboard, r_o is the outer cylinder radius, r_{pbo} is the inner radius of the outer cylinder pressboard, T is the temperature of the pressboard, M is moisture content of the pressboard.

C.3.1 Pressboard Dielectric Spectrum

Previous research in [5] has demonstrated a method of shifting a universal spectrum for the dielectric properties of pressboard in order to compensate for both temperature and moisture effects. A plot of the real and imaginary components of the complex permittivity for two moisture levels at 35°C are shown in Figure C-7. The universal curve data used to generate these plots existed for frequencies in the range of .005 Hz to 10KHz and therefore some assumptions were made as to the asymptotic behavior of the spectrum in order to make values available for all frequencies.

The universal curve data, shift algorithms for moisture and temperature, and asymptotic assumptions were combined in a Matlab function which was used in evaluating Eq. C.16 in simulations.

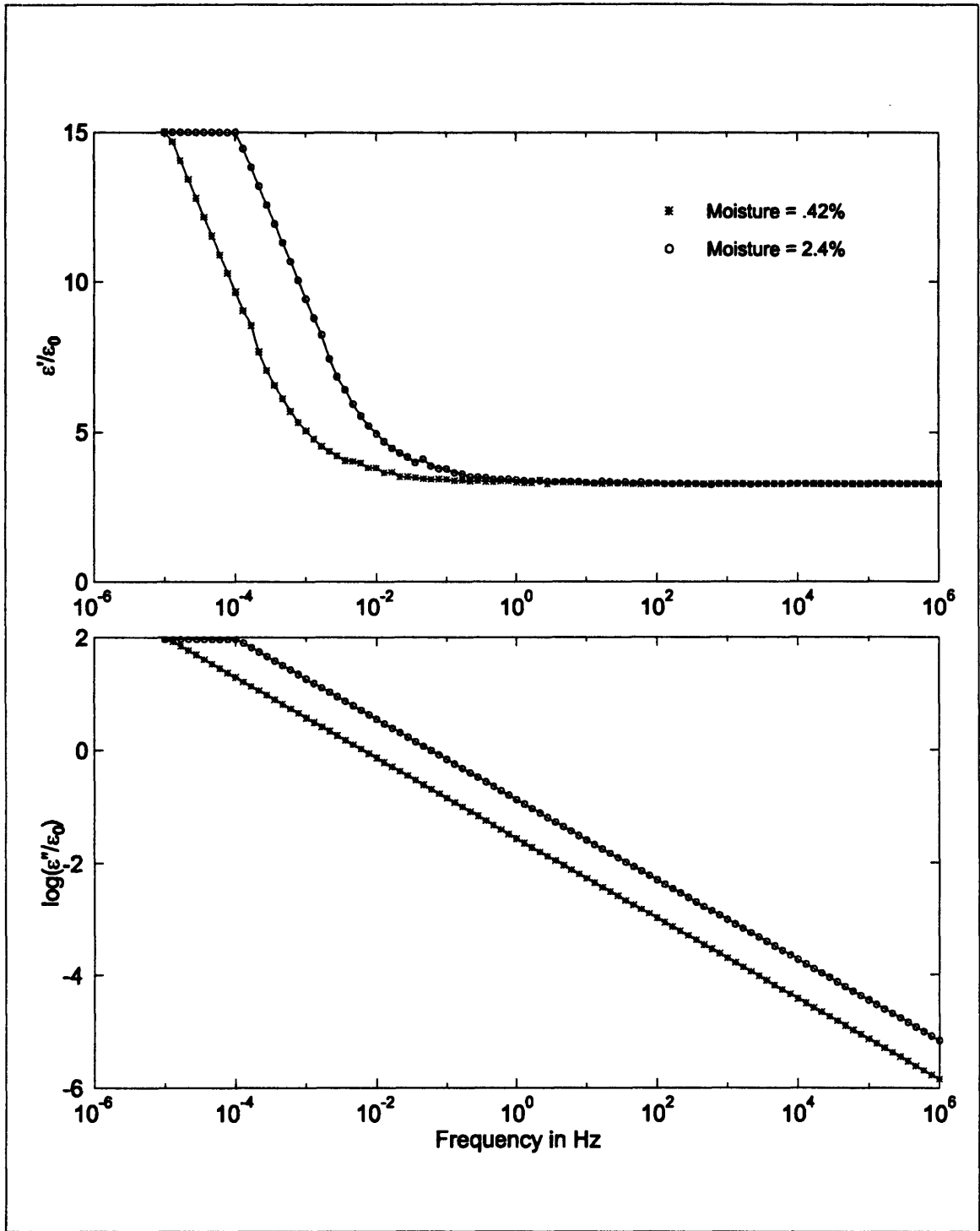


Figure C-7: Dielectric spectrum of pressboard at two levels of moisture.

C.3.2 Simulation of Recovery Voltage

Simulations for the recovery voltage in the oil/pressboard system were made using the calculated impedance spectrum of Eq. C.16, which was based on known geometric factors and dielectric properties. In this simulations the conductivity of the oil was chosen to be 3 pS, the pressboard on each cylinder was chosen to be 1.2 mm thick, while the temperature and moisture were chosen as 35°C and 1% respectively. Each step of simulation using previously described techniques is shown in Figure C-8 through Figure C-11.

No measurements of the physical system under these conditions were made, but the simulated recovery voltage has many qualitative similarities to previously simulated recovery voltages, but also some differences. The characteristic shape during the recovery period of a rise to a peak, followed by a decay is observed. However, the recovery voltage does not start out at zero and also does not seem to decay to zero as one might expect. The applied charging and discharging voltage also seem to be affected at the end of the simulation and do not exactly match the original applied voltage signal. Since this was not observed in the network simulations, it is believed that these effects resulted from the asymptotic assumptions of the pressboard dielectric spectrum. Improvements may be made here by making better choices of the asymptotic behavior to maintain causality of the pressboard response through Kramers-Krönig relations. An alternate solution may be to pre-filter the signals, so that most of the spectral power in the response is in the known frequency range of the pressboard spectrum.

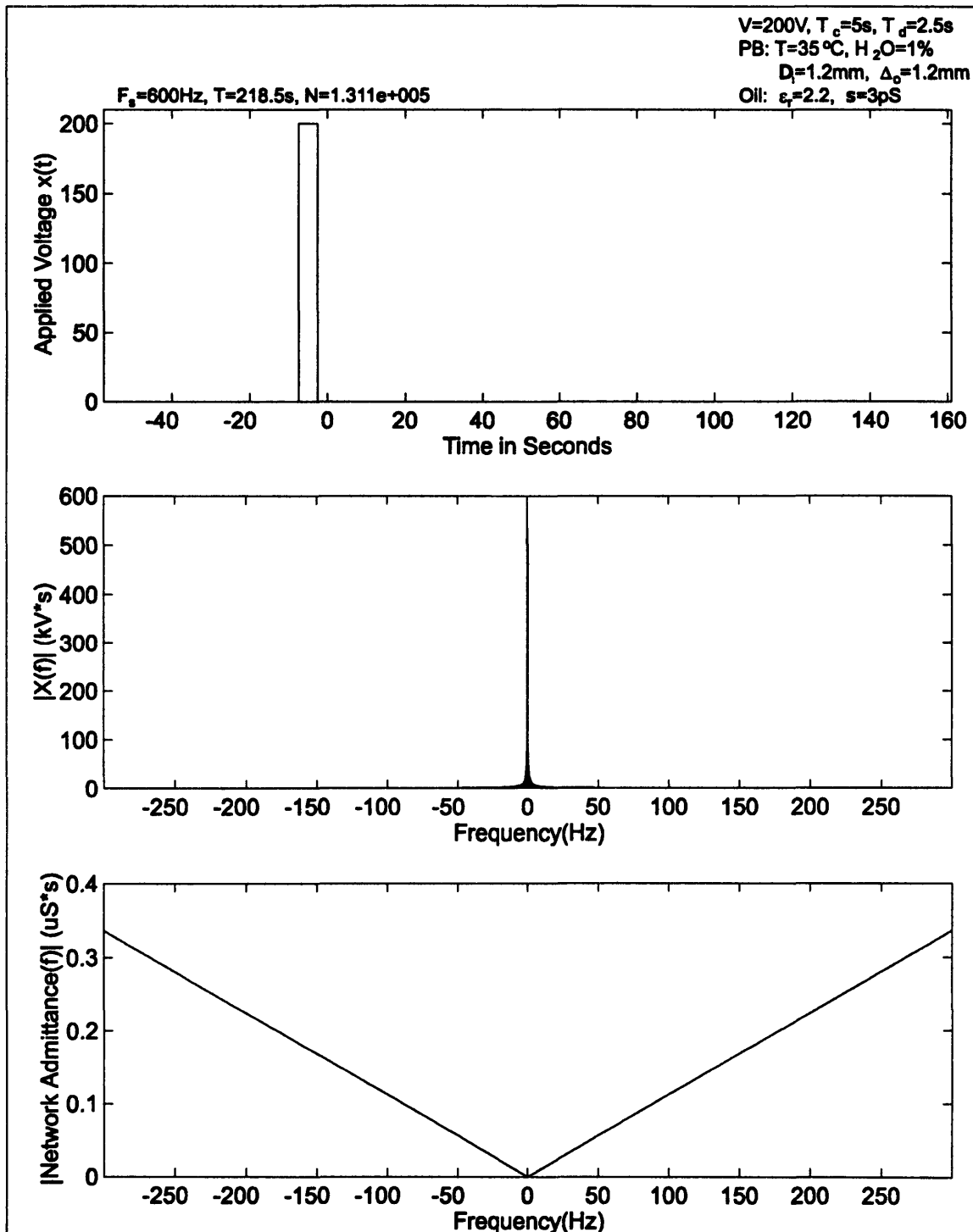


Figure C-8: Simulation of recovery voltage. Top) Applied voltage, recovery voltage is unknown and is therefore set to zero. Middle) FFT of applied voltage. Bottom) Magnitude of admittance as a function of frequency for modeled oil/pressboard system.

Appendix C: Recovery Voltage Simulation

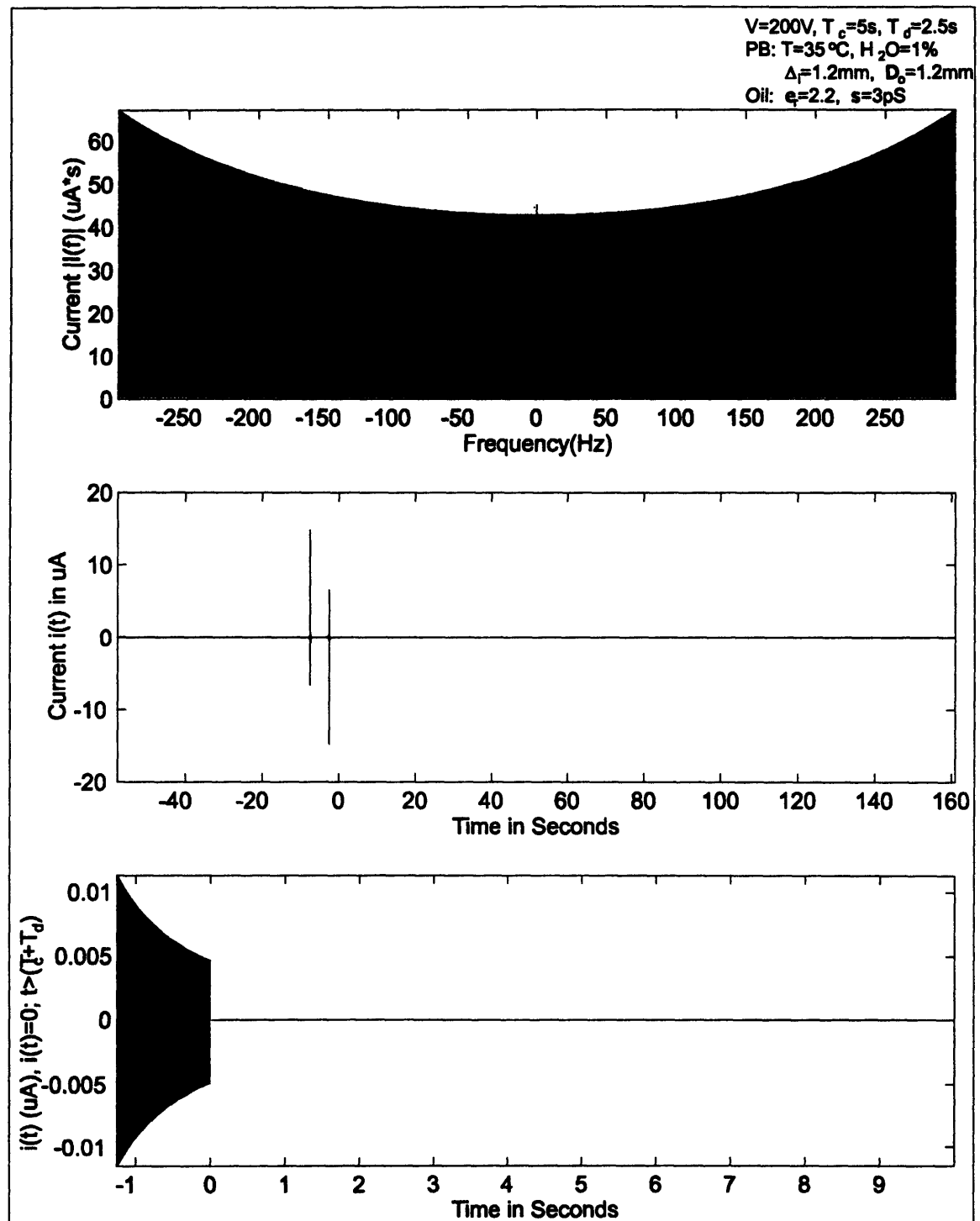


Figure C-9: Simulation of recovery voltage. Top) FFT of current flowing pressboard/oil system due to applied voltage. Middle) IFFT of current. Bottom) Current after imposing open circuit conditions at recovery period.

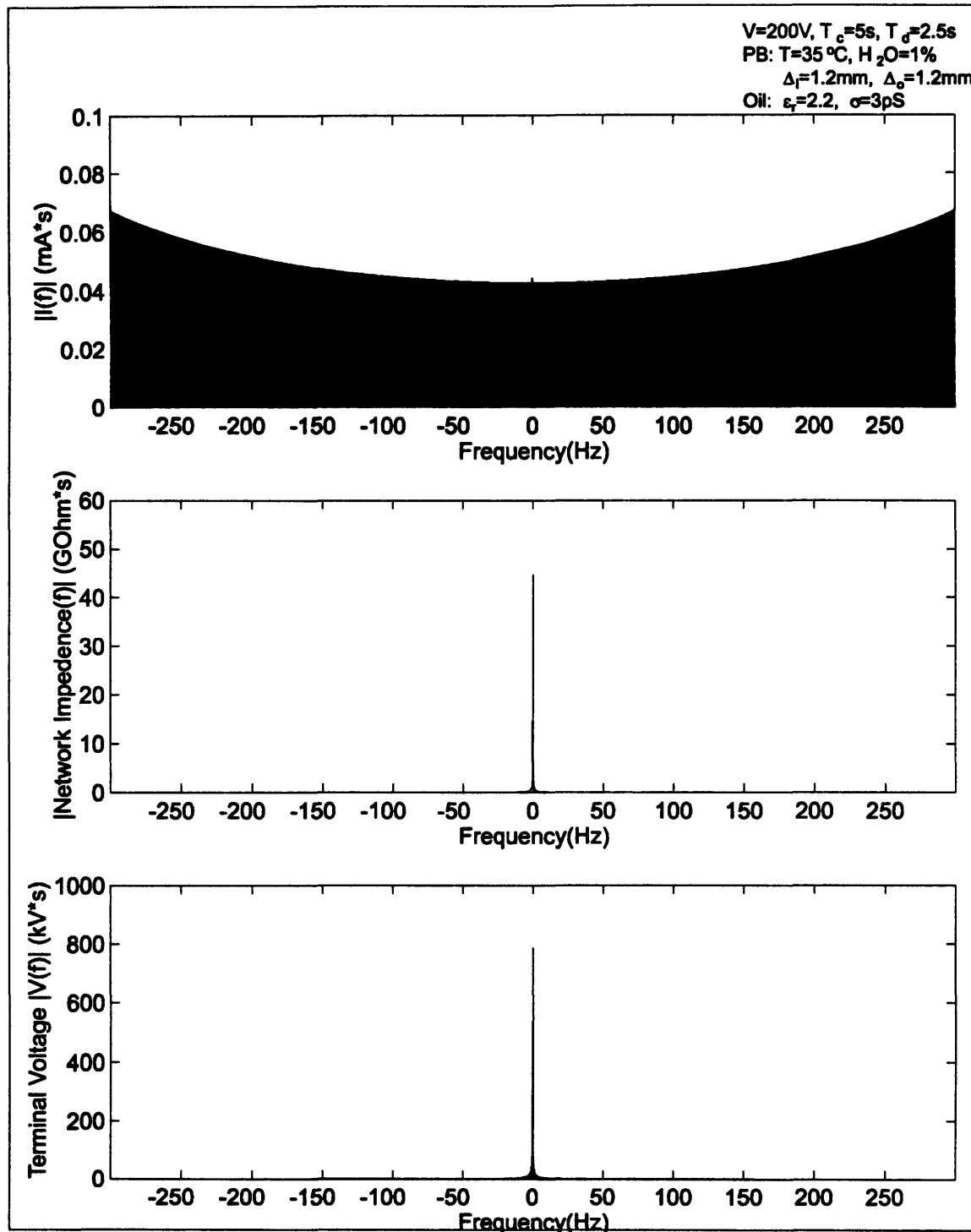


Figure C-10: Simulation of recovery voltage. Top) FFT of current after imposing zero current for recovery stage. Middle) Magnitude of network impedance. Bottom) FFT of network voltage after imposing open circuit condition for recovery period.

Appendix C: Recovery Voltage Simulation

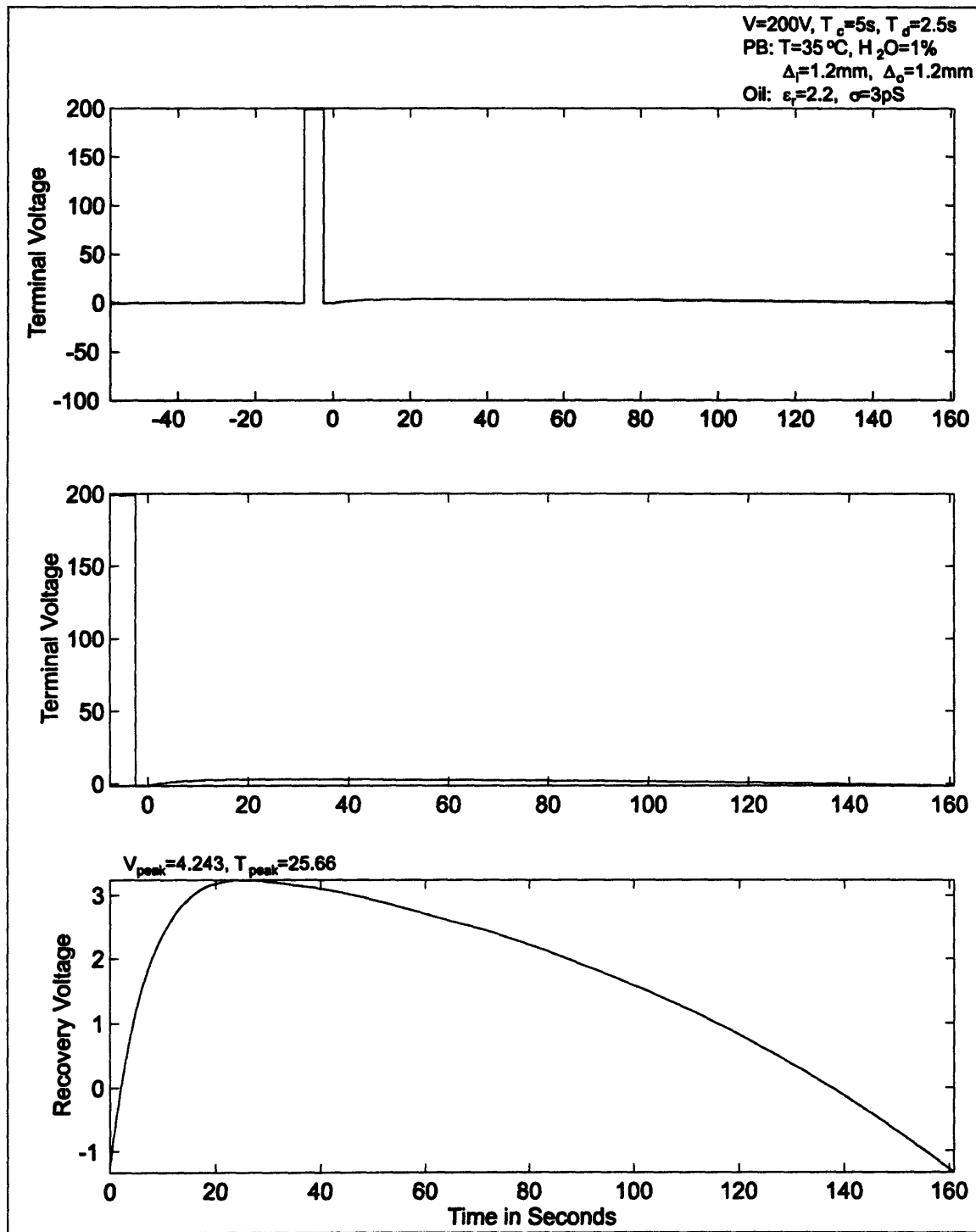


Figure C-11: Simulation of recovery voltage. Top) Applied and recovery voltage after IFFT. Middle) Applied and recovery voltage. Bottom) Simulated recovery voltage.

C.4 Scripts Used for Recovery Voltage Simulations

C.4.1 RC Network Simulation

The following Matlab script was used to simulate the recovery voltage for a second-order RC network, using only its impedance spectrum.

```
% Tettex Simulation
tic

% Sheet Stamp Info
% Line 1
SimType = 'Simulation: Max Cap';
% Line 2 Tettex Parameters
% Line 3
Params1 = '\10 R_{1}=1.05M{\sym W}, R_{2}=10.3M{\sym W},';
% Line 4
Params2 = '\10 C_{1}=.330{\sym m}F, C_{2}=.335{\sym m}F';

%Tettex Parameters
TC = 5 % Charge Time
TD = 2.5 % Discharge Time
V = 200 % Voltage

% Networkwork Params
G1 = 1/(1.05e6)
G2 = 1/(10.3e6)
C1 = .330e-6
C2 = .335e-6

% Simulation Parameters
TL = 2*TC % Zero input Lead Time
Fs = 300 % Sampling Rate
n = 16 % Total Samples in period = 2^n

% Build System Input
df = Fs/(2^n); % Calculate Frequency Spacing
dt = 1/Fs; % Calculate Sampling Interval
T = 1/df; % Calculate Periodicity of time signal
Nl = TL*Fs; % Calculate Number of Samples for Lead
Ncd = TC*Fs; % Calculate Number of Samples for Charge
Ndc = TD*Fs; % Calculate Number of Samples for Discharge
Noc = (2^n) - (Nl + Ncd + Ndc); % Use Remainer of Samples for OC

x = [zeros(1,Nl) V*ones(1,Ncd) zeros(1,(Ndc+Noc))];
N = length(x)
```

Appendix C: Recovery Voltage Simulation

```
time = (-(Nl + Ncd + Ndc):(Noc-1))*dt;

% FFT Input
disp('Forward Xforming...')
X = fftshift(fft(x));
Freq = df * (-(N/2 - .5):(N/2 - .5));

% Test Network(MAX Capacitor)
Yw = '(G1*G2 + i*w*(G1*C2 + G2*C1) - (w.^2)*C1*C2)/((G1+G2) + i*w*(C1+C2))'

% Filter Input
w = 2*pi*Freq;
Y = eval(Yw);
I = Y.*X;

% Find IFFT of Current
disp('Inverse FFT of Current...')
ii = ifft(fftshift(I));

% Extract Current and add Open Circuit Time
inew = real([ii(1:(Nl + Ncd + Ndc)) zeros(1,Noc)]);

% Xform Current Input
disp('Xforming Current with Open-Circuit...')
Inew = fftshift(fft(inew));

%Inverse Test Network
Zw = '((G1+G2) + i*w*(C1+C2))/(G1*G2 + i*w*(G1*C2 + G2*C1) - (w.^2)*C1*C2)'

% Apply Current to System
w = 2*pi*Freq;
Z = eval(Zw);
VO = Inew.*Z;

% Inverse Transform VO
disp('Inverse Xforming Vo...')
vo = real(ifft(fftshift(VO)));

% Calculate Measured Tettex Parameters
AvgCDV = mean(real(vo( (Nl + 2):(Nl + Ncd - 2) )))
AvgDCV = mean(real(vo( (Nl + Ncd + 2):(Nl + Ncd + Ndc - 2) )))
```

```
RealVmax = max(real(vo( (Nl + Ncd + Ndc):N )))
```

```
CorrectedVmax = RealVmax - (AvgDCV + (AvgCDV - V))/2  
Tmax = find(real(vo( (Nl + Ncd + Ndc):N )) == RealVmax)*dt
```

```
toc
```

```
% Sheet 1, Applied Voltage, Xform, Network Admittance
```

```
F1 = figure('PaperPosition',[.25 .75 8 9.5],'NumberTitle','off','Name','Tettex Simulation:  
sheet 1');
```

```
% Applied Voltage
```

```
subplot(3,1,1)  
plot(time,x)  
ax = axis;  
axis([min(time) max(time) 0 (V+10)]);  
xlabel('Time in Seconds')  
ylabel('Applied Voltage x(t)')
```

```
% Xform of Input
```

```
subplot(3,1,2)  
plot(Freq,(abs(X)/1000))  
ax = axis;  
axis([min(Freq) max(Freq) ax(3) ax(4)]);  
xlabel('Frequency(Hz)')  
ylabel('|X(f)| (kV*s)')
```

```
% Network Admittance
```

```
subplot(3,1,3)  
plot(Freq,abs(Y)*1000)  
ax = axis;  
axis([min(Freq) max(Freq) ax(3) ax(4)]);  
xlabel('Frequency(Hz)')  
ylabel('|Network Admittance(f)| (mS*s)')
```

```
% Sheet 1 Headings
```

Appendix C: Recovery Voltage Simulation

```
text('String','Tettex Simulation: Sheet 1','FontSize',19,'HorizontalAlignment','center',...  
'Units','Inches','Position',[3 8.65])
```

```
text('String',SimType,'FontSize',10,'HorizontalAlignment','left',...  
'Units','Inches','Position',[4.65 8.36])
```

```
stext('String',['\10 V=' num2str(V) ', T_c=' num2str(TC) ', T_d='  
num2str(TD)],'HorizontalAlignment','left',...  
'Units','Inches','Position',[4.65 8.19])
```

```
stext('String',Params1,'HorizontalAlignment','left',...  
'Units','Inches','Position',[4.65 8.02])
```

```
stext('String',Params2,'HorizontalAlignment','left',...  
'Units','Inches','Position',[4.65 7.85])
```

% Simulation Parameters

```
stext('String',['\10 F_s=' num2str(1/dt) 'Hz, T=' num2str(N*dt) 's, N='  
num2str(N)],'HorizontalAlignment','left',...  
'Units','Inches','Position',[.1 7.85])
```

% Sheet 2, Xform of Current, $i(t)$, $i(t)$ with $i(t) = 0; t > (TC+TD)$

```
F2 = figure('PaperPosition',[.25 .75 8 9.5],'NumberTitle','off','Name','Tettex Simulation:  
sheet 2');
```

%Plot I(f)

```
subplot(3,1,1)  
plot(Freq,abs(I))  
ax = axis;  
axis([min(Freq) max(Freq) 0 max(abs(I))]);  
xlabel('Frequency(Hz)')  
ylabel('Current |I(f)| (A*s)')
```

% Temporal Response of Current

```
subplot(3,1,2)  
plot(time,real(ii))  
ax = axis;  
axis([min(time) max(time) ax(3) ax(4)]);  
xlabel('Time in Seconds')  
ylabel('Current i(t) in Amps')
```

```

% Temporal Response of Current with OC current = 0
subplot(3,1,3)
plot(time,real(inew)*1000)
ax = axis;
axis([-TD/2 4*TD min(real(inew)((TL+TC+TD/2)/dt:(TL+TC+4*TD)/dt))*1000
max(real(inew)((TL+TC+TD/2)/dt:(TL+TC+4*TD)/dt))*1000]);

xlabel('Time in Seconds')
ylabel('i(t) (mA), i(t)=0; t>(T_c+T_d)')

% Sheet 2 Headings
text('String','Tettex Simulation: Sheet 2','FontSize',19,'HorizontalAlignment','center',...
'Units','Inches','Position',[3 8.65])

text('String',SimType,'FontSize',10,'HorizontalAlignment','left',...
'Units','Inches','Position',[4.65 8.36])

stext('String',[\10 V=' num2str(V) ', T_c=' num2str(TC) ', T_d='
num2str(TD)],'HorizontalAlignment','left',...
'Units','Inches','Position',[4.65 8.19])

stext('String',Params1,'HorizontalAlignment','left',...
'Units','Inches','Position',[4.65 8.02])

stext('String',Params2,'HorizontalAlignment','left',...
'Units','Inches','Position',[4.65 7.85])

% Sheet 3, Xform of New Current, Network Impedance, V(f)
F3 = figure('PaperPosition',[.25 .75 8 9.5],'NumberTitle','off','Name','Tettex Simulation:
sheet 3');

%Freq Spec of New Current
subplot(3,1,1)
plot(Freq,abs(Inew))
ax = axis;
axis([min(Freq) max(Freq) 0 ax(4)]);
xlabel('Frequency(Hz)')
ylabel('|I(f)| (A*s)');

% Network Impedance

```

Appendix C: Recovery Voltage Simulation

```
subplot(3,1,2)
plot(Freq,abs(Z)/1e6)
ax = axis;
axis([min(Freq) max(Freq) ax(3) ax(4)]);
xlabel('Frequency(Hz)')
ylabel('|Network Impedence(f)| (MOhm*s)')

%Voltage Response
subplot(3,1,3)
plot(Freq,abs(VO)/1000)
ax = axis;
axis([min(Freq) max(Freq) ax(3) ax(4)]);
xlabel('Frequency(Hz)')
ylabel('Terminal Voltage |V(f)| (kV*s)')

% Sheet 3 Headings
text('String','Tettex Simulation: Sheet 3','FontSize',19,'HorizontalAlignment','center',...
'Units','Inches','Position',[3 8.65])

text('String',SimType,'FontSize',10,'HorizontalAlignment','left',...
'Units','Inches','Position',[4.65 8.36])

stext('String',['\10 V=' num2str(V) ', T_c=' num2str(TC) ', T_d='
num2str(TD)],'HorizontalAlignment','left',...
'Units','Inches','Position',[4.65 8.19])

stext('String',Params1,'HorizontalAlignment','left',...
'Units','Inches','Position',[4.65 8.02])

stext('String',Params2,'HorizontalAlignment','left',...
'Units','Inches','Position',[4.65 7.85])

% Plot Response
F4 = figure('PaperPosition',[.25 .75 8 9.5],'NumberTitle','off','Name','Tettex Simulation:
sheet 4');

% Plot Terminal Voltage
subplot(3,1,1)
plot(time,real(vo))
ax = axis;
axis([min(time) max(time) ax(3) ceil(max(real(vo))]))
```

```
ylabel('Terminal Voltage')
```

```
% Plot Temporal Response of Voltage Zoom on OC Response
```

```
subplot(3,1,2)
```

```
plot(time,real(vo))
```

```
ax = axis;
```

```
axis([- (TC + TD) (20*Tmax) 0 ceil(max(real(vo))))])
```

```
ylabel('Terminal Voltage')
```

```
% Plot Temporal Response of Voltage Zoom on OC Response
```

```
subplot(3,1,3)
```

```
plot(time,real(vo))
```

```
ax = axis;
```

```
axis([0 10*Tmax 0 ceil(RealVmax)])
```

```
xlabel('Time in Seconds')
```

```
ylabel('Recovery Voltage')
```

```
% Headings
```

```
text('String','Tettex Simulation: Sheet 4','FontSize',19,'HorizontalAlignment','center',...  
'Units','Inches','Position',[3 8.65])
```

```
text('String',SimType,'FontSize',10,'HorizontalAlignment','left',...  
'Units','Inches','Position',[4.65 8.36])
```

```
stext('String',['\10 V=' num2str(V) ', T_c=' num2str(TC) ', T_d='  
num2str(TD)],'HorizontalAlignment','left',...  
'Units','Inches','Position',[4.65 8.19])
```

```
stext('String',Params1,'HorizontalAlignment','left',...  
'Units','Inches','Position',[4.65 8.02])
```

```
stext('String',Params2,'HorizontalAlignment','left',...  
'Units','Inches','Position',[4.65 7.85])
```

```
% Recovery voltage Parameters
```

```
stext('String',['\10 V_{peak}=' num2str(CorrectedVmax) ', T_{peak}='  
num2str(Tmax)],'HorizontalAlignment','left',...  
'Units','Inches','Position',[1 2.25])
```

```
% Print plots
```

```
pq = input('Print(y/n)? ','s');
```

Appendix C: Recovery Voltage Simulation

```
if (pq == 'y')
    pq = input('Print All(y/n)? ','s');
    if (pq == 'y')
        pnt = [1 1 1 1];
    else
        pnt = [0 0 0 0];
        pq = input('Print Sheet 1(y/n)? ','s');
        if (pq == 'y')
            pnt(1) = 1;
        end

        pq = input('Print Sheet 2(y/n)? ','s');
        if (pq == 'y')
            pnt(2) = 1;
        end
        pq = input('Print Sheet 3(y/n)? ','s');
        if (pq == 'y')
            pnt(3) = 1;
        end

        pq = input('Print Sheet 4(y/n)? ','s');
        if (pq == 'y')
            pnt(4) = 1;
        end
    end

    % Print
    FH = [F1 F2 F3 F4];
    for plt = 1:4
        if (pnt(plt))
            figure(FH(plt));
            printsto;
        end
    end
end
```

C.4.2 Function to Generate Pressboard Spectrum

The following Matlab function utilizes data and algorithms in [5], along with some assumptions on the asymptotic behavior of the spectrum to generate a complex dielectric constant for specified frequency, temperature and moisture of oil-impregnated pressboard.


```

% Function to Determine Dielectric Spectrum of Pressboard at

% Given Temp in degrees C and Moisture Content in % H2O by
% Oil impregnated Weight
%
% [e1, e2] = function pbspec(temp, moist, Freq)
%
% Written by D.Schlicker 3/8/96
% Utilizes Data by Yanko Sheiretov

function [e1, e2] = pbspec(temp, moist, Freq);

% Extrapolation Parameters
e1max = 15; % Maximum Extrapolated Epsilon1

% Calculate Temp Freq shift Using Yanko Temp Curve or Extrapolation
if ((temp <= 70) & (temp >=30))
    Tlogfs =interp1([30 40 50 60 70],[-0.71    -0.34 0 0.3 0.61],temp);
else
    Tlogfs = .0328*temp - 1.668;
end;

% Calculate Moisture Freq shift Using Linear Interpolation of Known Points
% These Points seem to have much experimental error, but are the only
% measured relation.

% Yanko Data for Moist vs. shift
Mstr = [.42 .83 1.1 1.8 2.2 2.4];
Fshift = [-0.96 -0.98 -0.54 -0.49 -0.48 0];

% Moisture Below .42 % results in Mlogfs = -.96
if (moist < .42)
    Mlogfs = -.96;
elseif (moist > 2.4)
    Mlogfs = 2.4*(moist-2.4); %?Extrapolate?
else
    % Interpolate
    Mlogfs = interp1(Mstr,Fshift,moist);
end

% Calculate Total Log Shift
Flogfs = Tlogfs + Mlogfs;

% Map Input Frequencies to Universal Curve Frequencies

```

Appendix C: Recovery Voltage Simulation

$$\text{FreqUniv} = 10.^{(\log_{10}(\text{Freq}) - \text{Flogfs})};$$

% Universal Curve Data

% Universal Curve(MA50) for epsilon2

e1univ = [4.000000 3.273295

3.907000 3.243553

3.796000 3.258656

3.699000 3.284077

3.606000 3.268672

3.495000 3.278840

3.398000 3.273792

3.305000 3.238986

3.194000 3.263941

3.097000 3.278581

3.000000 3.278855

2.907000 3.309288

2.796000 3.278764

2.699000 3.263931

2.606000 3.278964

2.495000 3.298983

2.398000 3.304171

2.305000 3.340130

2.194000 3.289129

2.097000 3.345390

2.000000 3.329418

1.907000 3.258389

1.796000 3.445536

1.699000 3.297144

1.606000 3.304375

1.495000 3.324654

1.398000 3.359997

1.305000 3.360532

1.200000 3.355151

1.100000 3.334554

1.000000 3.355126

0.900000 3.379080

0.800000 3.348224

0.700000 3.396824

0.600000 3.380633

0.500000 3.418789

0.400000 3.436322

0.300000 3.430781

0.200000 3.423026

0.100000 3.470855

| | |
|-----------|------------|
| 0.000000 | 3.492933 |
| -0.100000 | 3.503814 |
| -0.200000 | 3.516022 |
| -0.300000 | 3.673610 |
| -0.400000 | 3.636126 |
| -0.500000 | 3.812861 |
| -0.600000 | 3.778804 |
| -0.700000 | 3.877109 |
| -0.800000 | 4.114580 |
| -0.900000 | 3.950995 |
| -1.000000 | 4.131714 |
| -1.100000 | 4.241556 |
| -1.200000 | 4.379465 |
| -1.300000 | 4.539154 |
| -1.400000 | 4.768371 |
| -1.500000 | 5.005285 |
| -1.600000 | 5.242401 |
| -1.700000 | 5.557703 |
| -1.800000 | 5.906241 |
| -1.900000 | 6.331683 |
| -2.000000 | 6.693304 |
| -2.100000 | 7.179829 |
| -2.200000 | 7.783016 |
| -2.300000 | 8.609601]; |

% Universal Curve(MA50) for epsilon2

e2univ = [0.300000 -0.687281

| | |
|-----------|-----------|
| 0.200000 | -0.645519 |
| 0.100000 | -0.594973 |
| 0.000000 | -0.499918 |
| -0.100000 | -0.424902 |
| -0.200000 | -0.348219 |
| -0.300000 | -0.287623 |
| -0.400000 | -0.216944 |
| -0.500000 | -0.156109 |
| -0.600000 | -0.087847 |
| -0.700000 | -0.020810 |
| -0.800000 | 0.102455 |
| -0.900000 | 0.113128 |
| -1.000000 | 0.185288 |
| -1.100000 | 0.265020 |
| -1.200000 | 0.341081 |
| -1.300000 | 0.412631 |
| -1.400000 | 0.477242 |
| -1.500000 | 0.554613 |

Appendix C: Recovery Voltage Simulation

```
-1.600000    0.626924  
-1.700000    0.712905  
-1.800000    0.769886  
-1.900000    0.863848  
-2.000000    0.923977  
-2.100000    1.014168  
-2.200000    1.093876  
-2.300000    1.157271];
```

```
% Determine epsilon1
```

```
% Allocate Space
```

```
e1 = zeros(1,length(FreqUniv));
```

```
% Find Interpolatable Indexes and Interpolate
```

```
intr = find((FreqUniv >= 10^(-2.3)) & (FreqUniv <= 10^4));  
e1(intr) = interp1(10.^e1univ(:,1),e1univ(:,2),FreqUniv(intr));
```

```
% Set e1 for Frequencies > 10^4 to 3.273295
```

```
hf = find(FreqUniv > 10^4);  
e1(hf) = 3.273295*ones(1,length(hf));
```

```
% Extrpolate Frequencies < 10^-2.3 with Slope of Known epsilon at low freq until epsilon  
= e1max
```

```
% Determine Extrapolation Cut Off Frequency
```

```
lfcut = 10.^(e1max + 4.53616)/(-5.64555);
```

```
% Extrapolate Between 10^-2.3 and lfcut
```

```
lf = find((FreqUniv < (10^(-2.3))) & (FreqUniv >= lfcut));  
e1(lf) = (log10(FreqUniv(lf)) * (-5.64555)) - 4.53616;    % ?Extrapolate%
```

```
% Limit Expsilon for Frequencies Below lfcut
```

```
emaxf = find(FreqUniv < lfcut);  
e1(emaxf) = e1max*ones(1,length(emaxf)); % Set epsilon1 for Freq < lfcut
```

```
% Determine epsilon2 using best fit data line
```

```
% Allocate Space
```

```
e2 = zeros(1,length(FreqUniv));
```

```
% Find Data for Frequencies greater than lfcut and Line Fit
```

```
mhf = find(FreqUniv > lfcut);
```

```

e2(mhf) = 10.^(-0.71347 * log10(FreqUniv(mhf)) -0.50522);

% Limit Epsilon2 for Freq. below lfcut to epsilon2(lfcut)
lf = find(FreqUniv <= lfcut);
e2(lf) = 10.^(-0.71347 * log10(lfcut) -0.50522)*ones(1,length(lf));

% End

```

C.4.3 Recovery Voltage Simulation for Couette Charger

This is the Matlab script used to simulate the recovery voltage between inner and outer cylinders of the couette charger with pressboard on the inner and outer cylinder and oil filling the gap between cylinders.

```

% Tettex Simulation
% Test Object: Couette Charger
tic

% Simulation Description
SimType = 'Simulation: Couette Charger'

%Tettex Parameters
TC = 5      % Charge Time
TD = 2.5   % Discharge Time
V = 200    % Voltage

% CC Params
% PressBoard Dimensions
PBi = 1.2e-3
PBo = 1.2e-3

% Couette Dimensions
Ri = 7.62e-2
Ro = 10.16e-2
D = 40.64e-2

% Calculated Radius
R1 = Ri + PBi
R2 = Ro - PBo

% Oil Dielectric Properties

```

Appendix C: Recovery Voltage Simulation

$$E_{oil} = 2.2 * 8.85e-12$$

$$S_{IGoil} = 3e-12$$

% Pressboard Temp and Moisture

$$\text{Temp} = 35 \quad \% \text{ Temp in C}$$

$$\text{Moist} = 2 \quad \% \text{ Moist in \% Mass Wet}$$

% Simulation Parameters

$$TL = 10 * TC \quad \% \text{ Zero input Lead Time}$$

$$F_s = 800 \quad \% \text{ Sampling Rate}$$

$$n = 18 \quad \% \text{ Total Samples in period} = 2^n$$

% Build System Input

$$df = F_s / (2^n); \quad \% \text{ Calculate Frequency Spacing}$$

$$dt = 1 / F_s; \quad \% \text{ Calculate Sampling Interval}$$

$$T = 1 / df; \quad \% \text{ Calculate Periodicity of time signal}$$

$$N_l = TL * F_s; \quad \% \text{ Calculate Number of Samples for Lead}$$

$$N_{cd} = TC * F_s; \quad \% \text{ Calculate Number of Samples for Charge}$$

$$N_{dc} = TD * F_s; \quad \% \text{ Calculate Number of Samples for Discharge}$$

$$N_{oc} = (2^n) - (N_l + N_{cd} + N_{dc}); \quad \% \text{ Use Remainder of Samples for OC}$$

$$x = [\text{zeros}(1, N_l) \quad V * \text{ones}(1, N_{cd}) \quad \text{zeros}(1, (N_{dc} + N_{oc}))];$$

$$N = \text{length}(x)$$

$$\text{time} = (-(N_l + N_{cd} + N_{dc}) : (N_{oc} - 1)) * dt;$$

% FFT Input

disp('Forward Xforming...')

$$X = \text{fftshift}(\text{fft}(x));$$

$$\text{Freq} = df * (-(N/2 - .5) : (N/2 - .5));$$

% Couette Charger Equivalent Admittance

$$[E_{pb1} \quad E_{pb2}] = \text{pbspec}(\text{Temp}, \text{Moist}, \text{abs}(\text{Freq}));$$

$$E_{pb} = (E_{pb1} - i * E_{pb2}) * 8.85e-12;$$

$$Y_w = '(2 * \pi * D * i * w) / ((\log(R_1/R_i) + \log(R_o/R_2)) / E_{pb} + \log(R_2/R_1) / (E_{oil} - i * S_{IGoil} / w))'$$

% Filter Input

$$w = 2 * \pi * \text{Freq};$$

$$Y = \text{eval}(Y_w);$$

$$I = Y * X;$$

% Find IFFT of Current

disp('Inverse FFT of Current...')

$$ii = \text{ifft}(\text{fftshift}(I));$$

```

% Extract Current and add Open Circuit Time
inew = real([ii(1:(Nl + Ncd + Ndc)) zeros(1,Noc)]);

% Xform Current Input
disp('Xforming Current with Open-Circuit...')
Inew = fftshift(fft(inew));

% Couette Charger Equivalent Impedance
Zw = '( (log(R1/Ri) + log(Ro/R2))./Epb + log(R2/R1)./(Eoil - i*SIGoil./w)
)./(2*pi*D*i.*w)';

% Apply Current to System
w = 2*pi*Freq;
Z = eval(Zw);
VO = Inew.*Z;

% Inverse Transform VO
disp('Inverse Xforming Vo...')
vo = real(ifft(fftshift(VO)));

% Calculate Measured Tettex Parameters
AvgCDV = mean(real(vo( (Nl + 2):(Nl + Ncd - 2) )))
AvgDCV = mean(real(vo( (Nl + Ncd + 2):(Nl + Ncd + Ndc - 2) )))
RealVmax = max(real(vo( (Nl + Ncd + Ndc):N )))

CorrectedVmax = RealVmax - (AvgDCV + (AvgCDV - V))/2
Tmax = find(real(vo( (Nl + Ncd + Ndc):N )) == RealVmax)*dt

toc

% Sheet 1, Applied Voltage, Xform, Network Admittance

F1 = figure('PaperPosition',[.25 .75 8 9.5],'NumberTitle','off','Name','Tettex Simulation:
sheet 1');

% Applied Voltage
subplot(3,1,1)
plot(time,x)

```

Appendix C: Recovery Voltage Simulation

```
ax = axis;
axis([min(time) max(time) 0 (V+10)]);
xlabel('Time in Seconds')
ylabel('Applied Voltage x(t)')

% Xform of Input
subplot(3,1,2)
plot(Freq,(abs(X)/1000))
ax = axis;
axis([min(Freq) max(Freq) ax(3) ax(4)]);
xlabel('Frequency(Hz)')
ylabel('|X(f)| (kV*s)')

% Network Admittance
subplot(3,1,3)
plot(Freq,abs(Y)*1e6)
ax = axis;
axis([min(Freq) max(Freq) ax(3) ax(4)]);
xlabel('Frequency(Hz)')
ylabel('|Network Admittance(f)| (uS*s)')

% Sheet 1 Headings
text('String','Tettex Simulation: Sheet 1','FontSize',19,'HorizontalAlignment','center',...
'Units','Inches','Position',[3 8.82])

text('String',SimType,'FontSize',10,'HorizontalAlignment','left',...
'Units','Inches','Position',[4.65 8.53])

stext('String',[\10 V=' num2str(V) 'V, T_c=' num2str(TC) 's, T_d=' num2str(TD)
's'],'HorizontalAlignment','left',...
'Units','Inches','Position',[4.65 8.36])

stext('String',[\10 PB: T=' num2str(Temp) ' ^oC, H_2O=' num2str(Moist) '%]
,'HorizontalAlignment','left',...
'Units','Inches','Position',[4.65 8.19])

stext('String',[\10      {\sym D}_i=' num2str(PBi*1000) 'mm, {\sym D}_o='
num2str(PBo*1000) 'mm'],'HorizontalAlignment','left',...
'Units','Inches','Position',[4.65 8.02])
```



```
stext('String',[\10 Oil: {\sym e}_r=' num2str(Eoil/8.85e-12) ', {\sym s}='
num2str(SIGoil*1e12) 'pS'] , 'HorizontalAlignment','left',...
'Units','Inches','Position',[4.65 7.85])
```

```
% Simulation Parameters
stext('String',[\10 F_s=' num2str(1/dt) 'Hz, T=' num2str(N*dt) 's, N='
num2str(N)], 'HorizontalAlignment','left',...
'Units','Inches','Position',[.1 7.85])
```

```
% Sheet 2, Xform of Current, i(t), i(t) with i(t)=0;t> (TC+TD)
F2 = figure('PaperPosition',[.25 .75 8 9.5], 'NumberTitle','off', 'Name','Tettex Simulation:
sheet 2');
```

```
%Plot I(f)
subplot(3,1,1)
plot(Freq,abs(I)*1e6)
ax = axis;
axis([min(Freq) max(Freq) 0 max(abs(I)*1e6)]);
xlabel('Frequency(Hz)')
ylabel('Current |I(f)| (uA*s)')
```

```
% Temporal Response of Current
subplot(3,1,2)
plot(time,real(ii)*1e6)
ax = axis;
axis([min(time) max(time) ax(3) ax(4)]);
xlabel('Time in Seconds')
ylabel('Current i(t) in uA')
```

```
% Temporal Response of Current with OC current = 0
subplot(3,1,3)
plot(time,real(inew)*1e6)
ax = axis;
if (TD == 0)
    axis([-TC/2 4*TC min(real(inew((TL+TC/2)/dt:(TL+4*TC)/dt)))*1e6
max(real(inew((TL+TC/2)/dt:(TL+4*TC)/dt)))*1e6]);
else
    axis([-TD/2 4*TD min(real(inew((TL+TC+TD/2)/dt:(TL+TC+4*TD)/dt)))*1e6
max(real(inew((TL+TC+TD/2)/dt:(TL+TC+4*TD)/dt)))*1e6]);
```

Appendix C: Recovery Voltage Simulation

end

```
xlabel('Time in Seconds')
ylabel('i(t) (uA), i(t)=0; t>(T_c+T_d)')
```

% Sheet 2 Headings

```
text('String','Tettex Simulation: Sheet 2','FontSize',19,'HorizontalAlignment','center',...
'Units','Inches','Position',[3 8.82])
```

```
text('String',SimType,'FontSize',10,'HorizontalAlignment','left',...
'Units','Inches','Position',[4.65 8.53])
```

```
stext('String',[\10 V=' num2str(V) 'V, T_c=' num2str(TC) 's, T_d=' num2str(TD)
's'],'HorizontalAlignment','left',...
'Units','Inches','Position',[4.65 8.36])
```

```
stext('String',[\10 PB: T=' num2str(Temp) ' ^oC, H_2O=' num2str(Moist) '%']
,'HorizontalAlignment','left',...
'Units','Inches','Position',[4.65 8.19])
```

```
stext('String',[\10 {\sym D}_i=' num2str(PBi*1000) 'mm, {\sym D}_o='
num2str(PBo*1000) 'mm'],'HorizontalAlignment','left',...
'Units','Inches','Position',[4.65 8.02])
```

```
stext('String',[\10 Oil: {\sym e}_r=' num2str(Eoil/8.85e-12) ', {\sym s}='
num2str(SIGoil*1e12) 'pS'],'HorizontalAlignment','left',...
'Units','Inches','Position',[4.65 7.85])
```

```
% Sheet 3, Xform of New Current, Network Impedance, V(f)
F3 = figure('PaperPosition',[.25 .75 8 9.5],'NumberTitle','off','Name','Tettex Simulation:
sheet 3');
```

%Freq Spec of New Current

```
subplot(3,1,1)
plot(Freq,abs(Inew)*1e3)
ax = axis;
axis([min(Freq) max(Freq) 0 ax(4)]);
xlabel('Frequency(Hz)')
ylabel('|I(f)| (mA*s)');
```

% Network Impedence

```
subplot(3,1,2)
```

```

plot(Freq,abs(Z)/1e9)
ax = axis;
axis([min(Freq) max(Freq) ax(3) ax(4)]);
xlabel('Frequency(Hz)')
ylabel('|Network Impedence(f)| (GOhm*s)')

```

```

%Voltage Response
subplot(3,1,3)
plot(Freq,abs(VO)/1000)
ax = axis;
axis([min(Freq) max(Freq) ax(3) ax(4)]);
xlabel('Frequency(Hz)')
ylabel('Terminal Voltage |V(f)| (kV*s)')

```

```

% Sheet 3 Headings
text('String','Tettex Simulation: Sheet 3','FontSize',19,'HorizontalAlignment','center',...
'Units','Inches','Position',[3 8.82])

```

```

text('String',SimType,'FontSize',10,'HorizontalAlignment','left',...
'Units','Inches','Position',[4.65 8.53])

```

```

stext('String',[\10 V=' num2str(V) 'V, T_c=' num2str(TC) 's, T_d=' num2str(TD)
's'],'HorizontalAlignment','left',...
'Units','Inches','Position',[4.65 8.36])

```

```

stext('String',[\10 PB: T=' num2str(Temp) '^oC, H_2O=' num2str(Moist) '%]
,'HorizontalAlignment','left',...
'Units','Inches','Position',[4.65 8.19])

```

```

stext('String',[\10 {\sym D}_i=' num2str(PBi*1000) 'mm, {\sym D}_o='
num2str(PBo*1000) 'mm'],'HorizontalAlignment','left',...
'Units','Inches','Position',[4.65 8.02])

```

```

stext('String',[\10 Oil: {\sym e}_r=' num2str(Eoil/8.85e-12) ', {\sym s}='
num2str(SIGoil*1e12) 'pS'],'HorizontalAlignment','left',...
'Units','Inches','Position',[4.65 7.85])

```

```

% Plot Response
F4 = figure('PaperPosition',[.25 .75 8 9.5],'NumberTitle','off','Name','Tettex Simulation:
sheet 4');

```

```

% Plot Terminal Voltage

```

Appendix C: Recovery Voltage Simulation

```
subplot(3,1,1)
plot(time,real(vo))
ax = axis;
axis([min(time) max(time) ax(3) ceil(max(real(vo)))])
ylabel('Terminal Voltage')

% Plot Temporal Response of Voltage Zoom on OC Response
subplot(3,1,2)
plot(time,real(vo))
ax = axis;
if (20*Tmax > Noc*dt)
    Tend = Noc*dt;
else
    Tend = 20*Tmax;
end
axis([- (TC + TD) Tend min(real(vo)) ceil(max(real(vo)))])
ylabel('Terminal Voltage')

% Plot Temporal Response of Voltage Zoom on OC Response
subplot(3,1,3)
plot(time,real(vo))
ax = axis;
if (10*Tmax > Noc*dt)
    Tend = Noc*dt;
    Vst = min(real(vo)((NI + Ncd + Ndc):(NI + Ncd + Ndc + Noc)));
    Vend = max(real(vo)((NI + Ncd + Ndc):(NI + Ncd + Ndc + Noc)));
else
    Tend = 10*Tmax;
    Vst = min(real(vo)((NI + Ncd + Ndc):(NI + Ncd + Ndc + 10*Tmax/dt)));
    Vend = max(real(vo)((NI + Ncd + Ndc):(NI + Ncd + Ndc + 10*Tmax/dt)));
end
axis([0 Tend Vst Vend])
xlabel('Time in Seconds')
ylabel('Recovery Voltage')

% Sheet 4 Headings
text('String','Tettex Simulation: Sheet 4','FontSize',19,'HorizontalAlignment','center',...
'Units','Inches','Position',[3 8.82])

text('String',SimType,'FontSize',10,'HorizontalAlignment','left',...
'Units','Inches','Position',[4.65 8.53])
```

```
stext('String',[\10 V=' num2str(V) 'V, T_c=' num2str(TC) 's, T_d=' num2str(TD)
's'],'HorizontalAlignment','left',...
'Units','Inches','Position',[4.65 8.36])
```

```
stext('String',[\10 PB: T=' num2str(Temp) ' ^oC, H_2O=' num2str(Moist) '%']
,'HorizontalAlignment','left',...
'Units','Inches','Position',[4.65 8.19])
```

```
stext('String',[\10     {\sym D}_i=' num2str(PBi*1000) 'mm, {\sym D}_o='
num2str(PBo*1000) 'mm'],'HorizontalAlignment','left',...
'Units','Inches','Position',[4.65 8.02])
```

```
stext('String',[\10 Oil: {\sym e}_r=' num2str(Eoil/8.85e-12) ', {\sym s}='
num2str(SIGoil*1e12) 'pS'],'HorizontalAlignment','left',...
'Units','Inches','Position',[4.65 7.85])
```

% Recovery voltage Parameters

```
stext('String',[\10 V_{peak}=' num2str(CorrectedVmax) ', T_{peak}='
num2str(Tmax)],'HorizontalAlignment','left',...
'Units','Inches','Position',[.1 2.25])
```

% Print plots

```
pq = input('Print(y/n)? ','s');
if (pq == 'y')
    pq = input('Print All(y/n)? ','s');
    if (pq == 'y')
        pnt = [1 1 1 1];
    else
        pnt = [0 0 0 0];
        pq = input('Print Sheet 1(y/n)? ','s');
        if (pq == 'y')
            pnt(1) = 1;
        end

        pq = input('Print Sheet 2(y/n)? ','s');
        if (pq == 'y')
            pnt(2) = 1;
        end

        pq = input('Print Sheet 3(y/n)? ','s');
        if (pq == 'y')
            pnt(3) = 1;
        end
end
```

Appendix C: Recovery Voltage Simulation

```
        pq = input('Print Sheet 4(y/n)? ','s');
        if (pq == 'y')
            pnt(4) = 1;
        end
    end

    % Print
    FH = [F1 F2 F3 F4];
    for plt = 1:4
        if (pnt(plt))
            figure(FH(plt));
            printsto;
        end
    end
end
```


Appendix D

Impedance Measurement of Interdigitated Electrode Sensor

D.1 Interdigital Sensor

A sensor has been developed to measure the spatial profile of a material's dielectric properties[1]. This sensor consists of several sets of interdigital electrodes of varied spatial period which are formed on an insulating substrate and lie in contact with the plane of the measured material's surface. The insulating material also has a conductive plane on the surface opposite to the electrodes to shield the sensor from external fields and surface contamination. The region of the material that each set of electrodes is sensitive to is dependent on the period of the electrodes. As the period increases the fields tend to fringe more and the response of the set of electrodes becomes more dependent on the material farther below the surface. A sensor containing three such periods is shown in Figure D-1.

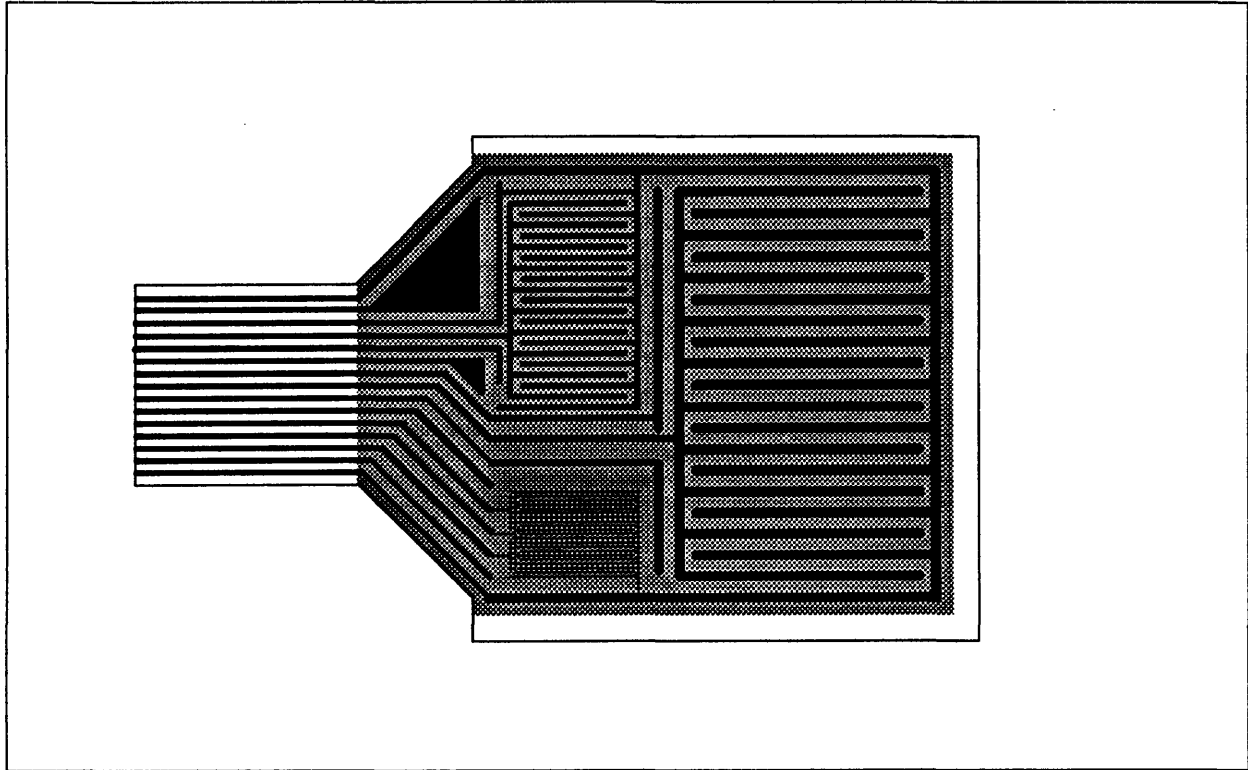


Figure D-1: Top view of interdigital electrode sensor containing three different spatial periodicity's.

Determination of the dielectric properties of the material requires several steps, the first of which is determining the admittance or impedance between electrodes of each sensor. A lumped-element circuit equivalent of one sensor is shown in Figure D-2. Terminals one and two, denoted T_1 and T_2 represent the connections to each group of alternating electrodes of a single sensor, while terminal T_3 represents the connection to the conductive plane opposite the substrate surface containing the electrodes. The capacitors C_{sub} are comprised of the capacitance due to the electric fields between the electrodes and the conductive plane. The value of these capacitors is mostly determined by the substrate, but also have a dependence on the measured material due to fields which pass through the measured material. The elements G_{ds} and C_{ds} result from the electric fields between electrodes and are highly dependent on the material properties which may also be a function of frequency. It is the measurement of this impedance which must first be made before material properties can be determined from further calculation.

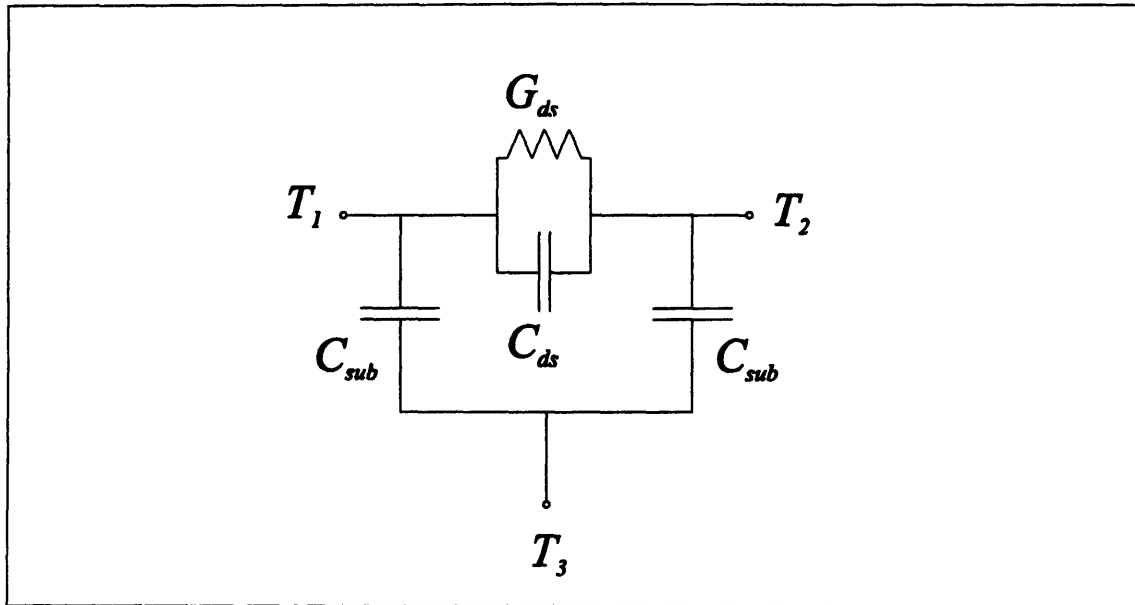


Figure D-2: Lumped-element equivalent circuit of one set of interdigitated electrodes.

D.2 Admittance Divider Technique

The technique used in previous research was to place the sensor in an admittance divider configuration as shown in Figure D-3. The first of the two admittances of the divider is formed by the parallel elements G_{ds} and C_{ds} , while the second is formed by the parallel combination of C_l (external load capacitor) and C_{sub} . The other substrate capacitance C_{sub} appears between the T_1 and T_3 terminals, but does not become part of the divider as a result of the voltage imposed across it by the source \hat{V}_d . The voltage \hat{V}_s can then be measured with a high impedance electrometer and related to the imposed voltage and unknown admittance. If the combined admittance of G_{ds} and C_{ds} are written as follows

$$\hat{Y}_t = G_{ds} + j\omega C_{ds} \quad (D.1)$$

then the system response can be written as

$$\hat{H} = \frac{\hat{V}_s}{\hat{V}_d} = \frac{\hat{Y}_t}{\hat{Y}_t + j\omega(C_l + C_{sub})} \quad (D.2)$$

Substitution of D.1 into D.2 yields the expression

$$\hat{H} = \frac{1 + j \frac{\omega}{G_{ds}/C_{ds}}}{1 + j \frac{\omega}{G_{ds}/(C_{sub} + C_l + C_{ds})}} \quad (D.3)$$

for which a Bode plot is shown in Figure D-4.

In observing the break points of the bode plot, one can see that the response is indeed dependent on both the material, substrate and load element values. Two major disadvantages exist for this type of measurement scheme. The first lies in the choosing of the load capacitor, while the second is a more practical problem related to stray admittance shielding during the actual measurement.

The care required in choosing of the load capacitor C_l can be seen by taking two limiting cases. When C_l is very large, the pole is moved to the left, this results in a significant attenuation of the response making measurements of magnitude and phase of the actual signal difficult. In the other limit, where C_l is very small, the pole and zero tend to move together. As they get close, a minimal phase of -90° is eventual reduced to 0° and the magnitude of the response remains the same. One can imagine that it will become difficult to determine the measured element values if the breakpoints they create result in no total break of the response.

The second disadvantage lies in protection against the inclusion of stray admittance in the measurement. Since in the measurement of a real sensor, the circuitry making the measurement will undoubtedly be located at a distance from the sensor, it becomes necessary to guard the wires leading from the sensor's terminal T_2 to either the electrometer measuring \hat{V}_s , or to the load capacitor. This is generally accomplished by providing an actively driven shield surrounding all such wires, which is maintained at a voltage equal to the wire's voltage. Therefore, if there is stray admittance between the shield and the protected wire, it will make no contribution. The disadvantage here is that an active circuit must provide a good guard voltage, which requires that the circuitry provide enough current with minimal phase delay.

Appendix D: Impedance Measurement of Interdigitated Electrode Sensor

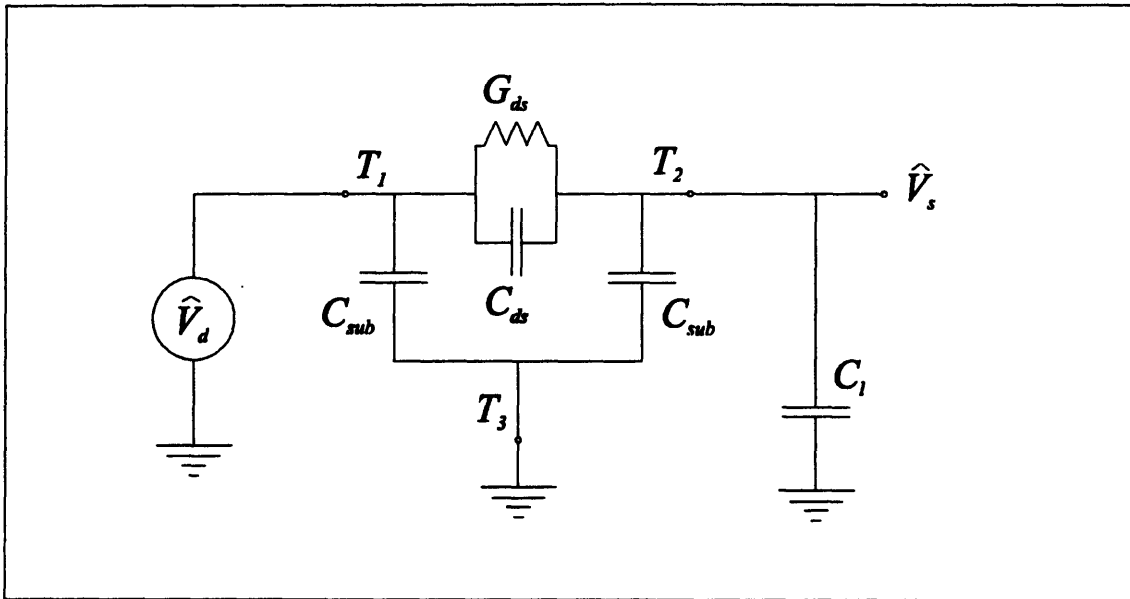


Figure D-3: Lumped-element equivalent circuit of dielectric sensor as an admittance divider.

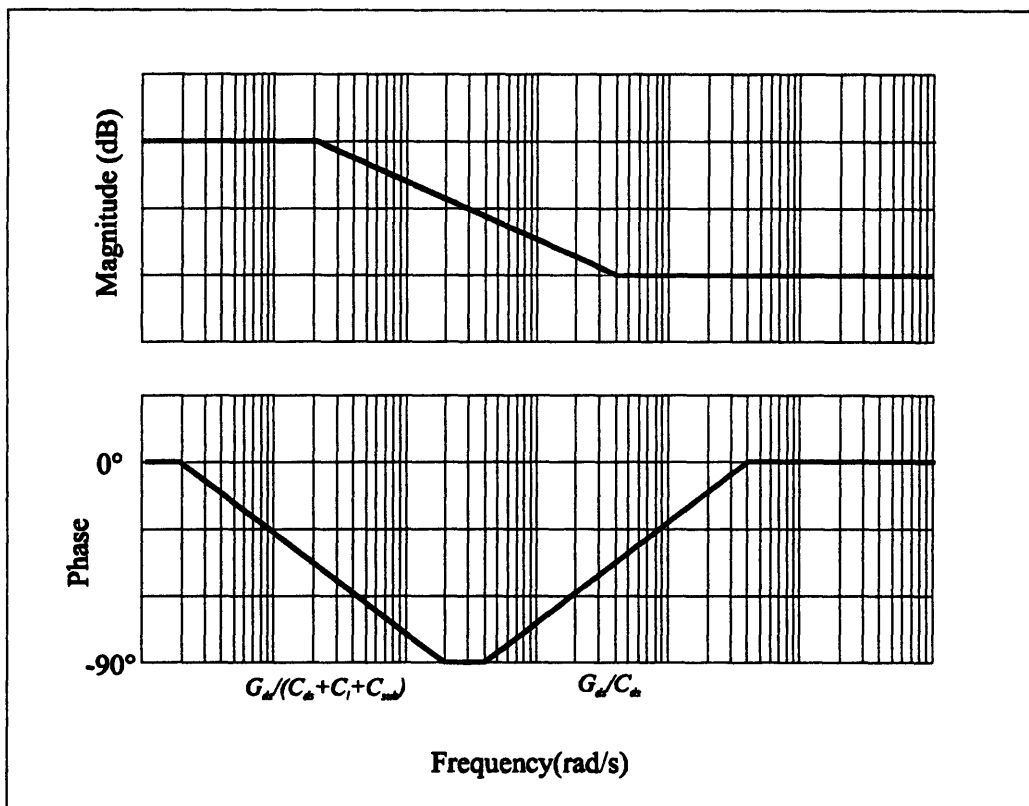


Figure D-4: Bode plot of admittance divider response.

D.3 Current Integration Technique

The idea of using an integration technique for measuring the current through an unknown admittance stems from the problems associated with measuring small currents. For example, take the reconnection of the sensor as in Figure D-5. Here the voltage source is connected directly between the T_1 and T_2 terminals. One thing to notice immediately is that the substrate capacitance between T_2 and T_3 has its voltage constrained to be zero and therefore no current will flow through it. So for the moment let's assume we have a method for determining the current \hat{I}_y , which flows out of T_2 and is also the current flowing through the unknown admittance. The voltage across the unknown admittance made up of G_{ds} and C_{ds} is now equal to \hat{V}_d and so the total admittance could be determined simply by

$$\hat{Y}_t = \frac{\hat{I}_y}{\hat{V}_d} \quad (\text{D.4})$$

where \hat{Y}_t is the total admittance of Eq. D.1. The element values of G_{ds} and C_{ds} are then solved for by equating the real and imaginary parts of Eq. D.1 and Eq. D.4. The solutions are

$$G_{ds} = \Re \left\{ \frac{\hat{I}_y}{\hat{V}_d} \right\} \quad (\text{D.5})$$

$$C_{ds} = \frac{1}{\omega} \Im \left\{ \frac{\hat{I}_y}{\hat{V}_d} \right\} \quad (\text{D.6})$$

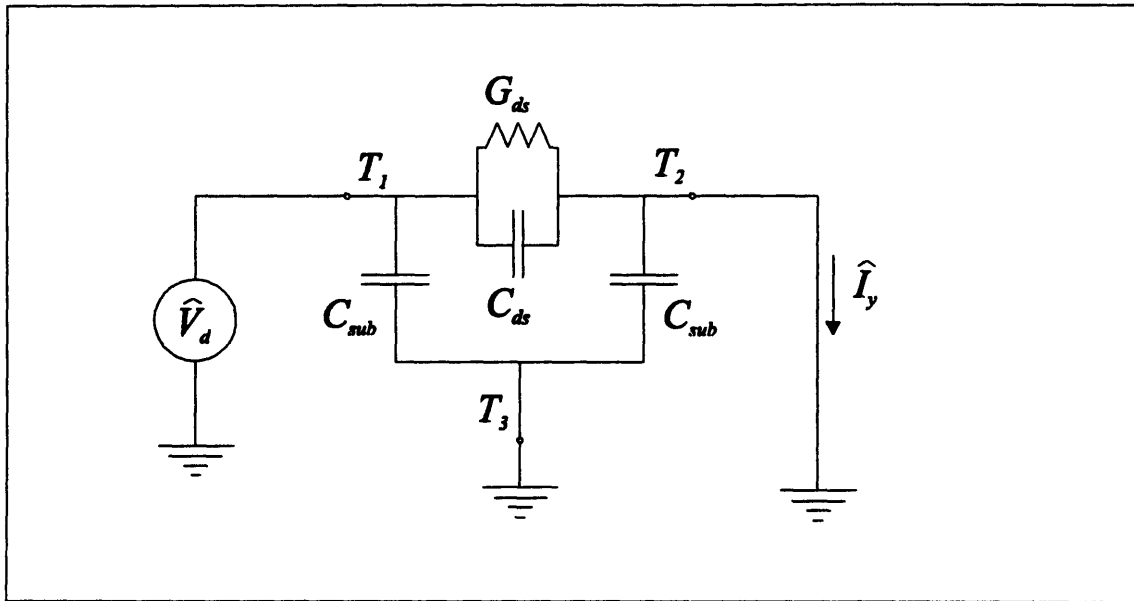


Figure D-5: Simple Current Measurement

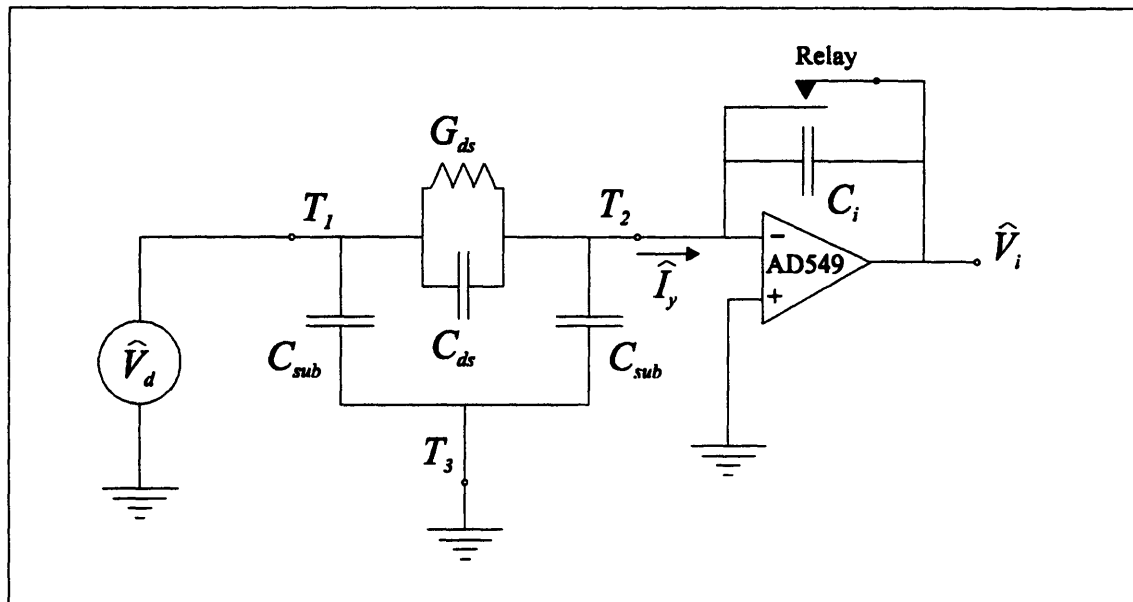


Figure D-6: Active current integration circuit.

Now a practical method of measuring the current \hat{I}_y , must be chosen. Current measurement is generally accomplished by using a load resistor to convert the current to a measurable voltage. Assuming G_{ds} is zero and taking C_{ds} to be 1 pF, a measurement at .005 Hz with a 1V peak sinusoid would yield a current with a peak amplitude of

approximately 30 fA. If it is assumed that a signal of at least 5 mV is required for measurement, a resistance of 160 GΩ would be necessary. This is an exceptionally large value for a resistor and is therefore not a very practical solution. However, an alternative solution is to use a capacitive element to accumulate the charge due to the current flow. As a quick check, assume the previous current of 35 fA and that a change of at least 5 mV must be observed over one tenth of the period. This would require a capacitor of 140pF, a small but practical value. Looking back on the original admittance divider we could view it as integrating the current from terminal T_2 on the capacitor C_l . However, in the divider, the current being integrated causes the voltage at T_2 to be non-constant and this feedback results in the poles dependency on C_l and C_{sub} . To remove the dependency, the T_2 voltage must be kept constant. This is achieved by utilizing an electrometer-grade operational amplifier in a current integrator configuration. The basic circuit along with the sensor connection is shown in Figure D-6. The circuit utilizes existing instrumentation to determine the actual magnitude and phase of the output voltage \hat{V}_i with respect to \hat{V}_d . The relay in parallel with the integration capacitor acts to discharge the capacitor before measurements.

The current \hat{I}_y can now be determined from the integration circuit using sinusoidal steady state techniques. The relationship between the measured voltage \hat{V}_i , the integration capacitance C_i , and the current is as follows:

$$\hat{V}_i = -\frac{\hat{I}_y}{j\omega C_i} \quad (D.7)$$

Now solving Eq. D.7 for \hat{I}_y and substituting into Eq. D.4, then solving for the system response yields

$$\hat{H} = \frac{\hat{V}_i}{\hat{V}_d} = -\frac{\hat{Y}_t}{j\omega C_i} \quad (D.8)$$

Further substitution of Eq. D.1 results in

$$\hat{H} = -\frac{G_{ds} + j\omega C_{ds}}{j\omega C_i} = \frac{-1}{G_{ds} C_i} \frac{1 + j\left(\frac{\omega}{G_{ds}/C_{ds}}\right)}{j\omega} \quad (D.9)$$

A bode plot has been constructed for this system response in Figure D-7.

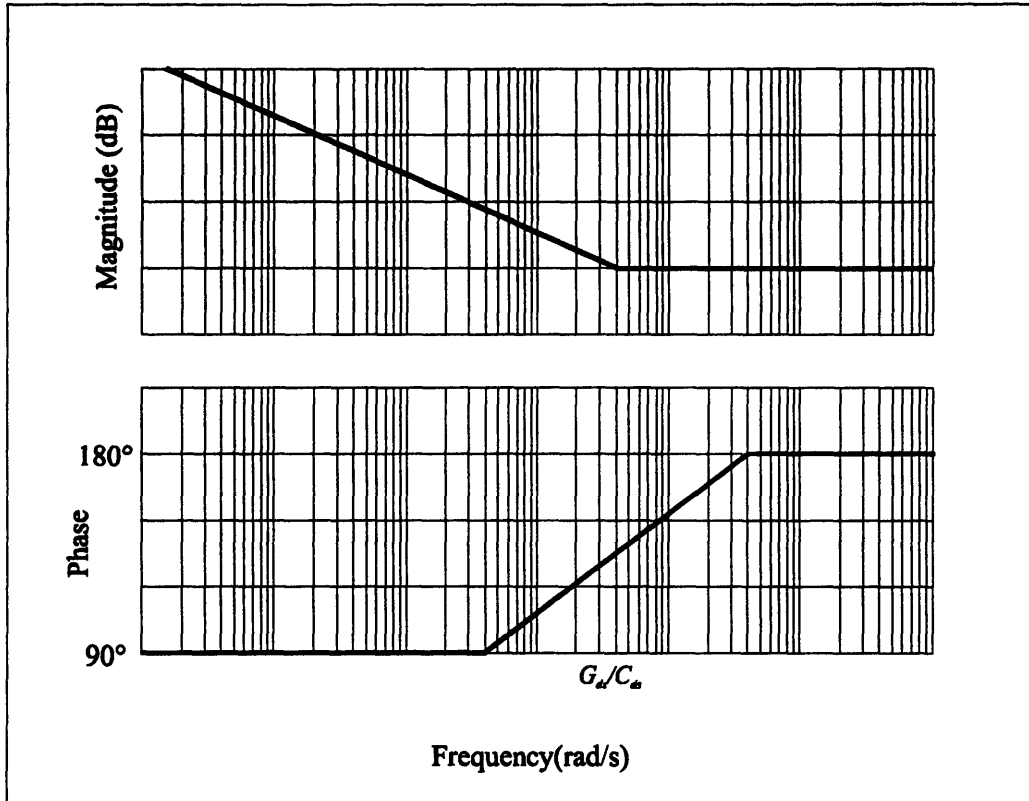


Figure D-7: Bode plot for system response of current integration technique.

The bode plot demonstrates the removal of the breakpoint due to the pole in the original divider circuit.

The current integration method offers two main advantages over the admittance divider technique. The first advantage is in the removal of the breakpoint due to the pole found in the admittance divider. C_i is now allowed to be decreased in order to maximize the signal without losing sensitivity of the response to the measured parameters. This is observed by the phase in Figure D-7 always making a 90° transition and the magnitude always exhibiting a breakpoint independent of C_i . The second advantage, briefly discussed earlier, is found in the fact that terminal T_2 is always held at a ground potential. This

allows shielding of connections from stray capacitance to be accomplished using only grounded shields, removing the necessity for active circuitry to maintain a guard potential. Since, the conductive plane on the substrate is already maintained at a ground potential the electrode connected to terminal T_2 is effectively shielded from the also unknown C_{sub} which is generally an unwanted unknown in further stages of calculation of material dielectric properties.

D.3.1 Representative Data

Some preliminary measurements using the described current integration methodology have been made with excellent results. Figure D-8 and Figure D-9 are measurements of the sensor in air, while Figure D-10 and Figure D-11 are measurements with the sensor in contact with pressboard, a material with dispersive dielectric properties.

Appendix D: Impedance Measurement of Interdigitated Electrode Sensor

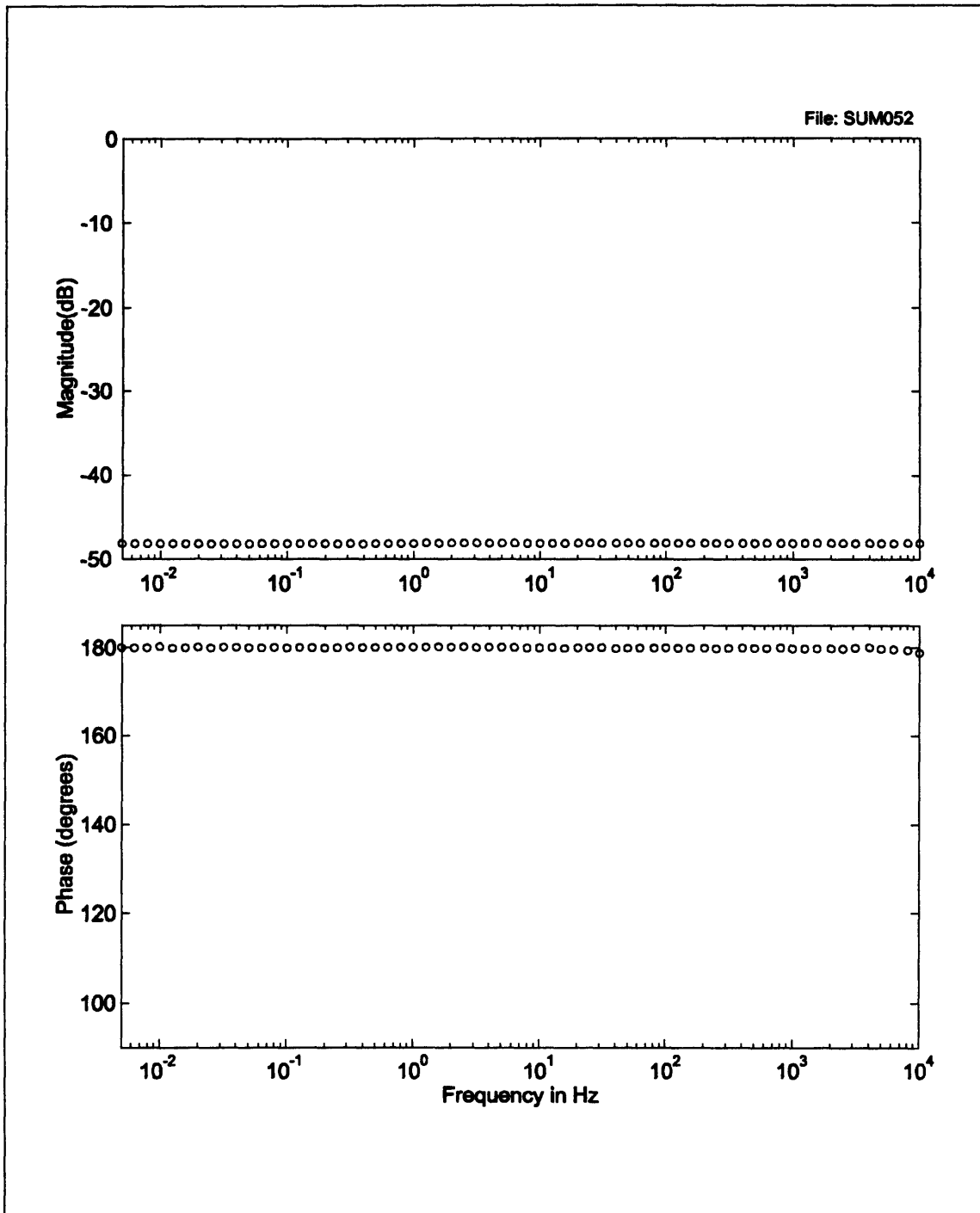


Figure D-8: Magnitude and phase measurement using current integration technique.

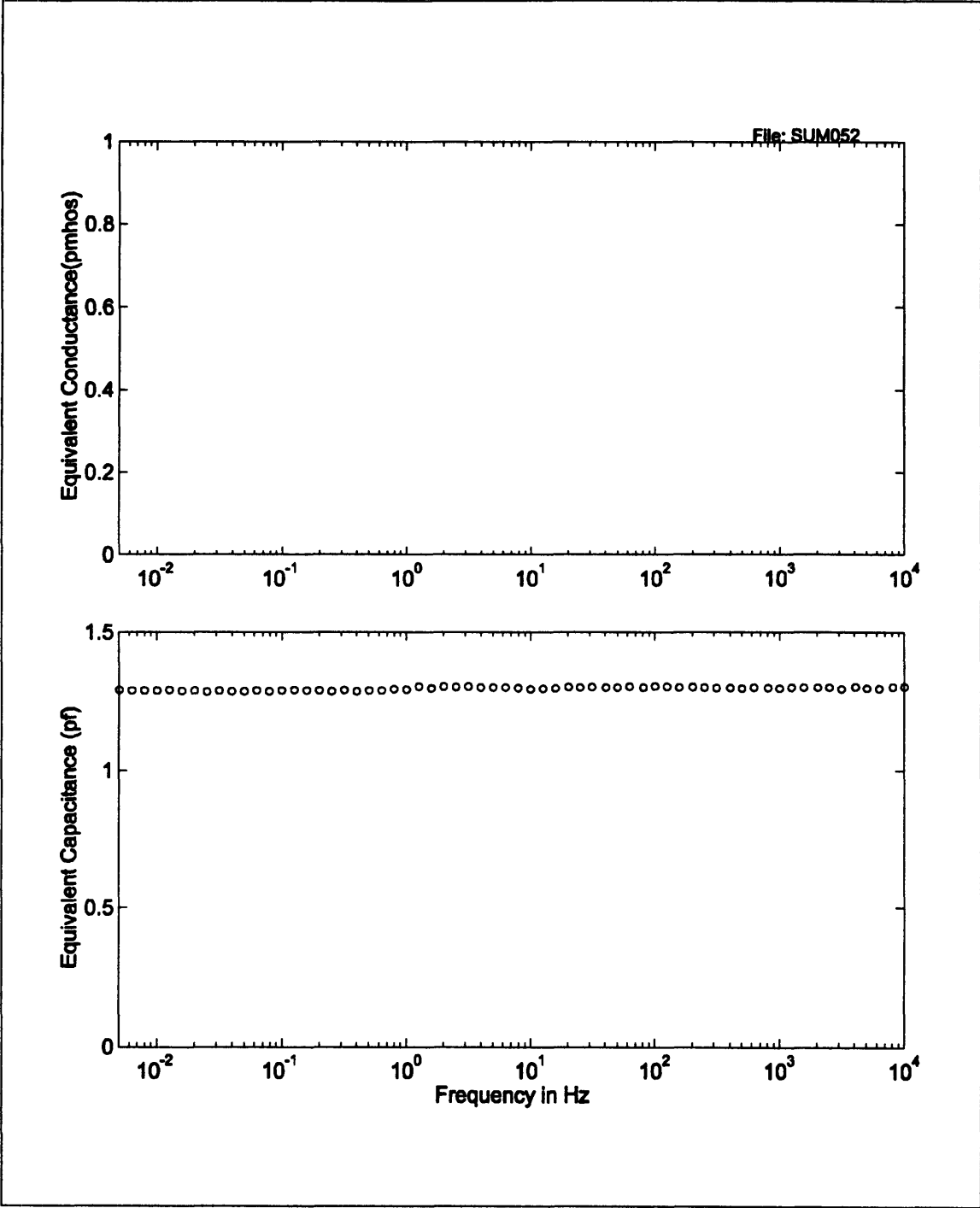


Figure D-9: Sensor capacitance and conductance measurement in air using current integration technique. Since both sensor and air are pure dielectrics, no conductance is observed.

Appendix D: Impedance Measurement of Interdigitated Electrode Sensor

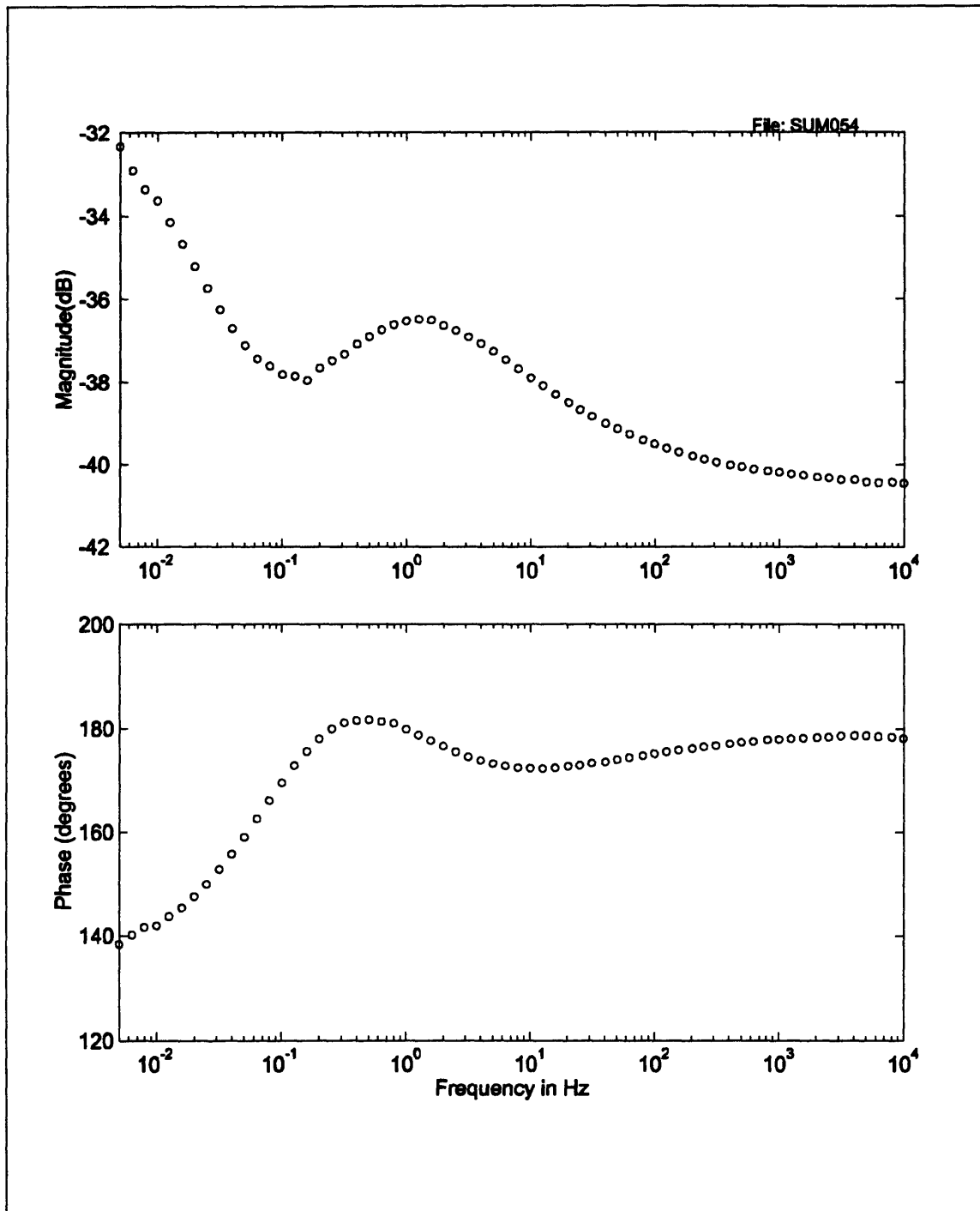


Figure D-10: Sensor magnitude and phase response in pressboard. The behavior of the gain and phase is due to the highly dispersive nature of the pressboard.

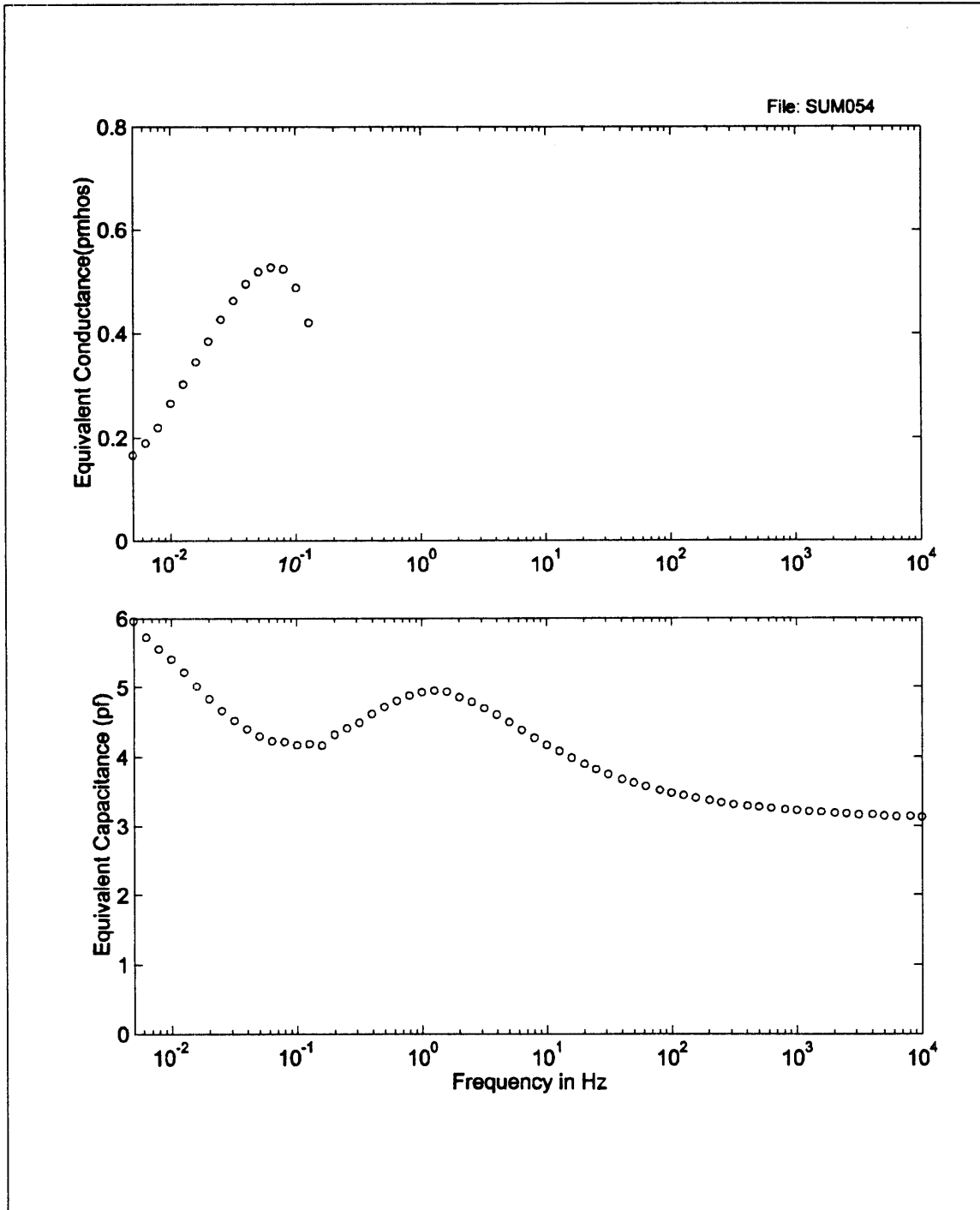


Figure D-11: Sensor capacitance and conductance when in contact with pressboard. The behavior of the capacitance and conductance signifies the known non-ohmic characteristics of the pressboard's dielectric spectrum.

Appendix D: Impedance Measurement of Interdigitated Electrode Sensor

D.3.2 Analysis Script

The magnitude and phase data was analyzed and plotted using the following Matlab m-file.

```
% TWS Admittance analysis for short circuit measurement technique
% By Darrell Schlicker 6-15-96

clear all;

% Analysis Parameters:

% Integrator Capacitance
Ci = [20 18.4 20 20] * 1e-12

% Drive Voltage
Vd = [1 1 1 1]

% Conduction Phase Limit
PhaseLimit = 5

% Admittance Divider Simulation Parameters
C11 = [20 60 100 150 200]*1e-12
C12 = [2 46]*1e-12
C13 = [20 60 100 150 200]*1e-12
C14 = [20 60 100 150 200]*1e-12

% Zero Order Dielectric Property Estimation
% Capacitance in Air
Ce0 = [1 2.55 1 1]*1e-12

% Capacitance with known material
Ce1 = [8 8 8 8]*1e-12
er1 = [3 3.1 3 3]

% End Analysis Parameters ----->

% Initialize e0
e0 = 8.85e-12;

% Get Data File Name
[filename pathname] = uigetfile('d:\darrell\twsensor\*.gpm','Plot TWS SS Current
Analysis');
```

```

if (filename==0)
    disp('Error Opening Data File!')
else

% Open File
DatID = fopen([pathname filename], 'rt');
if (DatID == -1)
    disp(' ');
    error('Error Opening Data File!');
end;

% Read off Header Data Line
[Head] = fscanf(DatID, '[GH,%f,%i,%i,%i,%i,%i]', 7);

% Read Data to Matrix
[Data, Number] = fscanf(DatID, '[GD,%i,%f,%f,%f,%f,%i]', [6, inf]);
Number = Number / 6;

% Close File
fclose(DatID);

% Divide Gain Phase Data

% Channel 1
ch_index = find(Data(1,:) == 1);

ch1Freq = 10.^Data(2, ch_index);
ch1Gain = Data(3, ch_index);
ch1Phase = Data(4, ch_index);
ch1Phase = ch1Phase + 360 * (ch1Phase < 0);
ch1Offset = Data(5, ch_index);
ch1Amp = Data(6, ch_index);

% Channel 2
ch_index = find(Data(1,:) == 2);

ch2Freq = 10.^Data(2, ch_index);
ch2Gain = Data(3, ch_index);
ch2Phase = Data(4, ch_index);
ch2Phase = ch2Phase + 360 * (ch2Phase < 0);
ch2Offset = Data(5, ch_index);

```

Appendix D: Impedance Measurement of Interdigitated Electrode Sensor

```
ch2Amp = Data(6,ch_index);

% Channel 3
ch_index = find(Data(1,:) == 3);

ch3Freq = 10.^Data(2,ch_index);
ch3Gain = Data(3,ch_index);
ch3Phase = Data(4,ch_index);
ch3Phase = ch3Phase + 360 * (ch3Phase < 0);
ch3Offset = Data(5,ch_index);
ch3Amp = Data(6,ch_index);

% Channel 4
ch_index = find(Data(1,:) == 4);

ch4Freq = 10.^Data(2,ch_index);
ch4Gain = Data(3,ch_index);
ch4Phase = Data(4,ch_index);
ch4Phase = ch4Phase + 360 * (ch4Phase < 0);
ch4Offset = Data(5,ch_index);
ch4Amp = Data(6,ch_index);

% Analysis

% Calculate Output Voltage
Vo1 = Vd(1) .* 10.^(ch1Gain/20) .* exp(i*ch1Phase*2*pi/360);
Vo2 = Vd(2) .* 10.^(ch2Gain/20) .* exp(i*ch2Phase*2*pi/360);
Vo3 = Vd(3) .* 10.^(ch3Gain/20) .* exp(i*ch3Phase*2*pi/360);
Vo4 = Vd(4) .* 10.^(ch4Gain/20) .* exp(i*ch4Phase*2*pi/360);

% Calculate Admittance
Y1 = (-Vo1/Vd(1)).* i .* Ci(1) .* 2 .* pi .* ch1Freq;
Y2 = (-Vo2/Vd(2)).* i .* Ci(2) .* 2 .* pi .* ch2Freq;
Y3 = (-Vo3/Vd(3)).* i .* Ci(3) .* 2 .* pi .* ch3Freq;
Y4 = (-Vo4/Vd(4)).* i .* Ci(4) .* 2 .* pi .* ch4Freq;

% Calculate Lumped G
G1 = real(Y1);
G2 = real(Y2);
G3 = real(Y3);
G4 = real(Y4);
```



```

% Calculate Lumped C
C1 = imag((-Vo1/Vd(1)).* i .* Ci(1));
C2 = imag((-Vo2/Vd(2)).* i .* Ci(2));
C3 = imag((-Vo3/Vd(3)).* i .* Ci(3));
C4 = imag((-Vo4/Vd(4)).* i .* Ci(4));

% Zero Order Estimation of Dielectric Properties epsilon, Sigma

% Determine Geometric Factors and Substrate Capacitance from Given Data
g = (Ce0 - Ce1)/(e0 - er1*e0);
Cs = Ce0 - g.*e0;

% Estimate Dielectric properties

E1 = (C1 - Cs(1))/g(1);
E2 = (C2 - Cs(2))/g(2);
E3 = (C3 - Cs(3))/g(3);
E4 = (C4 - Cs(4))/g(4);

S1 = G1/g(1);
S2 = G2/g(2);
S3 = G3/g(3);
S4 = G4/g(4);

% Simulate Admittance divider Gain Phase Response
H1 = zeros(length(C11),length(ch1Freq));
H2 = zeros(length(C12),length(ch2Freq));
H3 = zeros(length(C13),length(ch3Freq));
H4 = zeros(length(C14),length(ch4Freq));

if (length(ch1Freq) ~=0)
for loadindex = 1:length(C11)
    H1(loadindex,:) = Y1 ./ (Y1 + i*2*pi*ch1Freq*C11(loadindex) );
end
end

if (length(ch2Freq) ~=0)
for loadindex = 1:length(C12)
    H2(loadindex,:) = Y2 ./ (Y2 + i*2*pi*ch2Freq*C12(loadindex) );
end
end

```

Appendix D: Impedance Measurement of Interdigitated Electrode Sensor

```
end  
end
```

```
if (length(ch3Freq) ~=0)  
for loadindex = 1:length(CI3)  
    H3(loadindex,:) = Y3 ./ (Y3 + i*2*ch3Freq*CI3(loadindex) );  
end  
end
```

```
if (length(ch4Freq) ~=0)  
for loadindex = 1:length(CI4)  
    H4(loadindex,:) = Y4 ./ (Y4 + i*2*ch4Freq*CI4(loadindex) );  
end  
end
```

```
ADGain1 = 20*log10(abs(H1));  
ADGain2 = 20*log10(abs(H2));  
ADGain3 = 20*log10(abs(H3));  
ADGain4 = 20*log10(abs(H4));
```

```
ADPhase1 =angle(H1) * 360/(2*pi);  
ADPhase2 =angle(H2) * 360/(2*pi);  
ADPhase3 =angle(H3) * 360/(2*pi);  
ADPhase4 =angle(H4) * 360/(2*pi);
```

```
% Create Stamps
```

```
date = [ 'Date: ' num2str(Head(3)) '-' num2str(Head(4)) '-' num2str(Head(2))];  
time = [ 'Time: ' num2str(Head(5)) ':' num2str(Head(6)) ':' num2str(Head(7))];  
file = ['File: ' filename];
```

```
% Plot Data
```

```
% Sheet 1: Gain and Phase
```

```
F1=figure('PaperPosition',[.25 .75 8 9.5],'NumberTitle','off','Name','TWS Data: Sheet 1');
```

```
%Save Initial Position info
```

```
pos = get(F1,'Position');
```

```
%Enlarge figure to allow loaction of legend
```

```
set(F1,'Position',[0 0 1000 700]);
```

```
% Gain
```

```
subplot(2,1,1)
```

```

semilogx(ch1Freq,ch1Gain,'o',ch2Freq,ch2Gain,'x',ch3Freq,ch3Gain,'+',ch4Freq,ch4Gain,'
*','MarkerSize',4)
ylabel('Gain (dB)');
ax = axis;
axis([10^(-2.3) 10^4 ax(3) ax(4) ]);

```

```

lg = legend('o','Channel 1','x','Channel 2','+','Channel 3','*','Channel 4');
set(lg,'Box','off','FontSize',10,'Visible','off');
ch=get(lg,'Children');
set(ch(1),'MarkerSize',4)
set(ch(2),'FontSize',10)
set(ch(3),'MarkerSize',4)
set(ch(4),'FontSize',10)
set(ch(5),'MarkerSize',4)
set(ch(6),'FontSize',10)
set(ch(7),'MarkerSize',4)
set(ch(8),'FontSize',10)

```

```

% Phase
subplot(2,1,2)
semilogx(ch1Freq,ch1Phase,'o',ch2Freq,ch2Phase,'x',ch3Freq,ch3Phase,'+',ch4Freq,ch4Ph
ase,'*','MarkerSize',4)
ylabel('Phase (degrees)');
xlabel('Frequency in Hz')
ax = axis;
axis([10^(-2.3) 10^4 ax(3) ax(4) ]);

```

```

% Header
text('String','TWS SS Analysis: Sheet 1','FontSize',19,'HorizontalAlignment','center',...
'Units','Inches','Position',[3 8.5])

```

```

% FileStamp
text('String',file,'FontSize',10,'HorizontalAlignment','left',...
'Units','Inches','Position',[5 8.2])

```

```

% Time Stamp
text('String',time,'FontSize',10,'HorizontalAlignment','left',...
'Units','Inches','Position',[5 8.05])

```

```

% Date Stamp
text('String',date,'FontSize',10,'HorizontalAlignment','left',...
'Units','Inches','Position',[5 7.90])

```

Appendix D: Impedance Measurement of Interdigitated Electrode Sensor

```
%Restore figure size  
set(F1,'Position',pos);
```

```
% Sheet 2: Offset and Amplification
```

```
F2=figure('PaperPosition',[.25 .75 8 9.5],'NumberTitle','off','Name','TWS Data: Sheet 2');
```

```
%Save Initial Position info  
pos = get(F2,'Position');
```

```
%Enlarge figure to allow loaction of legend  
set(F2,'Position',[0 0 1000 700]);
```

```
% Offset
```

```
subplot(2,1,1)
```

```
semilogx(ch1Freq,ch1Offset,'o',ch2Freq,ch2Offset,'x',ch3Freq,ch3Offset,'+',ch4Freq,ch4Of  
fset,'*','MarkerSize',4)
```

```
ylabel('Offset in Volts');
```

```
ax = axis;
```

```
axis([10-2.3 104 ax(3) ax(4) ]);
```

```
lg = legend('o','Channel 1','x','Channel 2','+','Channel 3','*','Channel 4');
```

```
set(lg,'Box','off','FontSize',10,'Visible','off');
```

```
ch=get(lg,'Children');
```

```
set(ch(1),'MarkerSize',4)
```

```
set(ch(2),'FontSize',10)
```

```
set(ch(3),'MarkerSize',4)
```

```
set(ch(4),'FontSize',10)
```

```
set(ch(5),'MarkerSize',4)
```

```
set(ch(6),'FontSize',10)
```

```
set(ch(7),'MarkerSize',4)
```

```
set(ch(8),'FontSize',10)
```

```
% Amplification
```

```
subplot(2,1,2)
```

```
semilogx(ch1Freq,ch1Amp,'o',ch2Freq,ch2Amp,'x',ch3Freq,ch3Amp,'+',ch4Freq,ch4Amp,'  
*','MarkerSize',4)
```

```
ylabel('Amplification Factor');
```

```
xlabel('Frequency in Hz')
```

```
ax = axis;
```

```
axis([10-2.3 104 ax(3) ax(4) ]);
```

```

% Header
text('String','TWS SS Analysis: Sheet 2','FontSize',19,'HorizontalAlignment','center',...
'Units','Inches','Position',[3 8.5])

% FileStamp
text('String',file,'FontSize',10,'HorizontalAlignment','left',...
'Units','Inches','Position',[5 8.2])

% Time Stamp
text('String',time,'FontSize',10,'HorizontalAlignment','left',...
'Units','Inches','Position',[5 8.05])

% Date Stamp
text('String',date,'FontSize',10,'HorizontalAlignment','left',...
'Units','Inches','Position',[5 7.90])

%Restore figure size
set(F2,'Position',pos);

% Sheet 3: Real Admittance and Imaginary Admittance
F3=figure('PaperPosition',[.25 .75 8 9.5],'NumberTitle','off','Name','TWS Data: Sheet 3');

%Save Initial Position info
pos = get(F3,'Position');

%Enlarge figure to allow loaction of legend
set(F3,'Position',[0 0 1000 700]);

% Real part of Admittance
subplot(2,1,1)
semilogx(ch1Freq,real(Y1),'o',ch2Freq,real(Y2),'x',ch3Freq,real(Y3),'+',ch4Freq,real(Y4),'
*','MarkerSize',4)
ylabel('Real Admittance(mhos)');
ax = axis;
axis([10^(-2.3) 10^4 0 ax(4) ]);

lg = legend('o','Channel 1','x','Channel 2','+','Channel 3','*','Channel 4');
set(lg,'Box','off','FontSize',10,'Visible','off');
ch=get(lg,'Children');
set(ch(1),'MarkerSize',4)
set(ch(2),'FontSize',10)

```

Appendix D: Impedance Measurement of Interdigitated Electrode Sensor

```
set(ch(3),'MarkerSize',4)
set(ch(4),'FontSize',10)
set(ch(5),'MarkerSize',4)
set(ch(6),'FontSize',10)
set(ch(7),'MarkerSize',4)
set(ch(8),'FontSize',10)

% Imaginary Part of Admittance
subplot(2,1,2)
semilogx(ch1Freq,imag(Y1),'o',ch2Freq,imag(Y2),'x',ch3Freq,imag(Y3),'+',ch4Freq,imag(
Y4),'*', 'MarkerSize',4)
ylabel('Imaginary Admittance(mhos)');
xlabel('Frequency in Hz')
ax = axis;
axis([10^(-2.3) 10^4 0 ax(4) ]);

% Header
text('String','TWS SS Analysis: Sheet 3','FontSize',19,'HorizontalAlignment','center',...
'Units','Inches','Position',[3 8.5])

% FileStamp
text('String',file,'FontSize',10,'HorizontalAlignment','left',...
'Units','Inches','Position',[5 8.2])

% Time Stamp
text('String',time,'FontSize',10,'HorizontalAlignment','left',...
'Units','Inches','Position',[5 8.05])

% Date Stamp
text('String',date,'FontSize',10,'HorizontalAlignment','left',...
'Units','Inches','Position',[5 7.90])

%Restore figure size
set(F3,'Position',pos);

% Sheet 4: Conductance and Capacitance
F4=figure('PaperPosition',[.25 .75 8 9.5],'NumberTitle','off','Name','TWS Data: Sheet 4');

%Save Initial Position info
pos = get(F4,'Position');
```

```

%Enlarge figure to allow loaction of legend
set(F4,'Position',[0 0 1000 700]);

% Conductance

% Determine values for phase > phase limit
ftindex = find((abs(abs(ch1Phase)-180))>PhaseLimit);
ch1FreqRev = ch1Freq(ftindex);
G1Rev = G1(ftindex);

ftindex = find((abs(abs(ch2Phase)-180))>PhaseLimit);
ch2FreqRev = ch2Freq(ftindex);
G2Rev = G2(ftindex);

ftindex = find((abs(abs(ch3Phase)-180))>PhaseLimit);
ch3FreqRev = ch3Freq(ftindex);
G3Rev = G3(ftindex);

ftindex = find((abs(abs(ch4Phase)-180))>PhaseLimit);
ch4FreqRev = ch4Freq(ftindex);
G4Rev = G4(ftindex);

subplot(2,1,1)
semilogx(ch1FreqRev,G1Rev/(1e-12),'o',ch2FreqRev,G2Rev/(1e-
12),'x',ch3FreqRev,G3Rev/(1e-12),'+',ch4FreqRev,G4Rev/(1e-12),'*', 'MarkerSize',4)
ylabel('Equivalent Conductance(pmos)');

ax = axis;
axis([10^(-2.3) 10^4 0 ax(4) ]);

lg = legend('o','Channel 1','x','Channel 2','+','Channel 3','*','Channel 4');
set(lg,'Box','off','FontSize',10,'Visible','off');
ch=get(lg,'Children');
set(ch(1),'MarkerSize',4)
set(ch(2),'FontSize',10)
set(ch(3),'MarkerSize',4)
set(ch(4),'FontSize',10)
set(ch(5),'MarkerSize',4)
set(ch(6),'FontSize',10)
set(ch(7),'MarkerSize',4)
set(ch(8),'FontSize',10)

```

Appendix D: Impedance Measurement of Interdigitated Electrode Sensor

```
% Capacitance
subplot(2,1,2)
semilogx(ch1Freq,C1/(1e-12),'o',ch2Freq,C2/(1e-12),'x',ch3Freq,C3/(1e-
12),'+',ch4Freq,C4/(1e-12),'*',MarkerSize,4)
ylabel('Equivalent Capacitance (pf)');
xlabel('Frequency in Hz')
ax = axis;
axis([10^(-2.3) 10^4 0 ax(4) ]);

% Header
text('String','TWS SS Analysis: Sheet 4','FontSize',19,'HorizontalAlignment','center',...
'Units','Inches','Position',[3 8.5])

% FileStamp
text('String',file,'FontSize',10,'HorizontalAlignment','left',...
'Units','Inches','Position',[5 8.2])

% Time Stamp
text('String',time,'FontSize',10,'HorizontalAlignment','left',...
'Units','Inches','Position',[5 8.05])

% Date Stamp
text('String',date,'FontSize',10,'HorizontalAlignment','left',...
'Units','Inches','Position',[5 7.90])

%Restore figure size
set(F4,'Position',pos);

% Sheet 4: Sigma and Epsilon
F5=figure('PaperPosition',[.25 .75 8 9.5],'NumberTitle','off','Name','TWS Data: Sheet 5');

%Save Initial Position info
pos = get(F5,'Position');

%Enlarge figure to allow loaction of legend
set(F5,'Position',[0 0 1000 700]);

% Sigma
```



```

% Determine values for phase > phase limit
fltindex = find((abs(abs(ch1Phase)-180))>PhaseLimit);
ch1FreqRev = ch1Freq(fltindex);
S1Rev = S1(fltindex);

fltindex = find((abs(abs(ch2Phase)-180))>PhaseLimit);
ch2FreqRev = ch2Freq(fltindex);
S2Rev = S2(fltindex);

fltindex = find((abs(abs(ch3Phase)-180))>PhaseLimit);
ch3FreqRev = ch3Freq(fltindex);
S3Rev = S3(fltindex);

fltindex = find((abs(abs(ch4Phase)-180))>PhaseLimit);
ch4FreqRev = ch4Freq(fltindex);
S4Rev = S4(fltindex);

subplot(2,1,1)
semilogx(ch1FreqRev,S1Rev/(1e-12),'o',ch2FreqRev,S2Rev/(1e-
12),'x',ch3FreqRev,S3Rev/(1e-12),'+',ch4FreqRev,S4Rev/(1e-12),'*',MarkerSize',4)
ylabel('Sigma (pS/m)');

ax = axis;
axis([10^(-2.3) 10^4 0 ax(4) ]);

lg = legend('o','Channel 1','x','Channel 2','+','Channel 3','*','Channel 4');
set(lg,'Box','off','FontSize',10,'Visible','off');
ch=get(lg,'Children');
set(ch(1),'MarkerSize',4)
set(ch(2),'FontSize',10)
set(ch(3),'MarkerSize',4)
set(ch(4),'FontSize',10)
set(ch(5),'MarkerSize',4)
set(ch(6),'FontSize',10)
set(ch(7),'MarkerSize',4)
set(ch(8),'FontSize',10)

% Epsilon
subplot(2,1,2)
semilogx(ch1Freq,E1/e0,'o',ch2Freq,E2/e0,'x',ch3Freq,E3/e0,'+',ch4Freq,E4/e0,'*',Marker
Size',4)
ylabel('Relative Dielectric Constant');

```

Appendix D: Impedance Measurement of Interdigitated Electrode Sensor

```
xlabel('Frequency in Hz')
ax = axis;
axis([10^(-2.3) 10^4 0 ax(4) ]);

% Header
text('String', 'TWS SS Analysis: Sheet 5', 'FontSize', 19, 'HorizontalAlignment', 'center', ...
'Units', 'Inches', 'Position', [3 8.5])

% FileStamp
text('String', file, 'FontSize', 10, 'HorizontalAlignment', 'left', ...
'Units', 'Inches', 'Position', [5 8.2])

% Time Stamp
text('String', time, 'FontSize', 10, 'HorizontalAlignment', 'left', ...
'Units', 'Inches', 'Position', [5 8.05])

% Date Stamp
text('String', date, 'FontSize', 10, 'HorizontalAlignment', 'left', ...
'Units', 'Inches', 'Position', [5 7.90])

%Restore figure size
set(F5, 'Position', pos);

% Sheet 6: Simulated Admittance Divider Response for Channel 1
if (length(ch1Freq) ~= 0)

F6=figure('PaperPosition',[.25 .75 8 9.5], 'NumberTitle','off', 'Name','TWS Data: Sheet 6');

%Save Initial Position info
pos = get(F6, 'Position');

%Enlarge figure to allow loaction of legend
set(F6, 'Position', [0 0 1000 700]);

% Channel 1 Simulated Gain
```

```

subplot(2,1,1)

for loadindex = 1:length(C11);
    semilogx(ch1Freq,ADGain1(loadindex,:),'o','MarkerSize',4)
    text(ch1Freq(length(ch1Freq)/2),ADGain1(loadindex,(length(ch1Freq)/2)),['Cl='
num2str(C11(loadindex)/1e-12) ' pF'])
    hold on
end;
ylabel('Simulated Ch. 1 Gain(dB)');

ax = axis;
axis([10^(-2.3) 10^4 ax(3) ax(4) ]);

% Channel 1 Simulated Phase
subplot(2,1,2)

for loadindex = 1:length(C11);
    semilogx(ch1Freq,ADPhase1(loadindex,:),'o','MarkerSize',4)
    text(ch1Freq(length(ch1Freq)/2),ADPhase1(loadindex,(length(ch1Freq)/2)),['Cl='
num2str(C11(loadindex)/1e-12) ' pF'])
    hold on
end;
ylabel('Simulated Ch. 1 Phase(degrees)');

ax = axis;
axis([10^(-2.3) 10^4 ax(3) ax(4) ]);

% Header
text('String','TWS SS Analysis: Sheet 6','FontSize',19,'HorizontalAlignment','center',...
'Units','Inches','Position',[3 8.5])

% FileStamp
text('String',file,'FontSize',10,'HorizontalAlignment','left',...
'Units','Inches','Position',[5 8.2])

% Time Stamp
text('String',time,'FontSize',10,'HorizontalAlignment','left',...
'Units','Inches','Position',[5 8.05])

% Date Stamp
text('String',date,'FontSize',10,'HorizontalAlignment','left',...
'Units','Inches','Position',[5 7.90])

```

Appendix D: Impedance Measurement of Interdigitated Electrode Sensor

```
%Restore figure size
set(F6,'Position',pos);

end; % End Channel one Admittance Simulation Plots

% Sheet 7: Simulated Admittance Divider Response for Channel 2
if (length(ch2Freq) ~= 0)

F7=figure('PaperPosition',[.25 .75 8 9.5],'NumberTitle','off','Name','TWS Data: Sheet 7');

%Save Initial Position info
pos = get(F7,'Position');

%Enlarge figure to allow loacation of legend
set(F7,'Position',[0 0 1000 700]);

% Channel 2 Simulated Gain

subplot(2,1,1)

for loadindex = 1:length(CI2);
    semilogx(ch2Freq,ADGain2(loadindex,:),'o','MarkerSize',4)
    text(ch2Freq(length(ch2Freq)/2),ADGain2(loadindex,(length(ch2Freq)/2)),['CI='
num2str(CI2(loadindex)/1e-12) ' pF'])
    hold on
end;
ylabel('Simulated Ch. 2 Gain(dB)');

ax = axis;
axis([10^(-2.3) 10^4 ax(3) ax(4) ]);

% Channel 1 Simulated Phase
subplot(2,1,2)

for loadindex = 1:length(CI2);
    semilogx(ch2Freq,ADPhase2(loadindex,:),'o','MarkerSize',4)
    text(ch2Freq(length(ch2Freq)/2),ADPhase2(loadindex,(length(ch2Freq)/2)),['CI='
num2str(CI2(loadindex)/1e-12) ' pF'])
```

```

        hold on
    end;
    ylabel('Simulated Ch. 2 Phase(degrees)');

    ax = axis;
    axis([10^(-2.3) 10^4 ax(3) ax(4) ]);

% Header
text('String','TWS SS Analysis: Sheet 7','FontSize',19,'HorizontalAlignment','center',...
'Units','Inches','Position',[3 8.5])

% FileStamp
text('String',file,'FontSize',10,'HorizontalAlignment','left',...
'Units','Inches','Position',[5 8.2])

% Time Stamp
text('String',time,'FontSize',10,'HorizontalAlignment','left',...
'Units','Inches','Position',[5 8.05])

% Date Stamp
text('String',date,'FontSize',10,'HorizontalAlignment','left',...
'Units','Inches','Position',[5 7.90])

%Restore figure size
set(F7,'Position',pos);

end; % End Channel 2 Admittance Simulation Plots

```

```

% Print Plots

```

```

pnt = input('Print Plots y/n? ','s');
if (pnt == 'y')
    FG = [F1 F2 F3 F4];
    for plt = 1:4

```

Appendix D: Impedance Measurement of Interdigitated Electrode Sensor

```
        figure(FG(plt));  
        print;  
    end  
end  
end;
```

D.3.3 Circuit Board Layout

A circuit board was developed for utilizing the current integration technique for the interdigital sensor containing three individual set of electrodes. The circuit produces a voltage output which is used by existing instrumentation that also provides the sinusoidal source and determines the magnitude and phase of the signal. The circuit makes provisions for the discharge of the integration capacitor and also switching of the integration capacitor to increase the range dielectric materials which can be measured. In the layout of the circuit special attention was given to the shielding of the measurement leads.

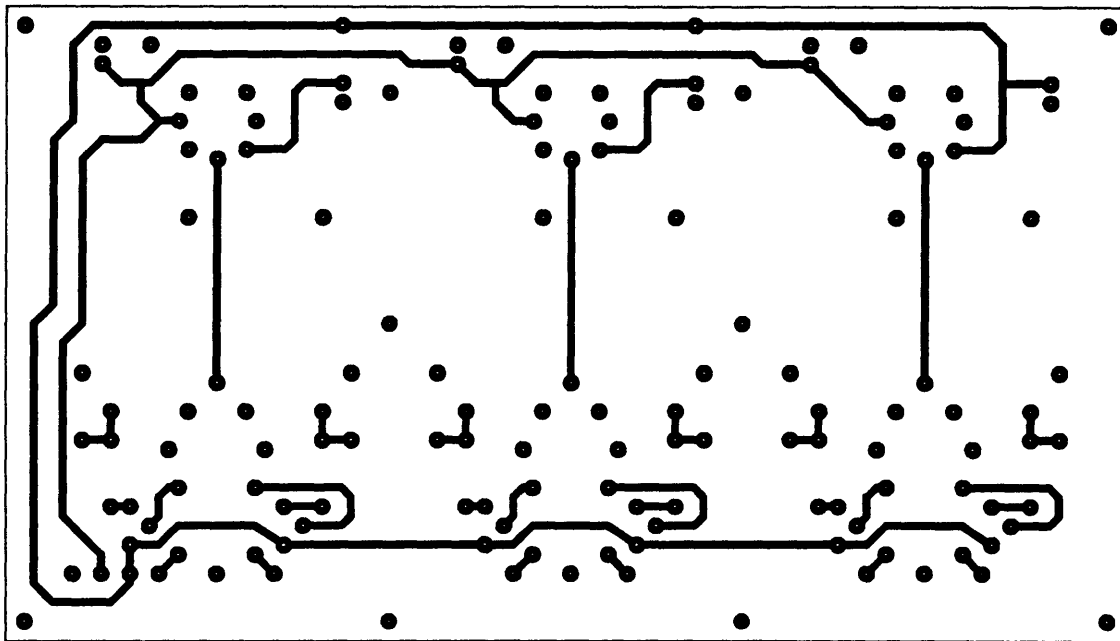


Figure D-12: Solder side of interdigital sensor interface using current intergration techniques (viewed from component side).

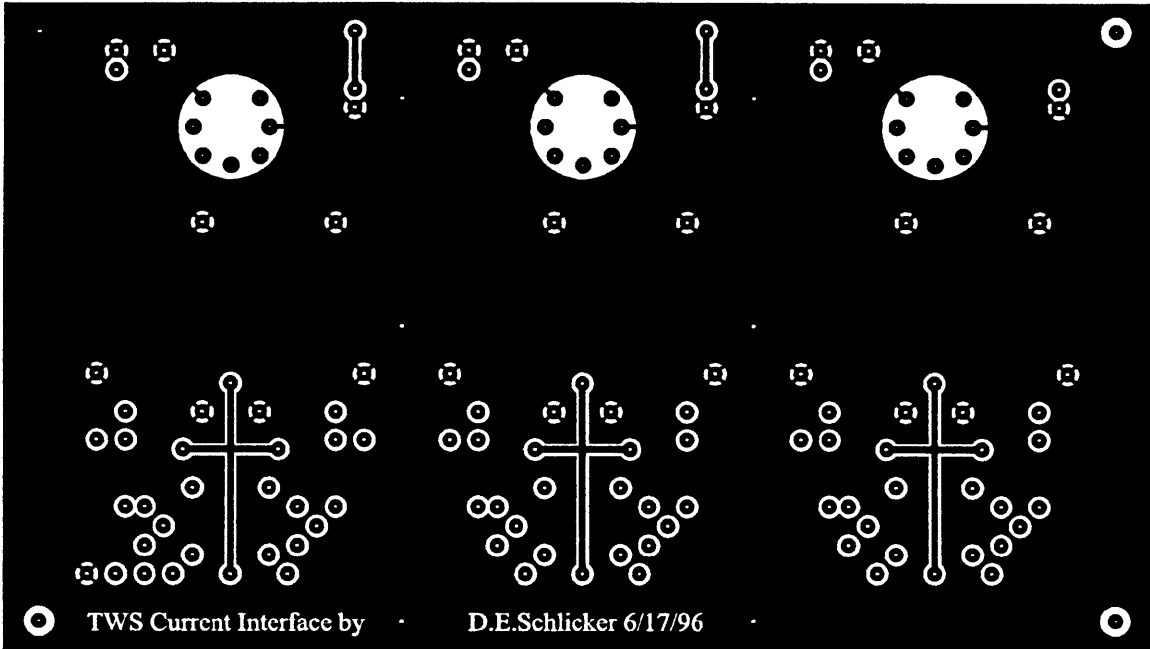


Figure D-13: Component side of interdigital sensor interface using current integration techniques (viewed from component side).

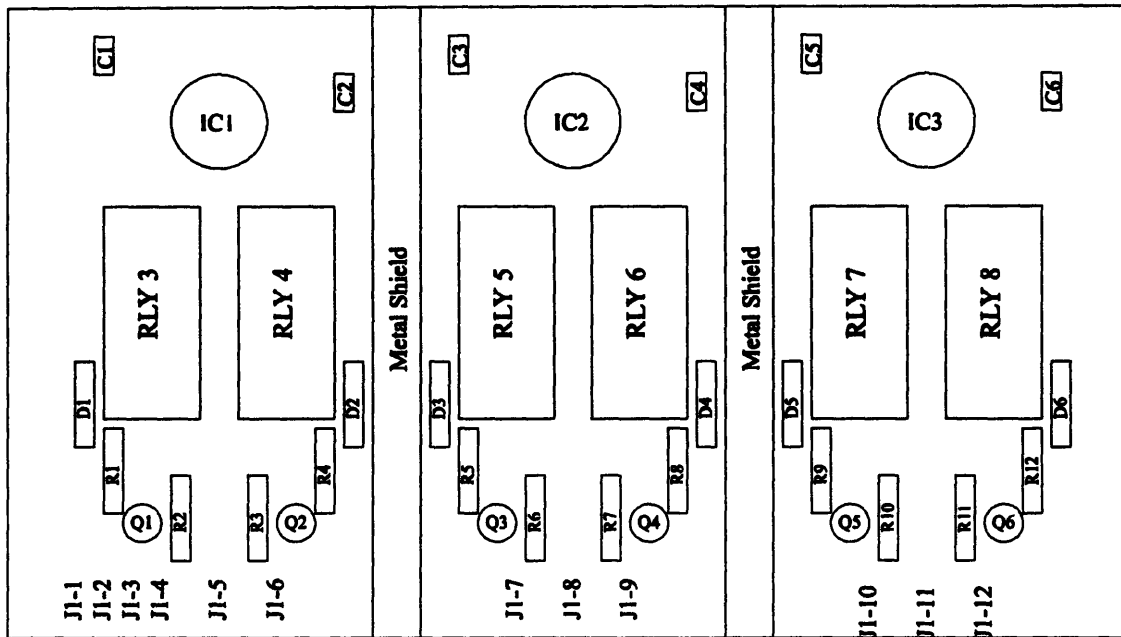


Figure D-14: Parts placement for interdigital sensor interface using current integration techniques (viewed from component side).

D.4 Proposed Zero-Order Inversion Technique for Homogeneous Material

Once the admittance between the interdigital electrodes has been determined, some analytical technique must be applied to recover the dielectric properties of the material which is being measured. Several techniques have been developed including the iterative use of a continuum model to match piecewise potential distributions along boundaries and pure calibration using known materials for homogeneous applications[7]. One very significant observation about the calibration curves is the linearity between measured sensor capacitance and dielectric constant over a wide range of dielectrics[2]. This fact helps to stimulate an assumption which can be used in getting an estimate of a homogeneous materials dielectric constant and conductivity based on a simple two point calibration of the sensor.

The assumption being made here is that the potential along the surface located between the sensor substrate and material being measured is completely constrained by the electrodes, independent of material properties. The reasoning behind this assumption is

that a major portion of this surface has its potential fixed by the conducting electrodes. The regions of the surface lying between electrodes must then have a potential distribution which varies from one electrode potential to the next and as long as the variation of material does not perturb this distribution too severely, the fields in the regions above and below the electrode surface will be relatively unchanged. If this is true, then the contribution of displacement and conduction currents flowing into the material side of the electrodes will be proportional to a geometric factor multiplied by the dielectric constant and conductivity of the material, respectively. Likewise, the displacement and conduction current flowing into the bottom of the electrode will be proportional to a second geometric factor multiplied by the dielectric constant and the conductivity of the substrate, respectively. This amounts to modeling the admittance between electrodes as two separate admittances, one due to the measured material and one due to the substrate. This assumption although obviously valid for only a limited range of materials is useful in creating a quick and simple method for inversion of a homogeneous material.

Based on the presented model, the two unknowns which must be determined before an inversion can be made are the geometric factors. First the admittances due to the material and substrate can be expressed as

$$\hat{Y}_{mat} = g_{mat} (\sigma_{mat} + j\omega\epsilon_{mat}) \quad (D.10)$$

$$\hat{Y}_{sub} = g_{sub} (\sigma_{sub} + j\omega\epsilon_{sub}) \quad (D.11)$$

where g is the geometric factor, σ is the conductivity, and ϵ is the dielectric constant. The subscript $_{mat}$ denotes the material, while $_{sub}$ denotes the substrate. Since the substrate is a pure dielectric with constant dielectric properties Eq. D.11 can be rewritten as

$$\hat{Y}_{sub} = j\omega C_{sub} \quad (D.12)$$

The total admittance can now be expressed as the sum of Eq. D.10 and Eq. D.12.

$$\hat{Y}_t = g_{mat} (\sigma_{mat} + j\omega\epsilon_{mat}) + j\omega C_{sub} \quad (D.13)$$

Appendix D: Impedance Measurement of Interdigitated Electrode Sensor

The two unknown parameters of the sensor needed for inversion have become g_{mat} and C_{sub} . These can be determined through two measurements of materials with differing dielectric properties. The calibration materials will be chosen to have no conductivity ($\sigma_{mat} = 0$) and to have dielectric constants denoted by ϵ_1 and ϵ_2 . The total admittance measured for each material will be denoted by \hat{Y}_1 and \hat{Y}_2 . Substituting into Eq. D.13 yields the following system of equations

$$\hat{Y}_1 = j\omega_{m1}(\epsilon_1 g_{mat} + C_{sub}) \quad (D.14)$$

$$\hat{Y}_2 = j\omega_{m2}(\epsilon_2 g_{mat} + C_{sub}) \quad (D.15)$$

where ω_{m1} and ω_{m2} are the radian frequencies at which \hat{Y}_1 and \hat{Y}_2 are measured, respectively. The solution to the system is as follows:

$$g_{mat} = \frac{\frac{1}{\omega_{m1}} \Im\{\hat{Y}_1\} - \frac{1}{\omega_{m2}} \Im\{\hat{Y}_2\}}{\epsilon_1 - \epsilon_2} \quad (D.16)$$

$$C_{sub} = \frac{\frac{1}{\omega_{m1}} \Im\{\hat{Y}_1\} - \frac{\epsilon_1}{\epsilon_2} \frac{1}{\omega_{m2}} \Im\{\hat{Y}_2\}}{1 - \frac{\epsilon_1}{\epsilon_2}} \quad (D.17)$$

Now that the unknown parameters of the sensor have been determined, the inversion can be completed by taking the real and imaginary parts of Eq. D.13 and solving for the material properties as

$$\epsilon = \frac{\frac{1}{\omega} \Im\{\hat{Y}_i\} - C_{sub}}{g_{mat}} \quad (D.18)$$

$$\sigma = \frac{\Re\{\hat{Y}_i\}}{g_{mat}} \quad (D.19)$$

This proposed technique has yet to be tested to determine its useful range of dielectric properties, but if even rough approximations can be achieved, its simplicity may be useful in certain instances.

Appendix D: Impedance Measurement of Interdigitated Electrode Sensor

Bibliography

- [1] P. A. von Guggenberg, Applications of Interdigital Dielectrometry to Moisture and Double Layer Measurements in Transformer Insulation, PhD thesis, Department of Electrical Engineering and Computer Science, Massachusetts Institute of Technology, Cambridge, MA, June 1993.
- [2] A. Marnishev and M. Zahn, "Techniques for Semi-Empirical Characterization of Material and Sensor Properties in Interdigital Dielectrometry," IEEE Symposium on Electrical Insulation, Montreal, Quebec, June 1996, pp. 486-489.
- [3] A.J. Morin II, M. Zahn, and J.R.Melcher, "Fluid Electrification Measurements of Transformer Pressboard/Oil Insulation in a Couette Charger," IEEE Transactions on Electrical Insulation, Vol. 26, No. 5, pp. 870-901, October 1991.
- [4] A.J. Morin II, M. Zahn, J.R.Melcher, and D.M. Otten, "An Absolute Charge Sensor for Fluid Electrification Measurements," IEEE Transactions on Electrical Insulation, Vol. 26, No. 2, pp. 181-199, April 1991.
- [5] Y.K. Sheiretov, Dielectrometry Measurements of Moisture Dynamics in Oil-Impregnated Pressboard, M.S. thesis, Department of Electrical Engineering and Computer Science, Massachusetts Institute of Technology, Cambridge, MA, May 1994.
- [6] A.P. Washabaugh, Flow Induced Electrification of Liquid Insulated Systems, PhD thesis, Department of Electrical Engineering and Computer Science, Massachusetts Institute of Technology, Cambridge, MA, December 1994.

- [7] M.C. Zaretsky, Parameter Estimation Using Microdielectrometry with Application to Transformer Monitoring, PhD thesis, Department of Electrical Engineering and Computer Science, Massachusetts Institute of Technology, Cambridge, MA, November 1987.